Technical University of Denmark

DTU

Formulation and validation of applied engineering equations for heat transfer processes in the food industry

Christensen, Martin Gram; Adler-Nissen, Jens; Løje, Hanne

Publication date:
2014

Document Version
Publisher's PDF, also known as Version of record

[Link back to DTU Orbit](#)

Citation (APA):
Christensen, M. G., Adler-Nissen, J., & Løje, H. (2014). Formulation and validation of applied engineering equations for heat transfer processes in the food industry. Technical University of Denmark (DTU).

DTU Library
Technical Information Center of Denmark

Formulation and validation of applied engineering equations for heat transfer processes in the food industry

DTU Food
National Food Institute

Formulation and validation of applied engineering equations for heat transfer processes in the food industry

Ph.D. Thesis

Martin Gram Christensen

2014

National Food Institute, Division of Industrial Food Research

Food Production Engineering Group

Technical University of Denmark

Supervisors:

Professor, dr.techn. Jens Adler-Nissen

Associate professor, Hanne Løje

Food Production Engineering Group

National Food Institute

Technical University of Denmark

National Food Institute
Division of Industrial Food Research

Formulation and validation of applied engineering equations for heat transfer processes in the food industry

Preface

This Ph.D thesis was carried out at the Food Production Engineering group, Division of Industrial Food Research, The National Food Institute at the Technical University of Denmark. The Ph.D thesis is carried out from December 1st 2009 to September 30th 2014, with the supervisors, dr.techn. Jens Adler-Nissen and Associate Professor, Hanne Løje.

First, I would like to express my deepest gratitude to my principal supervisor Professor, dr.techn. Jens Adler-Nissen and to my co-supervisor, Associate Professor, Hanne Løje. I am honoured to have been given the pleasure and opportunity to work under your wings. Your academic guidance, your advices, fruitful discussions, encouragement and especially your professional support through all phases of the project enabled this thesis to be realised. Your warm personalities, professionalism and honest dedication have been an inspiration.

Furthermore, I would like to send gratitude's towards all my colleagues at the division; it has been a real pleasure to work in such a friendly and inspiring environment. I would like to send special thanks to Associate Professor Emeritus, Jørgen Risum for his wisdom in the discussions of ideas and results, Ph.D candidate, Søren Juhl Pedersen for his creativity and dedication in our daily academic discussions and Assistant Professor Aberham Hailu Feyissa for supplying numerical data and for his skills and excellence which has really enlightened me.

I would also express my deepest gratitude for assisting with review on linguistics, cross references and nomenclature towards: Gine Ørnholt Johansson, Søren Juhl Pedersen, Taus Laurent Meincke, Søren Holm Rasmussen and Katrine Landerslev.

I would also like to thank all my students for sparking academic necessities; you have been a huge inspiration.

Finally, I would like to send my deepest gratitude's and warm thoughts to my family: My wife to become Katrine for your inspiration and joy through the process and for your love, care and understanding when times were tough. And to my beloved children Wilbur and Siv for cheering me up and warming my heart with your smiles, for your laughs and for your inconsiderate disturbances, without it I would not feel so alive. To You I am forever grateful.

Lyngby, September 2014

Martin Gram Christensen

Summary

The study is focused on convective heat transfer in the processing of solid foods, specifically with the scope to develop simple analytical calculation tools that can be incorporated into spreadsheet solutions. In areas of food engineering such as equipment manufacture the use of predictive calculations, modelling activities and simulations for improved design is employed to a high degree.

In food manufacture the use process calculations are seldom applied. Even though, the calculation of thermal processes is not a challenging task in academia; this is not the case for food manufacture. However; the calculations need fundamental validation and a generality that ensures a wide application, thus also the development of simplified approximations and engineering equations have to be conducted in academia. The focus group for the utilization of the presented work is; food manufacture, authorities ensuring food safety standards and students pursuing a food engineering career but lacks full engineering training.

The approach in this study is to identify possible simplifications to the complete Fourier series expansion [Fo-exp]. This is done through; a new method to non-iteratively find the Fourier exponents and lag factors needed in a 1st term approximation, expanding the use of the 1st term approximation to also cover low Fourier numbers [Fo], and investigating the input in the series expansion in terms of the determination of convective heat transfer coefficients. For the investigation it was crucial to establish a thorough understanding of the origin of both the standard [Fo-exp] solution and the criteria coupled with standard simplified solutions.

A new description of the internal and external resistance to heat transfer has been suggested in form of a normalization of the Biot number [Bi]. The normalized Biot number [Bi_{norm}] enables a simple, monotonically increasing expression, used to determine the Fourier exponents and lag factors needed in the [Fo-exp] solution to the heat equation. The proposed method has a low prediction error and can be used as an alternative to iterative methods or the use of charts. Additionally, [Bi_{norm}] provides a rational investigation of the sensitivity of important parameters such as the thermal conductivity and the heat transfer coefficients [h].

For the calculation of the thermal history during convective heating and cooling of solids, a solution is proposed that can also handle the initial heating/cooling period (Fo<0.2). In the construction of the new procedure the residual between a 1st term [Fo-exp] and the complete [Fo-exp] was modelled without introducing new parameters, except one experimental constant.

The combined procedure of the determination of Fourier exponents and lag factors have been used in excel calculations for the calculation of finite bodies. The developed method is validated with numerical solutions with comparable accuracy in two representative cases; cooling of packaged cream cheese and a three step processing of ham.

In the study, three investigations into the measurement methods for convective heat transfer coefficients [h_c] have been conducted.

The [h_c] for separate boundaries have been measured for a cooling operation, where also the influence of a present headspace was investigated. The contribution of the phenomena of boiling in the overall [h] to suspended particles was investigated in a new experimental setup. Experiments conducted at a comparison level emphasize that process control of vessel cooking should also include boiling rate instead of only using temperature.

A study in fluid to particle heat transfer coefficients [h_{fp}] have been conducted, where it is shown that potatoes can be used as a model food device for temperature measurements, in otherwise challenging environments. The method utilizes an observed gelatinization front in potatoes and inverse calculations of the thermal curve.

Based on a literature search it has been experienced that the common rules acknowledged in all textbooks and papers on the subject have not been properly investigated in terms of induced uncertainties coupled with the common rules. This includes the use of the lumped capacitance method for [Bi<0.1], and the criteria that a 1st term approximation is adequate for [Fo>0.2].

Whereas it was possible to trace the origin of the [Fo>0.2] criterion, the [Bi<0.1] criterion for the lumped capacitance method were unsuccessful. However, the error accompanied by this assumption is now documented and I believe it should be stated along with the criteria in future textbooks. The analysis shows that for elementary geometries the criteria [Fo>0.2], in worst case, generate calculation errors of up to 1.8%. The most troubling is that the worst case is for infinite slabs, which are used in the construction of general geometries, such as the shape of a box, increasing the induced error to almost 6%. The highest errors were observed at [Bi] around 2. For food manufacture [Bi] around 2 are extremely common.

The thesis presents an analysis and description of the [Fo-exp] to the heat equation, and also presents solutions to common challenges when calculations are conducted in food manufacture. The study provides a method where traditional processes can be calculated with a high precision by using an expanded 1st term approximation to the series expansion. This is an advantageous in terms of application in the industry where the solution can be incorporated into spreadsheet solutions. This feature is important in conducting process planning and scheduling, handling changes in products and processes and it is valuable in debottlenecking operations.

It is wished that the proposed work could help facilitate that the use of rational engineering calculations are performed in food manufacture. It is also hoped that the solutions provided and the insight to the [Fo-exp] will become a part of the engineering training for food science students. And most important, that the study will find application in the food industry.

Resumé

Dette studie omhandler konvektiv varmetransmission under produktion af faste fødevarer, med det specifikke fokus at udvikle nye beregningsværktøjer, der kan indbygges i regnearksløsninger. I nogle områder indenfor "Food Engineering", såsom produktion af procesudstyr, er brugen af prædikative beregninger, modelleringsaktiviteter og computersimuleringer meget anvendte værktøjer i forbindelse med design og optimering af udstyr. I den fødevare producerende industri er procesberegninger dog sjældnere anvendt. Selvom beregninger på simple termiske processer ikke er en stor udfordring i forskningsverdenen er situationen noget anderledes i dele af fødevareindustrien. Udviklingen af nye værktøjer, der kan højne anvendelsen af procesberegninger er dog en akademisk opgave, da de omhyggeligt skal valideres og udbredelsen skal sikres i form af generelle løsningsmetoder. Mens målgruppen for det præsenterede studie som helhed er forskningsverdenen er målgruppen for de udviklede ligninger fødevareproduktion, fødevarekontrolmyndigheder og studerende på de fødevarevidenskabelige uddannelser.

Formålet med studiet er at undersøge mulighederne for at udvikle nye analytiske metoder til beregning af opvarmning og nedkøling af faste fødevarer. Det primære mål er at muliggøre simplificering af Fourier´s serie ekspansion [Fo-exp] til Fourier's ligning til varmetransport. Dette indeholder en non-iterativ metode til bestemmelse af nødvendige faktorer og eksponenter til [Fo-exp], og en udvidelse af en simplificeret rækkeudvikling til også at muliggøre beregninger i starten af varmeprocesser hvor Fourier-tallet [Fo] er lavt. Til denne undersøgelse er det nødvendigt med en tilbundsgående undersøgelse af oprindelsen af den analytiske løsning til Fourier's ligning og de antagelser som danner grund for generelt accepterede antagelser for de simplificerede løsninger.

En ny beskrivelse af den eksterne og interne modstand imod varmetransport er blevet formuleret i form af en normalisering af Biot-tallet [Bi]. Det normaliserede Biot-tal [Bi_{norm}] muliggør en non-iterativ bestemmelse af Fourier-eksponenter og lag-faktorer som er nødvendige til beregning af [Fo-exp]. Den foreslåede metode har stor præcision i bestemmelsen af disse faktorer og eksponenter. Derudover muliggør [Bi_{norm}] en mere gennemsigtig bestemmelse af følsomheden i de vigtigste input i [Fo-exp]; varmeovergangstallet [h] og den termiske konduktivitet [k].

En simplificeret løsning til beregninger af temperaturhistorien under opvarmning/nedkøling af fødevarer er blevet formuleret som også omfatter startforløbet, hvor [Fo] er lavt. Ligningerne er gældende ved konvektiv varmeovergang i situationer hvor varmetransport er det eneste primære fænomen. Udviklingen af de nye beregninger er muliggjort ved modellering af residualet imellem en første terms [Fo-exp] og den komplette løsning til [Fo-exp]. Beregningerne introducerer ingen nye variable, og kun en enkelt empirisk bestemt konstant. Løsningen kan bruges til beregninger af uendelige legemer og sammensatte legemer.

Beregningsmetoden, som inkluderer både bestemmelsen af de nødvendige faktorer og eksponenter samt residual-modelleringen, er præsenteret og implementeret i regneark, hvor beregningen af to case studier er valideret med numerisk modellering. Det udviklede værktøj viste sammenlignelig præcision med en numerisk løsning for nedkøling af smøreost i en pakke med headspace (isolerende luftlag i toppen af pakken), og tretrins produktion af hamburgerryg indeholdende to opvarmningstrin og et nedkølingstrin.

I studiet er også bestemmelse af varmeovergangstal[h] behandlet, da dette er en central udfordring i forbindelse med beregninger på termiske processer. Fokus har været på det konvektive varmeovergangstal [h_c] og der er udviklet metoder indenfor tre områder:

Bestemmelse af [h_c] under blæstkøling for individuelle grænseflader ved at isolere en modelfødevare konstrueret i aluminium. Under bestemmelsen blev også indflydelsen af et isolerende luftlag i emballerede fødevarer undersøgt.

Bestemmelse af varmeovergangstal fra væsker til partiker [h_{fp}] under grydekogning er blevet udviklet, hvor en observeret gelatineringsfront i kartofler blev udnyttet som en non-invasiv temperatur måling til bestemmelse af [h_{fp}], i processer hvor det ikke ellers er muligt at måle temperaturen i partikler på normal vis.

Derudover er det blevet undersøgt, hvilken indflydelse kogningsgraden har på varmeovergangen fra ikke newtonske væsker til partikler under grydekogning. Resultatet af undersøgelsen indikerer, at også kogningsgraden bør indføres som proceskontrolparameter i disse processer.

På baggrund af gennemgang af litteratur er det ikke lykkedes at dokumentere oprindelsen af kriteriet for brugen af "lumped capacitance" modellen for [$Bi<0.1$]. Dog har en matematisk analyse af rækkeudviklingen resulteret i en dokumentation af usikkerheden, når dette kriterium anvendes. Oprindelsen til kriteriet for at bruge simplificerede [Fo-exp] til beregning, hvor [$Fo>0.2$] er dokumenteret. En analyse af de implicerede usikkerheder viste, at en fejl på op til 1.8% ville fremkomme i værste tilfælde. Dog er det tankevækkende, at den maksimale fejl er for uendelige plader, som udnyttes i beregningerne af endelige simple legemer (såsom kasser), hvor fejlen i disse tilfælde vil være op til 6%. Dette er problematisk specielt fordi de største fejl observeres ved [$Bi=2$], som er yderst normalt under produktion af fødevarer.

Denne afhandling dokumenterer en analyse og beskrivelse af [Fo-exp] til beregning af opvarmning og nedkøling af faste stoffer, og præsenterer en løsning til generelle problemstillinger under opvarmning og nedkøling af fødevarer. Den præsenterede løsning har en generel anvendelse og er i et format, der kan implementeres direkte i regnearksløsninger. Dette er en fordel i forbindelse med den industrielle anvendelse, specielt i form af udførelsen af rationel produktionsplanlægning, samt til at håndtere ændringer i proces eller produkt, og er et værdifuldt værktøj til identifikation af flaskehalse.

Det er et håb, at denne afhandling kan være en assistance til, at flere beregninger udføres i forbindelse med produktion af fødevarer. Det er også et ønske, at indsigten fra dette studie og de udviklede ligninger kan blive en del af undervisningen i fødevareteknologi for studerende i fødevarevidenskab. Og mest af alt er der ønske om at de udviklede løsninger vil finde anvendelse i fødevareindustrien.

Structure of the Thesis

This Thesis consists of 9 chapters and 8 appendices. The appendices to this thesis consist of both scientific papers (appendix 1-5) and extra material (appendix 6-8). The thesis can be read chronologically without referring to the appendices, hence there are similar sections in the papers (appendix 1-5) and in the thesis. A special note when reading this thesis is that chapter 7 (a synthesis chapter) which presents a thorough analysis of the Fourier series expansion, and thus also serves as central argumentation for deducing the simplified equation presented in chapter 3 and 4.

Contents

List of publications

Christensen, G. M., Adler-Nissen, J. (2014). Simplified equations for transient heat transfer problems at low Fourier numbers. *Journal of Applied Thermal Engineering – Submitted July 2014*

Christensen, G. M., Adler-Nissen, J. (2014). Proposing a normalized Biot number: For simpler determination of Fourier exponents and for sensitivity analysis of heating and cooling of solids. *Journal of Applied Thermal Engineering – Submitted September 2014*

Feyissa, A. H., **Christensen, M. G**., Adler-Nissen, J., Pedersen, S. J., Hickman, M. (2014). Potatoes as potential devices for studying fluid-to-particle heat transfer coefficients in vessel cooking processes. *Food Research International – submitted September 2014*

Christensen, M. G., Feyissa, A. H., Adler-Nissen, J. (2011). Computer aided simulation for developing a simple model to predict cooling of packaged foods. *In Proceedings of ICEF11, MCF 378, 2011, Athens Greece – Oral presentation http://www.icef11.org/main.php?fullpaper&categ=MCF*

Christensen, M. G., Adler-Nissen, J. (2014). Gentle vessel cooking of particles in viscous liquids. *Food Factory of the future 2014 in Uppsala Sweeden, Accepted for poster presentation*

Nomenclature, definitions and abbreviations

Biot number (Bi): Is the ratio between internal and external resistance to heat transfer and is the dimensionless description of a bodies thermal characteristics used in analytical calculation of non-stationary heat transfer

Fourier number (Fo): Is the dimensionless time which describes the process duration. Fo is mathematically convenient to enable the analytical description of the series expansion in a simple format not dependent of the geometry and size.

Dimensionless temperature difference (Ω): The dimensionless temperature difference is a normalization of the thermal response inside a body compared to the surrounding temperature. The normalization enables the mathematical representation of the series expansion to be independent of the temperatures involved in a given process.

Fourier exponent (b, λ^2): The Fourier exponent is a characteristic variable used in the series expansion which is dependent of the geometry, the size and the heat transfer coefficient in a given process lumped in the Biot number. For elementary geometries the Fourier exponents can be calculated based on given root equations.

Lag factor (a_x): The lag factor is a characteristic variable used in the series expansion, and is the intercept in a semi logarithmic regression of the dimensionless process scheme (Ω, Fo). Each term in the series expansion has a specific lag factor depending on the geometry and the given eigenvalue to the geometries given root function.

Elementary geometry: 3 elementary geometries exists corresponding to the 3 simple coordinate systems; Cartesian coordinates used for infinite slabs, Cylindrical coordinates used for infinite cylinders and spherical coordinates used for spheres.

General geometry: A general geometry is any geometry that can be expressed as cross-products of elementary geometries, where the most important are the finite box and the finite cylinder and infinite prisms.

Volume to Area ratio (V/A): The volume of any geometry divided by its corresponding surface area will in all cases correspond to the average distance from the surface to the centre of the geometry. Thus in some situations it is beneficial to use V/A for presenting the characteristic dimension

Heat transfer coefficient (h): The heat transfer coefficient is the rate of energy [J] transferred pr. [m^2] pr. temperature difference [K]. Several types of heat transfer can be observed in processing, but in this thesis only convective heat transfer is covered. Convective heat transfer is the transfer of energy between a moving fluid (gas or liquid) and a solid

Symbol	Description	Unit
A	Surface area	[m^2]
a_i	Lag factor used in the Fourier series expansion, general form	[-]
a_c	Lag factor used for centre temperature in the series expansion	[-]
$a_{x/l}$	Lag factor used for positional temperatures in the series expansion	[-]
b_i	The Fourier exponent used in the Fourier series expansion	[-]
Bi	Biot number	[-]
Bi_{norm}	Normalized Biot number	[-]
C	Empirical constant used in chapter 4	[-]
$CVRMSD$	Coefficient Variation of the Root Mean Squared Difference	[-]
c_p	Specific heat capacity	[J/kg$\cdot$K]
Fo	Fourier number	[-]
h	Heat transfer coefficient	[W/m^{2}K]
H	Enthalpy	[J/kg]
k	Thermal conductivity	[W/m$\cdot$K]
K	Consistency index in the power-law model	[Pa$\cdot$s^N]
L	Length (characteristic dimension) ½ height or radius	[m]
m	mass	[kg]
n	Number of dimensions	[-]
N	Power law exponent	[-]
R	Radius (characteristic dimension)	[m]
$RMSE$	Root mean squared difference	[-]
t	Time	[s]
T	temperature	[°C]
T_{gel}	Gelatinization temperature of potatoes	[°C]
V/A	Volume to surface area ratio	[m]

V	Volume	[m^3]
x/R	Relative characteristic dimension relative to the geometric centre	[-]

Greeks

α_{slope}	Slope of regression curve	[depends]
α	Thermal diffusivity	[W/m$\cdot$K]
β	Intercept of regression curves	[depends]
ε	Residual (ΔΩ)	[-]
λ	Eigenvalues for given root functions	[-]
ρ	Density	[kg/m^3]
Ω	Dimensionless temperature difference	[-]

Subscripts

aluminium	
cyl	Infinite Cylinder in cylindrical coordinates
evap	evaporation
fp	Fluid-to-particle
slab	Slab infinite slab in Cartesian coordinates
sphere	Sphere in spherical coordinates
c	Centre
m	volume average temperature
x/R	Normalized point distance 1=surface 0=centre
R	radius
norm	Normalised

1. Introduction

Heating and cooling of solid foods are central operations in food manufacture. These processes are often dominated by non-stationary heat transfer. This thesis is focus on processes where convective non-stationary heat transfer dominates. Examples of such processes are:

a) Cooling of packaged foods (for example ready-made meals, processed meat and cheese)
b) Sterilization of canned foods (solid or high-viscous liquid foods)
c) Heating of particles in a liquid food (soups and sauces)
d) Low temperature heating <100°C (for example processing of ham, sous-vide, blanching)

The overall goal of this thesis is to develop analytical engineering equations that can be implemented directly into the routines in food manufacturing. This, to increase productivity in food manufacture through a better quantitative understanding of the thermal processes.

1.1 Optimization and calculation of thermal processes in food manufacture

A key driver in industrial production is a continuous optimization of processes to improve productivity; in terms of optimal use of raw materials, workforce, machinery and energy etc. For the food industry, additional focus is on food safety and sensory quality products. Thermal processes play a key role in assuring food safety, and the sensory quality is also often critically influenced by the thermal treatment. Therefore, quantitative understanding of thermal processes is a cornerstone in striving for improved productivity without compromising on the demands for food safety and sensory quality.

To ensure an environment where continuous optimization of processes can flourish, it is important that knowledge on processes and products are documented and embedded in the companies. This was described more than a century ago in Frederick Winslow Taylor's classic *Scientific Management* (1911) which initiated an industrial culture of manufacturing goods and conducting operational tasks in a manner inspired by science and not only by traditional practices. The approach by Winslow Taylor was a systematic documentation of systems and use of best practice in order to optimize tasks and operations.

Traditionally, process changes in the food industry are performed by trial and error investigations; the changes can be in form of changes in recipes, introduction of new products or unit operations, or a general optimization of the process lines. Many of the operational specifications are thus based on experience and tacit knowledge among workforce, making the company knowledge fragile and less capable of process transition when changes in the production environment occur. Like other manufacturing industries, the food industry is therefore facing a need to change the procedures from trial and error based decisions into more rational and knowledge based documentation. The calculations performed in food manufacture needs simplicity for fast evaluation. Simplicity is an advantage because a crude answer before deadline is infinitely better than a detailed accurate one after the deadline (Chwif and Baretto 2000).

A more rational and knowledge based approach to food manufacture facilitate continuous optimization and allow knowledge to be anchored in the organizations and not bound to specific employees. Predictive

calculations and modelling of processes plays an important role for this change in production culture to take place.

The literature review in chapter 2, shows that change in manufacturing philosophy from empiricism to predictive calculations was implemented for heat sterilization in the canning industry already in the first decades of the 20th century. In a wider context, however, predictive calculations of thermal processes appear not to be used to the extent they deserve, probably because the mathematical-physical models for many predictive calculations of many thermal processes are rather complex. This statement, which will be elaborated on later, has motivated the present thesis and its title, *Formulation and validation of applied engineering equations for the calculation of heat transfer processes in the food industry*.

1.1.2 The role of modelling and predictive calculations

Modelling in the context of this work, is defined as the development of a mathematical-physical process model that can mimic the process settings, the product characteristics and subsequently solved numerically, so that the process can be reproduced as a simulation on a computer. Modelling is thus a way to conduct experiments on a computer to achieve knowledge of the physical phenomena in the products during processing. Modelling serves as a platform for deeper understanding in the same way as traditional experiments. Furthermore, modelling activities provide a setup where responses to a process impact can be investigated in situations where it is otherwise difficult to conduct experimental measurements (such as assessing volume average temperature or temperature gradients during a thermal process). Additionally, mathematical-physical models are powerful tools for validation of more simple predictive calculations.

Mathematical-physical models are based on an understanding and description of the physics of the process. Ideally, the model is based on combining fundamental physical laws, but in many situations, the modelling must also incorporate one or more empirical parameters to obtain a realistic prediction of the process. This is characteristic of many predictive engineering models, which are formulated as analytical equations.

A typical predictive engineering equation which immediately can be solved analytically is the well-known Nusselt relation describing the convective heat transfer for fluid flow through a pipe. For turbulent flow of Newtonian liquids it is usually presented as the following empirical equation (Singh and Heldman 2014: p. 309):

$$Nu = 0.023 \cdot Re^{0.8} \cdot Pr^{0.33} \cdot \left(\frac{\mu_b}{\mu_w}\right)^{0.14}$$

Re is the Reynolds number and Pr is the Prandtl number: they are both calculated based on measured or assumed inputs, namely viscosity, thermo-physical properties, fluid velocity and dimensions of the pipe. μ_b and μ_w are the viscosity in the bulk liquid and the viscosity at the wall of the pipe respectively – for low-viscous liquids like water, this viscosity correction term is often omitted, and other versions of the above equation are also found (Mills 1995: pp. 269-272). The factor 0.023 and the two exponents results from empirical investigations of fluid flow under controlled circumstances (Singh and Heldman 2014: pp. 306-307).The Nusselt relation and a multitude of other predictive engineering equations are fundamental in textbooks in the fields of chemical, mechanical, and food engineering.

Where the Nusselt relation is empirically determined the Fourier series expansion solution in non-stationary heat transfer is an exact theoretically derived equation (theory section 1.2). The Fourier series exapnsion needs an empirical input in form of the thermo-physical properties and the convective heat transfer coefficient associated with the Biot number and describes an ideal geometry. In context of this thesis a simplified solution that approximates the series expansion solution is also considered an engineering equation if it includes an empirically determined constant or parameter.

The central equation in this thesis is the Fourier heat equation. It is a second order differential equation, which is presented and discussed in section 1.2. The equation can be solved in two principally different ways:

1. Numerically, which is very versatile because a broad number of phenomena can be included in the calculation and the solution is not limited to for example specific elementary geometries. Numerical solutions are often very specific to the modelled interactions between process and product. Numerical solutions require dedicated software or programming and for more complex problems also considerable computing power. The use of numerical solutions to the heat equation is discussed more in section 2.1.
2. Analytically, by a series expansion which, however, is only valid under certain ideal conditions, such as specific elementary geometries. To the extent that the real process conditions can be simplified without losing too much of the connection to reality, analytical solutions are much less demanding on computing power and dedicated programming. For rapid, predictive calculations analytical solutions are much to be preferred for reasons expounded on below. A specific advantage of the analytical solutions is the price of the needed software.

It should be stressed that both numerical and analytical solutions to the heat equation require a thorough physical understanding of phenomena occurring during processing in order to set the correct conditions for the calculations. This statement may appear self-evident, but it is too important to be neglected. If the engineer has not investigated which physics are involved in the investigated process, the calculations could be useless. Because experimental validation sometimes have significant variations in measured parameters and responses it can even be difficult to assess the performance of the calculations and whether the correct frame for the calculations have been set. Generally, models and predictions are used to predict responses for new inputs. Only a calculation based on the correct understanding of the phenomena can be used for this. A model or a calculation that is not based on correct physical understanding is basically just data fitting.

Independent of the solution method used to the heat equation, the input parameters in form of thermo-physical properties and boundary conditions needs to be adequately assessed cf. section 1.3. A perfect model is a perfect correlation between input and output. If the input is uncertain it is a perfect correlation to an uncertain output. The sensitivity of the input parameters to the model determines how affected the output is by uncertainties in the input parameters. This is discussed in chapter 7.

Although the establishment of a model for a numerical solution to the heat equation may result in the best predictive power, it is not in all situations the most favourable strategy. This is mainly because the generation of such a model and its solution is knowledge intensive and a time consuming task, and many food producers do not have the required software to either conduct the modelling or acquire the knowledge generated in academically produced models. Thus, in the daily routines at the food manufacturers it is often an advantage to use more simple predictive calculations. The operational tasks can be crude calculation of process times and resulting temperatures. Crude calculations are valuable tools in e.g; implementation of new products or processes, conduction of process planning and in de-bottlenecking operations to optimize the scheduling of a

process line. Especially, the possibility of incorporating the equations into simple spreadsheet programs will serve as an advantage for food manufacturers lacking more advanced dedicated software. Though the use of simple analytical tools are most important in food manufacture, the development of the predictive calculation methods is an academic task. This is important because simple tools need to be thoroughly theoretically validated in order to ensure a wide application. An understanding of the physical phenomena dominating the calculations has to be established to ensure proper use of the calculations. If the equations are not based on a physical understanding and instead based on a high degree of data fitting, the models could perform poorly in terms of predictions outside the fitted area. Subsequently all models and equations also need industrial validation in context of intended use.

The majority of recent studies on the calculation of thermal processes are based on numerical solutions and a huge variety of models are constructed and reported in academic journals. Unfortunately, as stated above, many food producers do not have in-house qualifications and/or time to conduct or make use of numerical modelling. In addition, the costs for conducting advanced numerical simulations are high.

There is therefore still a need for analytical calculations that can be utilized with existing software in order to ensure a broad implementation at the food manufacturers. The motivation of this study is to derive such equations, which are user friendly and supply an adequate precision for utilization at the manufacturers.

In the production of food, a huge variety of product characteristics and unit operations is present within even a single production site. If the company has intentions of acquiring numerical modelling knowledge through academic collaboration, it is an advantage if the company can perform crude calculations on their unit operations and products to select the most suited process to ensure value for the money spend. Then the modelling activities can be focused towards processes and products where a simple calculation does not suffice.

The assumption of this work is that implementing simpler equations into the routine at food manufacturers ease the later implementation of more advanced numerical methods, and in general promote a culture where production management is conducted in more scientific way.

1.2 An introduction to the theory of analytical solutions for non-stationary heat transfer in food processing

The following section is as an introduction to non-stationary heat transfer giving the general theoretical background for the later chapters in this thesis. In this introductory theory section, equations that are specifically referred to later in the thesis are numbered in brackets, while equations of informational character and not directly referred to later are not numbered.

The evaluation and calculation of heat transfer processes is an old discipline that origins from the work of Isaac Newton with the law of cooling. This law states that the rate of cooling of an object is opposite proportional to the mass of the object and the heat capacity of the object, with the driving force being the temperature difference between the exposed surface area and the cooling media:

$$m \cdot c_p \cdot (T_t - T_0) = U \cdot A \cdot (T_s - T_t) \cdot t$$

Where integration over time yields what is called the lumped capacitance equation

$$\frac{(T_s - T_t)}{(T_s - T_0)} = e^{-\left(\frac{U \cdot A}{m \cdot c_p}\right) \cdot t} \qquad [1.1]$$

The lumped capacitance equation evaluates the temperature response inside a body where the internal resistance to heat transfer can be neglected (Biot number <0.1), yielding uniformity in temperature distribution. Situations where the internal resistance to heat transfer cannot be neglected are characterized by the Biot number:

$$Bi = \frac{h \cdot R}{k} \qquad [1.2]$$

h is the heat transfer coefficient [W/m²K], R is the characteristic dimension [m] (half thickness for infinite slabs, and the radius for infinite cylinders and spheres), k is the thermal conductivity [W/m·K]. The Biot number describes the ratio between the external resistance to heat transfer and the internal resistance to heat transfer.

The general equation describing the temperature response in solids subjected to convective heat transfer is derived from Fourier's law and the conservation of energy (Fourier 1822). The Fourier law states that the flow rate of energy through a surface is proportional to the negative temperature gradient across the surface:

$$q = -k\Delta T$$

Based on Fourier´s law and the conservation of energy the heat equation (here presented for 3 dimensions) becomes:

$$\frac{\delta T}{\delta t} = \alpha \left(\frac{\delta^2 T}{\delta x^2} + \frac{\delta^2 T}{\delta y^2} + \frac{\delta^2 T}{\delta z^2} \right)$$

Where α, is the thermal diffusivity [m²/s] determining the rate that heat is transported through a solid body. The thermal diffusivity is calculated from the thermo-physical properties of the solid:

$$\alpha = \frac{k}{\rho \cdot c_p}$$

Where k is the thermal conductivity [W/m·K], ρ is the density [kg/m³] and c_p is the specific heat capacity [J/kg·K].

In pure heat transfer processes the Fourier equation can be solved by a series expansion also initially proposed by Fourier (1822) and thoroughly described by Carslaw and Jaeger (1959):

$$\Omega = \left(\frac{T_s - T}{T_s - T_0}\right) = \sum_i^\infty a_i e^{-b_i \cdot Fo} \qquad [1.3]$$

Where Ω, is the dimensionless temperature difference [-] determined by the surrounding temperature T_s, the initial body temperature T_0 and the present temperature T, because the temperatures are measured in differences all units of temperature has the same equation, at time t [s]. Fo is the Fourier number [-] describing the dimensionless time:

$$Fo = \frac{\alpha}{R^2} \cdot t \qquad [1.4]$$

In non-stationary heat transfer the series expansion is conveniently expressed by its 1st term approximation when the Fourier number is above a certain limit. As discussed later in chapter 7, this limit is traditionally set at Fo>0.2 based on the pioneering work by Heissler (1947). The 1st term approximation is presented as:

$$\Omega = \left(\frac{T_s - T}{T_s - T_0}\right) = a_1 \cdot e^{-b_1 \cdot Fo} \qquad [1.5]$$

Where a_1 is the first lag factor and b_1 is the Fourier exponent, calculated from root functions (table 1.1.) given for the 3 elementary geometries (infinite slab, infinite cylinder and sphere). Below in figure 1.1 the behaviour of the 1st term approximation (equation 1.5) is presented in comparison to the entire expansion (equation 1.3). The figure presents an infinite cylinder with a Biot number of 10 as an example.
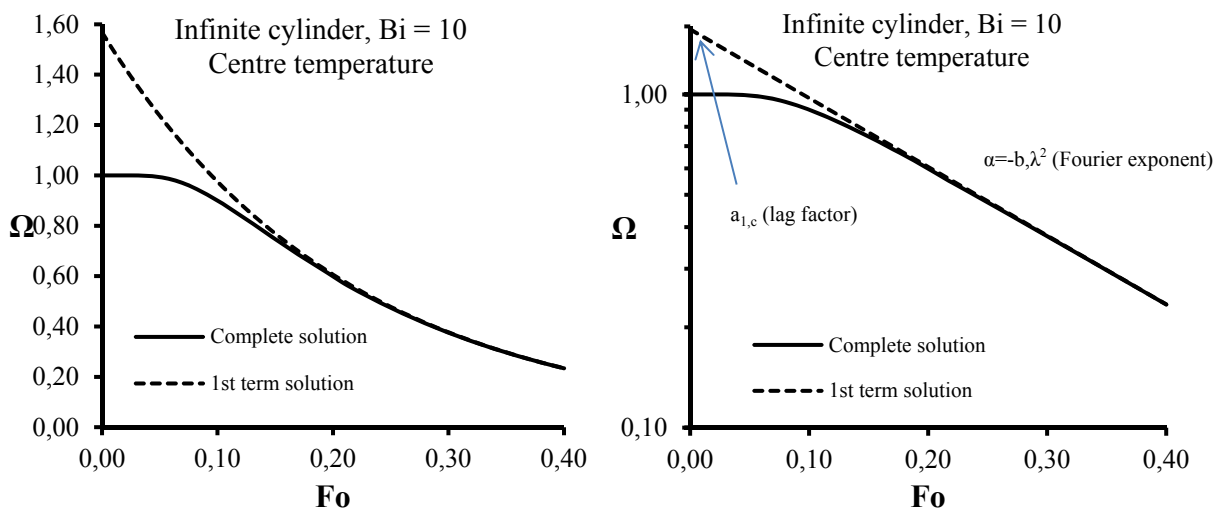

Figure 1.1 Graphical presentations of the 1st term approximation of the Fourier series expansion and explanation of the 1st lag factor and Fourier exponent.

From the presentation in figure 1.1 it is seen that the 1st term approximation is converging rapidly towards the entire series expansion solution for Fourier number above 0.2. In the graph to the right the lag factor a_1 is indicated as the crossing of the dimensionless temperature (Ω) axis in a semi logarithmic plot vs the Fourier number. The Fourier exponent (b, λ^2) is the slope of the linearized 1st term approximation.

The inputs in equation 1.3 are the Fourier number (Fo), the lag factors a_i and the Fourier exponents (b_i, λ_i^2). For the first term approximation only the 1st lag factor and 1st Fourier exponent are needed.

The Fourier exponent b_i in equation 1.3 is related to the eigenvalue λ_i to the respective root functions:

$$b_i = \lambda_i^2 \qquad\qquad [1.6]$$

The eigenvalues are calculated by iteration from the root functions in table 1.1 based on the Biot number. The equations for the derived lag factors a_i are presented along for the centre temperature a_c the volume average temperature a_m and positional temperatures $a_{(x/R)}$ within the body. The equations presented in table 1.1 are for the three elementary geometries (infinite slab, infinite cylinder and sphere).

Table 1.1 Mathematical presentation of the respective root function for the ideal geometries, lag factors for centre temperatures (a_c), the positional lag factors ($a_{x/R}$) and the lag factors for mean temperatures (a_m),

Geometry	Root function λ_i	a_c	$a_{x/R}$	a_m
Inf. Plate	$Bi = \lambda_i tan\lambda_i$	$\dfrac{2sin\lambda_i}{\lambda_i + sin\lambda_i cos\lambda_i}$	$a_c \cdot cos\left(\lambda_i \dfrac{x}{L}\right)$	$a_c \cdot \dfrac{sin(\lambda_i)}{\lambda_i}$
Inf. Cylinder	$Bi = \dfrac{\lambda_i J_1(\lambda_i)}{J_0(\lambda_i)}$	$\dfrac{2J_1(\lambda_1)}{\lambda_i(J_0^2(\lambda_i) + J_1^2(\lambda_i))}$	$a_c \cdot J_0\left(\lambda_i \dfrac{x}{R}\right)$	$a_c \cdot 2\dfrac{J_1\lambda_i}{\lambda_i}$
Sphere	$Bi = 1 - \lambda_i cot\lambda_i$	$\dfrac{2(sin\lambda_i - \lambda_i cos\lambda_i)}{\lambda_i - sin\lambda_i cos\lambda_i}$	$a_c \cdot \dfrac{sin\left[\lambda_i\left(\dfrac{x}{R}\right)\right]}{\lambda_i\left(\dfrac{x}{R}\right)}$	$a_c \cdot 3\dfrac{sin(\lambda_i) - \lambda_i cos(\lambda_i)}{\lambda_i^3}$

J_0 and J_1 is the Bessel function of the 1st kind with 0th and 1st order respectively. x/R is the relative distance from the centre

The behaviour of the complete series expansion (equation 1.3) in non-dimensional form for each of the 3 elementary geometries are presented in figure 1.2.
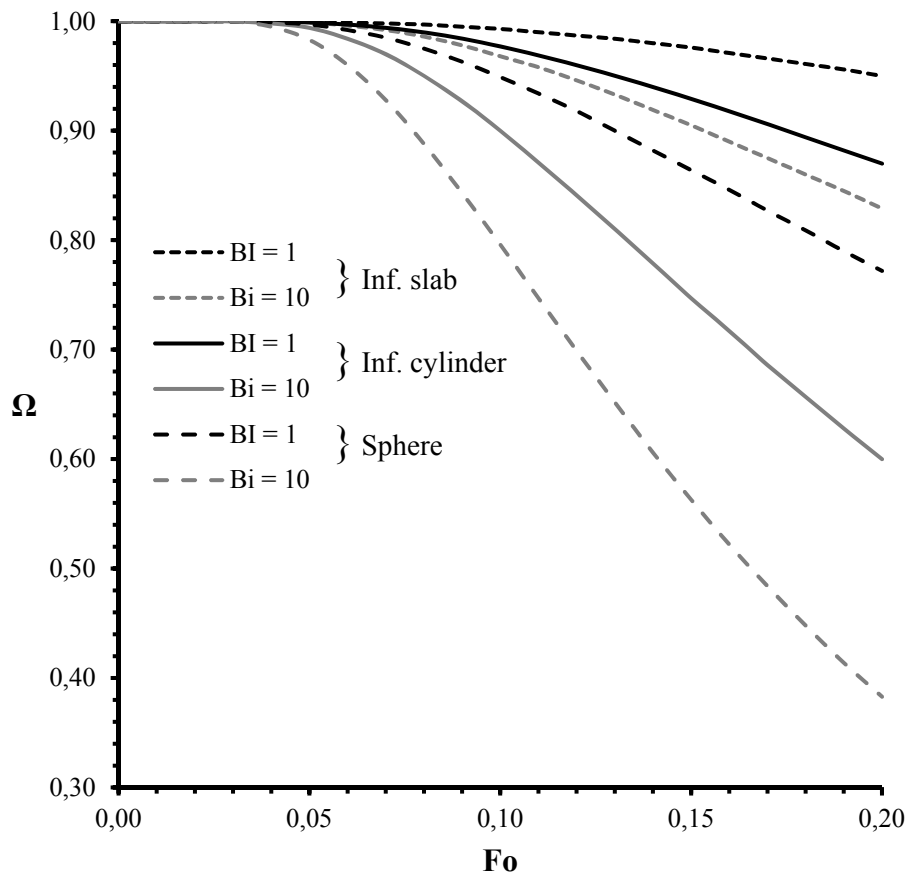
Figure 1.2 The non-dimensional temperature history in the center of the three elementary geometries for two selected Biot numbers

It is clear that the sphere exchanges heat with its surroundings faster than the infinite cylinder and the infinite slab for equal Biot numbers, where also the process time is equal for the geometries at equal Fo-numbers (figure 1.2). This is because the sphere has the largest surface are to volume ratio. For low Fourier numbers (Fo<0.05) $\Omega \approx 1$, indicating that the thermal response in the centre is not yet detectable.

The series expansion is an exact analytical solution to the heat equation for convective non-stationary heat transfer if all the series are considered under the given assumptions:

1. No phase change or mass transfer is occurring
2. No heat generation is considered
3. The initial conditions are uniform for both temperature and thermos-physical properties
4. The thermos-physical properties are assumed constant during processing
5. The geometry is either elementary or can be represented as cross products of elementary geometries
6. No changes in geometry

For applications in bodies that cannot be presented as an infinite slab, an infinite cylinder or a sphere Newman (1936) presented a method for the cross products of these elementary geometries. The cross products are an infinite prism (slab x slab), a box (slab x slab x slab) and a can (slab x cylinder) which expanded the application area of the series expansion to more common geometries. The procedure is

presented in equation 1.7, exemplified by the shape of a box. The cross product geometries are shown in figure 1.3

$$\Omega_{box} = \Omega_{length} \cdot \Omega_{width} \cdot \Omega_{height}$$

$$\Omega_{box} = \left[\sum_{i=1}^{\infty} a_i \cdot e^{(-\lambda_i^2 \cdot Fo)}\right]_{length} \cdot \left[\sum_{i=1}^{\infty} a_i \cdot e^{(-\lambda_i^2 \cdot Fo)}\right]_{width} \cdot \left[\sum_{i=1}^{\infty} a_i \cdot e^{(-\lambda_i^2 \cdot Fo)}\right]_{height} \qquad [1.7]$$
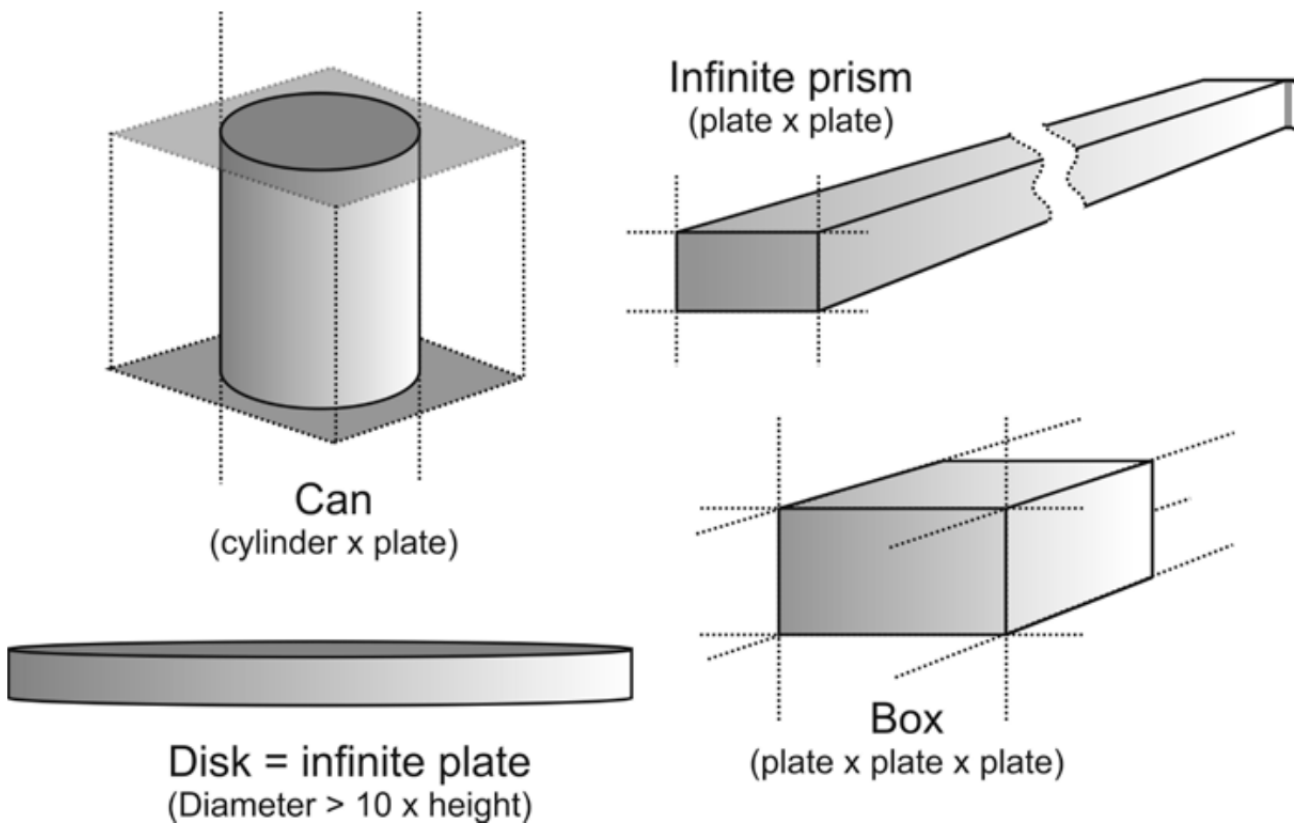
Figure 1.3 The general geometries generated by cross products of the elementary geometries, by courtesy of Jens Adler-Nissen (2014).

For crude calculations of the thermal history it is not practical to use the entire expansion. When the process time is sufficiently large (Fo>0.2) (Heissler 1947, Mills 1995, Singh and Heldman 2013) applying only the 1st term induces only small errors in the calculations (a further investigation in the prediction errors at Fo=0.2 is presented in chapter 7). Using the 1st term approximation is not only favourable in terms of simplicity in the calculation; it has furthermore the advantage that it can be used in the inverse form for calculating the time to reach a specific temperature. If two or more terms are used, it is only possible to calculate the temperature at a specific time input without iteration. Thus to reach a specific temperature it is necessary to produce a time-temperature curve and then find the time to reach the target temperature from the curve.

Heissler (1947) developed graphs for determining the temperature response at Fourier numbers below 0.2 which are still used today (Mills 1995, Singh and Heldman 2013). The graphs are a valuable fast tool for the evaluation but are not convenient for implementation into programming. Furthermore, the risk of misreading

is a problem. Pflug et.al (1965) published an approach where the Fourier exponents and lag factors for the 1st term approximation can be determined graphically. The procedure from Pflug et.al (1965) is still used today for crude calculations, and is a part of the curricula in food engineering education (Singh and Heldman pp. 377-380).

1.3   Thermo-physical properties and heat transfer coefficients

The series expansion solution (equation 1.3) to the heat equation is essentially exact under given assumptions. The input parameters in the equations are coupled with uncertainties. In addition to the definition of the geometry, the input parameters into the series expansion and to a numerical solution are the thermo physical properties of the food and the convective heat transfer coefficient(s) associated with the process. In all cases in this thesis the initial conditions are assumed uniform in terms of thermo-physical properties and temperature, which is essential for the applicability of the series expansion solution.

Thermo-physical properties

The relevant thermo-physical properties, in situations where only heat transfer is considered, are the density ρ, the thermal conductivity k and the heat capacity c_p. The thermo-physical properties can be obtained from literature for specific food items. Determination of the thermo-physical properties from knowledge of the composition of the food can also be done with reasonable accuracy (Nesvadba 2014; Singh and Heldman 2014: 275-282). For the temperature dependence of the properties the task is a bit more difficult but the standard equations based on Choi and Okos (1986) can be used. It should be noted that the procedure is coupled with some level of uncertainty as in this work (Choi and Okos 1986) the temperature dependence was determined experimentally for liquids and might not be directly applicable for the calculation of heat transfer in solids. Because solid foods (except for dried products) have high water content the use of Choi and Okos´s procedure is widely accepted. The incorporation of the temperature dependence of the properties is not directly applicable in an analytical solution based on the series expansion, which is why the utilized properties are often assumed constant at the value corresponding to the averaged product temperature in the duration of the process. For this thesis the procedure of using constant averaged thermo physical properties is used in all situations as this is a prerequisite for the series expansion solution.

Calculation of thermo-physical properties

For a given homogeneous product, the thermo physical properties can be calculated based on the content of macronutrients (Carbohydrates, lipids, protein, fibre, ash and water). The content of macronutrients can be evaluated based on the recipe. The content of macronutrients and general composition can be found in databases e.g. the National Food Institute: www.foodcomp.com. The formulas for calculating the thermo-physical properties are:

The density:

$$\rho_{product} = \frac{1}{\sum \frac{x_i}{\rho_i}} \quad [\frac{kg}{m^3}]$$

heat capacity:

$$c_{p,product} = c_{p,c} \cdot x_c + c_{p,p} \cdot x_p + c_{p,f} \cdot x_f + c_{p,a} \cdot x_a + c_{p,w} \cdot x_w \quad [\frac{J}{kg \cdot K}]$$

thermal conductivity:

$$k_{product} = k_{water} \cdot \frac{c_{p,product}}{c_{p,water}} \quad [\frac{W}{m \cdot K}]$$

Boundary conditions (driving temperature difference and heat transfer coefficients)

For convective heat transfer the energy transferred between the product and the surrounding medium (typically water or air) is determined by the heat transfer coefficient and the driving temperature difference between the surroundings and the surface of the object. In numerical solutions the driving temperature difference and the heat transfer coefficient are combined in the flux equations defining the boundary conditions for the calculation. In the analytical solutions to the heat equation using the Fourier series expansion they are handled individually.

For the surrounding temperature it is a fact that both small and large fluctuations will happen simply due to the nature of how processes are controlled, this is especially evident when air serves as the media because its thermal buffer is low compared to water. Using the series expansion solution it is necessary to assume a constant surrounding temperature equal to the process average value.

The heat transfer coefficient, h, is defined as the energy [W] transferred pr. surface area [m^2] of the boundary between the solid and the liquid pr. temperature difference [K] between the solid and the liquid, have the unit: [W/m^{2}K].

A more detailed description of convective heat transfer coefficients is presented in chapter 6, where also determination methods and uncertainties in the determinations are discussed.

1.4 Research question

As discussed above, the overall aim of this project is to deduce new equations for easier calculations of heat transfer in food manufacture. The format of the equations should allow for implementation into simple calculation tools and guidelines, preferably the equations could be implemented directly into spreadsheet solutions.

This thesis deals with calculations at a unit operation level, and specifically focuses on thermal processes where transient heat conduction is dominant, and where mass transfer and phase transition are negligible. In this context the Fourier series expansion solution to the heat equation introduced in the theory section 1.2 is central.

The overall research question for this thesis is:

- **Is it possible to deduce and validate new engineering equations in heat transfer for food processing, which are user-friendly and provide adequate precision?**

In the next chapter the overall research question will be analysed in terms of a literature review of the subject and operationalized into sub-sections describing the tasks needed in order to fully answer the research question.

1.5 Overview of the thesis structure

The structure of the thesis is schematically presented in figure 1.4. The general introduction and literature review is followed by an operationalization of the research question in chapter 2. A simplification track (green) and an experimental section on heat transfer coefficients (orange) serves as the fundament for the synthesis of a proper work frame for the series expansion and the discussion of the application of the developed predictive calculations.
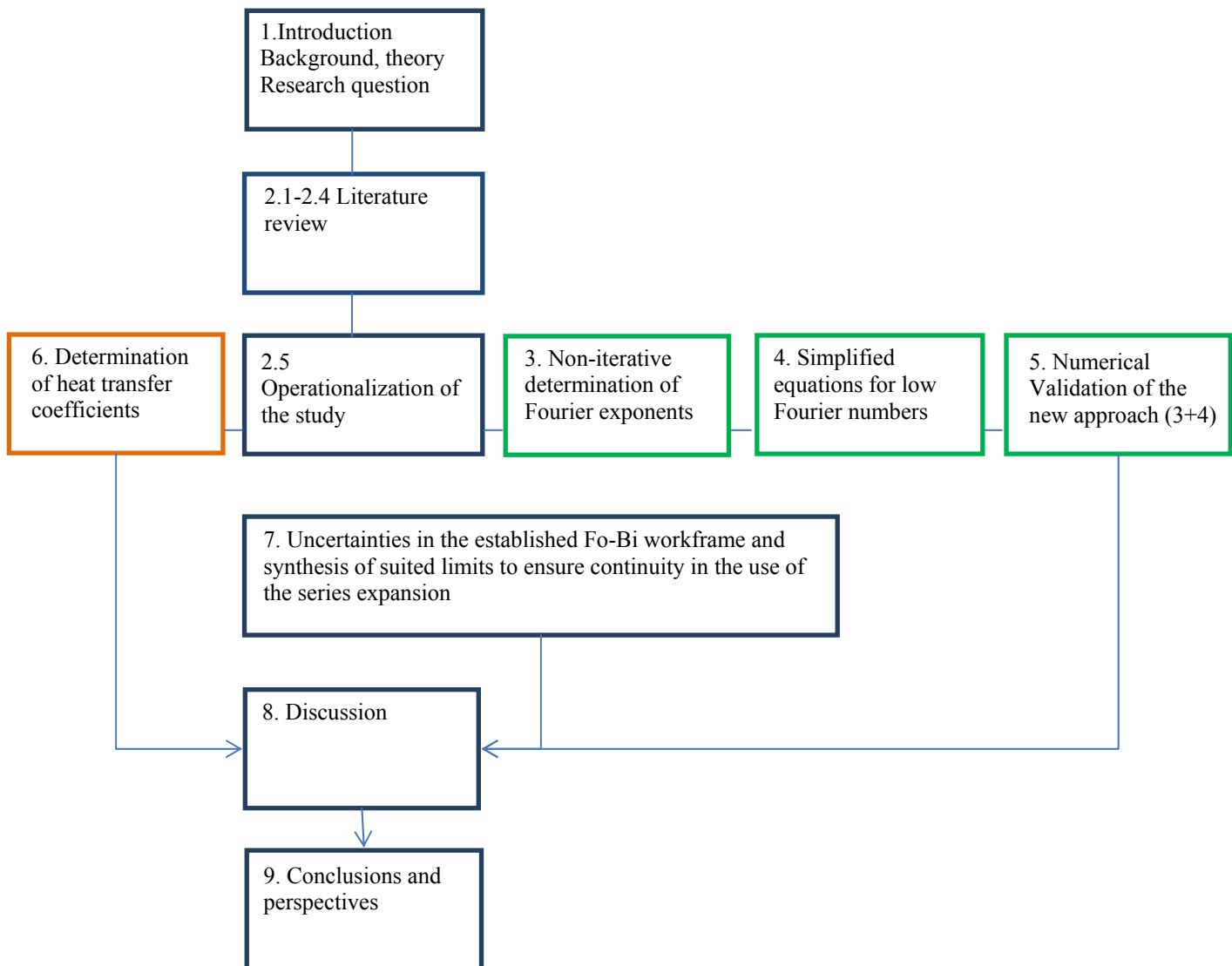

Figure 1.4 Schematic overview of the thesis structure, and the division into chapters

2. Literature review and operationalization of the research question

This section reviews the research related to the research question presented in chapter 1.4. In this context the review is primarily focusing on studies dealing with simplification of the Fourier series expansion and the application of the series expansion for non-stationary heat transfer in food processing. The literature search has been conducted in research databases through google scholar and DTU-Library, and by browsing through scientific journals deemed to be central to the field: *Journal of Food Engineering, Journal of Food Science and Technology, Journal of Food Process Engineering, Applied Thermal Engineering, Food Engineering Reviews, International Journal of Heat Transfer, Journal of Heat and Mass Transfer.* Various combinations of typical search words have been: *food, engineering, heat transfer, transient conduction, non-stationary heat transfer, heat equation, series expansion, analytical solutions, calculation, application, unit operation, thermal processes, heating, cooling.*

The review covers; determination and application of analytical solutions to the heat equation and briefly introduce how adaptations to the series expansion have been utilized in the calculations of food processes.

For a part of the review a historical backtracking was needed for accessing important pioneering studies, such as the work from (Fourier (1822), Ball (1923), Pflug et al. (1965), Newman (1936), Gurnay and Lurie (1923) and Heissler (1947)). This was also needed to investigate where common guidelines originate for example the limits for using the lumped capacitance model and the 1st term approximation to the series expansion.

Because many studies related to analytical solutions to the heat equation and simplification of the series expansion are old and often scarcely cited, a broad database search was also necessary for acquiring the literature.

The primary input in the equations is the energy flux governed by the heat transfer coefficient. Quantitative knowledge on heat transfer coefficients are crucial for all calculations of heat transfer into solids and a prerequisite for predictive calculations on thermal processes. Methods for determination of heat transfer coefficients are also reviewed in this chapter.

2.1 Review

This thesis is focusing on solutions to the heat equation. Basically two types of solutions exist: numerical solutions and analytical solutions. In addition, also simplified engineering equations and graphical solutions are evaluated in this review. The numerical solutions are introduced briefly, because in this project numerical solutions are used for validation of generated equations; however, it is outside the scope of the thesis to review all the literature dealing with numerical solutions of heat transfer in solid foods. In contrast, analytical solutions to the heat equation are reviewed thoroughly as these solutions constitute the basis for the construction of the simplifications and applied engineering equations.

2.1.2 Historical background

The historical background of the Fourier equation is condensed from Narasimhan (1999) and a translated English version of Fourier´s work "*Analytical theory of heat*" (Freeman; 1878). In 1822 Joseph Fourier presented his monograph "*Theorié analytique de la chaleur*" which still stands as the founding reference work for the mathematical description of heat transfer, introducing the heat equation. In the same monograph Fourier also supported an analytical solution to the heat equation based on trigonometric series. In 1804, a few years earlier than Fourier, Jean Baptiste Biot had also addressed the problem of heat conduction, but he was unsuccessful in including convective heat transfer in his work. Fourier read the work from Biot and started to formulate a solution to this challenge and submitted his work "*Théorie de la propagation de la chaleur dans les solides*" in 1807. Initially, Fourier´s work was rejected publication and it was not accepted for publication before 1822 (Narasimhan; 1999).

For application of the series expansion solution, graphical solutions were presented in the early-mid 20th century. Amongst others, Gurnay and Lurie (1923) presented graphical solutions for the distributions of temperature in heating and cooling of solids known as the Gurney Lurie diagrams. They exemplify how charts can be used for the evaluation of temperature history for few selected Biot numbers ranging from 0-2 for the elementary geometries. In 1947 Heissler published sets of graphical solutions for a large range of Biot numbers and Fourier numbers (Fo>0.2) that are still presented in present textbooks (Singh and Heldman 2013, Mills 1995) for easy calculation of the 1st term approximation. The charts presented by Heissler are presented in figure 2.1 directly copied from his original article.
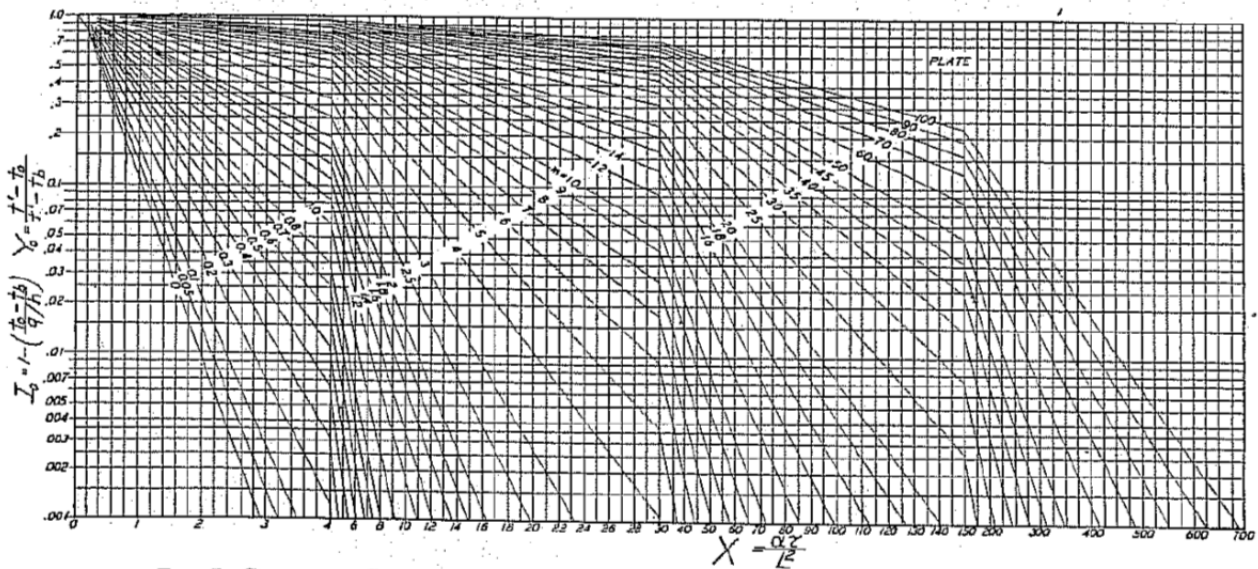
FIG. 7 CHART FOR DETERMINING TEMPERATURE HISTORY AT CENTER OF SEMI-INFINITE PLATE

Figure 2.1 Example of a Heissler chart, from his original work for the calculation of thermal response in a semi-infinite plate for Fo numbers above 0.2. Heissler (1947), line numbering referring to the reciprocal Biot number.

It is also in the work from Heissler (1947) that the limit (Fo>0.2) for the use of the 1st term approximation originates. In addition to these charts Heissler also introduced charts for determining thermal response in the low Fourier region (Fo<0.2) in the same work from 1947. The charts for low Fourier numbers are more difficult to read and interpret, as can be seen in figure 2.2 and are seldom presented in modern textbooks.
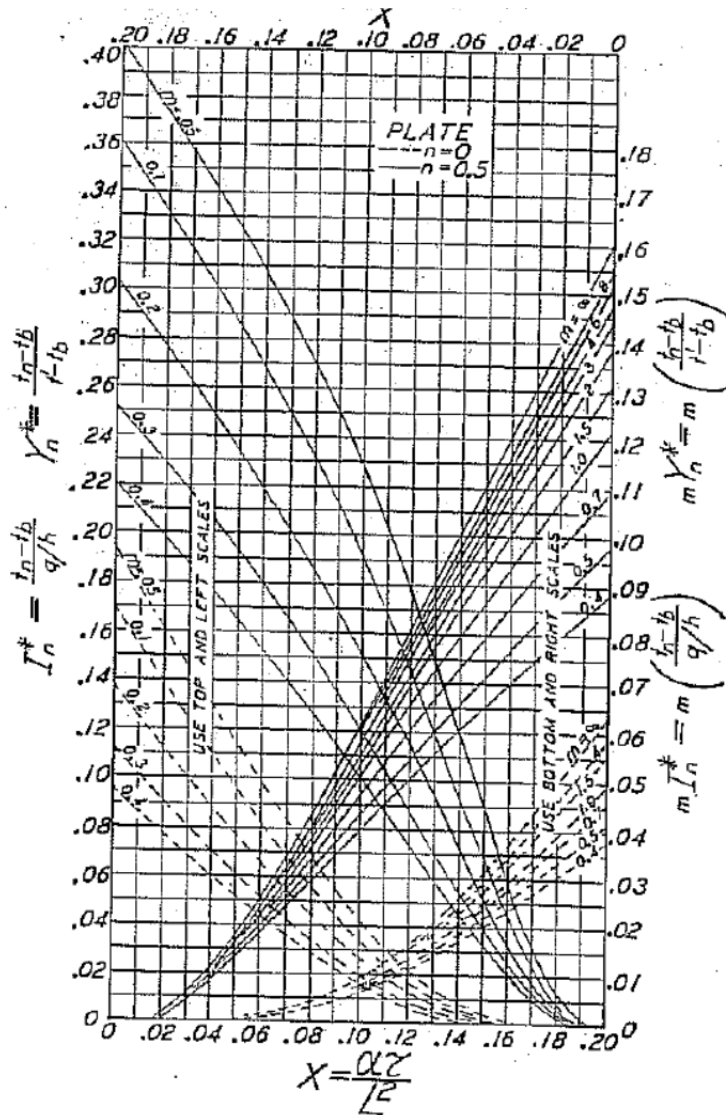
FIG. 2 CHART FOR DETERMINING TEMPERATURE HISTORY AT CENTER (n = 0) AND MID-PLANE (n = 0.5) OF SEMI-INFINITE PLATE

Figure 2.2 Example of charts produced by Heissler for the determination of centre temperature and mid-plane temperature at Fourier numbers below 0.2 (Heissler 1947)

Similar charts can be viewed in e.g. (Mills 1995 pp.1210-1216) for selected Biot numbers. These are easier to interpret.

Even though the graphical methods supplied by e.g. Gurnay and Lurie (1923) and Heissler (1947) have found great use in industrial production they only cover bodies that can be approximately described by one of the elementary geometries (infinite slab, infinite cylinder and sphere). The analytical calculation of finite bodies (general geometries) was presented by Newman (1936) and is briefly introduced in chapter 1. This enabled the analytical calculation for geometries that are more presentative for food processing e.g. the sterilization of cans cf. chapter 1.2.

A cornerstone in the analytical calculation of heating and cooling of solids is presented by Carslaw and Jaeger (1959) where different solution methods for the heat equation is deduced from Fourier´s work and published in the extensive work "*Conduction of Heat in Solids*" where chart-based solutions, analytical

derivations of the Fourier equation with several terms and even analytical handling of semi-infinite bodies are presented. In this work also the Fourier exponents and lag factors are presented as tabulated values for several terms. Whereas the lag factors and exponents can be acquired in this extensive work for several terms in the series expansion, the values for the 1st term are presented in most textbooks covering heat transfer in solids (Mills 1995, Singh and Heldman 2013).

In many situations it is reasonable to assume that a 1st term approximation to the series expansion is adequate (Fo>0.2) (Mills (1995) p. 152). It was thus worthy to determine the 1st Fourier exponent and 1st lag factor in a simple procedure. (Pflug et al. 1965) presented a graphical solution to determine these two important variables as a function of the Biot number. Their solution is an alternative to the use of the Heissler charts presented in figure 2.1. The use of the 1st term approximation under the condition (Fo>0.2) from Heissler (1947), is in some cases problematic and the uncertainties are not thoroughly presented in literature or textbooks. This issue is analysed in chapter 7.

2.1.3 The Fourier expansion applied in food engineering

Ball (1923) was apparently the first to apply the series expansion to food engineering where the sterilization curves of canned foods were investigated to ensure food safety. Ball used two factors to describe the heat equation. He introduced the heating rate as *1/f*, where *f* is the thermal decimation in a log10 plot of the temperature as a function of the time, describing the heating rate in the exponential phase (basically this is where the 1st term approximation applies, as later determined by Heissler (1947) to be Fo>0.2). Ball also introduced a lag factor he called *j* representing the intercept of the equation (in this thesis this is denoted as *a*, according to the nomenclature of Mills (1995)). The relation between the Fourier exponent *b* and the heating rate *f* is:

$$b_1, \lambda_1^2 = \frac{2.303}{f} \cdot \frac{R^2}{\alpha}$$

Where R is the characteristic dimension and α is the thermal diffusivity. The procedure from Ball (1923) is reproduced in (Singh and Heldman 2013 p. 378) and presented in figure 2.3.
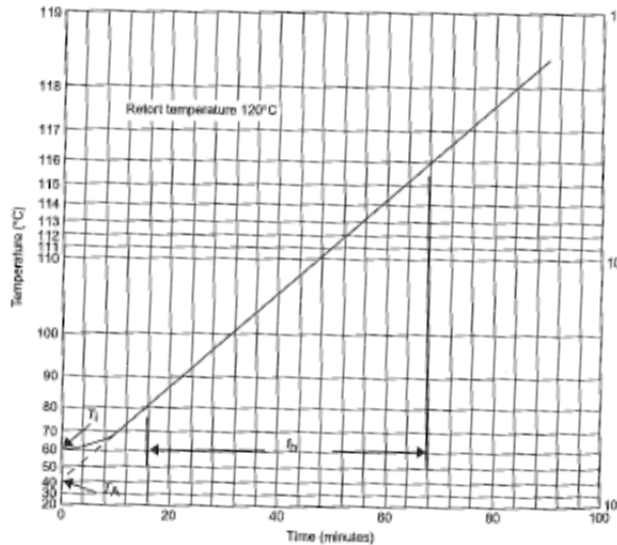
Figure 2.3 The procedure used by Ball (1923-1924) for experimental determination of the heating rate and the lag-factor

The investigation from Ball is interesting because it was conducted on a finite geometry (a cylindrical can) before the analytical calculation of finite geometries was established by Newman in 1936. The work by Ball was based on a 1st order approximation of the sterilization curve based on experimental observations.

The Fourier series expansion has since then been widely used in classical food engineering to evaluate thermal history, initially for sterilization processes. Hayakawa (1969) presented calculations also covering the initial heating and cooling period in sterilization processes limited to the geometry of a can. Together, Hayakawa and Ball (1971) published theoretical calculations for sterilization of cans, also including a time varying process temperature for 5 typical process situations. These studies are presented at the same time period where Teixeira et al. (1969) presented some of the first numerical solutions to the heat equation, which changed the focus in Food Engineering research towards more numerical solutions and modelling.

2.1.4 Numerical solutions

The application of numerical calculations of heating/cooling of solid foods was applied along with the development of computer technologies and was initiated by the work by Teixeira et al. (1969). Along with technological advances in hard- and software the computer assisted numerical calculations have been used in numerous applications in food engineering. Since the work from Teixeira in 1969 the physical models have incorporated numerous phenomena in the calculations of food processes. Recently the larger knowledge heavy corporations have started to include modelling activities (Datta 2008).

In recent decades the research on heat transfer in solid foods has focused on modelling and simulations of numerical solutions in often advanced software such as the MATLAB based COMSOL Multiphysics (Trystram 2012, Dehghannya et al. 2010). The numerical solutions have the advantage that more advanced and coupled physics can be included into the calculations accounting for mass transfer, geometry changes, chemical reactions and structure changes within the products (Lemus-Mondaca et al. 2011). Such calculations are, if conducted properly, precise and can handle real processing situations; however, they are often targeted at specific products in specific processes making them less versatile for general engineering

26

calculations. It is crucial that constructed models are not too complex to avoid misunderstanding of model results, in some cases a simple approach is preferable(Chwif and Baretto 2000).

2.1.5 Simplification to the series expansion

In the use of the series expansion for the calculation of heat transfer in solids also studies in possible simplifications of the expansion have been proposed. Three challenges in the use of a series expansion solution covered: The determination of the crucial parameters, the lag factor and the Fourier exponent by approximating the root functions (cf. chapter 1.3), calculation of the initial cooling/heating phase to avoid the use of multiple terms in the expansion, and incorporation of correction factors for the calculation of irregular geometries.

Fourier exponents and lag factors
One of the big challenges using the solutions devised by Pflug et al. (1965) is the determination of the Fourier exponents given by the eigenvalues to the respective root functions (Table 1.1, chapter 1.2). As mentioned, the root functions are of iterative character and are thus cumbersome to solve. Alternatively, the Fourier exponents can be found tabulated in textbooks or papers on the subject (Mills 1995 pp.173; Pflug et.al 1965), where it is often needed to interpolate between tabulated values, or they can be found in charts (Singh and Heldman 2013 pp.379) where there is a risk of misreads. Neither the tabulated values nor the graphical representation are suited for implementation in simple programs or spreadsheets. Thus, it would be an advantage to develop non-iterative equations for calculating the Fourier exponents, and a few authors have presented such equations.

Ramaswamy et al. (1982) fitted the Fourier exponents to ideal geometries using trigonometric regressions of the Biot number with good precision. The trigonometric regression made by Ramaswamy et al. (1982) introduces many new constants and equations which hampers the application in food manufacture. Lacroix and Castaigne (1987) used a logarithmic polynomial fit to determine the Fourier exponents. Ostrogorsky and Mikic (2008), developed explicit equations for the determination of Fourier exponents with a good precision at Bi<2. Ostrogorsky and Mikic (2009) also determined explicit equations for the Fourier exponents for Bi>2 with a good prediction. Ostrogorsky (2009) presented equations that cover the entire Biot range also with good accuracy.

All the above-mentioned four studies provide non-iterative solutions that could be incorporated into spreadsheets. However the suggested solutions by Ramaswamy et al. (1982) and Lacroix and Castaigne (1987) are rather complex for easy interpretation, hence the application of these studies has not been transferred outside academia or made their presence in textbooks on the subject. The solutions from Ostrogorsky and Mikic are split into two sets of equations one for Bi<2 and another set for Bi>2 which is not favourable. Additionally, Ostrogorsky (2009) published other simple explicit equations for the whole Biot range with a good overall precision. The methodology and robustness of Ostrogorsky (2009) is, however, less transparent. If the work was presented in a single paper the procedure and results might have been easier to interpret and use. All the four mentioned studies are compared and discussed more extensively in chapter 3.

The lag factors needed in the series expansion has been modelled separately to the Fourier exponent (Ramaswamy et al. 1982 and Ostrogorsky 2009), both with good precision. However in a spreadsheet solution it is not necessary to model the lag factors separately as they can be calculated non-iteratively if the Fourier exponent is determined.

New procedures for calculation on thermal response have also been proposed. Cuesta and Lemúa (1995) published a new method based on asymptotic modelling of the heating curves where the entire expansion is essentially known for Bi→0 in form of the lumped capacitance model, and for Bi→infinity where the exponents and lag factors of the expansion is known a priory. Their work is a simplified solution in the sense that the Fourier exponents and lag factors do not need to be determined; their model is validated for elementary and general geometries for Fo=0.5 with prediction errors of up to 8%. In comparison, the use of a 1st term approximation where the lag factors and Fourier exponents are determined based on either Ramaswamy et al. (1982) or Ostrogorsky (2009), inducing errors less than 1% at an even lower Fourier number (0.2).

Low Fourier numbers

It was only possible to track one paper that has been published on a simple analytical solution for heat transfer also including the initial phase (Fo<0.2). Ramaswamy and Shreekanth (1999) presented such a solution where the low Fourier number region could be calculated as well. Their approach was a stepwise regression of the residual between the entire series expansion and the 1st term approximation. The resulting equations from their work are rather precise and could be incorporated into a spreadsheet solution. However the procedure in establishing the equations with a set of 13 new parameters in 3 different equations for each of the 3 elementary geometries is very comprehensive for practical industrial application. This work is discussed more extensively in chapter 4.

Irregular geometries

A numerical solution performed in a suited software package is often the preferred choice for researchers because the solution works for all geometrical shapes. But also analytical solutions for irregular geometries have been presented.

The calculation of irregular geometries with a series expansion solution is challenging because the solution is bound to one of the three coordinate systems (Cartesian, cylindrical or spherical). If a geometry cannot be represented by these coordinate systems or orthogonal cross products of them (elementary geometries cf. chapter 1.2) no root function or calculation of the lag factor exists to describe the product.

For the calculation of irregular geometries with the series expansion Cleland and Earle (1982) published a method of averaging the heat transfer through the concept of EHTD (Equal Heat Transfer Dimensionality). The procedure is quite similar to the use of the Volume to Area ratio as the characteristic dimension but is somewhat more complex to interpret. Their proposed solution is after their own conclusion rather precise with an accuracy of +- 10%. However, it is not their proposed EHTD that has most impact in reducing the uncertainty but the additional inclusion of what they call the lag time, which restricting the dimensionless temperature response (Ω=1 if Ω>1). The EHTD procedure is also used in their pioneer work on freezing prediction (Cleland and Earle 1987). A procedure where the temperature response is corrected in the same manner (Ω=1 if Ω>1) is also proposed by Merts et al. (2007) for irregular geometries.

Uyar and Erdogdu (2012) presented a method where the calculation of sphere-like geometries (pears, apples, potatoes etc.) could be calculated as if they were spherical by using the calculation of a sphere with the same V/A ratio. Their procedure is validated with good accuracy as long as the product has a high sphericity, but for products with low sphericity the procedure is imprecise, according to their own conclusion.

Christensen et.al (2011)[1] investigated the possibility of expressing irregular geometries by their Volume to Area ratio as the characteristic dimension in predictive calculations of cooling processes. The procedure had only a narrow operation window and is thus not widely applicable.

It seems that no simple calculations have been proposed with a large operation window covering irregular geometries of different character with an acceptable accuracy.

2.1.6 Adaptation of the series expansion solution to incorporate other phenomena

In the application of the series expansion solution also other phenomena than heat transfer have been included in the calculations. Cuesta and Lamúa (2009) included the respiration phenomena by a correction of the Fourier exponent and in addition found that a 1st term approximation was converging with the complete solution for Fo>0.2 as for the series expansion solution without internal respiration. The respiration has been included as an empirical parameter based on data from the American Society of Heating, Refrigeration and Air condition Engineers (ASHRAE). Dincer (1993) coupled the respiration to the complete series expansion by incorporating the phenomena of transpiration and respiration in a lumped heat transfer coefficient with good validation when the complete series is solved under the tested conditions.

Lacroix and Castaigne (1987) presented an equation for freezing processes, where the initial cooling phase was calculated through a series expansion. The simplification of the series expansion is in form of the determination of lag factors and Fourier exponents by adapting a logarithmic polynomial (Lacroix and Castaigne; 1987). For the application, the phase change of water is included through Plank´s freezing equation, (Singh and Heldman 2014, p 537).

Van der Sman (2003) presented a shell and core model to calculate cooling times that also involved mass transfer. The approach for his simplification was to incorporate the evaporation into the external resistance to heat transfer in the Biot number. His model is based on the assumption that the mean volume averaged temperature can be presented as a single point throughout the process; this is according to his own figures and results not correct, however, a position that equals the volume average temperature initially will be close to the surface and in the very end close to the centre. Because the study is validated with a small driving temperature difference it is difficult to establish the uncertainties of the model. It would be interesting though to see a full validation of the study in order to investigate the versatility of the work. Though the study is not a direct simplification of the series expansion, his view on how an evaporation phenomena can be included the description of the process through the Biot number is a simple approach for coupled heat and mass transfer worth for further investigation.

The works from Cuesta and Lamúa (2009), Dincer (1993), Lacroix and Castaigne (1987) and van der Sman (2003) imply that the application of the series expansion solution can be adapted for the calculation of other processes than purely heat transfer.

---

[1] The publication is difficult to access, but is attached also as appendix 3

Beside the mentioned studies numerous papers have been published on simplified calculations of other occurring phenomena in food processing. These studies are not included in this review because the heat transfer phenomenon is not the primary driving phenomena in these processes.

Application of analytical solutions to the heat equation and evaluation of thermal response in solids are also a task related to other engineering fields. The challenges of other engineering fields are often of a different character. For example in building construction the Biot numbers associated with the heat transfer processes are often very high due to insulation and in the metallurgy industry the associated Biot numbers are often very low due to the high conductivity of metals. Also the process time in heating and cooling of solid foods differ from other industries where heating/cooling of solids is central; In quenching processes in the metallurgy industry and hardening of rubber in the chemical industry where the thermal response is fast (Baïri and Laraqi 2003), and in geology and building construction the heat transfer rate is very low (Lü et al. 2006). The heating and cooling of solid foods is of a different character as the associated Biot numbers have a wide span from low Biot numbers (Bi<0.5) in chilling of small products to large Biot numbers (Bi>30) in the canning industry. Also the process time differs substantially.

2.1.7 Determination of heat transfer coefficients

Basically two general procedures are used in the determination of a convective heat transfer coefficient h_c to a solid: evaluation of the fluid media or evaluation of a product exposed to the fluid media. In this context the fluid media could be a liquid (food or water) noted as a fluid to particle heat transfer coefficient h_{fp}, and it could be a gas (typically air) where the heat transfer coefficient is in this thesis denoted a convective heat transfer coefficient h_c.

In the investigation on the fluid media Computational Fluid Dynamics (CFD) has been used to determine flow profiles around a solid based on the inlet velocity in the equipment and the geometry of the equipment and the product, (Denys et.al 2003). This procedure is most commonly used by equipment manufacturers in optimizing the design of cooling towers, heat exchangers, spray-dryers etc. For some simple designs also engineering equations in form of Nusselt-relations have been used, most often in closed equipment with a liquid media as the fluid.

The other possibility is to investigate the heat transfer coefficient through measurements on the product by inverse calculation from the temperature response (Zuritz et al. 1990). This can be done by either analytical or numerical methods for the curve fitting.

But also more exotic measurement techniques have been applied in order to determine heat transfer coefficients; The use of time temperature integrators based on microbial inactivation kinetics, (Maesmans et al. 1994 and Weng et al. 1992), Particles with embedded liquid crystals, (Balasubramaniam and Sastry 1995), Magnetic Resonance Imaging (MRI) (Kantt 1998). These methods are not elaborated further.

Investigations through Computational Fluid Dynamics (CFD)
Many studies have used computational fluid dynamics (CFD) to quantify fluid flow and thereby approximate the convective heat transfer coefficient. Two examples are; Verboven et al. (1997) investigated local convective heat transfer coefficients across a rectangular body for sous-vide application, Augusto et al.

(2012) determined convective heat transfer coefficients for heating and cooling of bottles using a CFD approach.

The CFD approach have played an active part in the design and control of process equipment in the food industry and are in these fields widely applied, (Norton and Sun 2006). This has since become even more evident as can also be observed in the candidates sought for by process equipment manufacturers, where CFD skills are highly appreciated. Bhutta et al. (2012) reviewed application of CFD in the design, development and optimization of heat exchangers, concluding that the approach is a cost effective and very efficient method in the equipment manufacturing industry. An advantage of using CFD for the determination is that it is possible to quantify local heat transfer coefficients. In food manufacture however CFD is seldom used outside academic collaboration mainly due to cost.

Heat transfer coefficient determination from fluid to a particle (h_{fp})
An extensive listing of references is out of scope here, as the literature (the majority of references are from the 1980s and 1990s) is well covered by three extensive reviews (Maesmans et al. 1992; Ramaswamy et al. 1997; Barigou et al. 1998). The most common approach is to measure the temperature-time curve inside a real food particle or replicas made either in materials having thermal properties close to those of the food product or made in a highly conductive material, usually aluminium. By fitting the temperature-time curve to a mathematical solution of the Fourier equation for non-stationary convective heat transfer into a body of the relevant geometry, it is possible to estimate h_{fp} (Maesmans et al. 1992 and Barigou et al. 1998). For convective heat transfer coefficients it is important that the geometrical shape of a model product is as close to a real product as possible because the flow pattern around the food item is shape dependent.

The advantage of using model replicas in metal, for which the Biot number is very low (Bi < 0.1), is that the solution to the heat transfer equation is simple and allows a high precision in the determination of heat transfer coefficients (Barigou et al. 1998). Besides, the position of the temperature sensor inside the body is not critical (Ramaswamy et al. 1997). For particles with food-like thermo-physical properties, Bi is higher, which generally results in a less precise determination and the heat transfer equation must be solved by a more complicated series expansion of the Fourier equation (Maesmans et al. 1992 and Barigou et al. 1998). Also the position of the temperature sensor is sensitive in order to achieve precise measurements. A numerical solution matched with several temperature sensors are in case of real food products more reliable.

An advantage of using model particles with food-like thermo-physical properties is that the heat transfer conditions are more realistic than for replicas constructed in metal; this holds in particular in cases were natural convection is a significant mode of heat transfer (Åström & Bark 1994). This will be the case in many vessel cooking processes, as agitation should be gentle to avoid destroying the often fragile particles.

Heat transfer coefficient determination where the fluid is a gas (h_c)
In situations where the fluid is a gas is primarily for this thesis covering cooling operations where products are cooled by circulating air. In heating processes where air is the media (primarily ovens) the determinations are often more difficult to conduct and the process physics more complex, and in relation to the focus of this thesis, oven processes are out of scope (heat transfer is seldom the only governing phenomena as also evaporation and considerable mass transport often occurs). Primarily in research CFD is used for determination of h_c in cooling with circulating air. Because the characteristics of the air flow applied often

induce varying heat transfer coefficients dependent on the relative position of the boundary to the flow direction, a flow quantification that allows for local heat transfer investigation (like CFD) is an advantage.

Since the h_c is both product (geometry) and process (design and setting) dependent it is crucial that they are also determined at the production sites for predictive calculations on the operation of equipment. For these determinations both measurements using model foods made from a high conductive material and real food items are possibilities. The standard procedure is an inverse calculation of the temperature curve (Maesmans et al. 1992). The choice of method however can have very different results. In the extensive review from Maesmans et al. (1992) differences of up to a factor of 3 was observed for measuring using a real food item compared to aluminium, with aluminium showing the highest values. The reason for this is unknown and a thorough investigation into the original data is needed.

2.2 Reflections on the literature review

The academic community has transferred from discovering physical phenomena in the renaissance, describing them in the 18th and 19th century by mathematics, supplying graphical solutions for applications in the early 20th century to conducting advanced mathematical solutions to applied problems in the mid-late 20th century.

The 21st century has transferred the industrial production into the IT age with smart censor technologies, advanced numerical solutions for coupled phenomena and processes, and incorporated smart process control through e.g. genetic algorithms and artificial neural networks.

Based on decades of collaboration with the food industry, in the Food Production Engineering group at the Technical University of Denmark, we are convinced that the history is somewhat different in industrial food manufacture. Even though equipped with modern process equipment with incorporated process control systems and advanced censor technologies belonging to the 21st century, the majority of food manufactures have not included a culture where process calculations are performed as a general activity.

When handling the calculation of thermal processes in food manufacture the food engineer have a choice in preferred solution method. The level of detail needed and the calculation possibilities and availability of suited software of the company often sets boundaries for whether a numerical solution or an analytical solution is the most suited. Independent of the chosen solution method a reasonable heat transfer coefficient must be determined.

In 2013 Saguy et.al published an important paper with viewpoint on the challenges focusing the area of food engineering (Saguy et al. 2013) especially with regards to academic focus and education of the food engineers of the future. They discuss the many advances accomplished in food technology and also supply thorough and thoughtful recommendation for future academic focus and curricula for food technology educations.

What is not discussed as thoroughly is how the advance in food engineering can be applied also into the operational tasks in food manufacture and how food manufactures actively can improve their production by utilizing the knowledge generated from the academic projects, independently whether they have been a part

of the specific project or not. It is this issue that the aim of developing engineering equations for heat transfer is addressing.

2.3 Operationalization of the research question

This section presents an operationalization of the research question presented in the introduction in chapter 1. To answer the research question:

"**Is it possible to deduce and validate new engineering equations in heat transfer for food processing, which are user-friendly and provide adequate precision?**"

This thesis is an analysis of the series expansion to the heat equation. The thesis is formulated around the challenges in the use of the series expansion solution. How the chapters are related to the Fourier series expansion for heat transfer in solids is presented in figure 2.4
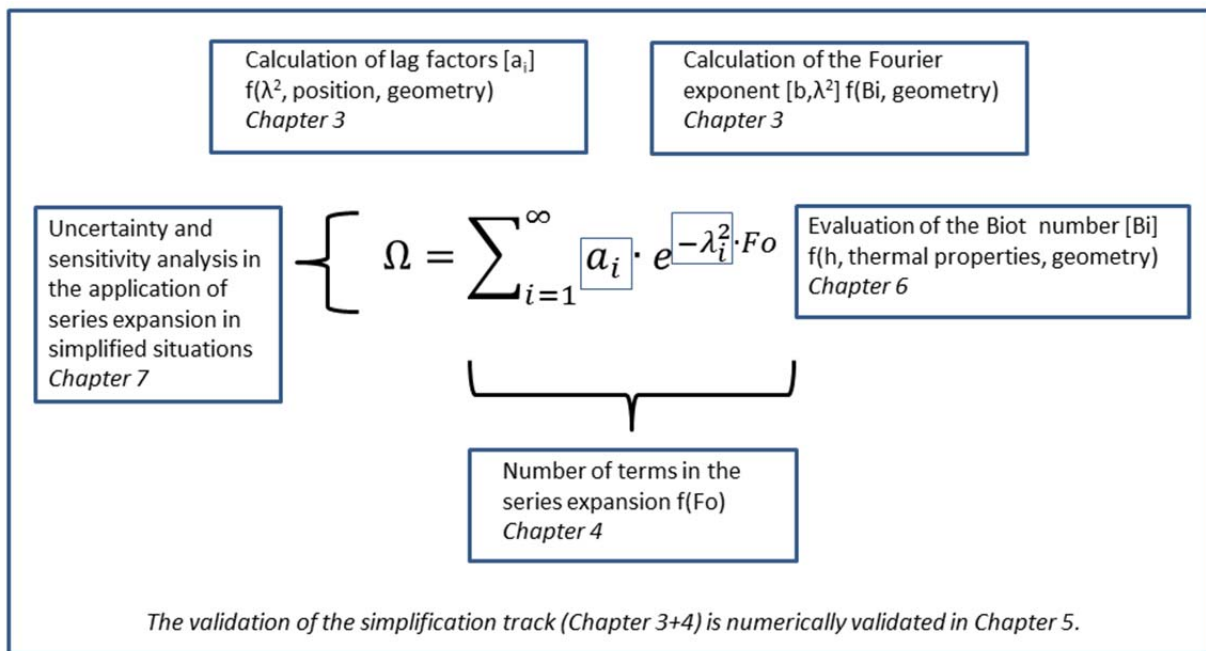
Figure 2.4 Graphical description of the overall theme in this thesis. The figure serves as an overview of how the thesis is connected.

The task is split up into four Objectives.

- Analytic determination of eigenvalues in chapter 3
- Thermal calculations at low Fourier numbers in chapter 4
  - Validation of the developed model (chapter 3 and 4) is presented in chapter 5
- Determination of heat transfer coefficients in chapter 6
- Continuity and sensitivity in the series expansion in chapter 7

The first two objectives are theoretical work on simplification of the analytical solution to the heat equation, the third objective is an experimentally based section on the determination of heat transfer coefficients and part four is a synthesis section. In the fourth objective the uncertainty and sensitivity in the utilization of the series expansion is investigated in order to establish guidelines and frames for the utilization of the series

expansion solution to the Fourier equation. In the end of each description of the four objectives, the corresponding chapter is highlighted in italic bold.

The literature review has pinpointed two challenges in simplification of the series expansion, namely; the determination of lag factors and Fourier exponents, and the calculation of the thermal history at low Fourier numbers.

Objective 1: Analytic determination of eigenvalues to the root functions.

A simple non-iterative solution to determine eigenvalues for the root functions to the general geometries should be established. The solution should dispense with the need for charts or tables for giving input parameter values in the series expansion solutions, and thus promote the application of predictive calculations on thermal processes. ***Chapter 3***

Objective 2: Formulating equations for low Fourier numbers, to evaluate process history also valid in the initial phase (Fo<0.2)

A simplification of the series expansion where the initial heating/cooling period can be evaluated should be deduced and validated, in order to dispense with the use of the graphs or programming. ***Chapter 4***

Validation of the simplified model:

The combined procedure for a simplified series expansion is validated against a numerical solution of two typical commercial products: ***Chapter 5***

- Pre cooling of packaged cream cheese before storage: After processing the cream cheese is pasteurized and packaged at app. 70°C. After packaging the cheeses are cooled in a blast cooler to an average temperature set-point of 30-40°C.
- Three-step processing of hamburgerryg (brined, smoked and salted saddle of pork): In the processing of hamburgerryg, it is initially smoked before the heat treatment process, followed by a cooling step.

In all solution methods for thermal calculation it is essential to determine the heat transfer coefficients driving the thermal process. Sub-task 3 is presenting methods for the determination of convective heat transfer coefficients that can be measured on site at food manufacturers.

Objective 3: Determination of heat transfer coefficients and handling of complex heat transfer situations.

Determination methods for heat transfer coefficients are investigated and discussed based on a review of procedures. Specific measurement methods and results are also supplied: Determination of fluid to particle heat transfer coefficients, heat transfer to particles during boiling and the variation in heat transfer coefficients depending on position relative to the flow of the media and presence of a headspace in packaged foods. ***Chapter 6***

The last part of the thesis is a characterization of the Fourier-Biot workspace for the Fourier equation based on an analysis of the uncertainties and sensitivities in the use of the series expansion solution.

Objective 4: Continuity and sensitivity of different simplified solutions to transient heat transfer is investigated.

It has been experienced that there is a discontinuity between the different heat transfer equations for transient heat conduction. The possibility of creating continuity between the equations is discussed for 3 different aspects *Chapter 7*

- The challenge deciding the number of terms needed in the series expansion should be investigated in terms of setting proper limits for the utilization of the 1 term approximation
- The continuity between low Biot numbers in the heating of solid foods, and the lumped capacitance analysis ($0<Bi<0.1$) should be investigated and reported.
- To assess the uncertainty in the calculation of heating and cooling of solids it is needed to establish a conceptual understanding of the sensitivity of the parameters used in the calculation. This is also expounded in objective 4.

As a result from the investigation in chapter a work frame with proper guidelines is presented for the use of simplified approximations to the series expansion.

2.4 Calculation programs

The general methodology of this thesis is primarily a theoretical study where different solution forms to the Fourier heat equation is solved and compared. These solutions are conducted in specific programs. A brief introduction to the used calculation programs is described in this section.

The theoretical calculations have been conducted in Microsoft Excel 2010, the freeware program "R - HEATMAN" and the commercial software COMSOL Multiphysics. Where the specific methodology for the excel procedure is described in the belonging chapters chapter 3, 4 and 5. The essential procedure for the use of HEATMAN and COMSOL Multiphysics are described in the following two sections.

Solving the series expansion in "R"

Civil engineer Peter Reimer Stubbe[2] has coded a solution method to the series expansion in an R (R 2008) platform in a library under the name HEATMAN (the description of the program and manual for usage is attached in appendix 7). The function of the program is as follows:

Initiating the program, the number of terms needed in the calculation is typed (100 is the standard). After applying the wanted number of roots, each of the roots is solved by iteration by applying the Biot number for the investigated geometry. The series expansion is solved directly from the roots for the centre temperature, positions in the body or volume average temperature, either by point investigation (input of a process time in form of a scalar) or curve (input of several process times in form of a vector).

Modelling of heat transfer in COMSOL Multiphysics

In the heat transfer module in COSMOL Multiphysics the wanted geometry is constructed and divided into small elements by meshing. The specific partial differential equation governing the phenomena for heat transfer is approximated by a finite element method (FEM). In FEM the investigated domain is divided into a finite number of defined elements which are connected through node points. The governing equation is

---

[2] Food production Engineering Group, National Food Institute, Technical University of Denmark

solved individually for each element and the unique solution in each element is combined by iteration of the input and output temperature of each node, until all points converge and a continuous solution is obtained (Tijskens et al. 2001).

The needed input in the program is the initial conditions (temperature, thermo-physical properties), the boundary conditions (temperature and heat transfer coefficients) applying the investigated physical phenomena (transient heat conduction).

3 Fourier exponents

This chapter is the foundation for the submitted paper "Proposing a normalized Biot number: for simpler determination of Fourier exponents and for sensitivity analysis of heating and cooling of solids" attached in appendix 1.

In this chapter the series expansion solution to the heat equation is investigated and a simplified solution to the two important variables is presented, namely the first Fourier exponent (b_1, λ_1^2) and the lag factor a_1. The series expansion is recalled from the theory section in chapter 1:

$$\Omega = \left(\frac{T_s - T}{T_s - T_0}\right) = \sum_i^\infty a_i e^{-b_i \cdot Fo} \qquad\qquad b_i = \lambda_i^2$$

For each term applied in the series expansion the corresponding Fourier exponent needs to be calculated by solving the given root functions to obtain the eigenvalues of the functions, which are λ_i for i=1 to i (table 3.1). The Fourier exponents are λ_i^2, cf. chapter 1. The lag factor needed in the series expansion solution can be directly calculated from the λ_i –values, as shown in table 3.1.

Table 3.1 Mathematical presentation of the respective root function for the ideal geometries, lag factors for centre temperatures (a_c), the positional lag factors ($a_{x/R}$) and the lag factors for the volume average temperatures (a_m),

Geometry	Root function λ_i	a_c	$a_{x/R}$	a_m
Inf. Plate	$Bi = \lambda_i \tan\lambda_i$	$\dfrac{2\sin\lambda_i}{\lambda_i + \sin\lambda_i \cos\lambda_i}$	$a_c \cdot \cos\left(\lambda_i \dfrac{x}{L}\right)$	$a_c \cdot \dfrac{\sin(\lambda_i)}{\lambda_i}$
Inf. cylinder	$Bi = \dfrac{\lambda_i J_1(\lambda_i)}{J_0(\lambda_i)}$	$\dfrac{2J_1(\lambda_1)}{\lambda_i(J_0^2(\lambda_i) + J_1^2(\lambda_i))}$	$a_c \cdot J_0\left(\lambda_i \dfrac{r}{R}\right)$	$a_c \cdot 2\dfrac{J_1\lambda_i}{\lambda_i}$
Sphere	$Bi = 1 - \lambda_i \cot\lambda_i$	$\dfrac{2(\sin\lambda_i - \lambda_i \cos\lambda_i)}{\lambda_i - \sin\lambda_i \cos\lambda_i}$	$a_c \cdot \dfrac{\sin\left[\lambda_i\left(\frac{r}{R}\right)\right]}{\lambda_i\left(\frac{r}{R}\right)}$	$a_{c.} \cdot 3\dfrac{\sin(\lambda_i) - \lambda_i \cos(\lambda_i)}{\lambda_i^3}$

J_0 and J_1 is the Bessel function of the 1st kind with 0th and 1st order respectively.

In chapter 4, a solution for the series expansion where the 1st Fourier exponent is central in order to predict thermal response also valid at Fo<0.2 is presented. Thus, the development of a non-iterative solution to the root functions is central.

The Fourier exponents may be calculated by iterations of the root functions for any given Bi number. However, the iterative character of the root functions results in cumbersome calculations. In general, the values of the 1-term Fourier exponents and the associated lag factors are found in charts or tables in textbooks on the subject, while values of the higher order terms are rarely available as tables or graphs. Solutions which require more terms, that is when Fo<0.2, are based on graphs of Ω as a function of Fo, as explained in chapter 1. This situation is dealt with further in chapter 4.

For solutions based on the 1st term (Fo>0.2) it is beneficial to determine the Fourier exponents from a non-iterative analytical solution. This is a classical challenge and for the 1st Fourier exponent used in the 1st term approximation of the series expansion several studies have suggested good solutions cf. chapter 2.

(Ramaswamy et al. (1982), Ostrogorsky (2009) and Lacroix and Castaigne (1987)) are good examples serving adequate precision. This study proposes a new way of calculating the first Fourier exponent ($b_1=\lambda_1^2$) which is more transparent and intuitive which will be shown later. The studies are presented, compared and discussed in section 3.2 in this chapter.

The Fourier exponents is in this study determined through a normalisation of the Biot number, which enables a more simple and intuitive procedure. The normalisation and the resulting determined Fourier exponents are presented in the next section.

3.1 Normalisation of the Biot number and determination of Fourier exponents

The Biot number (Bi), describing the ratio between the internal and external resistance to heat transfer, is recapitulated below for better interpretation of the procedure in formulating a normalized Biot number:

$$Bi = \frac{h}{k} \cdot R$$

For easier calculation of the Fourier exponents, this study proposes a normalisation of the Biot number (Bi_{norm}) in equation 3.1. Where (Bi) is the fraction of internal resistance to external resistance to heat transfer, (Bi_{norm}) is the fraction of internal resistance to overall resistance of heat transfer. The internal resistance to heat transfer, *R/k,* is described as the characteristic dimension (R), divided by the thermal conductivity (k). The external resistance to heat transfer is the reciprocal heat transfer coefficient (1/h). The total resistance to heat transfer can be defined as:

$$total\ resistance = \frac{1}{h} + \frac{R}{k}$$

And the ratio of the internal resistance to the total resistance will be defined as:

$$ratio\ of\ internal\ resistance = \frac{\frac{R}{k}}{\frac{1}{h} + \frac{R}{k}}$$

Multiplying with the heat transfer coefficient (h), gives a rational description of Bi_{norm}:

$$Bi_{norm} = \frac{\frac{h}{k} \cdot R}{\frac{h}{h} + \frac{h}{k} \cdot R} = \frac{Bi}{Bi+1} \tag{3.1}$$

The constructed normalized Biot number has some advantages: it has an s-shaped curvature as a function of Bi enabling a more simple expression to determine Fourier exponents without iteration. It enables a presentation of the Fourier exponent in a linear scale in graphical presentation instead of a logarithmic scale for Bi, which notoriously has been a road to misreads. The relation between Bi_{norm}, Bi and the Fourier exponents is presented graphically in figure 3.1.
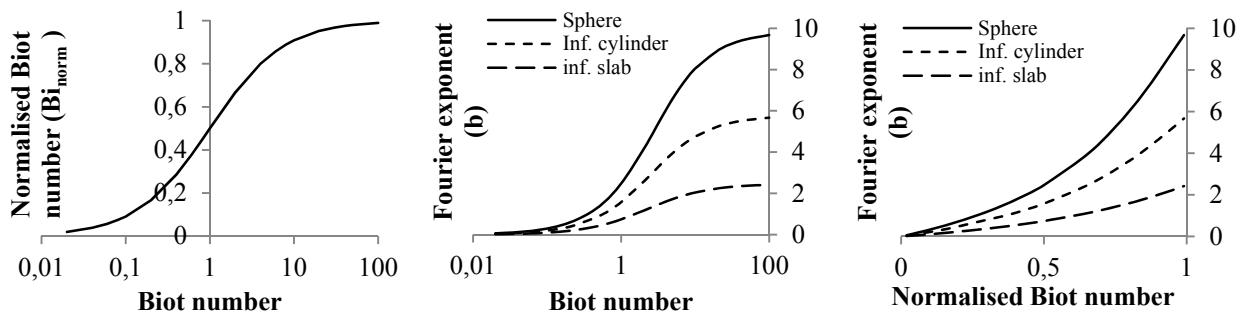
Figure 3.1 Normalisation of the Biot number (left), Fourier exponents as a function of the Biot number (middle) and the Fourier exponents as a function of the normalised Biot number (right). Fourier exponents are from Mills (1995) p. 173.

The normalized presentation (Bi_{norm}) of (Bi) has the advantage of having the same s-shaped curvature as the Fourier exponents, making (Bi_{norm}) easier to utilize as a base for regression determination of Fourier exponents (b, λ^2), (figure 3.1). The behaviour of the Fourier exponent is monotonically increasing as a function of (Bi_{norm}), where both the 1st and the 2nd derivative are positive, making polynomial fitting suitable with very small residuals (figure 3.2, 3.3 and 3.4). This enables a simple procedure where engineers can construct a spreadsheet themselves, from which the Fourier exponents can be determined.

In this study twenty one Biot numbers have been chosen to illustrate the procedure (0.02; 0.04; 0.06; 0.08; 0.1; 0.2; 0.4; 0.6; 0.8; 1; 2; 4; 6; 8; 10; 20; 30; 40; 50; 100; ∞) (all available data from Mills 1995 p. 173). The twenty one Fourier exponents from Mills (1995) are plotted as a function of Bi_{norm}. A polynomial regression of the third order gave a reasonable fit (figure 3.2-3.4); higher order polynomials have also been tried without improving the fit substantially and a lower order polynomial gave a less precise fit over the whole range.
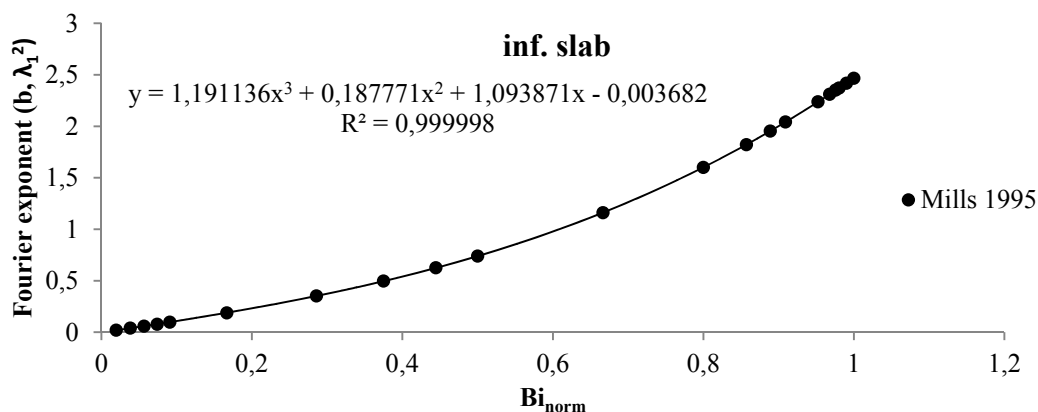

Figure 3.2 The b values (λ_1^2) as a function of the normalised Biot number, The dots represents b-values from Mills (1995), the line represents the polynomial fit.

Figure 3.3 The b values (λ_1^2) as a function of the normalised Biot number, The dots represents b-values from Mills (1995), the line represents the polynomial fit.
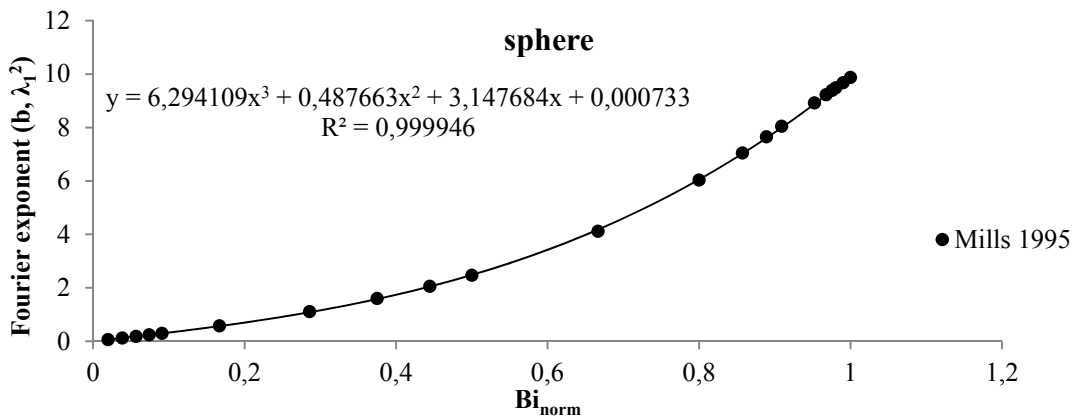
Figure 3.4 The b values (λ_1^2) as a function of the normalised Biot number, The dots represents b-values from Mills (1995), the line represents the polynomial fit.
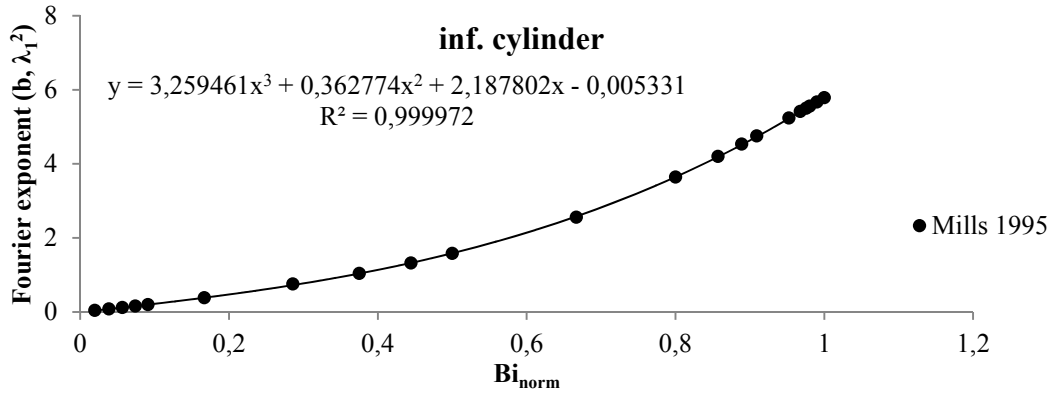
From visual inspection of the plots, and by means of the regression coefficients, the Fourier exponents can be predicted fairly precise by these 3rd order polynomial regressions (R^2>0.9999). By this procedure the calculation of the Fourier exponents, eigenvalues and lag factors associated with the series expansion can be determined without iterations. The regression equations are summarized in table 3.2.

Table 3.2 Summation of the regression polynomials to determine the Fourier exponents for the series expansion

Geometry	Regression polynomials
Inf. slab	$b = \lambda_1^2 = 1.1911 \cdot (Bi_{norm})^3 + 0.1878 \cdot (Bi_{norm})^2 + 1.0939 \cdot (Bi_{norm}) - 0.0037$
Inf. cylinder	$b = \lambda_1^2 = 3.2595 \cdot (Bi_{norm})^3 + 0.3628 \cdot (Bi_{norm})^2 + 2.1878 \cdot (Bi_{norm}) - 0.0053$
Sphere	$b = \lambda_1^2 = 6.2941 \cdot (Bi_{norm})^3 + 0.4877 \cdot (Bi_{norm})^2 + 3.1477 \cdot (Bi_{norm}) + 0.00073$

All the polynomial regressions have positive coefficients and they are monotonically increasing (table 3.2). The residual in the regressions should optimally be 0 for Bi→0. However when Bi→0, then the Fo→ infinity for all t > 0; thus the series expansion is less suited for Bi → 0. Instead, the lumped capacitance model

(equation 1.1) should be used, cf. chapter 1, when Bi<0.1 (Mills 1995 p. 30 and Singh and Heldman 2013 p. 359). This assumption is discussed further in chapter 7 where the uncertainty in this assumption is evaluated.

3.2 Validation

The polynomial regression fit is used to determine Fourier exponents and the eigenvalues for the series expansion based on the equations from table 3.1. The results are validated by comparison with tabulated values from Mills (1995) p.173. The results are presented in figure 3.5 for the Fourier exponent (b_1).
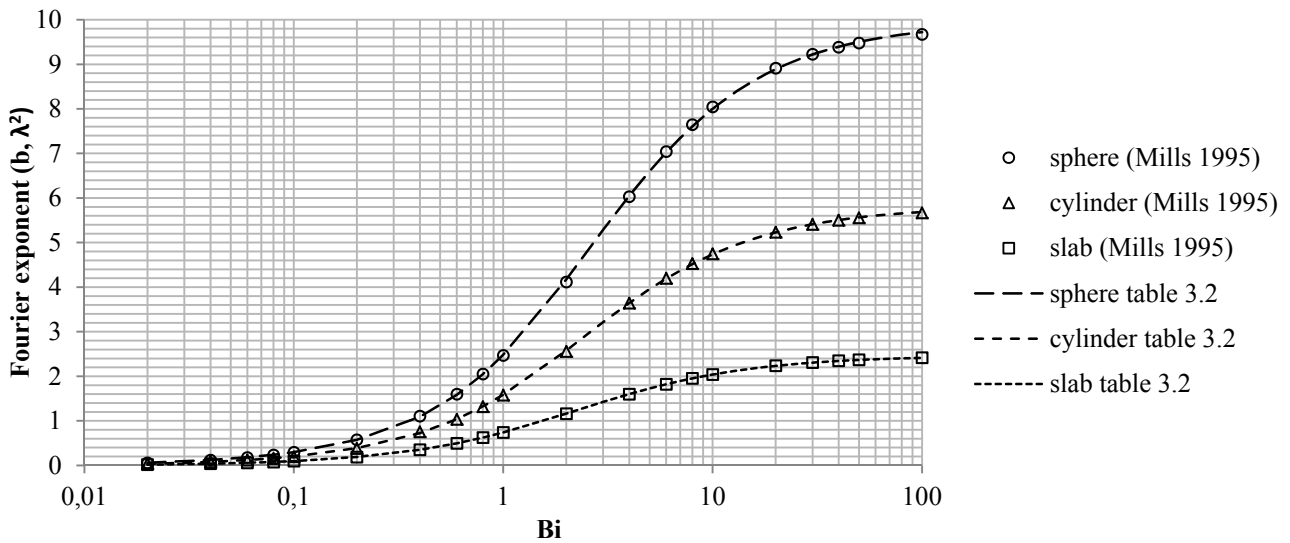
Figure 3.5 Validation of the calculated Fourier exponents (b_1 , λ_1^2) on the polynomial fits. The dashed lines are calculated values, the open dots represents data from Mills (1995).

It is clear that the calculated Fourier exponents match the actual values (figure 3.5). It is thus reasonable to believe that the regressions also predict the exponents in between the tabulated values and hence interpolation is not necessary using this new approach.

To validate that the approach could also be used for calculating the lag factors used in the series expansion, the eigenvalues λ, derived from the Fourier exponents ($\lambda^2=b$ from table 3.2) are used to calculate the lag factors (table 3.1). These are presented in figure 3.6 for the lag factor used when considering centre temperatures, (a_c) and figure 3.7 for lag factors considering the volume averaged temperatures (a_m). The calculated values are compared with tabulated values from Mills (1995) p. 173.
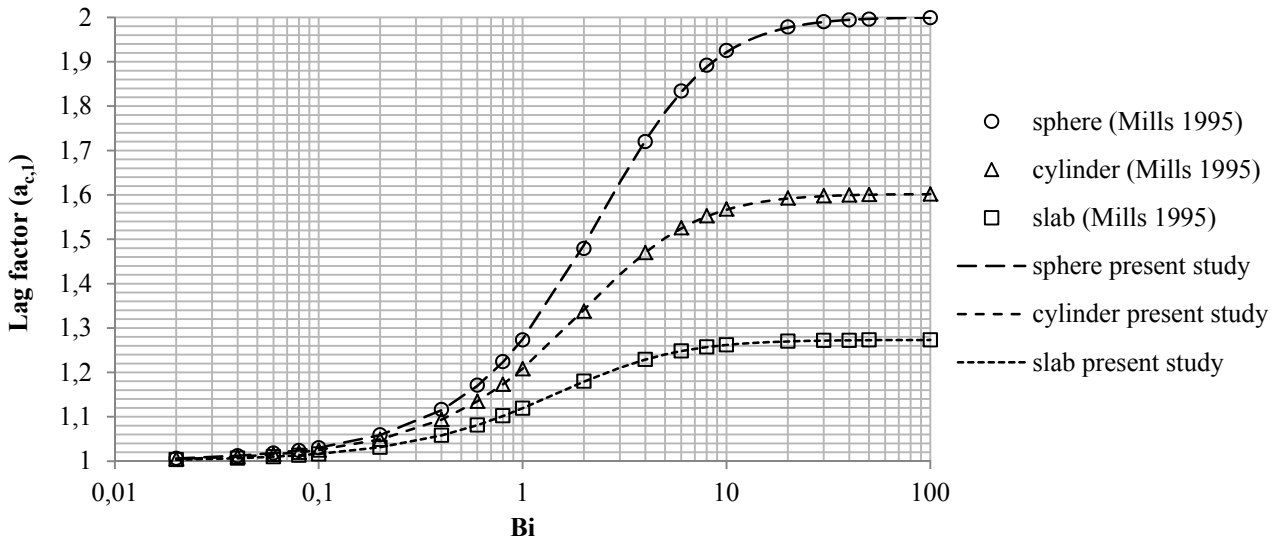
Figure 3.6 Validation of the calculated lag factors for centre temperatures (a_c) in the Fourier expansion compared to tabulated values from Mills (1995).
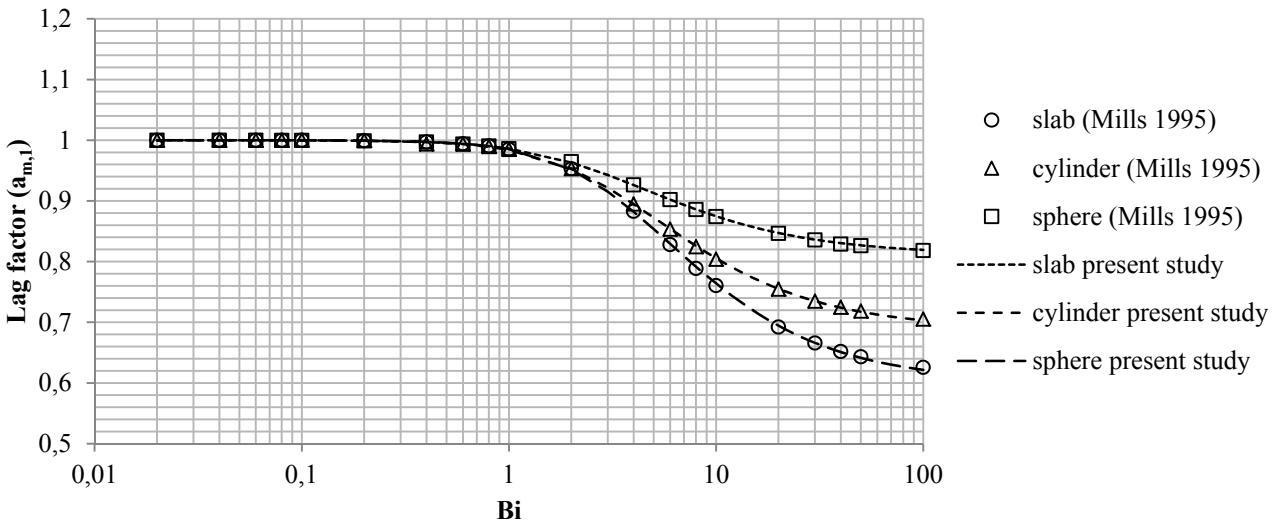
Figure 3.7 Validation of the calculated lag factors for volume averaged temperatures (a_m) in the Fourier expansion compared to tabulated values from Mills (1995).

From the validation of the lag factors (figure 3.6 and figure 3.7) it is seen that the derived lag factors based on the predicted lag factors have a good fit with the actual lag factors as presented in Mills (1995). The average variation coefficients, CVRMSD (Coefficient of Variation of the Root Mean Squared Deviance) (equation. 3.2) for the three fits in figure 3.5, 3.6 and 3.7 are presented in table 3.3.

$$CVRMSD = \frac{1}{\bar{x}_2} \sqrt{\sum_{t=1}^{n} \left(\frac{(x_{1,t} - x_{2,t})^2}{n} \right)}$$ [3.2]

Table 3.3 CVRMSD values for the fit of the Fourier exponents and the lag factors needed in the series expansion calculation for non-stationary heat transfer for centre and volume average temperatures

	Fourier exponent (b, λ_1^2)	Lag factor centre (a_c)	Lag factor mean (a_m)
Inf. Slab	*0.0011*	*0.00033*	*0.00034*
Inf. Cylinder	*0.0043*	*0.00076*	*0.00082*
Sphere	*0.0059*	*0.0018*	*0.0017*

The CVRMSD values from table 3.3 shows that the Fourier exponents and the derived lag-factors can be determined with high accuracy. Because the positional lag factors $(a_{x/R})$ are also derived from the same eigenvalues as the centre lag factor (a_c) they can also be precisely calculated from this approach.

3.3 Comparison with related studies

The presented approach is compared to existing studies (Ramaswamy et al, 1982; Lacroix and Castaigne 1987, and Ostrogorsky, 2009) that provide a good precision. These studies are described in the literature review (cf. 2.1.5) and introduced in the beginning of this chapter. The proposed equations are presented in table 3.4.

Table 3.4 Proposed equations for determining Fourier exponents for the series expansion

	Proposed equations
Ramaswamy et al. (1982)	

Infinite slab

$$\lambda_1^2 = \frac{2.0738Bi}{(Bi+2)} + 0.2795\ arctan\left(\frac{Bi}{3}\right) - 0.02915\ arctan(5Bi) + 0.001171$$

Infinite cylinder

$$\lambda_1^2 = \frac{4.1093Bi}{Bi+2} + 1.2365\ arctan\left(\frac{Bi}{3}\right) - 0.1641\ arctan(2Bi) - 0.007762$$

Sphere

$$\lambda_1^2 = \frac{4.0704Bi}{Bi+2} + 3.5560\ arctan\left(\frac{Bi}{3}\right) + 0.1781\ arctan\left(\frac{Bi}{8}\right) - 0.04036arctan(7Bi) + 0.002262$$

Lacroix and Castaigne (1987)

Infinite slab

$$\lambda_1 = 0.860972 + 0.312133(\ln(Bi)) + 0.007986(\ln(Bi))^2 - 0.016192(ln(Bi))^3 - 0.001190(\ln(Bi))^4 + 0.000581(\ln(Bi))^5$$

Infinite cylinder

$$\lambda_1 = 1.257493 + 0.487941(\ln(Bi)) + 0.025322(\ln(Bi))^2 - 0.026568(\ln(Bi))^3 - 0.002888(\ln(Bi))^4 + 0.001078(\ln(Bi))^5$$

Sphere

$$\lambda_1 = 1.573729 + 0.642906(\ln(Bi)) + 0.047859(\ln(Bi))^2 - 0.03553(\ln(Bi))^3 - 0.004907(\ln(Bi))^4 + 0.001563(\ln(Bi))^5$$

Ostrogorsky (2009)

Infinite slab

$$\lambda_1 = \frac{\pi/2}{(1 + 2.62/Bi^{1.07})^{0.468}}$$

Infinite cylinder

$$\lambda_1 = \frac{2.4048}{(1 + 3.28/Bi^{1.125})^{0.446}}$$

Sphere

$$\lambda_1 = \frac{\pi}{(1 + 4.1/Bi^{1.18})^{0.4238}}$$

When evaluating the equations from the three studies and the present work it is important also to establish the users of such equations. In academia the calculation using a 1st term approximation to Fourier's heat equation is no big challenge and academic research is certainly not the focus group. The proposed solutions have their real value in the teaching of students lacking full engineering training and employees in food manufacture (food process engineers) who needs crude calculations in their daily process operations.

The proposed equations from Ramaswamy et al. (1982) and Lacroix and Castaigne (1987) comprise of several new parameters/constants and neither of the equations is monotonically increasing. This could lead to wrong calculations. From experience in teaching food technology at universities and collaborating with food manufacturing industries this issue is important. The equations proposed by Ostrogorsky (2009) are simple in their expression; however the methodology in the construction of these equations is not explained. Thus it is difficult to assess the variability in the presented parameters. The visibility of the procedure in the present study through the formulated normalised Biot number makes the study more transparent and the parameter sensitivity easier to assess.

The error of prediction (equation 3.3) of the solutions from the three studies is compared to the present study (in figure 3.8, 3.9 and 3.10).

$$error = \frac{\lambda_{1,calculated}^2 - \lambda_{1,actual}^2}{\lambda_{1,actual}^2}$$ [3.3]
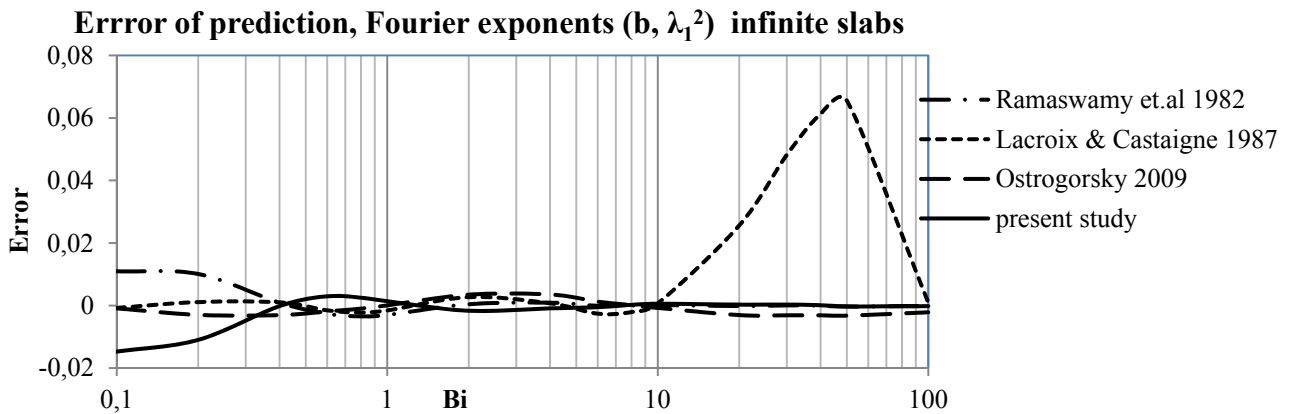

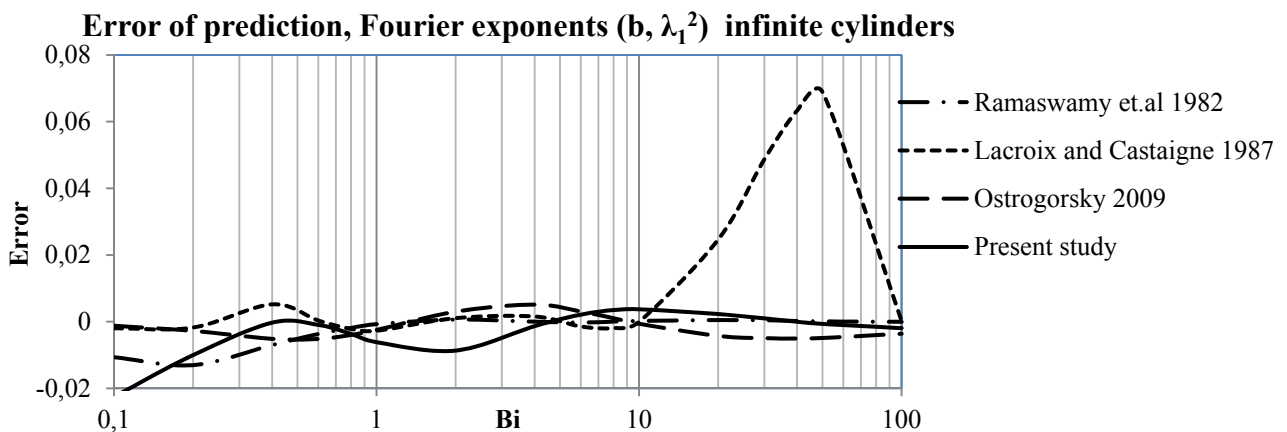Figure 3.8 Comparison of prediction errors for related studies for infinite slabs

Figure 3.9 Comparison of prediction errors for related studies for infinite cylinders

46

Error of Fourier exponents (b, λ_1^2) prediction spheres
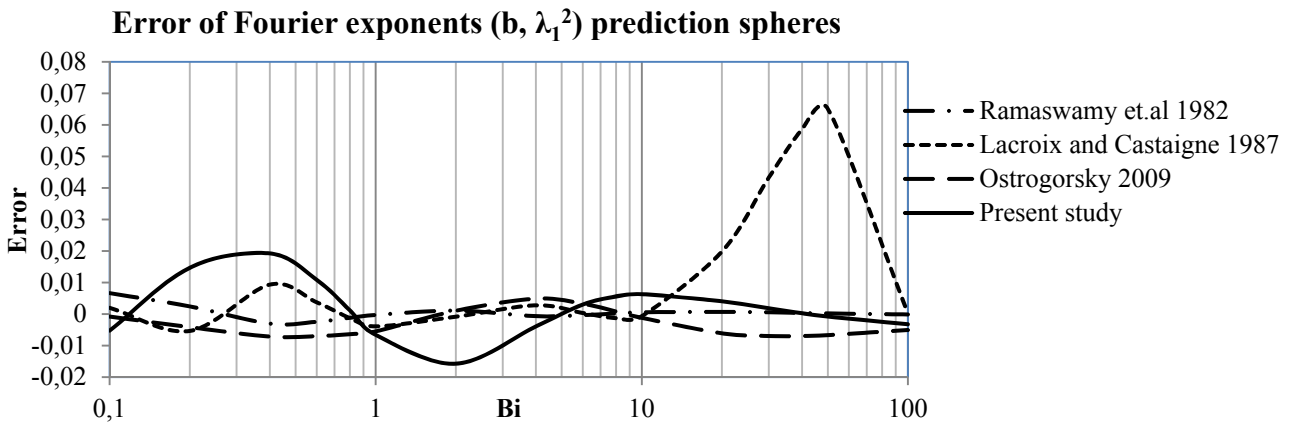
Figure 3.10 Comparison of prediction errors for related studies for spheres

From the comparison between the related studies it can be extracted that all the studies are promoting a good fit for Bi<10 with an overall prediction error <0.02 for all the studies (figure 3.8, 3.9 and 3.10). The study by Lacroix and Castaigne (1987) is less suited for high Biot numbers (10-100). The best overall fit is performed by Ramaswamy et al. (1982) with an overall maximum error<0.01 (which was also the set point in their multiple regression). The present study has the same overall maximum error of 0.01 for the slab at all Biot numbers and for the cylinder at all Bi > 0.2. The prediction error in the elementary geometries of an infinite plate and an infinite cylinder is more sensitive because they are used to generate cross product geometries such as cans and boxes. In all cases for all elementary geometries the maximum prediction error is less than 0.02 for the present study.

The propagation of the prediction error of the Fourier exponents from the present study is evaluated in the worst case scenarios for the three elementary dimensions at Biot 2 and 10. The propagation is presented as the residual Ω_{actual}-$\Omega_{predicted}$ in figure 3.11.
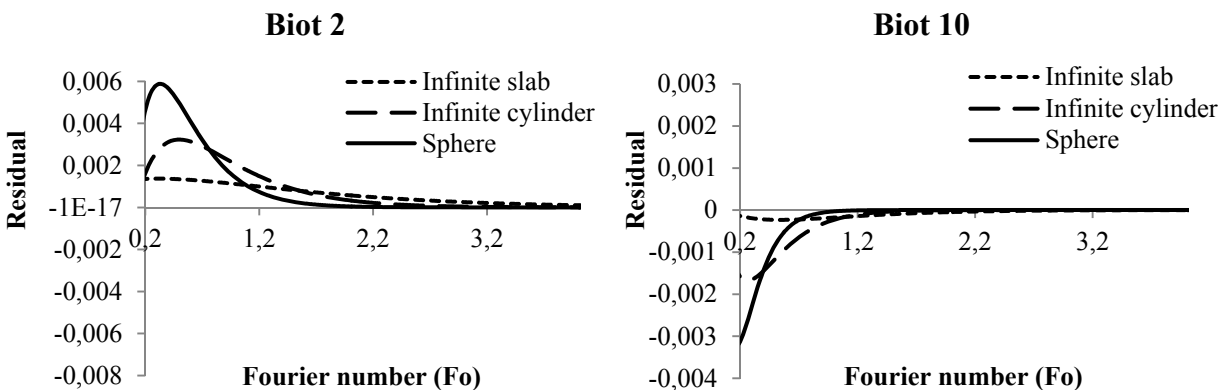
Figure 3.11 Residual logarithmic temperature difference ($\Delta\Omega$) for the worst case predictions of the centre temperatures of infinite slabs, infinite cylinders and spheres for Fo>0.2

The residual can be extracted to a maximum of $\Delta\Omega$=0.006 for spheres at Bi=2. In food processing the driving temperature difference is seldom above 100°C in situations where mass transfer and phase changes can be neglected (figure 3.11). Thus the maximum residual will induce an error in the predicted temperature of maximum 0.6°C for spheres. For the infinite slabs and infinite cylinders the residuals are considerably lower (<0.3°C); therefore the construction of finite bodies by cross products of these does not induce any appreciable error.

47

3.4 Discussion

The determination of the eigenvalues (λ) and hence Fourier exponents (b) to the series expansion without the need for iterations and interpolation, is a clear advantage in the construction of simple programs for evaluating thermal history. The solution provided supports the study in modelling the low Fourier region presented in chapter 4, where the 1st eigenvalue is used in the modelling.

In addition Bi_{norm} is a more direct description of the influence of internal and external resistance to heat transfer. This is valuable in assessing the sensibility in heat transfer calculations, especially the determination of heat transfer coefficients and thermal conductivity. For example if Bi is calculated to be 10 based on an average heat transfer coefficient of 100 +/-20 [W/m^{2}K] the implications can be seen directly. By means of the resulting Bi (8, 10 and 12) the sensibility in the estimation of h is difficult to assess. By using Bi_{norm}, the internal fraction of the resistance is calculated in the three possible situations to be: 0.89, 0.91 and 0.923.

The presentation of the sensibility in terms of internal resistance is more direct because the Fourier equation is a calculation of internal conduction, based on an external impact. Because [Bi_{norm}] has a more direct relation to the Fourier exponent compared to [Bi] the resulting calculation uncertainty is easier to assess, cf. figure 3.1. Because the thermal calculations are primarily dominated by the internal resistance in this example a variation of 20% in the heat transfer coefficient determination is less sensitive in the determination of the internal resistance.

In cases where the Biot number is high it is thus more important to determine the conductivity with small uncertainties. The opposite will be the case for low Biot numbers (Bi<1). In general the determination of the thermal conductivity (k) is prone to less uncertainty than the determination of the heat transfer coefficients (h).

4. Solutions for low Fourier numbers

This chapter is the foundation for the submitted paper "Simplified equations for transient heat transfer problems at low Fourier numbers" attached in appendix 2.

The following section presents a solution to heat transfer problems at low Fourier numbers (Fo<0.2). The main focus is to approach the challenge described in the introduction; the lack of precision in the low Fourier region (Fo<0.2). The solution and validation is also presented for the calculation of centre temperatures and volume average temperatures. The implementation and versatility in industrial applications is discussed.

The challenge of heat transfer calculations for low Fourier numbers is traditionally solved by the use of charts such as Heissler (1947) (figure 2.2), by using the complete series expansion (equation 1.3) or by a numerical solution. As described in the introduction, food manufacturers are often limited to a 1st term approximation (equation 1.5) and applying chart based solutions for the initial phase (Fo<0.2). This procedure is still central in textbooks on food engineering (Singh and Heldman, 2013).

The aim of this task is to derive more simple equations which are valid for all Fourier numbers, also for Fo<0.2 and to avoid the use of graphs normally required for the standard procedures (1st term approximation).

Studies directed towards more simple engineering equations to handle low Fourier numbers are scarce. Ramaswamy and Shreekanth (1999) used a stepwise multiple regression approach to approximate the summarized series solution at Fo<0.2 for infinite geometries. Their general idea was to model the residual between the summarized series and the 1 term approximation, as is also done in the present study. Their solution included 13 new parameters for each of the three infinite geometries in a set of three equations. This chapter is presenting a solution only including one new empirically determined constant.

4.1 General approach

The theory for the series expansion solution to the heat equation is introduced in section 1.2. The solution to the series expansion (equation 1.3) is obtained using the freeware program R (R Development Core Team 2008) see HEATMAN manual in the appendix 7. 100 terms is used to represent the virtually exact solution to the complete expansion.

The difference between the 100 term solution and the 1 term solution (residual) is then evaluated for 16 Biot numbers (0.1; 0.2; 0.4; 0.6; 0.8; 1; 2; 4; 6; 8; 10; 20; 30; 40; 50; 100) for the three elementary geometries (infinite slab, infinite cylinder and sphere). Because the residual between the 1 term solution and the 100 term solution to the thermal history is only of practical significance at Fo<0.2 the analysis of the residual is conducted for the range 0<Fo<0.2.

Following the procedure from Ramaswamy and Shreekanth (1999), an approximate solution to the series expansion is achieved by splitting the expansion into the 1st term minus a residual, where the residual is be the difference between the complete series and its 1st term (equation 4.1) covering the full range of Fourier numbers (Fo>0):

$$\Omega = a_1 \cdot e^{-\lambda_1^2 \cdot Fo} - \epsilon \qquad\qquad [4.1]$$

where:

$$\epsilon = \Delta\Omega = \left(a_1 \cdot e^{-\lambda_1^2 \cdot Fo} - \sum_{i=1}^{\infty} a_i \cdot e^{-\lambda_i^2 \cdot Fo}\right) \qquad\qquad [4.2]$$

In the procedure of constructing a simplified expression covering the low Fourier numbers it is an advantage only to model the residual from equation 4.2 and subtract it from the 1st term approximation. Because the series expansion truncates at its first term at Fo>0.2 the remaining series in the series expansion can be lumped in the residual for a finite timescale. In the formulation of the residual it is important that the residual also truncates rapidly at Fo>0.2.

The method represented by eq. 4.1 is illustrated in figure 4.1, where Ω for a sphere of Bi=4 is plotted against the Fourier number [0:0.2] for the 1st term solution, the 100 term solution and the residual (equation 4.2).
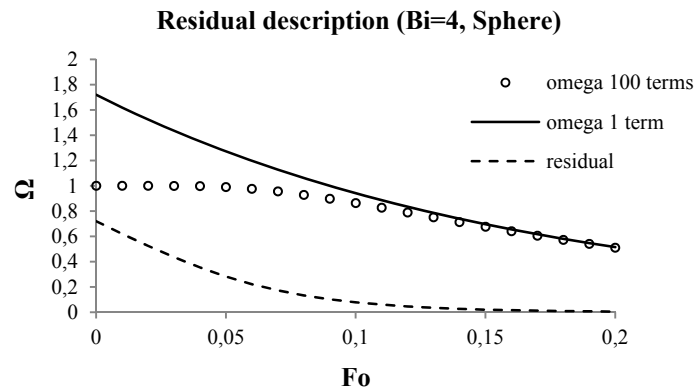
Figure 4.1 Graphical method description of equation 4.2

4.2 Centre temperatures – derivation of equations

The procedure for the formulation of an expanded 1st term approximation is identical for the centre temperature and the volume average temperature. The procedure is presented in detail for the centre temperature.

The natural logarithm to the residual ($\epsilon = \Omega_{1\ term} - \Omega_{100\ terms}$) calculated from equation 4.2, is investigated as a function of the Fourier number [0; 0.2; 0.02]. This is chosen in order to express the residual in the same format as the series expansion solution. In figure 4.2 it is exemplified for a sphere with a Biot number of 4.

The initial residual is known a priory through the lag-factor. The intercept in the regression is thus forced at $\ln(a_{c,1}-1)$. This is convenient because the lag factor is the intercept of the 1st term approximation and (a_c-1) is the initial residual. The determination of $a_{c,1}$ is calculated from the 1st eigenvalue through the equations presented in table 1.1. In chapter 3 a solution is proposed for an accurate and easy calculation of the Fourier exponent λ_1^2 and hence also the eigenvalue λ_1 needed in this calculation (see table 3.2).
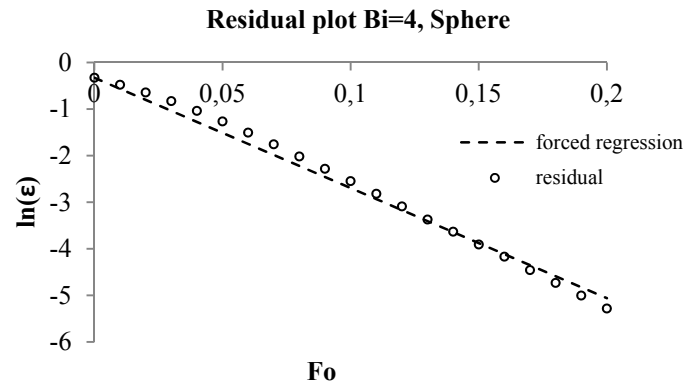
Figure 4.2. Regression plot of the residual (eq. 4.2) as a function of the Fourier number, for a sphere with a Biot number of 4, fitted by a minimal squared error regression with a forced intercept

The regression equation 4.3 crudely represents the development in the residual over process time (Fo):

$$\ln \epsilon = \alpha_{slope} \cdot Fo + \ln(a_{c,1} - 1) \qquad [4.3]$$

All the regressions are presented in appendix 5. The regression slopes (appendix 5) for the 16 tested Biot numbers are plotted against ln[Bi] for infinite slabs (figure 4.3), for infinite cylinders (figure 4.4) and for spheres (figure 4.5).

Because it is desirable to introduce as few new variables as possible in the calculation of the residual it is chosen to express the regression slope as a function of the Biot number and the first eigenvalue λ_1 to the respective root function. The choice of representing the slope as a function of the Biot number also enables a single regression equation to fit for all Biot numbers.

Testing a number of simple combinations it is found that the regression slope α, follow rather closely equation 4.4: This expression is also convenient because the introduced parameter in the slope λ_1 is already known from the 1st term approximation. Thus only the constant C is not already known from the 1st term approximation.

$$\alpha_{slope} = -(\lambda_1 \cdot \ln(Bi) + C) \qquad [4.4]$$

Where *C* is a constant which depends on the geometry and is close to the regression slope at Bi=1, the value of C represents the best global fit of the forced regressions. The predicted regression slopes from equation 4.4 are presented in figure 4.3, 4.4 and 4.5.
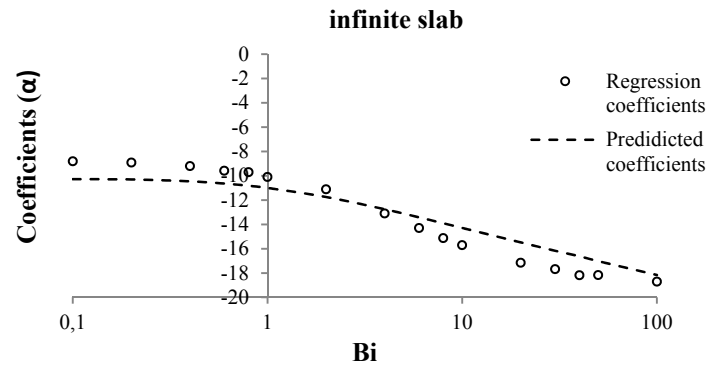
Figure 4.3. Plot of the slopes of the residual plots as a function of ln(Bi) for infinite slabs, the line represents the predicted coefficients from equation 4.4.
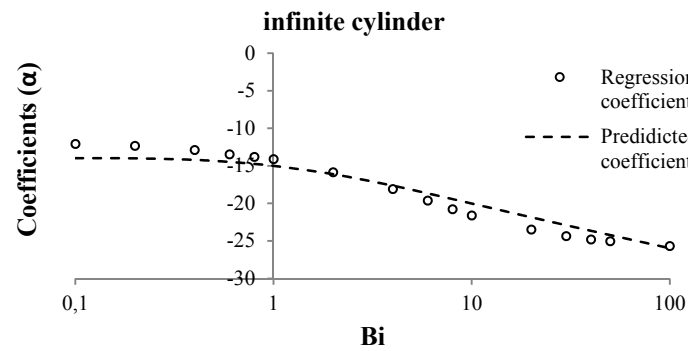
Figure 4.4. Plot of the slopes of the residual plots as a function of ln(Bi) for infinite cylinders, the line represents the predicted coefficients from equation 4.4.
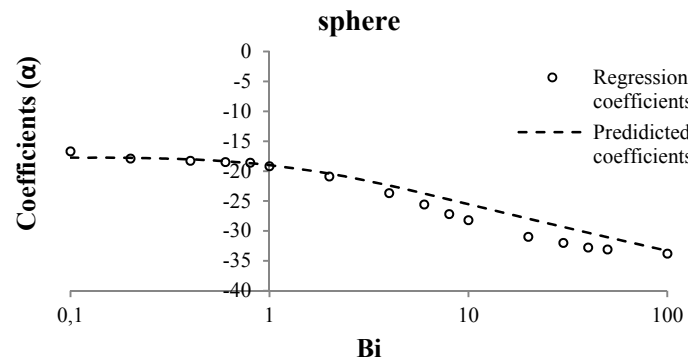
Figure 4.5. Plot of the slopes of the residual plots as a function of ln(Bi) for spheres, the line represents the predicted coefficients from equation 4.4.

The construction of a simplified equation that describes the residual propagation as a function of the dimensionless time (Fo) is constructed by the combination of the residual description in equation 4.3, and the regression for the slope of the residual behaviour from equation 4.3.

Inserting equation 4.4 in equation 4.3 gives:

$$\ln(\epsilon) = -(\lambda_1 \cdot \ln(Bi) + C) \cdot Fo + ln(a_{c,1} - 1) \qquad [4.5]$$

52

Taking the antilogarithm to equation 4.5 and rearranging gives:

$$\epsilon = (a_{c,1} - 1) \cdot e^{-\lambda_1 \cdot \ln(Bi) \cdot Fo} \cdot e^{-C \cdot Fo} \qquad [4.6]$$

Equation 4.6 may be simplified to:

$$\epsilon = (a_{c,1} - 1) \cdot Bi^{-\lambda_1 \cdot Fo} \cdot e^{-C \cdot Fo} \qquad [4.7]$$

For the infinite slab, the infinite cylinder and the sphere, the rounded values of C equals: 11, 15 and 19, respectively.

Equation 4.6 and 4.7 predicts that the residual, ε approaches 0 when the Fourier number becomes large and approaches $a_{c,1}$ when the Fourier number approaches 0, in full accordance with the complete series expansion. For Bi<0.1 $a_{c,1}$ approaches 1 and the residual is negligible, and in these cases the lumped capacitance method can also be used (Mills 1995 p.,32) For Bi>100 the surface resistance is negligible and these situations can be calculated as if Bi=100. The parameter C is not sensitive to small variations; however, the global fit of the model is best at the suggested values of C. The inputs needed are summarised in table 4.1.

Table 4.1 Formulae input to calculate the thermal history based with the suggested equation

Geometry	λ_1	a_c	a_m	C
Inf. Plate	$Bi = \lambda_1 tan\lambda_1$	$\dfrac{2sin\lambda_1}{\lambda_i + sin\lambda_1 cos\lambda_1}$	$a_c \cdot \dfrac{sin(\lambda_i)}{\lambda_i}$	11
Inf. Cylinder	$Bi = \dfrac{\lambda_1 J_1(\lambda_1)}{J_0(\lambda_1)}$	$\dfrac{2J_1(\lambda_1)}{\lambda_1(J_0^2(\lambda_1) + J_1^2(\lambda_1))}$	$a_c \cdot 2 \cdot \dfrac{J_1\lambda_i}{\lambda_i}$	15
Sphere	$Bi = 1 - \lambda_1 cot\lambda_1$	$\dfrac{2(sin\lambda_1 - \lambda_1 cos\lambda_1)}{\lambda_1 - sin\lambda_1 cos\lambda_1}$	$a_c \cdot 3 \cdot \dfrac{sin(\lambda_i) - \lambda_i cos(\lambda_i)}{\lambda_i^3}$	19

The values of λ_1, $a_{c,1}$ and $a_{m,1}$ for different Biot numbers are presented in most textbooks on the subject based on the equations summarized in table 4.1, and as presented in chapter 3, these can be predicted with very good accuracy using the proposed polynomial fit in table 3.2 recapitulated below in table 4.2:

Table 4.2 regression equations for the determination of the 1st Fourier exponent from chapter 3

Geometry	Regression polynomials
Inf. Slab	$b = \lambda_1^2 = 1.1911 \cdot (Bi_{norm})^3 + 0.1878 \cdot (Bi_{norm})^2 + 1.0939 \cdot (Bi_{norm}) - 0.0037$
Inf. Cylinder	$b = \lambda_1^2 = 3.2595 \cdot (Bi_{norm})^3 + 0.3628 \cdot (Bi_{norm})^2 + 2.1878 \cdot (Bi_{norm}) - 0.0053$
Sphere	$b = \lambda_1^2 = 6.2941 \cdot (Bi_{norm})^3 + 0.4877 \cdot (Bi_{norm})^2 + 3.1477 \cdot (Bi_{norm}) + 0.00073$

Also the solutions for determining λ_1, $a_{c,1}$, and $a_{m,1}$ suggested by Ramaswamy et al. (1982) and Ostrogorsky (2009) provides accurate determinations. However, as discussed in chapter 3 they are more complex and less transparent equations.

For the combined approximation for the complete series expansion, the calculated residual in equation 4.7, is combined with the description of the complete expansion by a 1st term approximation – subtracted a residual in equation 4.8.

Inserting eq. 4.7 into eq. 4.1 gives:

$$\Omega = a_{c,1} \cdot e^{-\lambda_1^2 \cdot Fo} - \left(a_{c,1} - 1\right) \cdot Bi^{-\lambda_1 \cdot Fo} \cdot e^{-C \cdot Fo} \qquad\qquad [4.8]$$

For an improved precision at Fo<≈0.05-0.08, where equation 4.8 tends to overshoot the predicted value of Ω (see figure 4.6 later), the rational restriction $\Omega \leq 1$ should be applied, since a value of $\Omega > 1$ is not physical because no internal heat generation is considered. The consequence of the restriction can be seen in section 4.4.

$$\Omega = a_{c,1} \cdot e^{-\lambda_1^2 \cdot Fo} - \left(a_{c,1} - 1\right) \cdot Bi^{-\lambda_1 \cdot Fo} \cdot e^{-C \cdot Fo} \qquad [\text{ where } \Omega \leq 1] \qquad [4.9]$$

4.3 Volume average temperatures

The same procedure as in section 4.2 is used for constructing a similar equation for the volume average temperature. The residual between a 1st term approximation and a complete solution to the series expansion is investigated. As in section 4.2 the residual is plotted against Fo in a log scale and the regression equations are based on a forced regression with a known intercept. For the volume average temperature, the forced regression is at $(a_{m,1}-1)$, all regressions can be found in appendix 5. The following expression was obtained to describe the residual as a function of the Fourier number generalised for all Bi-numbers:

$$\ln(\epsilon) = -(3 \cdot \lambda_1 \cdot \ln(Bi) + C) \cdot Fo + ln(a_{m,1} - 1)$$

Antilog gives:

$$\epsilon = (a_{m,1} - 1) \cdot e^{-3 \cdot \lambda_1 \cdot \ln(Bi) \cdot Fo} \cdot e^{-C \cdot Fo}$$

Simplifies to

$$\epsilon = (a_{m,1} - 1) \cdot Bi^{-3 \cdot \lambda_1 \cdot Fo} \cdot e^{-C \cdot Fo}$$

Combining the 1st term approximation with the residual determination gives the simplified equation for volume average temperature also covering low Fourier numbers.

$$\Omega = a_{m,1} \cdot e^{-\lambda_1^2 \cdot Fo} - (a_{m,1} - 1) \cdot Bi^{-3 \cdot \lambda_1 \cdot Fo} \cdot e^{-C \cdot Fo} \qquad [4.10]$$

The exponential term $(3 \cdot \lambda_1 \cdot Fo)$ in equation 4.10 for volume average temperatures is larger than the exponential term $(\lambda_1 \cdot Fo)$ in equation 4.8 for the centre temperatures. This is because the 1-term approximation is converging more rapidly for the volume average temperature than for the centre temperature (see figure 7.8 in chapter 7). The convergence of the 1st term approximation for centre, volume average and positional temperatures is presented and discussed thoroughly in chapter 7.

The restriction $\Omega \leq 1$ does not need to be applied in the case of volume average temperatures because the theoretical value of the dimensionless temperature response never goes above 1 for the volume average temperature.

The temperature predictions at very low Fourier numbers are not challenging. The centre temperature is equal to the initial temperature before the heat has significantly reached the centre (app. Fo<0.04). The volume average temperature is more difficult to predict at very low Fourier numbers (Fo<0.04) and needs many terms in the series expansion to be exact. The presented study is not suited for this calculation. For heat transfer operations this is not crucial because the Fourier numbers are seldom extremely low within a reasonable process window, and the initial volume average temperature is of no big concern. However in the application of the procedure to mass transport processes (where the same basic Fourier expansion is used) such as salting operations this is important. The issue of calculating the volume average temperature at very low Fourier numbers (Fo<0.04) is not within the theme of this dissertation.

4.4 Validation

To test the validity of the new equation (equation 4.9) it is compared with the solution to infinite series solution at representative Biot numbers (1 and 10 for the centre temperature, 4 and 20 for the volume average temperature). The validation is presented in the figures 4.6.a-f for the centre temperature and 4.7.a-f for the volume average temperature. Even though the restriction should always be used (equation 4.9), the prediction without the restriction is presented in graphs to show the behaviour.
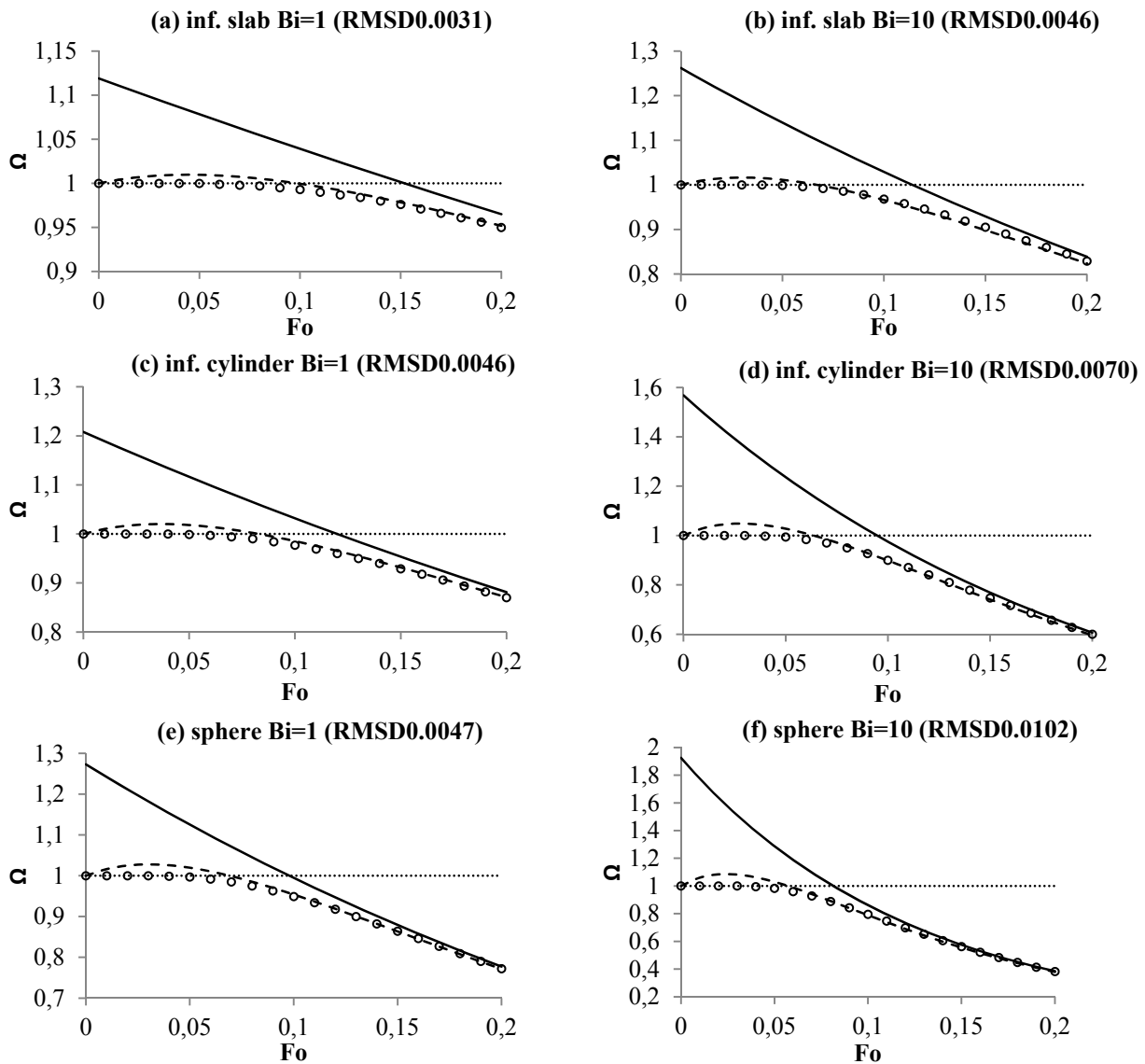
Figure 4.6. a-f. Centre temperature validation by comparing the 1- term solution from equation 1.5 (full line), the exact solution with 100 terms from equation 1.3 (open circles), and the new equation 4.8 (dashed line). The restriction from equation 4.9 ($\Omega \leq 1$) is included in the charts.

Figure 4.6 shows that equation 4.8 generally overshoots slightly at low Fo; by including the restriction ($\Omega \leq 1$) in equation 4.9 predicts the temperature response in the centre with good precision at all Fo-numbers.

The results from the validation of the volume average temperature calculation (equation 4.10) are presented in figure 4.7. a-f.
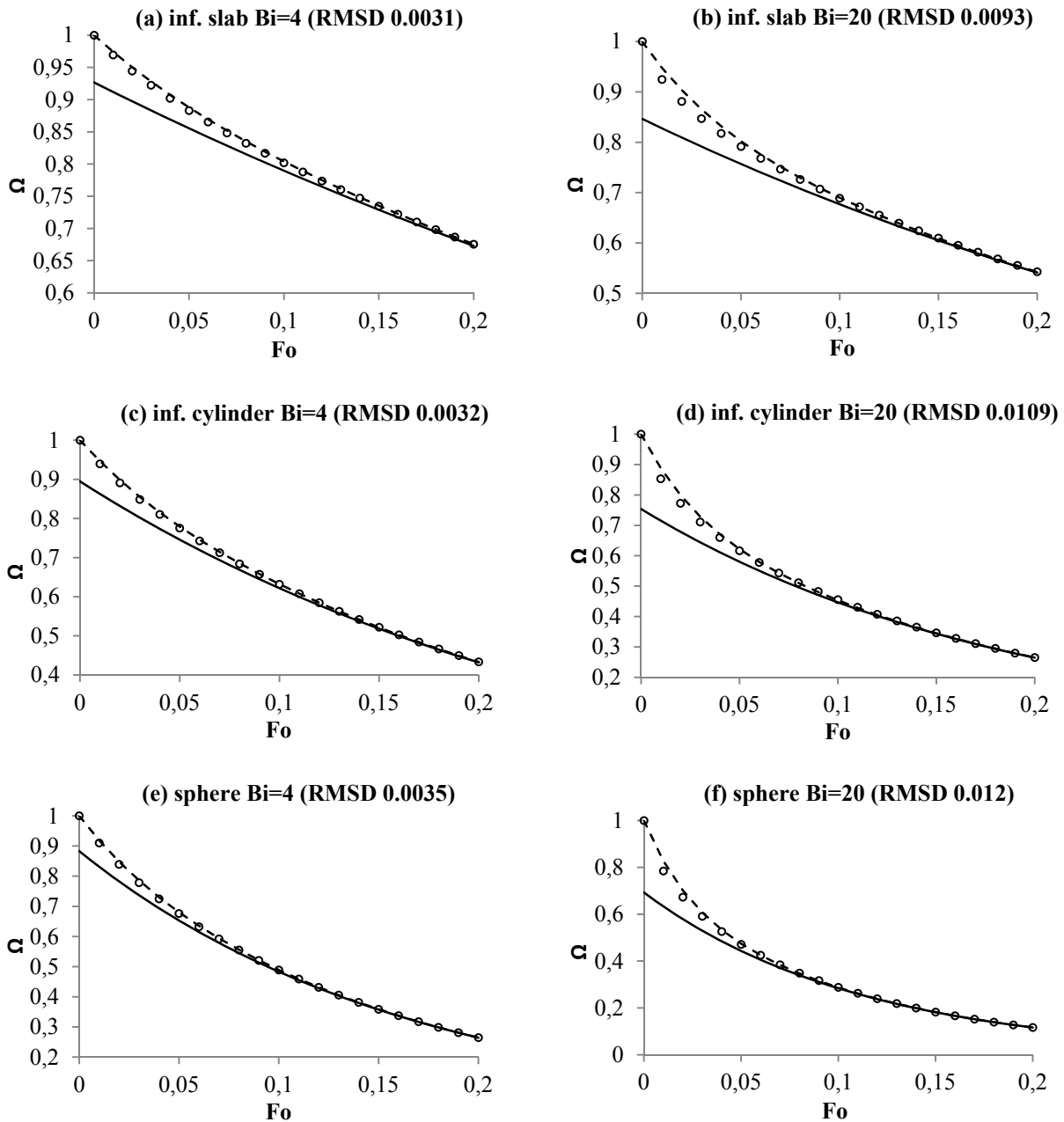
Figure 4.7. a-f. Volume average temperature validation by comparing by comparing the 1- term solution from equation 1.5 (full line), the exact solution with 100 terms from equation 1.3 (open circles), and the new equation 4.10 (dashed lines).

As for the centre temperature, the precision of the prediction is good also at low Fourier numbers as can be observed in the graphs in figure 4.7.a-f.

For investigating the full validation the precision of the developed equations (4.9 and 4.10) is supported by the calculation of the error of prediction in terms of Root Mean Squared Difference (RMSD) (equation 4.11) for all tested Biot numbers ($0<Fo<0.2$). The investigation is based on a comparison between the 100 term solution and the solution from equations 4.9 and 4.10, for the centre and volume average temperature respectively. The RMSD values of all the tested geometries are presented in table 4.2.

$$RMSD = \sqrt{\sum_{t=1}^{n}\left(\frac{(x_{1,t}-x_{2,t})^2}{n}\right)} \hspace{3cm} [4.11]$$

Table 4.2 The calculated RMSD values for the comparison between the new equation and the 100 term solution at 0<Fo<0.2 for the centre temperature and volume average temperature.

	Centre temperature (equation 4.9) *(Restriction: Ω≤1)*			*Volume average temperature* *(equation 4.10)*		
	Inf. slab	Inf. cylinder	sphere	Inf. slab	Inf. cylinder	sphere
Bi	RMSD	RMSD	RMSD	RMSD	RMSD	RMSD
0.1	0.0008	0.0010	0.0005	-	-	-
0.2	0.0013	0.0017	0.0012	-	-	-
0.4	0.0019	0.0026	0.0021	-	-	-
0.6	0.0024	0.0034	0.0030	-	-	-
0.8	0.0030	0.0041	0.0039	-	-	-
1	0.0031	0.0046	0.0047	0.0007	0.0006	0.0011
2	0.0035	0.0060	0.0072	0.0020	0.0018	0.0022
4	0.0031	0.0066	0.0089	0.0031	0.0032	0.0035
6	0.0035	0.0067	0.0101	0.0046	0.0047	0.0045
8	0.0041	0.0066	0.0102	0.0058	0.0062	0.0067
10	0.0046	0.0070	0.0102	0.0068	0.0074	0.0080
20	0.0046	0.0074	0.0103	0.0093	0.0109	0.0121
30	0.0041	0.0077	0.0107	0.0085	0.0123	0.0135
40	0.0042	0.0080	0.0115	0.0108	0.0126	0.0140
50	0.0037	0.0086	0.0124	0.0105	0.0128	0.0141
100	0.0041	0.0111	0.0161	0.0101	0.0123	0.0140

- *At Bi<1, the error (RMSD) is insignificant for the volume average temperature because $a_{m,1} \approx 1$*

As seen from the RMSD values (table 4.2) it is obvious that the error of the new equation is increasing at higher Biot numbers. The maximum error is for spheres (Bi=100) with a maximum RMSD of 0.016. In general RMSD is about 0.01 or lower, and this precision is adequate in most practical situations.

4.5 General geometries

Calculation of general geometries represented as cross sections of infinite bodies (cans, boxes and infinite prisms) the method suggested by Newman (1936) (equation 1.7) is adopted with the new approach, keeping in mind that the restriction (equation 4.9) should be applied for all individual dimensions.

Two representative cases have been chosen. The first case is the heating of a can with the dimensions: r=54 [mm], h=108 [mm], a heat transfer coefficient of 150 [W/m²K], an initial product temperature of 20°C and a surrounding temperature of 120°C. The resulting heating profile is presented in figure 4.8.

The second case is convective cooling of a box with the dimensions 80x80x40 [mm], a heat transfer coefficient of 40 [W/m²K], an initial product temperature of 70°C and a surrounding temperature of 2°C. The resulting heating profile is presented in figure 4.9 where the Fourier number refers to the largest dimension (80mm). The corresponding process time for the can in case 1 is 5000s at Fo=0.2, and for the box in case 2 it is 2700s at Fo=0.2.
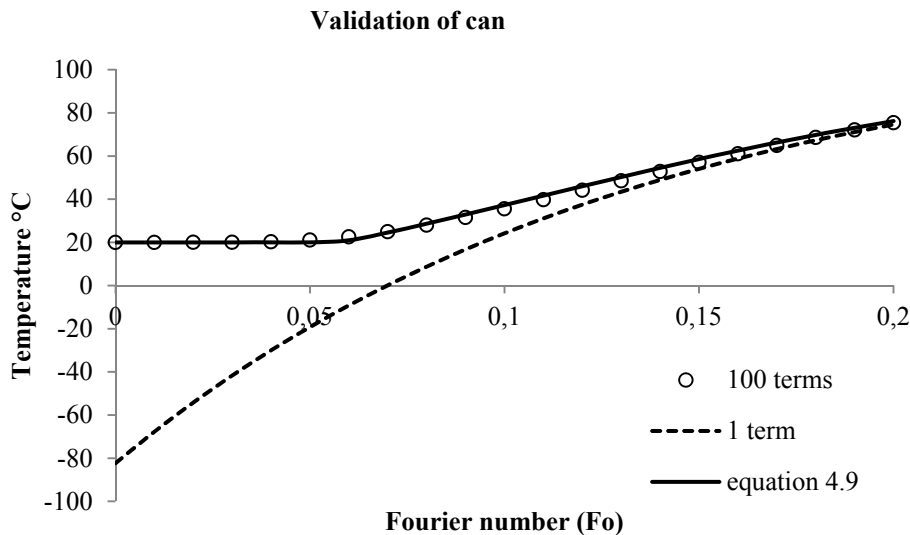
Figure 4.8. Validation of the heating profile of a can geometry during the initial heating period. The exemplified heat transfer coefficient is considered 150 [W/m²K], and the can dimensions are r=54mm and h=108mm. Bi$_{radius}$=20, Bi$_{1/2h}$=20
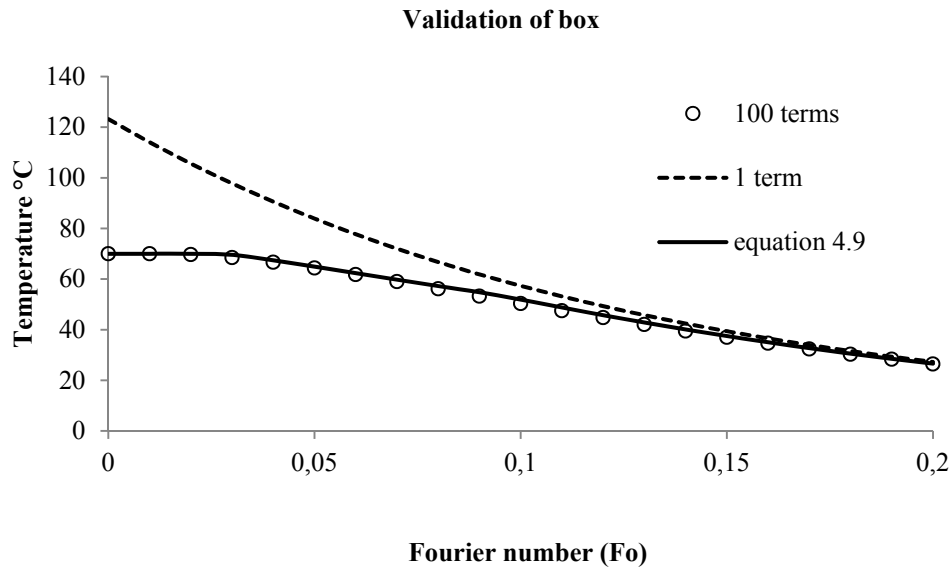
Validation of box

Figure 4.9. Validation of the cooling profile of a box geometry during the initial cooling period. The exemplified heat transfer coefficient is considered 41 [W/m²K]. The box dimensions are 80x80x40 [mm]. The box geometry has two sets of Fo numbers, here it is presented by the lowest Fourier numbers (the two dimensions of 80mm) at the x-axis. $Bi_h=4$, $Bi_w=8$, $Bi_l=8$

From figure 4.8 and 4.9 it is seen that the proposed new equation 4.9 is able to predict the thermal history in the initial phase with a high level of precision. the maximum error for the two cases is 2°C for the can in case 1 and 1.5°C for the box in case 2. The maximum error occurs in the beginning of the process where it is usually less important to know the temperature with a high precision.

The developed equations are compared with a numerical solution to two industrial examples in the next chapter to validate the equations for more real-life examples.

4.6 concluding remarks

The equations formulated in this study (equations 4.8-4.10) gives good precision for the thermal response in the centre and for the volume average temperature of simple geometries (slabs, cylinders, spheres, cans, boxes and prisms), covering the whole process time (Fo>0) and all Biot numbers in the range 0.1<Bi<100. In general, RMSD is about 0.01 or lower; for the sphere at high Bi the prediction error (RMSD) increases up to 0.016. This precision is adequate in most practical situations, considering that the driving temperature difference in most cases in the food industry is below 100°C. The variable input to the new equation is identical to the information needed in a 1-term solution to non-stationary heat transfer problems and an additional constant depending on the geometry.

For the utilization of this procedure the geometry of investigated product and the thermo-physical properties needs to be assessed which in most situations is not problematic. However, also the Biot number have to be calculated where a determination of the heat transfer coefficient is crucial. Determination of heat transfer coefficients for different process situation is presented and discussed in chapter 6.

Equation 4.9 applies for the full Fo range for the center-temperatures, equation 4.10 for the volume average temperatures is less precise at very low Fourier numbers(Fo<0.02).

5. Numerical validation of real products

The combined simplification method, developed and presented in chapter 3 and 4, has been validated for the elementary geometries in the previous chapters against the complete series expansion (exemplified by 100 terms). The validation of finite bodies in terms of general geometries (cans, quadratic prisms and boxes) that can be represented as cross sections of elementary geometries (infinite slab, infinite cylinder and sphere), the method is straight forward by applying the procedure from Newman (1936). In these cases it is important that the restriction ($\Omega \leq 1$) is applied to individual dimensions following equation 4.9.

For the validation of industrial products, this chapter presents the predictive calculation of two product examples from food manufacture, also presented in the operationalization section to this thesis (Chapter 2.3).

The method used for this validation is a numerical solution calculated using the commercial software COMSOL Multiphysics. For the first case presented, regarding the cooling of packaged cream cheese I have performed the modelling during the Ph.D study, for the second case (processing of hamburgerryg), Assistant Professor Aberham Hailu Feyissa has supported with numerical data.

5.1 Industrial application - Cream cheese case study

The case is inspired by a project where a Danish dairy production of cream cheese is investigated with regards to the cooling profile of a packaged product. In the project former bachelor student Søren Holm Rasmussen, investigated the influence of cooling of cream cheese under my co-supervision. From meetings with the company we got insight to the production and cooling of the cream cheese products. The modelling work and the predictive calculations presented in this thesis is formulated and calculated in the thesis study solely.

For this validation it is desired to know the heat transfer coefficients for individual boundaries. Due to the design of the cooling equipment, the supplied airflow is perpendicular (figure 5.1) which induces varying heat transfer coefficients at the different surfaces of the package.
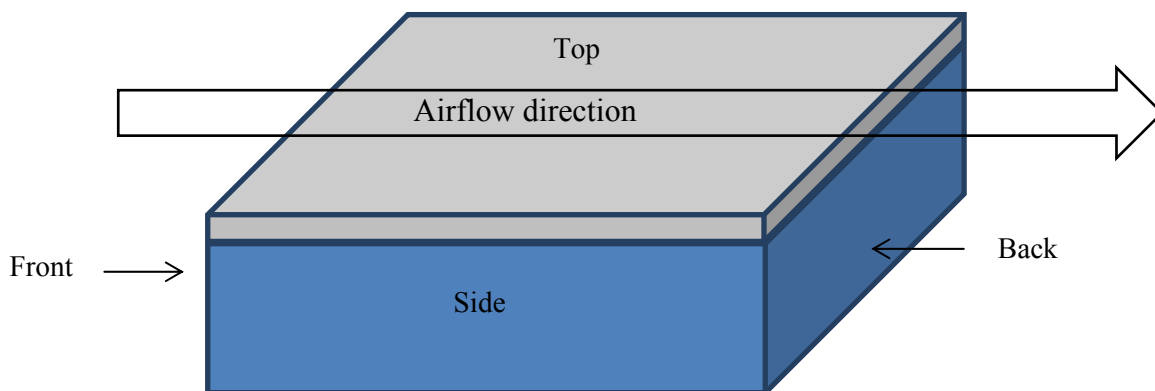

Figure 5.1 Description of the cooling during the processing of cream cheese in case 1. The package has a headspace and is exposed to perpendicular airflow across the sides and the insulated headspace insulated surface at the top. The boundaries are named according to their relative position to the flow i.e. Front, Back, Side and Top

A set of heat transfer coefficients for each boundary is assumed based on the experience from an earlier investigation where individual heat transfer coefficients were measured in a laboratory setup (see chapter 7.1). These are presented in table 5.1. Optimally, the convective heat transfer coefficients need to be measured at the production site. The procedure for determining heat transfer coefficients for separate boundaries is presented in chapter 6.

The description of the equipment and product characteristics are as follows:

The air tunnels comprises of a moving band inside a big housing with circulating air that surrounds the surface of the products. In the theoretical setup there is a slight insulation at the bottom surface touching the conveyor band (a plastic material, with assumed low thermal conductivity), and there is an insulating headspace at the product top between the attached lid and the product domain.

Process settings: The cream cheese is to be pre-cooled before storage to allow the gel to set at a volume average temperature set-point of around 30-40°C (the actual set-point is anonymised). The initial temperature is 70°C and the surrounding temperature is 0°C. The volume average temperature is important as a set point for the cooling process, but also the centre temperature (more precisely the global maximum temperature) is important in order to conduct process evaluation at the production site, as this can be directly measured.

5.1.1 Heat transfer coefficients in the process

The cream cheese is cooled in a conventional cooling spiral by circulating air. The air is considered a perpendicular airstream as presented in figure 5.1 inducing a non-uniform heat transfer around the package. The assumed heat transfer coefficients for the calculations are presented in table 5.1.

Table 5.1 Heat transfer coefficients used in the calculations of the cooling profiles of the cream cheese.

Dimension	Heat transfer coefficient
Top	30 [W/m^{2}K]
Bottom	10 [W/m^{2}K]
Sides	22 [W/m^{2}K]
Back	18 [W/m^{2}K]
Front	35 [W/m^{2}K]

For the numerical calculations the heat transfer coefficients in table 5.1 are applied to the respective boundary. In the analytical calculations the heat transfer coefficient is averaged in direction (x, y, z) top/bottom, side/side and front/back.

The headspace below the lid acts as an insulating layer, and the heat transfer coefficient to the top of the cream cheese is therefore equal to the overall heat transfer coefficient U (the air in the headspace is assumed stagnant in both the numerical and the analytical solution).

$$\frac{1}{U} = \frac{1}{h} + \frac{L_{headspace}}{k_{air}} = \frac{1}{\left(\frac{1}{30} + \frac{0.0237}{0.002}\right)} = 7.5 \, [\text{W}/m^2\text{K}]$$

For the analytical calculations based on the equations presented in this study (chapter 3 and chapter 4), the average values of h in each dimension are used, cf. the boundary conditions above:

- Top/bottom: 8.75 [W/m²K] $\left(\frac{7.5+10}{2}\right)$
- Sides: 22 [W/m²K] $\left(\frac{22+22}{2}\right)$
- Front/back: 26.5 [W/m²K] $\left(\frac{18+35}{2}\right)$

The thermo physical properties of the cream cheese (T, 50°C): ρ_{cheese}=998 [kg/m³], k_{cheese}=0.45[W/m·K], $c_{p,cheese}$=3261[J/kgK], $k_{headspace}$=0.0237[W/m·K], calculated from the content of macronutrients in the product and the temperature dependence described by Choi and Okos (1986). The dimensions of the product is (half height=0.01 [m], half-length=0.04 [m] and half width=0.065

Based on the dimension averaged heat transfer coefficients, the resulting Biot numbers for the cream cheese domain is:

- Top/bottom: $Bi = \frac{8.75}{0.45} \cdot 0.01 = 0.194$
- Sides: $Bi = \frac{22}{0.45} \cdot 0.06 = 2.93$
- Front/back: $Bi = \frac{26.5}{0.45} \cdot 0.04 = 2.36$

5.1.2 Numerical Calculation

The developed equations (4.9 and 4.10) are compared to a numerical simulation of the Fourier equation 5.1 solved in COMSOL Multiphysics®.

$$\rho c_p \frac{\partial T}{\partial t} = \nabla \cdot (k \nabla T) = k \left[\frac{\partial^2 T}{\partial x^2} + \frac{\partial^2 T}{\partial y^2} + \frac{\partial^2 T}{\partial z^2}\right] \tag{5.1}$$

The simulation describes the temperature as a function of time and position using the following boundary conditions:

$$-k\frac{\partial T}{\partial x} = h_x(T - T_{air})$$

$$-k\frac{\partial T}{\partial y} = h_y(T - T_{air})$$

$$-k\frac{\partial T}{\partial z} = h_z(T - T_{air})$$

The packaged cream cheese is considered as a box with the dimensions (20×80×120 [mm]) and an apparent headspace of 2 [mm] on the top boundary caused by an attached lid. In figure 5.2 the geometry is presented along with the applied mesh for the numeric calculations. In the simulations and the predictions with the developed equations, all thermo physical properties are assumed constant, and no convection is considered in the headspace. The study is performed as a pure conduction study, with applied convective heat transfer at the boundaries.
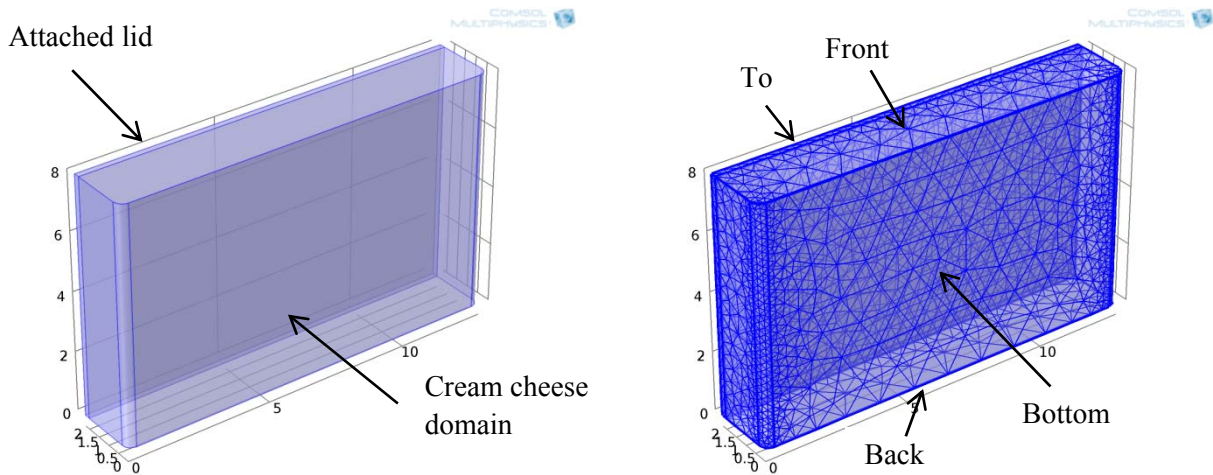
Figure 5.2. The constructed geometry for the modelling of cream cheese to the left and the applied mesh to the right. The dimension unit is [cm]. The attached lid is positioned at the top. The cream cheese domain is in the bottom.

5.1.3 Analytical calculation with the developed method

The simplified prediction using the procedures presented in chapter 3 and 4 is implemented in Excel where the inputs needed for the calculations are the Biot numbers calculated above, the thermo physical properties and the characteristic dimensions. From the Biot numbers presented in section 5.1.1 normalised Biot numbers are calculated for each of the three dimensions.

$$Bi_{norm} = \frac{Bi}{1 + Bi}$$

$$Bi_{norm,(top,bottom)} = \frac{0.194}{1 + 0.194} = 0.162$$

$$Bi_{norm,(front,back)} = \frac{2.36}{1 + 2.36} = 0.703$$

$$Bi_{norm,(sides)} = \frac{3.15}{1 + 3.15} = 0.759$$

The normalised Biot numbers are used to determine the Fourier exponents needed in the series expansion solution by the polynomial regressions determined from chapter 3, table 5.2 shows the calculation of the 3 Fourier exponents. In the table only the first two decimals are presented in the parameters, for the full regression equations see table 3.2.

Table 5.2 Polynomial regressions determination (from table 3.2) for the first Fourier exponent for the three dimensions

dimension	Regression polynomia
Top,bottom	$b = \lambda_1^2 = 1.19 \cdot (0.162)^3 + 0.19 \cdot (0.162)^2 + 1.09 \cdot (0.162) - 0.0037 = \quad 0.185$
Front,back	$b = \lambda_1^2 = 1.19 \cdot (0.703)^3 + 0.19 \cdot (0.703)^2 + 1.09 \cdot (0.703) - 0.0037 = \quad 1.269$
sides	$b = \lambda_1^2 = 1.19 \cdot (0.759)^3 + 0.19 \cdot (0.759)^2 + 1.09 \cdot (0.759) - 0.0037 = \quad 1.456$

The square root of the Fourier exponents, calculated from table 5.2, gives the eigenvalue belonging to the specific root function in table 1.1 used as input value to determine the lag factors.

$$\lambda_{1,top,bottom} = 0.185^{0.5} = 0.4295$$

$$\lambda_{1,front,back} = 1.269^{0.5} = 1.1264$$

$$\lambda_{1,sides} = 1.456^{0.5} = 1.2079$$

For the specific case, only the equations for infinite slabs are used in the calculations in table 5.3

Table 5.3 Calculation of the lag factor based on the first eigenvalues calculated in table 5.2

Geometry	a_c	a_m
Top,bottom	$\dfrac{2\sin(0.43)}{0.43 + \sin(0.43)\cos(0.43)} = 1.031$	$a_c \cdot \dfrac{sin(0.43)}{0.43} = 0.999$
Sides	$\dfrac{2\sin(1.13)}{1.13 + \sin(1.13)\cos(1.13)} = 1.192$	$a_c \cdot \dfrac{sin(1.13)}{1.13} = 0.956$
Front,back	$\dfrac{2\sin(1.21)}{1.21 + \sin(1.21)\cos(1.21)} = 1.214$	$a_c \cdot \dfrac{sin(1.21)}{1.21} = 0.94$

The Fourier exponents b_1, lag factors $a_{c,1}$, $a_{m,1}$ and 1st eigenvalues λ_1 are used as input in the developed simplified equations, for the centre temperature response (equation 4.9) with the time interval in dimensionless form (Fo). The procedure is presented as an example for the calculation of the centre temperature. The procedure in calculating the volume average temperature is analogue.

$$\Omega = a_{c,1}e^{-b \cdot Fo} - (a_{c,1} - 1)Bi^{-\lambda_1 \cdot Fo}e^{-C \cdot Fo} \quad (\Omega = 1 \; if \; \Omega > 1)$$

For the calculation of infinite slabs C=11. For calculation of general geometries that can be exemplified as cross sections of elementary geometries the approach described by Newman (1936) is adopted, in this specific case as a finite box. Keeping in mind that the restriction of the temperature response (Ω=1 if Ω>1) should be used on separate dimensions before they are multiplied. This can in practice be done in two ways in Excel. Either the response can be changed manually in the cells which is timeconsuming, or more elegantly an IF function can be used in the output cells.

$$\Omega_{top,bottom} = 1.031 \cdot e^{-0.185 \cdot Fo} - (1.031 - 1)Bi^{-0.4295 \cdot Fo}e^{-11 \cdot Fo} \quad (\Omega = 1 \; if \; \Omega > 1)$$

$$\Omega_{front,back} = 1.192 \cdot e^{-1.269 \cdot Fo} - (1.192 - 1)Bi^{-1.1264 \cdot Fo}e^{-11 \cdot Fo} \quad (\Omega = 1 \; if \; \Omega > 1)$$

$$\Omega_{sides} = 1.214 \cdot e^{-1.456 \cdot Fo} - (1.214 - 1)Bi^{-1.2079 \cdot Fo}e^{-11 \cdot Fo} \quad (\Omega = 1 \; if \; \Omega > 1)$$

For the temperature response in the cream cheese the 3 dimensions are multiplied (Newman 1936)

$$\Omega_{cream \; cheese} = \Omega_{top,bottom} \cdot \Omega_{front,back} \cdot \Omega_{sides}$$

For the volume average temperature the procedure is the same as for the centre temperature. Equation 4.10 is used for volume average temperatures, recapitulated below:

$$\Omega = a_{m,1}e^{-b \cdot Fo} - (a_{m,1} - 1)Bi^{-3\lambda_1 \cdot Fo}e^{-C \cdot Fo}$$

5.1.4 Results

The results from the simulation are the temperature history of the volume average temperature and the global maximum. Figure 5.2 demonstrates, also in this case, a good agreement between the numerical simulations and the calculations according to the new equations developed in the present work.

Figure 5.2 Comparison between the 1ˢᵗ term series expansion solution and the present work with the model result from COMSOL for the thermal history of the average temperature (left) and the global maximum temperature (right) for the simulation setup described in the case, the "new equation" label cover the combined procedure from chapter 3+4.

The prediction of the volume average temperatures using the new approach fits well with the numerical simulation of the process and is an improvement compared to the presently used 1ˢᵗ term approximation. Also the centre temperature can be predicted with high accuracy.

Where the simplified solution tested is predicting the geometrical centre, the numerical solution is in this validation predicting the thermal centre in the cream cheese domain. For this validation the thermal centre and the geometrical centre is close because the boundary heat transfer coefficients are similar in the same dimensions (top/bottom, sides, front/back), (figure 5.3).
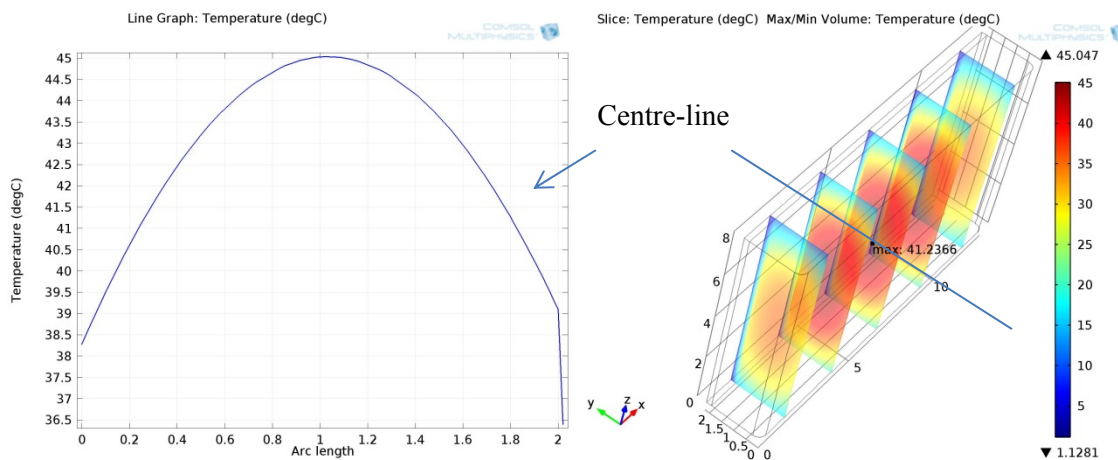
Figure 5.3 The temperature at the vertical centreline at the end of the cooling step after 1800s (left) and the position of the global maximum temperature in the midplane symmetric slice (right).

The thermal gradient is small around the thermal centre (figure 5.3). This is because the Biot numbers are small.

An additional comparison is presented in figure 5.4, where the bottom heat flux is increased to 20 [W/m²K]. Because the product has an apparent headspace below the lid of the product, it is assumed that the biggest potential for optimising the cooling time is through the bottom of the package. In this theoretical optimization setup, it is proposed that a high conductive material in the conveyor band can increase the heat transfer coefficient to the bottom of the package. This simulation was conducted for two reasons; in order to

investigate the optimisation potential, and to validate whether the developed equations could be used for such an investigation.
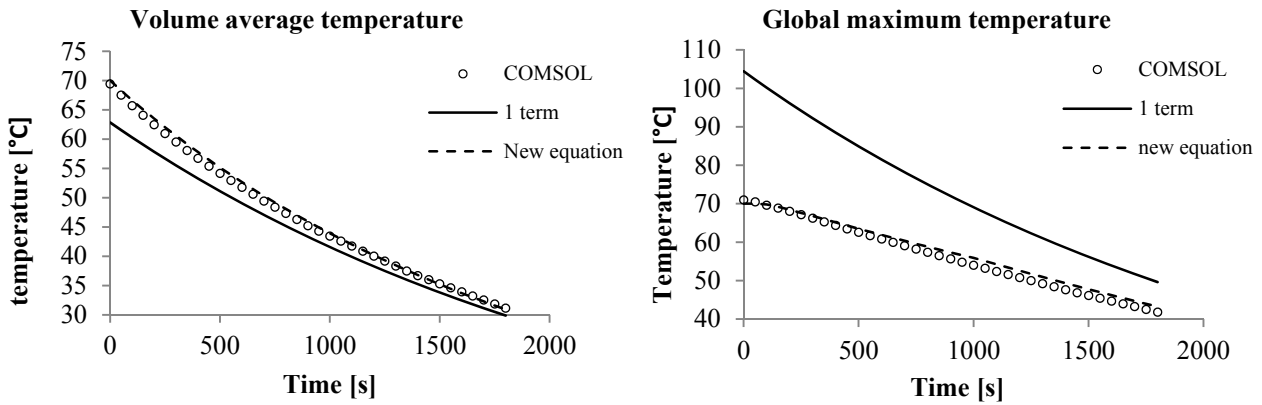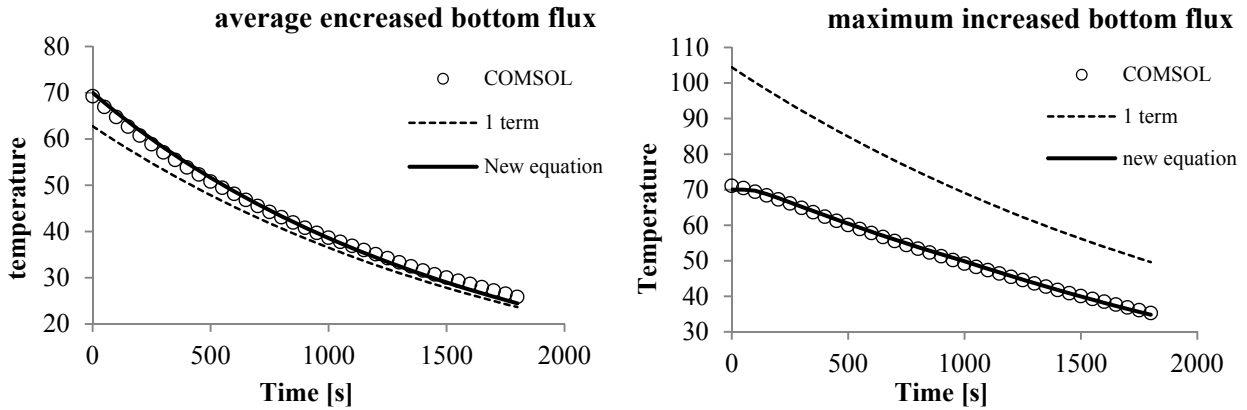

Figure 5.4 Comparison between the 1ˢᵗ term series expansion solution and the recently developed equation with the model result from COMSOL for the thermal history of the average temperature (left) and the global maximum temperature (right) for the simulation with an increased heat transfer at the bottom boundary

From the comparison in figure 5.4 of the process with an increased heat transfer coefficient to the bottom it can be seen that the developed equation has a high accuracy when compared to the numerical simulation for both the volume average temperature (left) and the centre temperature (right). For optimisation purposes, the target of a volume average temperature of e.g. 30°C is recalled from the case description. This is reached in the traditional process after 1800 [s], and in the optimization setup after 1500s, a reduction in cooling time of 300 [s] or 16%.

For this case it has been shown that the developed equations from the previous chapters can be used for predictive calculations of products with different heat transfer coefficients at the boundaries.

5.2 Industrial application – 3 step processing of "hamburgerryg"

In the second case the processing of hamburgerryg (brined, smoked and boiled saddle of pig) is modelled by a numerical simulation and compared to the simplified solution for predicting the thermal history as described in chapter 3 and 4. The experimental results and numerical simulations come from another project and are provided with courtesy of dr. Aberham Hailu Feyissa. The description of the process is provided below

Process description

Cylindrical hamburgerryg are manufactured in a three step process. The heat treatments are conducted after the brining step, which are not covered by this analysis. The hamburgerryg, which consists of brined meat cuts, have a length of 540 [mm] and a diameter of 85 [mm]. The thermo physical properties of the hamburgerryg are at process average temperature. The data used in this project has been transposed by a factor multiplied with the time and another factor multiplied with the temperature in the graphs due to confidentiality of the data. The set-points for the process are changed to an interval instead of a target.

Density: ρ=1064.5 [kg/m^3]

Specific heat capacity: c_p= 3535.5 [J/kg$\cdot$K]

Thermal conductivity: k= 0.47[W/m$\cdot$K]

Processing can be described as the following;

1. Initially the products are placed in a smoker where they are smoked until the desired quality is obtained. The conditions in the smoker is an average surrounding temperature of 50-60°C and a convective heat transfer coefficient of 20 [W/m^{2}K]
2. After the initial smoking of the products they are transferred to a steamer where they are processed at 70-85°C and a heat transfer coefficient of 3790 [W/m^{2}K]. In the transition period between the two heating steps the ambient temperature is 25°C under free convection at a heat transfer coefficient of 8 [W/m^{2}K]. The set-point of the steaming process is 70-80°C in the centre.
3. After steaming the hamburgerryg is cooled with water in a falling film inducing a heat transfer coefficient of 80 [W/m^{2}K] at 10-40°C
4. After the active cooling step they are placed for passive cooling at 0-10°C with a heat transfer coefficient of 13 [W/m^{2}K]

In the simplified prediction only the first three steps are modelled. The hamburgerryg is considered an infinite cylinder based on the numerical results. The product is also considered an infinite cylinder in the numerical solution. The resulting Biot numbers in the three steps are.

1. Bi=1.81 – initial heating and smoking
2. Bi=342 – heating with steam
3. Bi=7.23 – cooling with falling water

Following the same procedure as described in section 5.1.3 the centre temperature is calculated as a function of time.

5.2.1 Numerical solution

The numerical modelling of the process is conducted as a pure conduction process as no significant mass transfer or phase change need to be considered. The procedure of the modelling is in principal identical to the procedure used for the cream cheese calculation. However, the boundaries in the hamburgerryg process changes during the process history. This is included in the model by a sequential boundary where the boundaries vary over time. In the simulations the boundaries are equal to the equipment setting. The numerical calculations for the hamburgerryg case will not be elaborated further in this study as it only serves as comparative input for developed method. The numerical data are provided with courtesy of Aberham Hailu Feyissa, 2013.

5.2.2 Analytical calculation with the developed method

The predictive calculations are adapted using the developed method (equation 4.9 and 4.10). The Biot numbers and the normalised Biot numbers are calculated. The Fourier exponents and the derived eigenvalues and lag factors are determined as a function of the normalised Biot number by polynomial regression (table 3.2), and the equations presented in table 1.1. The procedure is identical to the procedure in section 5.1.3 for the calculation on the cooling profile for the cream cheese.

The processing of hamburgerryg differs substantially from the cooling of the cream cheese due to a change in the boundaries with regards to temperature and heat transfer coefficients during processing. In the case of the hamburgeryg processing it is possible to model a change in the boundary conditions with a series expansion solution because the surrounding temperatures are close to the target temperature of the product in each step. The assumption of initial uniform product temperature in the beginning of each of the process steps is approximately fulfilled.

5.2.3 Boundary temperature

The boundaries used in the numerical solution, the actual measured boundary temperature and the temperature used for the simple calculations are presented in figure 5.5, to exemplify the simplification of the boundary temperature of measurements and the used boundaries for the calculation. In figure 5.5 the temperatures and time scales have been removed from the graph to anonymise the experimental results.
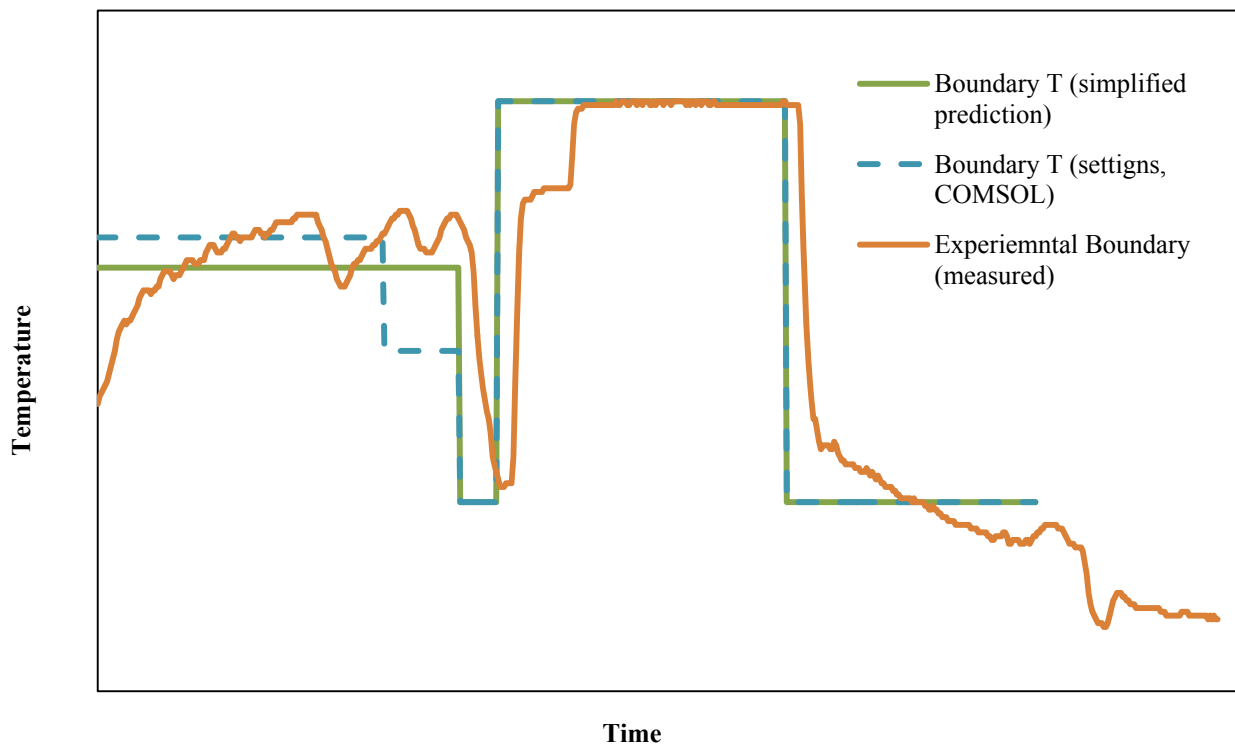
Figure 5.5 Boundary temperatures measured in during the experiment (orange) the equipment setup used in the numerical simulation (blue) and the used temperature for the simplified predictions (green)

In the simplified calculations it is an advantage that the expression of the boundary temperature is as simple as possible.

5.2.4 Results

The results from this study are divided in three sections: the provided experimental data, prediction of the temperature by a numerical solution and the developed equations from chapter 3 and 4, and a validation of the comparison of the numerical and developed solutions against the experimental data.

Experimental measurements

During the experiment, 16 products had an inserted thermocouple in the centre point to validate the thermal response in the expected coldest point during processing. The resulting measurements are presented in figure 5.6 for the average with included standard deviations. The time and temperature scale is removed for anonymising the experimental results.
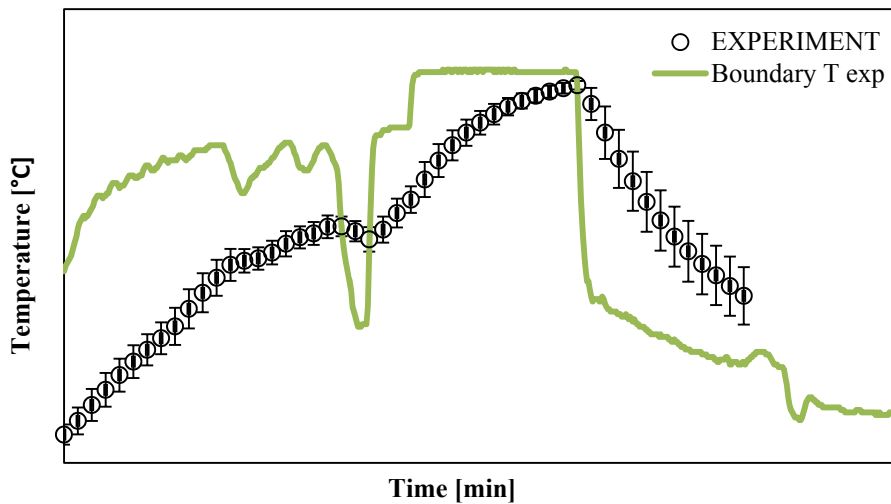
Figure 5.6 Experimental centre temperatures for the processing of ham, and the measured boundary temperature

Temperature predictions

The process is calculated numerically and with the developed method, eq. 4.9. The input for the Fourier exponents is the Biot numbers from section 5.1.3 and the temperature boundaries presented in figure 5.5. In the comparison in figure 5.7 the input boundary temperatures are not included, and the measured temperature is presented for the average enabling a more clean interpretation of the results. The boundaries can be viewed unit less in figure 5.5. The residuals of the numerical simulation and the developed simplified equations are presented in figure 5.8.
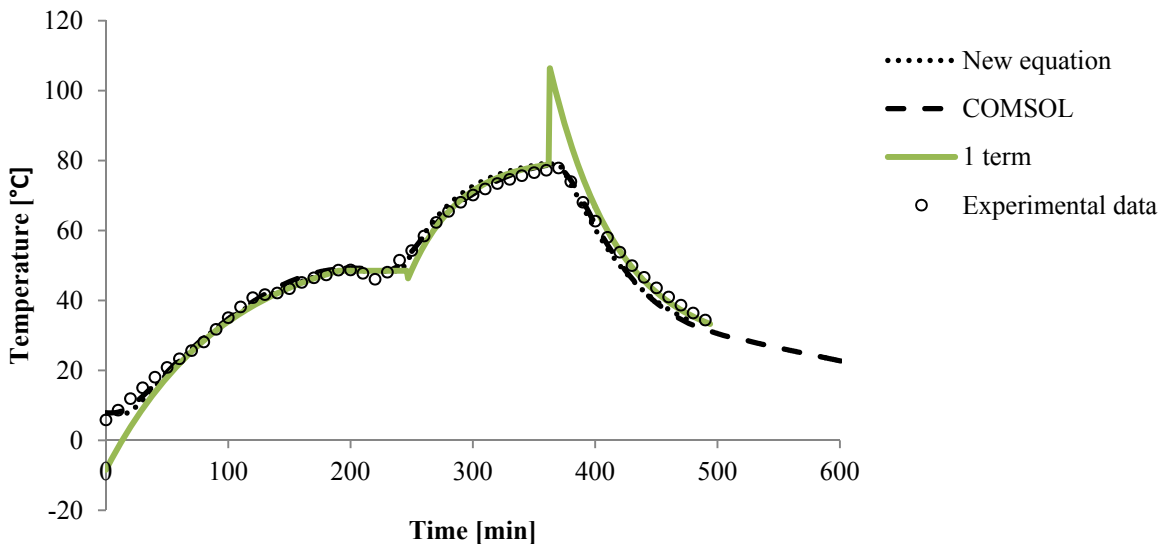
Figure 5.7 Comparison of the measured centre temperature with the temperature predicted by the numerical model and the predictive calculation from equation 4.9.

The measured average centre temperature in the experiments can be modelled by the numerical calculation and the predictions with the developed approach (figure 5.7). For analysing the precision of the prediction

from both the numerical solution and the new approach the residuals between the measured and the predicted is presented as a function of time in figure 5.8. It can be observed that the developed method predicts the temperature with comparable precision to a numerical solution (figure 5.8). It is also be observed that for the majority of the process a standard 1st term approximation gives a good prediction (figure 5.7). This is because for a big part of the process steps the Fourier number is above 0.2, where the approximation is valid. However, the 1st term approximation is less precise in the initial phase of the process steps. Especially for the cooling step this is problematic. Overshoot of the maximum temperature in this area disables the possibility of evaluating food safety with lethality calculations where the cooling step is included.
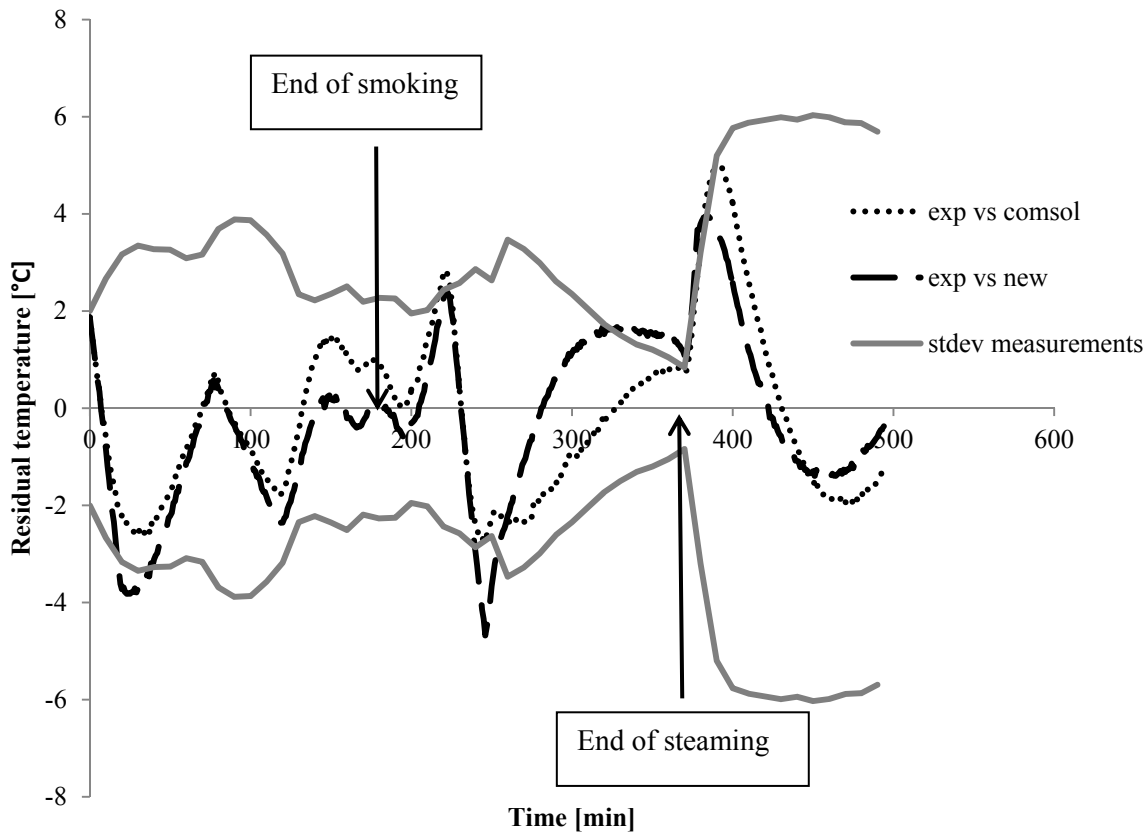
Figure 5.8 Residual between the measured and predicted temperature in the centre of the processed hams. Based on 16 thermocouples.

The accuracy of the temperature prediction using the numerical solution and the developed equations is comparable (figure 5.8). In addition it is also seen that the variance in the experimental measured values is larger than the prediction residuals. For a more in depth investigation the prediction of specific products is a more precise validation. However, this is out of scope for this specific case, where the comparison between the performance of a numerical solution and the developed equations is the focus.

The results from case two indicate that the developed equations can be used also for connected unit operations when the condition of initial uniform temperature is only approximately fulfilled. The results from the study also indicate that it is possible to use an average value for the boundary temperature in the calculations. This is important because process temperatures do vary, and a series expansion solution can only be calculated with an assumed constant boundary temperature.

5.3 Concluding remarks

The results from the two cases investigated shows that the developed equation for the Fourier exponents and the calculation of the initial heating and cooling time can be combined and used for the temperature prediction in industrial cases. The solution provides good accuracy and has been directly used in a spreadsheet. However, the solution needs to be used with caution. In case one (cooling of cream cheese) the geometry does not have big irregularities and the individual heat transfer coefficients are comparable. If bigger differences are seen in the heat transfer coefficients, and if the products are more irregular the solution could be less precise. In case two (processing of hamburgerryg) the target temperature in each step of the processing is close to the boundary temperature which implies that only a small temperature gradient is observed in the product in the initial phase of the subsequent step. Because one of the assumptions that allow a good accuracy for a series expansion solution is that the initial temperature is uniform the solution provides good accuracy in the investigated case. If the target temperature (in the centre of the product) differs substantially from the boundary temperature the temperature prediction over several process steps is less accurate.

In order to investigate the industrial versatility of the developed equations it is needed to conduct a larger validation study of various geometries, for a wider range of processes, optimally with comparison to both experimentally determined temperature profiles and to numerical solutions. These investigations should be performed in close industrial collaboration and is a definite future scope.

6. Convective heat transfer coefficients

In heat transfer processes, the thermal response is characterized by the energy transport within the product, determined by the thermo physical properties, and the energy transferred to the product at the product surface governed by the boundary conditions the product is subjected to. The theory on heat transfer coefficient determination is presented in chapter 2.1.

All the presented methods in this section are with an industrial focus, meaning that the procedures in principle could be conducted at the food manufacturing sites.

This part of the study concerns method development for the determination of convective heat transfer coefficients. Two focus areas have been chosen, namely situations when the heating/cooling media is air, and when the heating/cooling media is a liquid.

Convective heat transfer coefficients in air cooling of packaged foods. The determination of different heat transfer coefficients at individual boundaries, and the consequence of an apparent headspace are presented.

Fluid-to-particle heat transfer during vessel cooking of suspended particles. A new method is proposed using a potato as the measuring device, which has practical advantages. In vessel cooking equipment, the often non-Newtonian properties of the liquid, supplied agitation, and induced boiling makes the possibilities of using a CFD approach extremely challenging, and due to agitation it is not easy to acquire the particle temperature with thermo-couples and use inverse calculations.

6.1. General procedure

In this section, the determination of the heat transfer coefficient through evaluation of the solid and an inverse calculation of the thermal curve is presented. The generalized inverse calculations are done through solving the heat equation with either a numerical or analytical solution (cf. 2.1.7). If aluminium is used as product replica, the thermal conductivity is very large (app. 170 [W/m·K] and the Bi-number is low. Below is an example where the characteristic dimension of the aluminium replica is 0.04 [m] and the heat transfer coefficient is 100 [W/m²K].

$$Bi = \frac{h \cdot R_{aluminum}}{k_{aluminium}} = \frac{100 \cdot 0.04}{170} = 0.024 \, [-]$$

The method presented in section 6.2 is an aluminium replica and calculation through the lumped capacitance model. In section 6.3 a real food item (potato) is used and the thermal curve is fitted with the Fourier series expansion.

The methodology is presented as an example using aluminium as the solid. For very low Bi-numbers the curve can be calculated using the lumped capacitance model (equation 1.1), recapitulated below:

$$\Omega = \left(\frac{T_s - T}{T_s - T_o} \right) = e^{-\left(\frac{h \cdot A}{m \cdot c_p} \right) t}$$

Where h [W/m^{2}K] is the heat transfer coefficient, A [m^2] is the exposed surface area, m [kg] is the mass, c_p [J/Kg·K] is the specific heat capacity and t [s] is the time. The dimensionless temperature difference Ω is calculated from measured temperature T at time t, the surrounding temperature T_s, and the initial product temperature T_0. In the experimental heating curve of the aluminium product the slope is equal to [$-(h·A)/(m·c_p)$] when ln(Ω) is plotted against the time. From the slope, the heat transfer coefficient can be determined from knowledge on the mass, the exposed surface area and the specific heat capacity. An example of the procedure is presented in figure 6.1, for an aluminium block having a surface area of 0.0332 [m^2], a mass of 0.648 [kg], a c_p of 2700 [J/kg·K] and an initial temperature 70°C, exposed to media of 5°C.
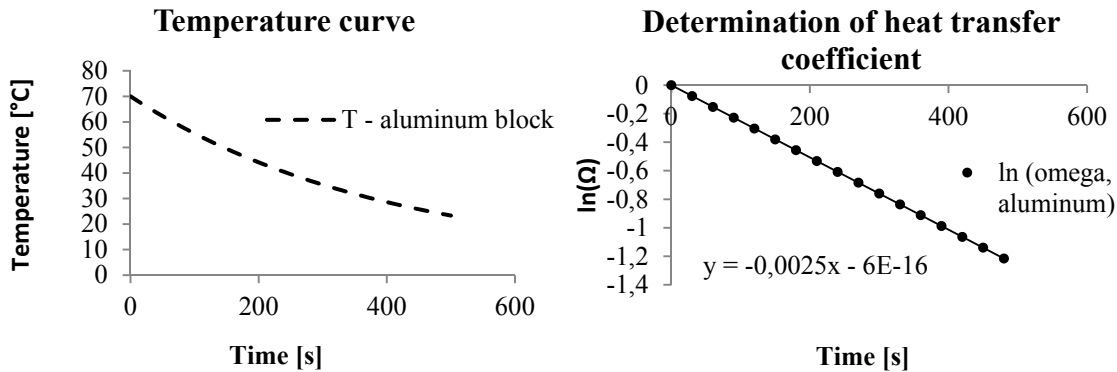
Figure 6.1 Procedure for determining heat transfer coefficients with aluminium.

From the temperature profile in figure 6.1 (left) the dimensionless temperature difference Ω is calculated and plotted logarithmically against the time. From the slope the heat transfer coefficient is calculated, in this particular case it is 50 [W/m^2·K]. The measured heat transfer coefficient resembles the average value exposed to the surface of the aluminium block.

In all experiments connected to this chapter the temperature is recorded using sensors (T-type thermocouples) connected to a computer with a data logger (Tc-08 Pico Technology, Cambridgeshire, UK) where the temperature is recorded every second.

6.2 Heat transfer coefficients in convective cooling

This part covers the convective heat transfer in the cooling of food products with circulating air. The general approach is to follow the method described in section 6.1.

In many situations the flow around the food creates a non-uniform heat flux depending on the boundary´s relative position to the direction of the airflow. Because many food products are cooled in the package, this investigation is focused towards packaged foods.

Often packaged foods have an apparent headspace, either because the package is not entirely filled with product before it is sealed or if a lid is attached before the cooling step, creating a narrow space with stagnant air in between.

This investigation is split into two small parts. Part one being the determination of individual heat transfer coefficients for boundaries that have a different relative position to the airflow. Part two is investigation of the influence of a headspace.

6.2.1 Heat transfer for individual boundaries

The heat transfer coefficients for individual boundaries are measured with an aluminium block. The aluminium block is heated to app. 45°C and placed in a large kitchen scale blast cooler (Gram KPS 18/30, Gram A/S Kolding, DK)

To investigate individual boundaries, a mould was carved in polystyrene wherein the aluminium block was inserted, only exposing the top surface of the aluminium block (figure 6.2). The experiments with the insulated block are conducted for all six relative positions to the airflow (top, bottom, side x 2, front and back). The results from the measurements are presented in table 6.1. In the experiments, the block can be rotated so that the aluminium surface is facing the airflow

Table 6.1 measured individual heat transfer coefficients

Geometry position	Local heat transfer coefficient [W/m^2·K]
Back	24.5
Sides	27
Front	33
Bottom	35
Top	32
Average	30
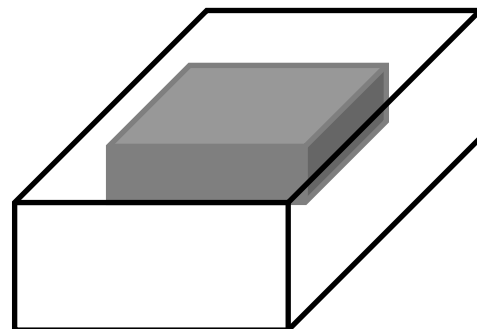
From the measurements in table 6.1 it can be seen that the values of the heat transfer coefficient is dependent of the relative position of the product to the airflow. However, these results should be considered with caution as the polystyrene insulation (being rather large) could change the flow pattern. In addition the measurements are only conducted to mimic one individual product. In a process line, several products could be placed close to each other which could change the airflow around the packages. For situations where the heat transfer coefficients are comparable, an average value would suffice, which makes the determination more straight forward. This is important because these have to be conducted on site at food manufacturers for enabling thermal calculations representable of their processes.

If the heat transfer coefficients for each boundary differs substantially it could be necessary to study the individual heat transfer coefficients. If a headspace is present or the product is placed on a conveyor band that provides insulation the heat transfer coefficient for each boundary differs substantially. In these cases it is necessary to study the individual heat transfer coefficients. This issue is presented in the following section

6.2.2 Influence of a headspace

In food processing the finished products are often cooled in the package. This is an advantage because they can be hot-filled in the package increasing the shelf life without the necessity of aseptic filling. In the design of food packages a headspace is often present. Due to package design, the headspace is often insulating the smallest characteristic dimension of the package. Because the smallest characteristic dimension is governing the cooling rate it is crucial to determine the effect on the heat transfer coefficient in the presence of a headspace.

To investigate the influence of a headspace, an aluminium block is inserted in a polystyrene insulated mould with an adjustable bottom. In the setup the heat transfer coefficient is measured for the exposed surface without a headspace and with a headspace of 5 [mm], 10 [mm] and 28 [mm]. The experimental setup is presented in figure 6.3.
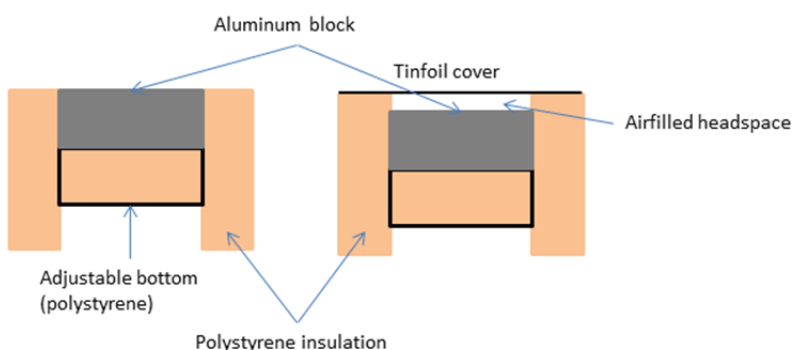
Figure 6.3 Experimental setup for the investigation of the headspace influence to the convective heat transfer coefficient

The results from the investigation are presented in table 6.2 where the results are compared to a calculation of the theoretical headspace influence through the overall heat transfer coefficient ($k_{headspace}$=0.0237[W/m·K], 50°C)

$$\frac{1}{U} = \frac{1}{h} + \frac{L_{headspace}}{k_{air}}$$

(eq.6.1)

NB: The assumption for using equation 6.1 in the presence of a headspace is that the air is stagnant.the difference between measured values and calculated values are presented in table 6.2

Table 6.2 Measured heat transfer coefficients with influence of headspace

Geometry position	Local heat transfer coefficient [W/m²·K]	Overall heat transfer coefficient (equation 6.1)
Exposed surface	32	32
Headspace 28 mm	7	1.1
Headspace 10 mm	9	2.2
Headspace 5 mm	10	4

It can be seen that a headspace influence the convective heat transfer coefficient. It is also seen that an overall heat transfer coefficient calculation cannot be used for investigation of large headspaces. A reason for this is that the air is not stagnant in these situations. For small headspaces (1-2 mm) use of the overall heat transfer coefficients will induce smaller errors because the air is more stagnant. Because the aluminium block was not perfectly insulated at the other boundaries the actual heat transfer coefficient is assumed to be lower than the measured.

6.3 Fluid-to-particle heat transfer coefficients (h_{fp}) – the use of potatoes as temperature indicators

This section presents the foundation for the submitted paper "Potatoes as potential devices for studying fluid-to-particle heat transfer in vessel cooking processes" attached in appendix 4.

Heating of suspended particles in a liquid is a very common operation in the food industry, for example in vessel cooking of soups and sauces with suspended pieces of meat and/or vegetables (Bouvier et al. 2011).

A theoretical calculation of fluid-to-particle heat transfer coefficients, (h_{fp}), under these conditions is very difficult if not close to the impossible because of the complicated movement of the particles. In agitated vessels the mode of heat transfer cannot be expected to be fully forced convection, because suspended particles generally follow the movement of the liquid, the slip velocities are low, and natural convection must contribute to the heat transfer as well. Natural convection evidently dominate if stirring is not applied or only used intermittingly to minimize mechanical damage (Bouvier et al. 2011).

This section describes a new method for evaluating h_{fp}, by using a potato as a model food particle and utilizing an observed gelatinization front as a temperature measurement. For further background information and validation of the method see appendix 4.

6.3.1 Methodology

The first step is to develop a simple procedure for determining the progression of the gelatinization front in potatoes immersed for a given time in a medium. The second step is to study the progression of the gelatinization front and the temperature profile in real time. From the gelatinization front, positional temperatures are indirectly measured as the gelatinization temperature is known through step one.

From the indirect temperature measurements an inverse calculation of the temperature profile enables a prediction of the fluid to particle heat transfer coefficient. For the full procedure description see appendix 4.

6.3.2 Results

The results are presented in three sections: Determination of the gelatinization temperature and conformation that the observed front in the potatoes is due to gelatinization of the native starch. Calculation of the heat surface to particle heat transfer coefficient with a standard Fourier series expansion for three theoretical examples. The feasibility of using a 1st term approximation to evaluate the heat transfer coefficient is investigated through a comparison with the complete series expansion solution.

The results are followed by a discussion of the sensitivity of the measurements based on position of the gelatinization front and determination of the gelatinization temperature.

The comparison of the experimentally determined heat transfer coefficient with a numerical solution of the experimental setup is found in the submitted paper, attached in appendix 4.

Fluid-to-particle heat transfer coefficients
Because the observed gelatinization front can be used as an indirect temperature measurement, a thermal history can be produced (appendix 4). The thermal history is not the temperature in a known position over time, but the position of a known temperature (67°C) over time. The heat transfer coefficient can be calculated from the relative position of the gelatinisation front, either by a numerical solution or an analytical solution to the heat equation. Only the analytical procedure is presented here. The Fourier series expansion for heat conduction in spheres is presented in equation 6.2 for relative positions (x/R) in the solid.

$$\Omega = \frac{(T_s - T)}{(T_s - T_0)} = \sum_i^\infty a_{\frac{x}{r},i} \cdot e^{-b_i \cdot Fo} = \sum_i^\infty \frac{sin\left[\lambda_i\left(\frac{x}{R}\right)\right]}{\lambda_i\left(\frac{x}{R}\right)} \cdot \frac{2(sin\lambda_i - \lambda_i cos\lambda_i)}{\lambda_i - sin\lambda_i cos\lambda_i} \cdot e^{-\lambda_i^2 \cdot \left(\frac{\alpha}{R^2}\right) \cdot t}$$ [6.2]

Where λ_i is the eigenvalue to the respective root function (cf. chapter 1.2), x/R is the position relative to the centre. In this case r is the diameter of the potato, x is the gelatinization front distance from the centre, α is the thermal diffusivity calculated from the composition (cf. chapter 1.2) and t is the time. T_s is the temperature of the heating medium, T_0 is the initial potato temperature and T is the gelatinization temperature, in this case 67°C. For the investigation with a first term approximation only the first eigenvalue is needed.

An example of the calculation is presented below for a 1st term approximation. The result is validated by a complete expansion solution at the determined Biot number.

Example calculations
A potato (R = 0.021 [m]) is heated in a media of 90°C with an initial temperature of 20°C. The thermo-physical properties (table 6.3) are estimated from the composition.

Table 6.3 Thermo-physical properties of potatoes (estimated from composition)

parameter	value	Unit
k_p	0.54	[W/(m·K)]
$C_{p,p}$	3671.6	[J/(kg·K)]
ρ_p	1076	[kg/m^3]
A	1.37·10^{-7}	[m/s]

Three situations are evaluated, all hypothetic x/R to a given time:

Case 1: After 600 [s] the potato is removed from the liquid and plunged into ice-water. The relative position of the gelatinization front to the centre is x/R=0.33 (0.014 [m] from the surface)

Case 2: After 900 [s] the potato is removed from the liquid and plunged into ice-water. The relative position of the gelatinization front to the centre is x/R=0.33 (0.0014 [m] from the surface)

Case 3: After 600 [s] the potato is removed from the liquid and plunged into ice-water. The relative position of the gelatinization front to the centre is x/R=0.62 (0.008 [m] from the surface)

The relative position *x/R* of the three cases at the respective time *t* are inserted into equation 6.2 and solved by iteration to find the roots that gives the solution:

$$\Omega = \frac{(T_s - T)}{(T_s - T_0)} = \frac{(90 - 67)}{(90 - 20)} = 0.329$$

In the calculation also an investigation in the sensitivity of the measured values (gelatinization temperature, position of the gelatinization front) is presented. The investigated sensitivity is conducted under assumption that the gelatinization temperature is known with 1°C precision (66.5-67.5 [°C]) and the gelatinization front can be measured with a precision of 1 [mm] (+/- 0.005 [m]). The calculation results from the three cases are presented in table 6.4.

Table 6.4 Predicted heat transfer coefficients using a 1st term approximation to equation 6.1

Case 1

Measured distance [m] x/R =0.33 (600s)	T_{gel}=66.5°C	T_{gel}=67°C	T_{gel}=67.5°C
0.0135	365 [W/m²K]	415 [W/m²K]	470 [W/m²K]
0.0140	328 [W/m²K]	**360 [W/m²K]**	410 [W/m²K]
0.0145	288 [W/m²K]	316 [W/m²K]	360 [W/m²K]

Case 2

Measured distance [m] x/R =0.33 (900s)	T_{gel}=66.5°C	T_{gel}=67°C	T_{gel}=67.5°C
0.0135	68 [W/m²K]	71 [W/m²K]	73 [W/m²K]
0.0140	66 [W/m²K]	**69 [W/m²K]**	71 [W/m²K]
0.0145	65 [W/m²K]	67 [W/m²K]	70 [W/m²K]

Case 3

Measured distance [m] x/R =0.62 (600s)	T_{gel}=66.5°C	T_{gel}=67°C	T_{gel}=67.5°C
0.0075	112[W/m²K]	118[W/m²K]	123[W/m²K]
0.008	104[W/m²K]	**108[W/m²K]**	113[W/m²K]
0.0085	96[W/m²K]	100[W/m²K]	104[W/m²K]

Based on the measured position and the predicted heat transfer coefficients in table 6.4, the gelatinization temperature is predicted by back calculation using the complete series expansion of equation 6.1, for validating whether a 1st term approximation is suited for the calculation. The validation is conducted for the

centre measurements from table 6.4 for the three cases. Figures 6.4-6.6 show the temperature curves using the entire expansion of equation 6.2.

Figure 6.4 Temperature profile for a spherical potato (radius=0.021m) heated in liquid media with a heat transfer coefficient of 360 [W/m²K] at relative position to the centre of (x/r=0.33) (left) residual between the complete expansion (equation 6.1) and a 1st term approximation (equation 1.5) in the process window of interest (right)
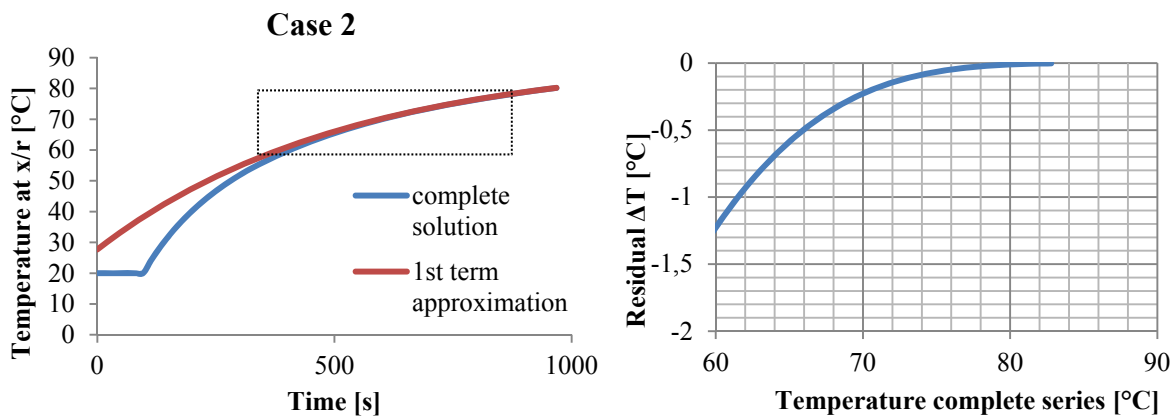
Figure 6.5 Temperature profile for a spherical potato (radius=0.021m) heated in liquid media with a heat transfer coefficient of 108 [W/m²K] at relative position to the centre of (x/r=0.62) (left) residual between the complete expansion (equation 6.1) and a 1st term approximation (equation 1.5) in the process window of interest (right)
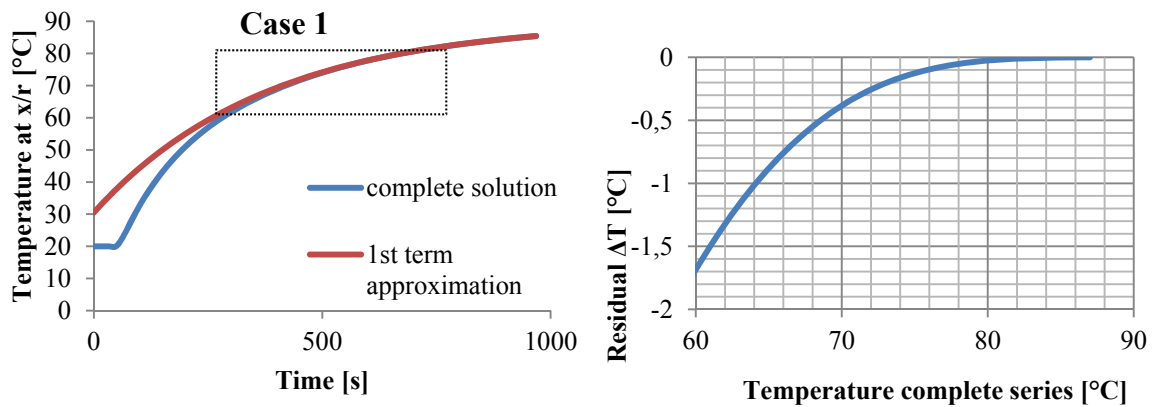
Figure 6.6 Temperature profile for a spherical potato (radius=0.021m) heated in liquid media with a heat transfer coefficient of 69 [W/m²K] at relative position to the centre of (x/r=0.33) (left) residual between the complete expansion (equation 6.1) and a 1st term approximation (equation 1.5) in the process window of interest (right)
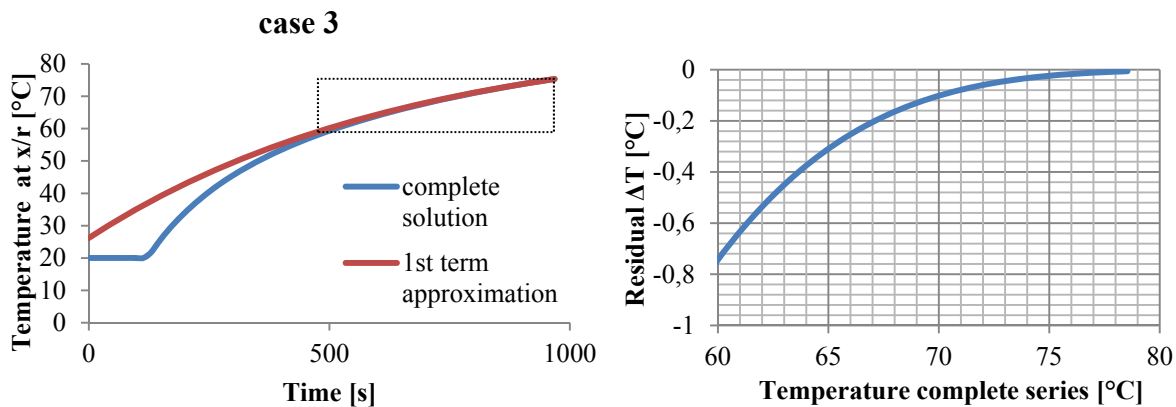
From the figures 6.4-6.6 (left) it can be seen that a 1st term approximation is only valid late in the process for predicting the temperature in the investigated positions (x/R). From the residual plot (right) it can be seen that the 1st term approximation predicts the gelatinization (67°C) temperature with a precision of (error<0.6°C). The error induced by the use of a 1st term approximation compared to the complete expansion is thus comparable to an error of 0.5°C in the assumed/determined gelatinization temperature. In the three cases the respective Fo-number is below 0.2 normally used as a criterion for the 1st term approximation. However chapter 7 (figure 7.8) it is presented that the point temperature in the middle between the surface and the centre calculated with a 1st term approximation converges much faster with the complete solution.

The conducted study presented in appendix 4, and further elaborated in this chapter is validated for particles heated in water. If the liquid is more viscous (soups or sauces) the heat transfer coefficients are generally lower. If the liquid is boiling the heat transfer coefficient is increased due to condensation of vapour to the particle surface and an increased convection. A small comparative study of the influence of boiling in water and non-Newtonian liquids is found in appendix 8. The results from the study emphasise that boiling is reducing the heating time for viscous fluids, but for water the convective heat transfer coefficients without boiling is sufficient (no significant decrease in heating time for the particles). In the comparative study (appendix 8) the heat transfer coefficient in commercial soups and sauces could be ten times lower than for water. In the submitted paper (appendix 4) on heat transfer coefficients the induced fluid to particle heat transfer coefficient was found to be around 400-500 [W/m²K].

The sensitivity of a determined heat transfer coefficient is calculated for four typical particles (green peas, frankfurter sausages, carrot cubes and potatoes) heated with varying heat transfer coefficients. In the study only heat transfer is included as a phenomenon. The heating time for the particles is defined as: the time to reach 78°C in the centre calculated from equation 1.3.

Figure 6.7 represents the heating time to reach 78°C from an initial temperature of 20°C as a function of the heat transfer coefficient. The thermal properties of the particles are calculated from the content of macronutrients. The characteristic dimensions of the investigated particles are: Peas (R=0.003 [m], sphere), frankfurters (R=0.095 [m], infinite cylinder), carrot cubes (L=0.005 [m], cubic) and potatoes (R=0.02 [m], sphere).
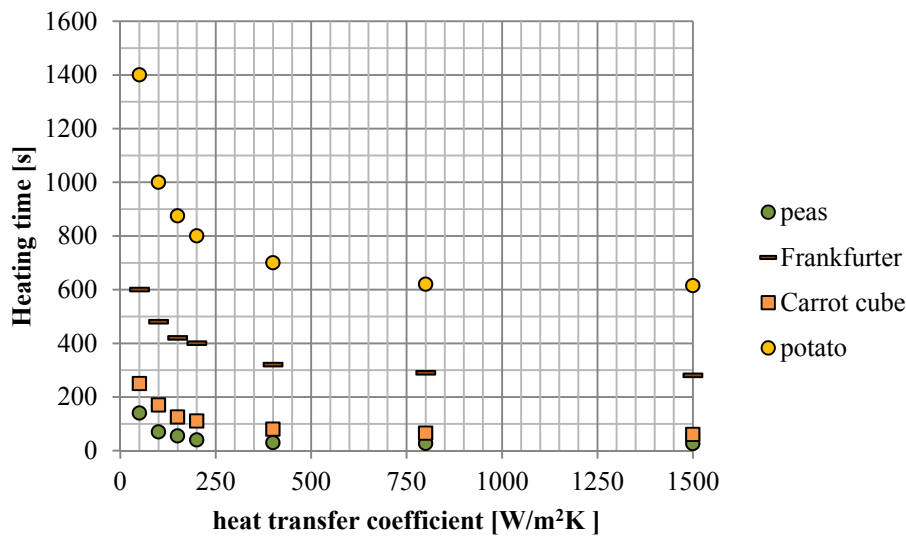
Figure 6.7 Heating time for selected food particles as a function of the fluid to particle heat transfer coefficient

From figure 6.7 it can be observed that the heating time for investigated particles does not decrease substantially with an increase in the heat transfer coefficient above app. 500 [W/m^{2}K].

6.4 Conclusion remarks

In this chapter two methods have been presented for determining convective heat transfer coefficients. For the determination of heat transfer coefficients for individual boundaries a method using aluminium is proposed where the other boundaries are insulated with polystyrene. The influence of a headspace was investigated and it was found that the use of overall heat transfer coefficient, assuming that the air in the headspace was stagnant is insufficient.

For the determination of fluid to particle heat transfer coefficients in vessel cooking a new procedure is presented where an observed gelatinisation front in potatoes could be used as a thermal indicator for inverse calculation of the heat transfer coefficient. Additional validation has shown that a 1st term approximation for the calculation can be applied with good accuracy.

The presented methods can be applied without the need for extensive modelling, and in most situations in the presented procedures a 1st term approximation or a lumped capacitance calculations of a thermal curve is adequate. The procedures can be used at the production sites but some staff education is needed to ensure a proper measure of the heat transfer coefficients.

7. Continuity and sensitivity

This chapter presents an analysis of the series expansion solution to the heat equation. The methodology in this chapter is to investigate the consequences of general assumptions and the sensitivity of parameters in the series expansion. For presenting the dynamics of the series expansion some of the deductions are also presented in this chapter whilst the explanation of the asymptotes is placed in appendix 6.

For predictive calculations of heating and/or cooling of solids it is important to be aware of the uncertainties induced by the choice of solution. To determine the precision of a predictive calculation an important activity is to assess the sensitivity of the parameters used in the calculation. Even though the focus of this chapter is the series expansion solution to the Fourier heat equation, the sensitivity analysis for the thermo-physical properties and the Biot number is more general and equally important in a numerical solution.

The Fourier series expansion for calculating the thermal response in solids during heating or cooling is described thoroughly in chapter 1.2 (equation 1.5), recapitulated below:

$$\Omega = \sum_{i=1}^{\infty} a_i \cdot e^{-\lambda_i^2 \cdot Fo}$$

In the analysis of the series expansion, two focus areas have been chosen: the continuity between the simplified solutions (1st term approximation and the lumped capacitance model) and the sensitivity of the Fourier expansion.

Continuity

Two criteria have been established where simplified expressions are adequate. For low Biot numbers (Bi<0.1) the lumped capacitance method can be used (equation 1.1) and for high Fourier numbers (Fo>0.2) the 1st term approximation can be used (equation 1.5). For crude calculations this is a big advantage.

The two criteria are well established in educational textbooks as well as acknowledged in research papers.

1. When the Biot number is below 0.1 the lumped capacitance method (equation 1.1) can be applied assuming negligible surface resistance to heat transfer (Singh and Heldman 2013 pp., Mills 1995 pp.32, Incropera and DeWitt 1996 pp. 216, Cengel and Ghajar 2011 pp.228, Ramaswamy et al. 1982, Ramaswamy and Shreekanth 1999, Balasubramaniam and Sastry 1994, Baptista et al. 1997)

2. When the Fourier number exceeds 0.2 the 1st term of the expansion (equation 1.5) is sufficient to evaluate the thermal response in the geometry (Mills 1995 pp.152, Singh and Heldman 2013 pp. Incropera and DeWitt 1996 pp. 226, Cengel and Ghajar 2011 pp.238, Heissler 1947, Ramaswamy et al. 1982, Ramaswamy 1999, Awuah et al. 1992)

The magnitude of the uncertainty induced by assuming the simplicity criteria is not presented in either textbooks or in literature and the continuity between the simplified solutions is not clear. The criterion for the use of the 1st term approximation is based on the temperature response in the centre. This chapter additionally presents how the convergence depends on relative position inside a product.

Sensitivity

The focus areas are in this section sensitivity of the thermo-physical properties and the sensitivity of the Biot number. The consequence of the number of terms used in a series expansion is also investigated to evaluate how many terms is needed for an accurate calculation.

Section 7.1 discusses the lumped capacitance model. Section 7.2 discusses the 1st term approximation and section. Section 7.3 discusses the sensitivity in the parameters used in the Fourier series expansion.

7.1 The limitations of the usage of the lumped capacitance method for infinite and finite specimens

The general equation for the series expansion used to calculate non stationary heat transfer for solids is presented in simple form (only the 1st term) below in equation 7.2. Because a process rapidly exceeds Fo<0.2 for situation at low Biot numbers (Bi<0.1), the 1st term approximation (equation 1.5), recapitulated below, is suitable for this analysis.

$$\Omega = a \cdot e^{-\lambda^2 \cdot \frac{k}{c_p \cdot \rho \cdot R^2} \cdot t} \qquad [7.1]$$

For situations where the Biot number is very low it is difficult to obtain the lag factor (a) and the Fourier exponent λ^2 in charts with a good precision. In these situations the internal resistance to heat transfer is negligible and it is standard procedure to use the lumped capacitance model recapitulated in equation 7.2.

$$\Omega = e^{-\left(\frac{A \cdot h}{V \cdot c_p \cdot \rho}\right) \cdot t} \qquad [7.2]$$

The consequences of utilising the lumped capacitance model as a function of the Biot number is investigated for elementary geometries (Infinite slabs, Infinite cylinders and spheres). From the standard presentation of the 1st term approximation (equation 7.1) and the lumped capacitance model (equation 7.2) it is difficult to see how they converge because equation 7.1 and equation 7.2 is represented by different characteristic dimensions, *R* and *A/V* respectively.

It is convenient to express the lumped capacitance model on a basis of the characteristic dimension (1/2 height for slabs and radius for cylinders and spheres). This is achieved by calculation of the area to volume ratio (A/V) of the infinite bodies.

Slab:

$$\frac{A}{V} = \frac{2 \cdot (length \cdot Width)}{Length \cdot Width \cdot Height} = \frac{2}{Height} = \frac{1}{1/2 height}$$

Cylinder:

$$\frac{A}{V} = \frac{\pi \cdot 2 \cdot R \cdot height}{\pi \cdot R^2 \cdot height} = \frac{2}{R}$$

Sphere:

$$\frac{A}{V} = \frac{4 \cdot \pi \cdot R^2}{\frac{4}{3} \cdot \pi \cdot R^3} = \frac{3}{R}$$

Generalised:

$$\frac{A}{V} = \frac{n}{R}$$

Where n, refers to the dimensionality (n=1 for infinite slabs, n=2 for infinite cylinders and n=3 for spheres). A generalized form of the lumped capacitance equation 7.2 can be written for infinite specimens as:

$$\Omega = e^{-\cdot\frac{n}{R}\cdot\frac{h}{c_p\cdot\rho}\cdot t} \qquad\qquad\qquad\qquad [7.3]$$

7.1.1 The continuity between the series expansion and the lumped capacitance method at low Biot numbers

The following describes the continuity between the series expansion and the lumped capacitance method. Initially it is relevant to investigate the limits for the series expansion exemplified by the 1st term:

$$\Omega = a \cdot e^{-\lambda^2 \cdot Fo}$$

$$1: a \to 1 \; when \; Bi \to 0$$

$$2: \lambda^2 \to n \cdot Bi \; when \; Bi \to 0$$

The mathematical explanation for the behaviour of the series expansion for Bi→0 is presented in appendix 6.

The mathematical reason for the behaviour of the Fourier exponent λ^2 at low Biot numbers is thoroughly described in appendix 6.

For Bi→ 0:

$$\Omega = e^{-n \cdot Bi \cdot Fo}$$

Written out:

$$\Omega = e^{-n \cdot \frac{h \cdot R}{k} \cdot \frac{k}{c_p \cdot \rho \cdot R^2} \cdot t} \;\leftrightarrow\; \Omega = e^{-\left(\frac{n \cdot h}{R \cdot C_p \cdot \rho}\right)t}$$

As recalled from the definition of the A/V ratio:

$$\frac{A}{V} = \frac{n}{R}$$

Thus:

$$\Omega = e^{-\left(\frac{A \cdot h}{V \cdot c_p \cdot \rho}\right)t} = e^{-n \cdot Bi \cdot Fo}$$

The consequences for the lumped capacitance assumption are as follows:

$$\Omega = a \cdot e^{-\lambda^2 \cdot Fo} = e^{-n \cdot Bi \cdot Fo} = e^{-\left(\frac{A \cdot h}{V \cdot c_p \cdot \rho}\right)t} \; (for \; Bi \rightarrow 0)$$

Hence the lumped capacitance assumption can be split into two assumptions:

Assumption 1: $a = 1$

Assumption 2: $\lambda^2 = n \cdot Bi$

The consequences of utilizing the lumped capacitance model is presented in figure 7.1 for low Biot numbers (0.02<Bi<1). Because the 1st term approximation is only valid in situations where the Fourier number is above 0.2, the consequences are presented at Fo=0.2 to exemplify the uncertainties.

The generally acknowledged criteria (Bi<0.1) and the uncertainties induced are not fully documented. The errors in the lumped capacitance assumption is clarified and documented below.

Residual when utilising the lumped capacitance method at Fo=0.2
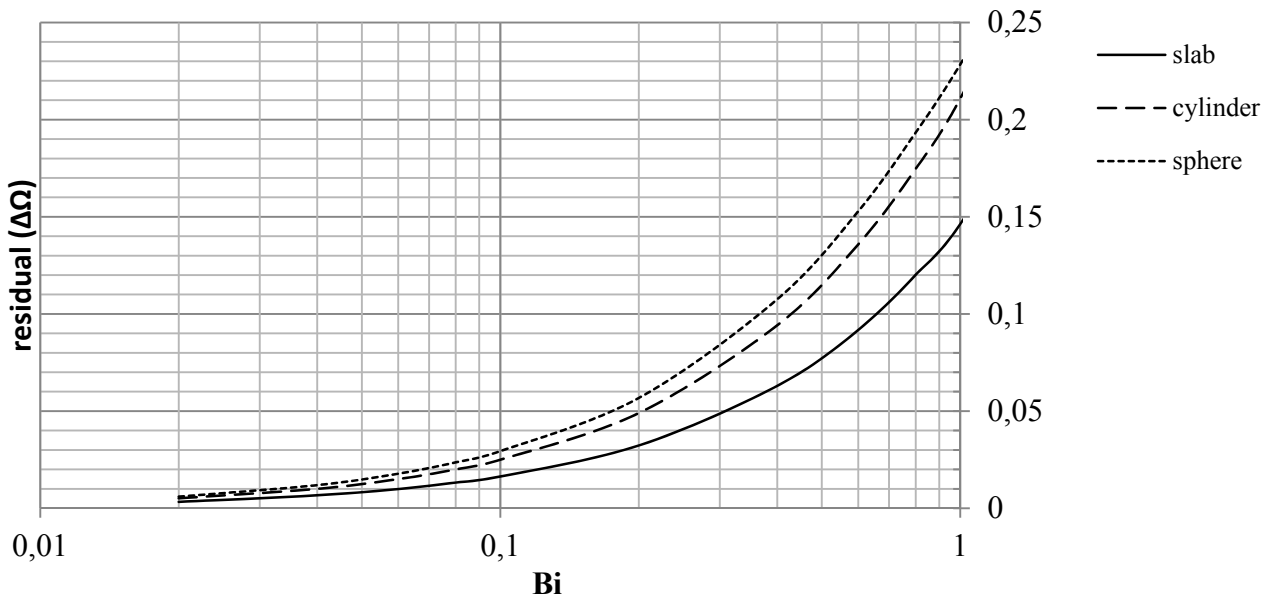
Figure 7.1 The residual between the series expansion solution (equation 7.1) and the lumped capacitance solution (equation 7.2) for low Biot numbers

At Bi=0.1 the residual ($\Delta\Omega$) is 0.015 for infinite slabs, 0.025 for infinite cylinders and 0.03 for spheres (figure 7.1). For interpretation of these residuals the dimensionless temperature difference Ω is used.

$$\Omega = \left(\frac{T_s - T}{T_s - T_0}\right) \hspace{6cm} [7.4]$$

Where T_s is the surrounding temperature, T_0 is the initial product temperature and T is the temperature at Time t. Following equation 7.4:

$$T = T_s - \Omega \cdot (T_s - T_0)$$

The residual ($\Delta\Omega$) converted to temperature difference:

$$\Delta T = \Delta\Omega \cdot (T_s - T_0)$$

The driving temperature difference (T_s-T_0) is seldom above 100°C in food processing (at atmospheric pressure). The consequence of utilizing the lumped equation is a maximum prediction error of 1.5°C for infinite slabs, 2.5°C for infinite cylinders and 3°C for spheres at Bi=0.1 based on the calculation results from figure 7.1.

NB: If the residual is required to be less than 1% ($\Delta\Omega$<0.01) the limitations for the use of the lumped capacitance model is: Bi<0.06 for infinite slabs, Bi<0.04 for infinite cylinders and Bi<0.03 for Spheres according to the results in figure 7.1.

7.1.2 Assumption $\lambda^2 = n \cdot Bi$

Further investigation of the error induced by the use of the Lumped capacitance is investigated in terms of the lag factor for the centre temperatures a_c , and the Fourier exponent λ^2.

Error in the Fourier exponent assumption (λ^2=n*Bi)
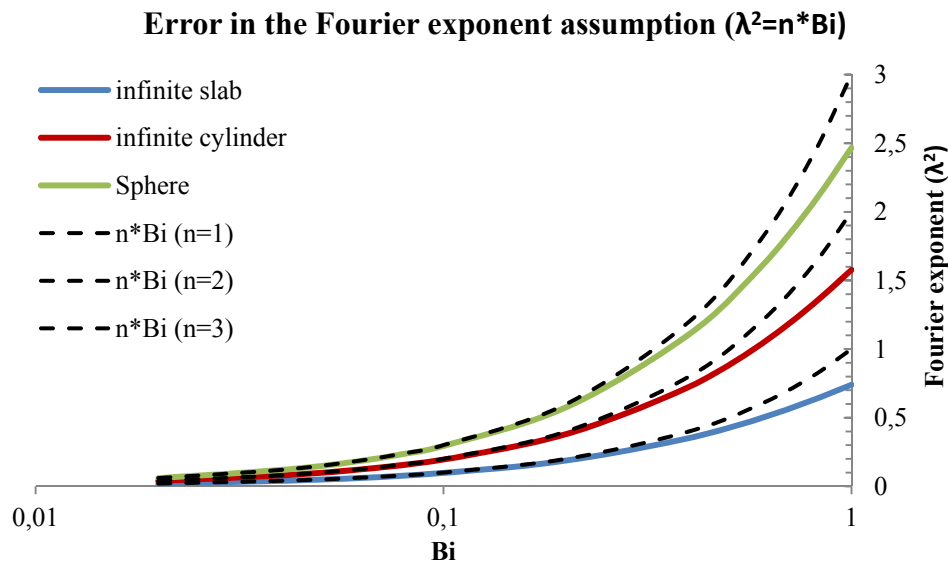
Figure7.2 The error induced in the Fourier exponent determination by the lumped capacity assumption for the 3 elementary geometries

The error in assuming negligible surface resistance to heat transfer does not induce big errors at Bi<0.1 in the determination of the Fourier exponent (figure 7.2). For Biot number above 0.1, the error increases dramatically. The resulting calculation error ($\Delta\Omega$) is presented in figure 7.3.

Residual difference induced by the Fourier exponent
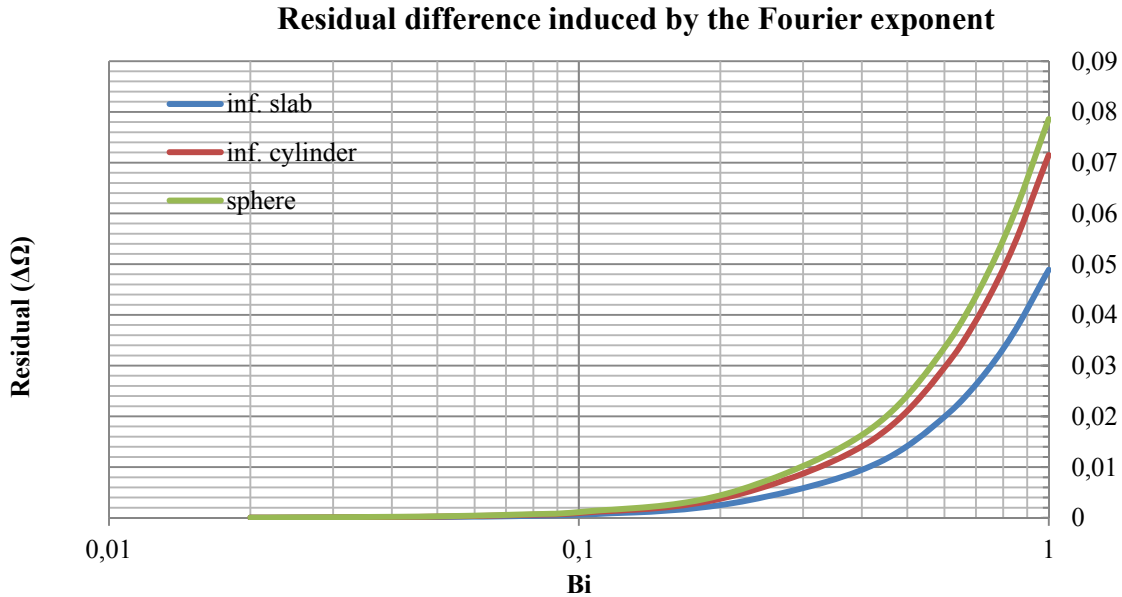
Figure 7.3 The residual from the lumped capacitance assumption induced by the error in the determination of the Fourier exponent

At Bi<0.1 the error in assuming the lumped capacitance model ($\lambda^2=n*Bi$) is only introducing a small residual in induced by the Fourier exponent $\Delta\Omega<0.002$, thus the residual from figure 7.1 is not induced by the error in the prediction of the Fourier exponent.

7.1.3 Assumption a=1

The lumped capacitance model also assumes that the lag factor is insignificant (a=1) according to equation 7.3, the actual lag factor as function of the Biot number is presented in figure 7.4

lag factor at low Biot numbers
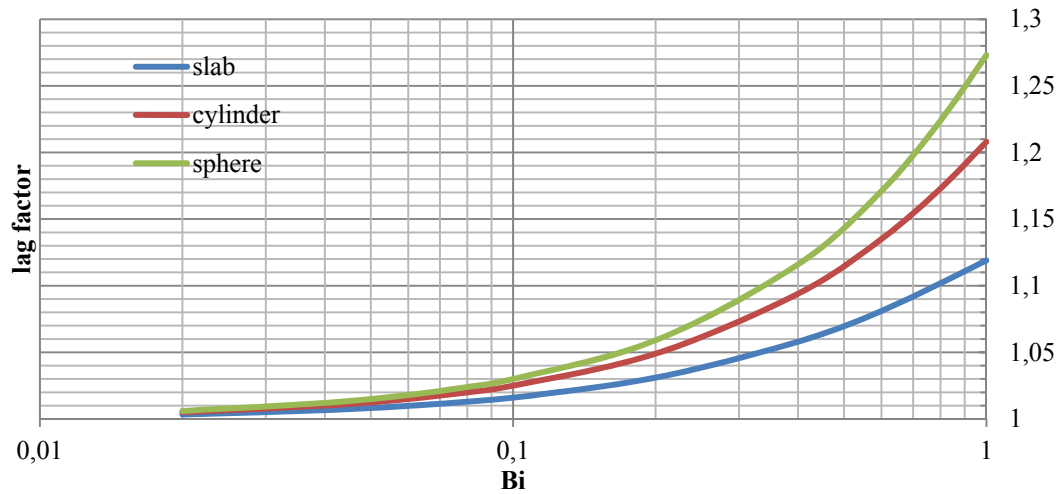
Figure 7.4 The error induced in the lag factor determination by the lumped capacity assumption for the 3 elementary geometries

The error in assuming the lag factor $a=1$ is accompanied by an error of up to 3% at Bi=0.1. The residual ($\Delta\Omega$) at Fo=0.2 is investigated in figure 7.5 as a function of the Biot number.

Residual difference induced by the lag factor (a) at Fo=0.2
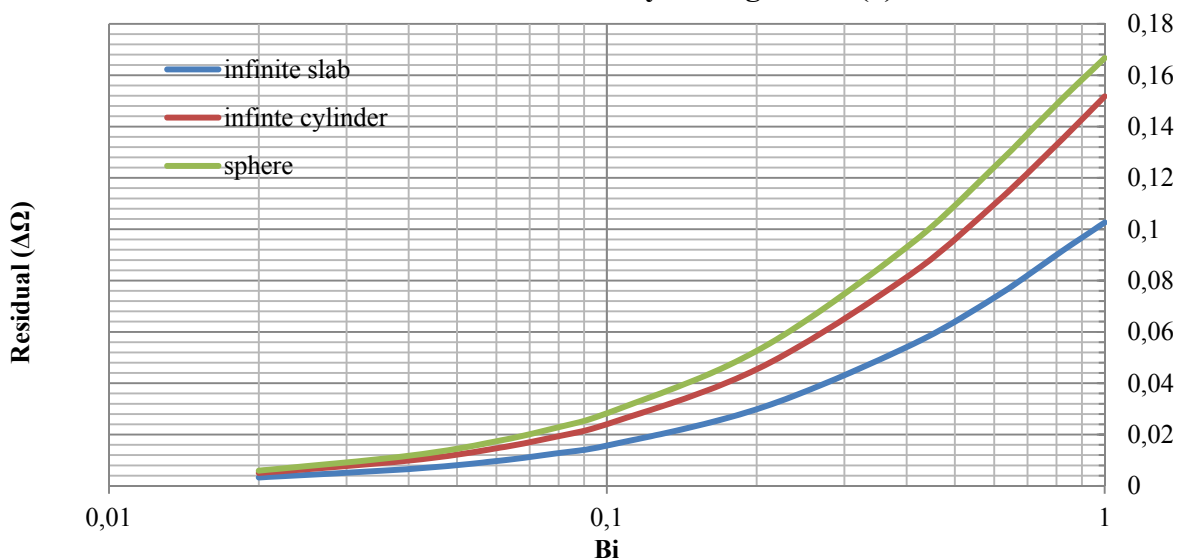
Figure 7.5 The residual from the lumped capacitance assumption induced by the error in the determination of the lag factor

From the investigation of the errors in assuming the lumped capacitance model ($a=1$, $\lambda^2=n*Bi$) it has been shown that the induced error is primarily caused by the lag factor for Bi<0.1. This is an important result because an error ($\Delta\Omega$) induced by the lag factor is static and do not propagate with time, if the error ($\Delta\Omega$) was induced by the Fourier exponent it would propagate with time as seen from equation 7.1.

It is thus convenient to have a simple estimation of the lag factor at low Biot numbers to correct for this static error. One example of this is presented by Ostrogorsky (2009), which has a good precision in this area. The approximation equations for the lag factor at low Biot numbers are presented in table 7.1

Table 7.1 Proposed simple equations for approximation of the lag factor for center temperatures in low Bi processes by Ostrogorsky (2009)

Geometry	Lag factor center (a_c) for Bi<1
Infinite slab	*(1+Bi/7)*
Infinite cylinder	*(1+Bi/4)*
sphere	*(1+Bi/3.5)*

The approximation of the lag factors presented by Ostrogorsky (2009) increase the accuracy of the lumped capacitance model without the need for determining the Fourier exponents. However since the presented simple calculations from chapter 3 and chapter 4 is valid for Bi>0.02 it would be more easy and transparent to change the criteria for the use of the lumped capacitance model from the present (Bi<0.1) to a more precise (Bi<0.02) where the static error is very low (less than 1%). The propagation of the lumped capacitance model as af unction of time (Fo) is presented in figure 7.6 the progression of the residuals from the lumped capacitance assumption is presented for the original criterion (Bi<0.1) and the proposed criterion (Bi<0.02) in figure 7.7. Both figures are presented by the geometry of a sphere.

Lumped capacitance propagation
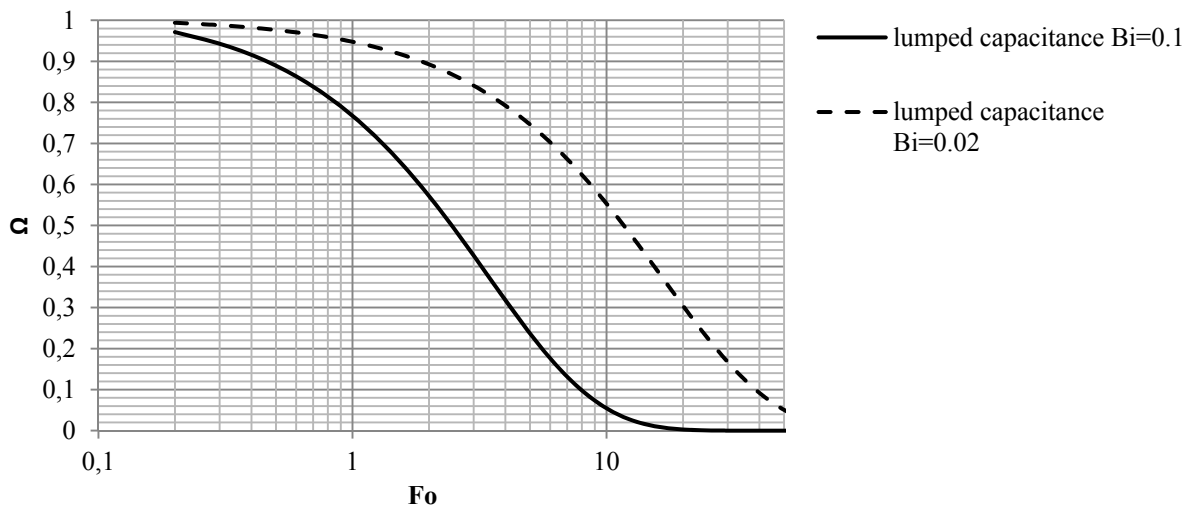
Figure 7.6 Propagation of the lumped capacitance model for the original criterion (Bi<0.1) and the proposed criterion (Bi<0.02)

The residual between the series expansion solution (equation 1.1) and the lumped capacitance solution (equation 1.3) for Bi=0.1 and Bi=0.02.

residual of the Lumped capacitance
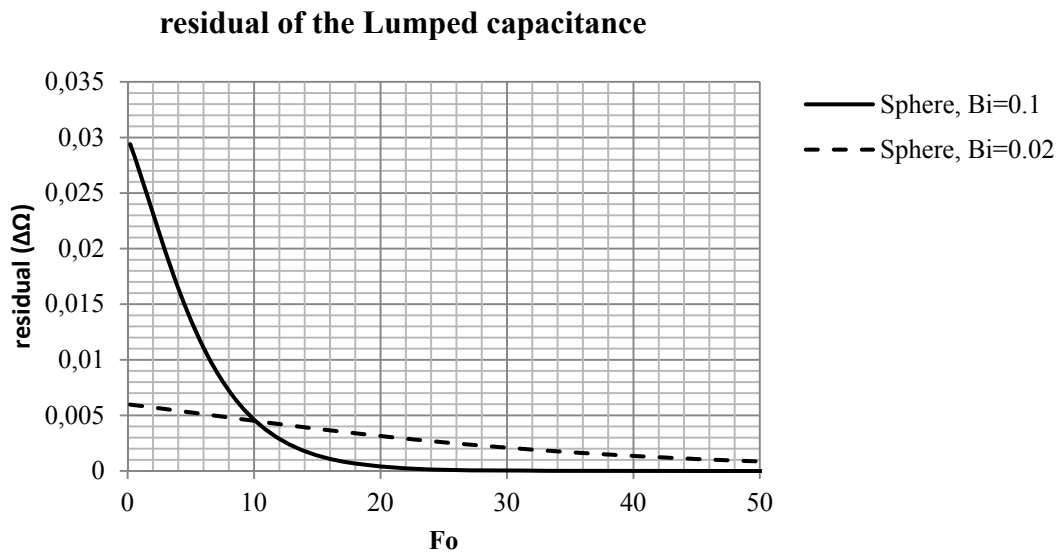
Figure 7.7 Propagation of the residual induced by the lumped capacitance assumption for the original criterion (Bi<0.1) and the proposed criterion (Bi<0.02)

From figure 7.6 it is seen that a significant temperature response only for rather large Fourier number (Fo>0.3). From the residual plot in figure 7.7 it is seen that the residual is reducing with time and the worst prediction error is at the beginning of the process as expected from the analysis in the previous sections.

7.2 Uncertainties accompanied with the 1st term approximation

The criterion acknowledged for the adequacy of the 1st term approximation to the heat equation at Fo>0.2 is investigated in this section. The centre temperature response, the spatial temperature response and the volume average temperature response is covered.

The thermal response in a given geometry is calculated from the series expansion using "HEATMAN" with 100 terms applied in the solution used as the complete analytical solution subtracted from the 1st term approximations is subtracted to obtain the residual. Figure 7.8 exemplifies the procedure for a sphere at Bi=4, 0<Fo<0.2 calculated from equation 4.2 recapitulated below.

$$\epsilon = \Delta\Omega = \left(a_1 \cdot e^{-\lambda_1^2 \cdot Fo} - \sum_{i=1}^{\infty} a_i \cdot e^{-\lambda_i^2 \cdot Fo} \right)$$
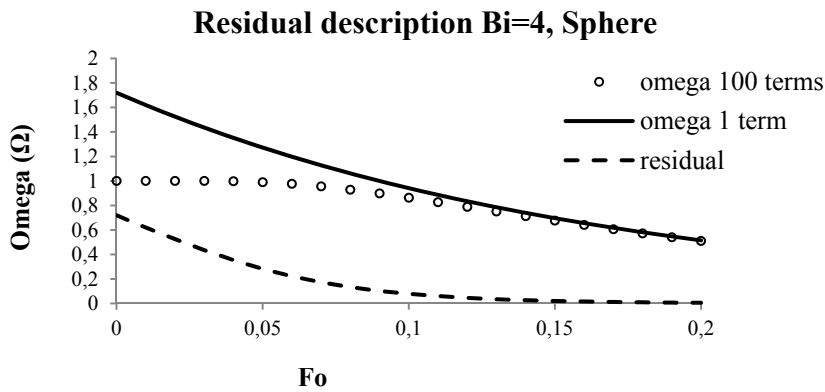
Figure 7.8 graphical representation of the residual between the exact series solution and the 1st term approximation to the series expansion.

This procedure is conducted for the elementary geometries as a function of the Fourier number for 21 selected Biot numbers (0.02:0.1:0.02, 0.2:1:0.2, 2:10:2, 10:50:10, 100). From this investigation the residuals for the criteria Fo>0.2 can be studied.

7.2.1 Induced error at Fo=0.2

The general criteria for utilization of the 1st term approximation for non-stationary heat transfer (Fo>0.2) is investigated with regards to induced uncertainty. As described in the above section, the residual ($\Delta\Omega$) is presented at Fo=0.2 as a function the Biot number. Initially the residual error introduced by assuming that the 1st term approximation is sufficient at Fo=0.2 is presented in figure 7.9.

Residual error at Fo=0.2
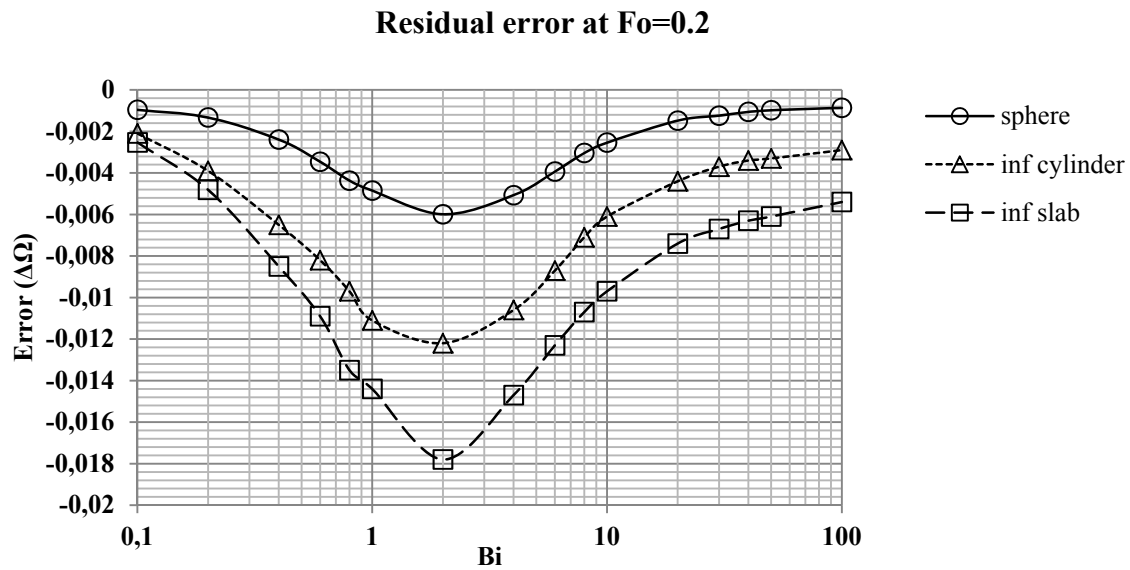
Figure 7.9 Maximum residual calculated from eq.6 for the elementary geometries at Fo=0.2

As it can be seen from figure 7.9 the nominal residual error for all elemental geometries is largest at Bi=2 (0.006 for spheres, 0.012 for infinite cylinders and 0.018 for infinite slabs). Biot numbers close to the value of 2 where the largest residual is introduced is very common in food manufacture.

7.2.2 Corresponding Fourier number at $\Delta\Omega<0.01$

As described in the beginning of this chapter, the criterion in literature is Fo>0.2 for acceptance of the residual in using only the 1st term in the series expansion. However this criterion is not presented along with the induced prediction errors as calculated here and presented in figure 7.9. Additionally this criterion is based only on the centre temperature. It is of interest to know at which process time (Fo) the residual ($\Delta\Omega$) is less than 0.01 as a function of the position in the specimen. To achieve this, the residual is calculated based on equation 4.2 for (0.1<Bi<100: 0<Fo<0.5: 0<x/R<1). The maximum Fo number to obey the criterion is presented in figure 7.10 as a function of the position in the specimen (0=centre, 1=surface). In general the maximum Fourier number that obeys $\Delta\Omega<0.01$ is found for 2<Bi<4, as expected from figure 7.9.
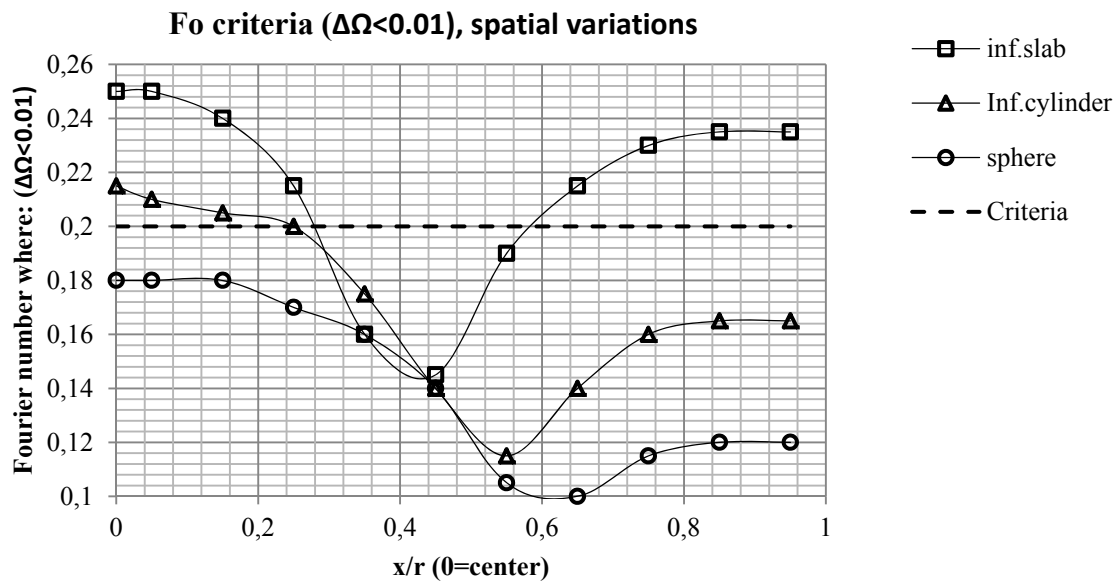
Figure 7.10 Fourier number obeying the criterion ΔΩ<0.01 as a function of the internal position within elementary geometries.

The convergence criterion is very dependent on the position inside the specimen (figure 7.10), and in general the centre temperature converges at the highest Fo number, notably higher than the in literature acknowledged 0.2. It should also be noted that the corresponding Bi numbers (not presented here) referring to the slowest convergence is close to 2 in all situations as expected from the investigation from figure 7.9.

7.2.3. General geometries - case example

For general geometries the situation is more complex because even though the process time is obviously the same for the different dimensions of a given product, the corresponding Fourier number is different if the dimensions have a different characteristic length. The situation is discussed with the following example:

A box shaped packaged food item is to be cooled in a blast cooler. The product dimensions are width=0.1[m], height=0.04[m] and length=0.2[m]. The heat transfer coefficient is 25 [W/m^{2}K] and the thermal conductivity is assumed to 0.45 [W/mK]. Giving the following Biot numbers for the three dimensions:

1. Bi_{width} =5.6
2. Bi_{length}=11.1
3. Bi_{height}=2.2

Because all Fourier numbers needs to be above 0.2 in order to agree with the criterion for the use of the 1st term expansion, and the Fo-number scales by $1/L^2$

1. Fo_{length}=0.2
2. Fo_{width}=0.8

3. $Fo_{height}=5$

Thus for a finite specimen the criteria for using the 1st term approximation is more complicated. Because the smallest dimension is the main contributor to the rate of cooling it might not be possible to evaluate the process by a 1st term approximation, as presented in figure 7.11 for the volume average temperature and 7.12 for the centre temperature. The 1st term approximation is in this case compared with the developed equations (4.9 for the centre temperature and 4.10 for the volume average temperature), presented and validated in chapter 3, 4 and 5. The blue lines represent the 1st term approximation (eq 1.5) for the investigation and the red lines represent the approximated complete solution (equation 4.9).

Volume average temperature
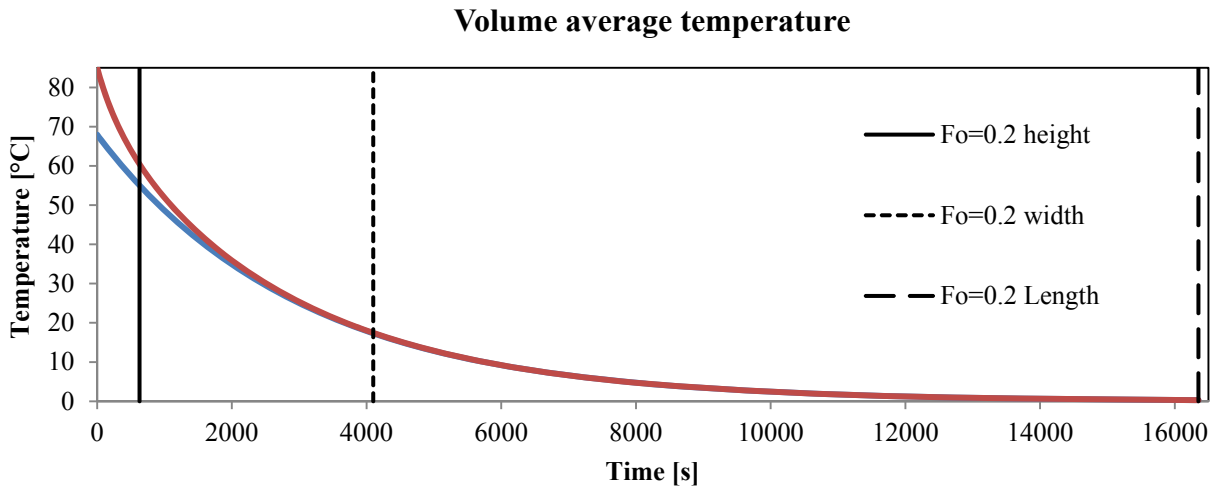
Figure 7.11 Volumetric average temperature history of the cooling case with indication of the dimensional Fourier number criteria

Center temperature
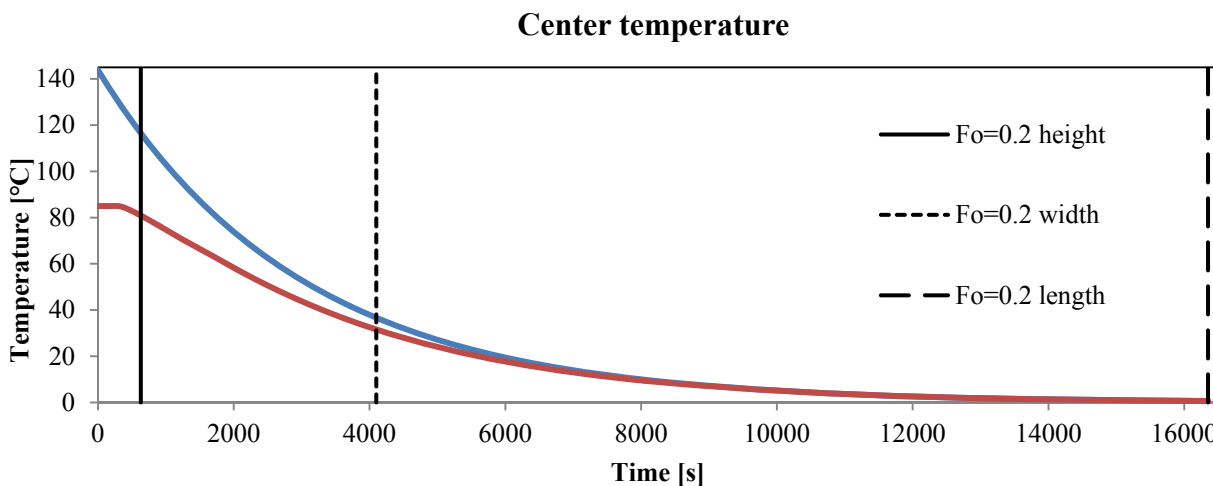
Figure 7.12 Centre average temperature history of the cooling case with indication of the dimensional Forier number criteria

From the case results in figure 7.11 and 7.12 it is observed that the criterion Fo<0.2 is very sensible to the interpretation of dimensions. Also it is observed that upon calculation of the temperature history (especially for the centre temperature) the 1st term approximation is only valid late in the process for the tested finite

geometry. To solve this, the developed equation (eq. 4.9) or more terms in the expansion (eq. 1.1) could be used

7.3 Sensitivity of the Fourier series expansion

The sensitivity using the Fourier expansion is here defined as the variations in the calculation results caused by a specific variation in the input parameters. Covered in this section are: the precision of the series expansion depending on the number of terms used for the calculation, the sensitivity of the thermo-physical properties and the sensitivity of the Biot number.

7.3.1 Number of terms used in a series expansion

It is well acknowledged that for high Fourier numbers (Fo>0.2) only 1 term in the series expansion is needed in order to achieve a good approximation of the thermal response. If the initial part of the thermal history curve is of interest, then how many terms is actually needed to achieve a good prediction?

In a recent paper Uyar and Erdogdu (2012) used a method where 10.000 terms were used in the calculation of the centre and volume average temperature with the scope to identify how a simple model (series expansion solution) could be used in process control.

Even though the computer power is not a limiting factor for the number of terms used in a series expansion solution, there is no need for using excessive number of terms. The evaluation of the number of terms needed is exemplified in this section for the centre temperature and the volume average temperature of a sphere. The example is representative for all elementary geometries as can also be seen in figure 1.2 in chapter 1.

Centre temperature
The number of terms needed in the series expansion for the prediction of the centre temperature depends on which level of prediction is accepted at low Fourier number. For this investigation the complete series is presented by a 100 term solution. The convergence of the first 5 terms is presented in figure 7.13 and 7.14.

Sphere, Bi=2, Center temperature
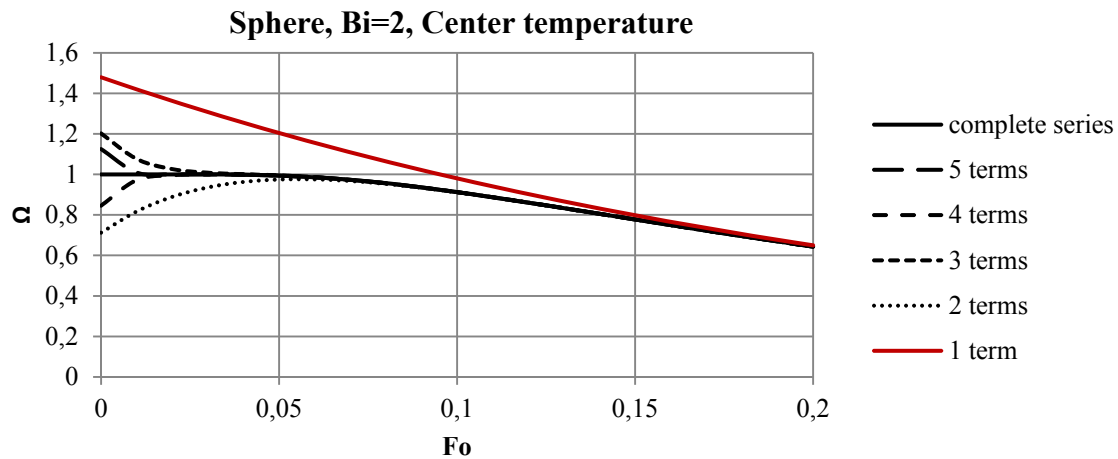
Figure 7.13 Convergence to the complete expansion when an increased number of terms are applied in the series expansion for a sphere with a Bi-number of 2.

Sphere, Bi=50, Center temperature
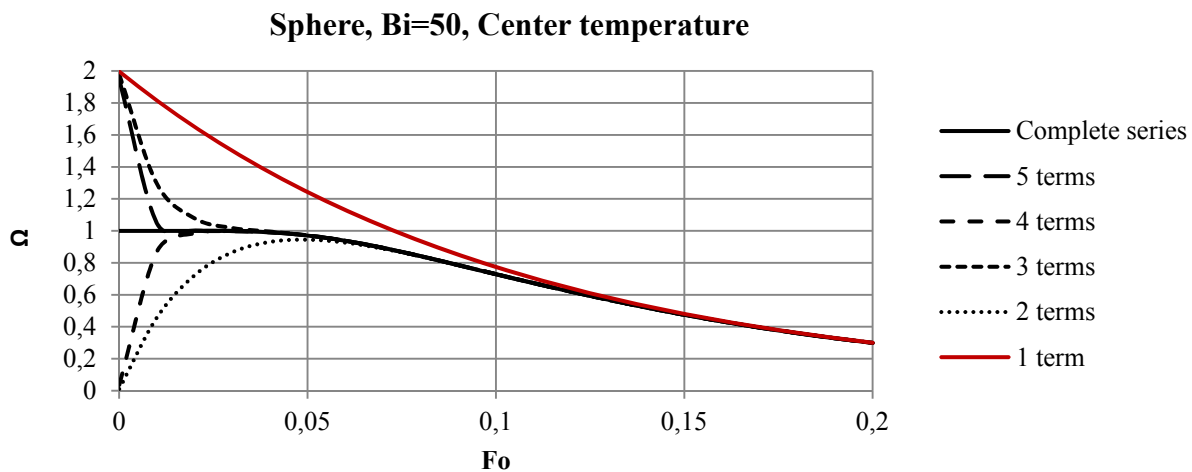
Figure 7.14 Convergence to the complete expansion when an increased number of terms are applied in the series expansion for a sphere with a Bi-number of 50.

From the investigation presented in figure 7.13 and 7.14 it can be seen that only using a few terms it is possible to predict the entire history curve for the centre. Before the heat has penetrated to the centre (Fo<0.03) the dimensionless temperature response, $\Omega=1$.

Volume average temperature
The convergence of the volume average temperature is also of interest in food processing (often a target in cooling processes). The convergence to the complete series expansion is investigated and exemplified in the presentation of a sphere with a Biot number of 10, and 50 in figure 7.15 and 7.16.

Sphere, Bi=10, Volume average temperature
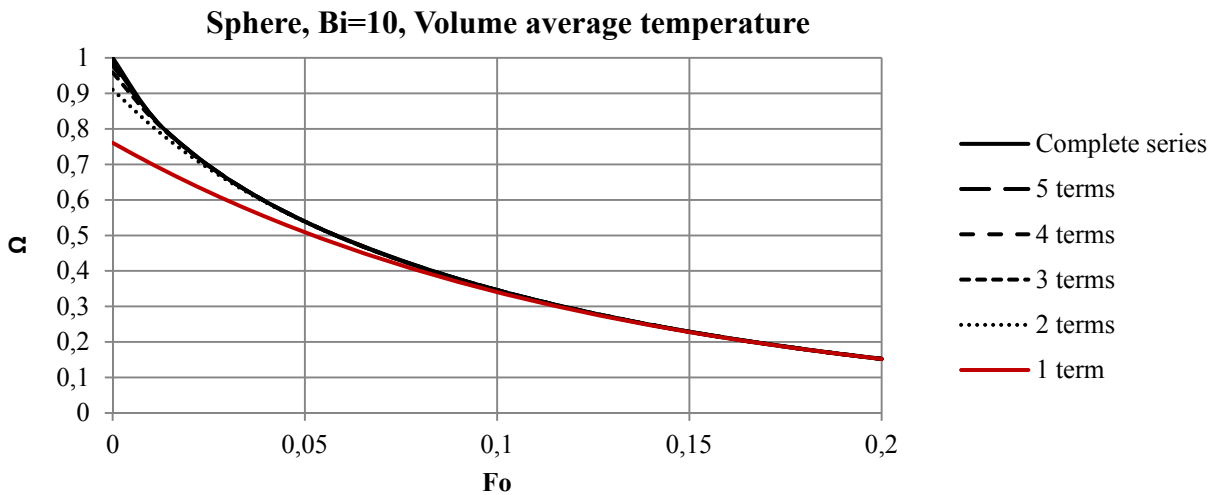
Figure 7.15 Convergence to the complete expansion when an increased number of terms are applied in the series expansion for a sphere with a Bi-number of 50.

Sphere, Bi=50, Volume average temperature
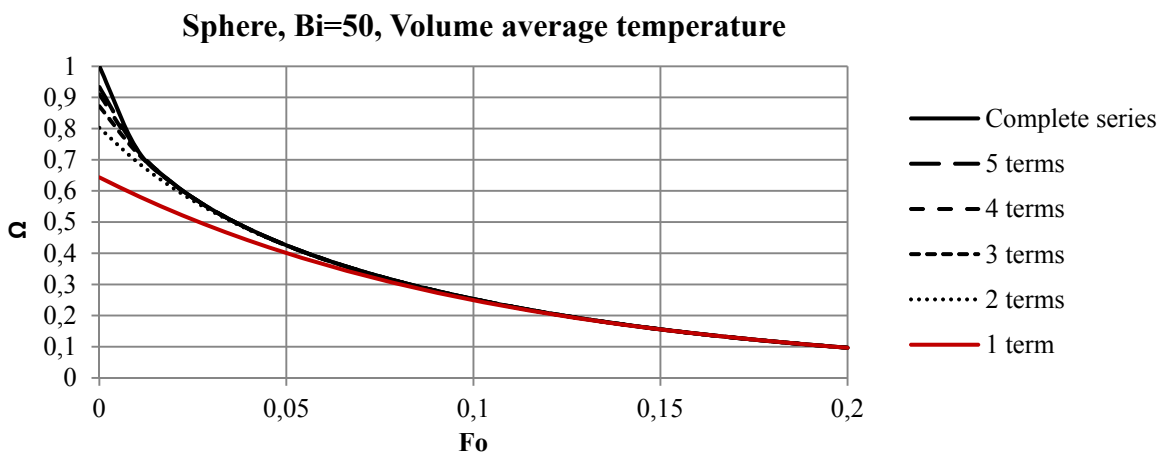
Figure 7.16 Convergence to the complete expansion when an increased number of terms are applied in the series expansion for a sphere with a Bi-number of 50.

From figure 7.15 and 7.16 it is seen that also for the volume average temperature only a few series is needed in order to have a convergence with the complete expansion for Fo>0.03. However for the volume average temperature also the very initial phase is diverging from a 1st term approximation. If a good prediction is needed in the very initial phase, several terms are thus needed. In heat transfer processes the volume average temperature in the very initial phase is of little interest. This is in contrast to mass transfer processes, where the same mathematics is used in a series expansion solution, the very initial phase is of great interest (e.g. in salting and brining operations).

The number of terms needed to investigate point temperatures outside the centre is more challenging because it is very dependent on the relative position to the centre. For positions close to the centre, only a few terms are needed whilst for positions close to the surface (x/R =0.95) many terms are needed to get a good approximation for the initial phase (Fo<0.2). The convergence for the surface temperatures are presented in figure 7.17 for a sphere with a Biot number of 2 and figure 7.18 for a Biot number of 10.
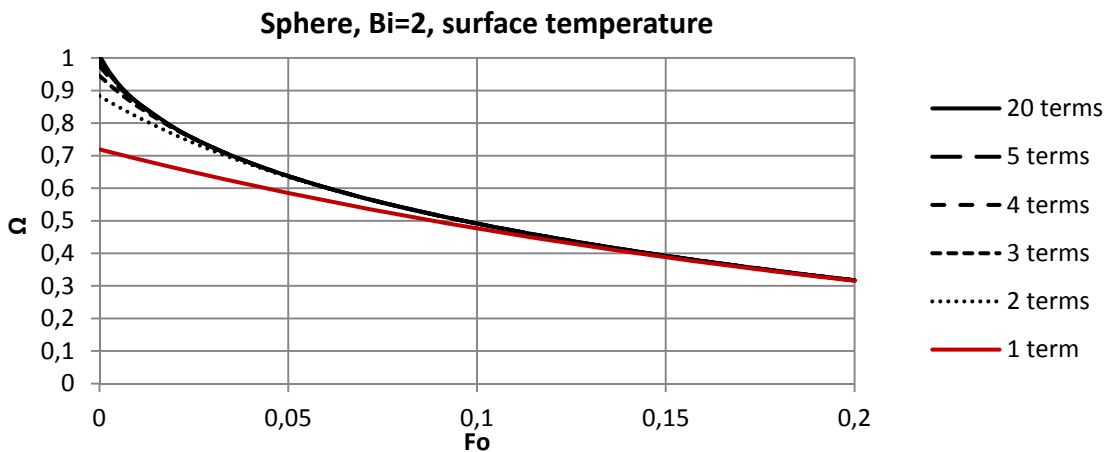
Figure 7.17 Convergence of the series expansion using an increasing number of terms for the surface temperature of a sphere with a Biot number of 2
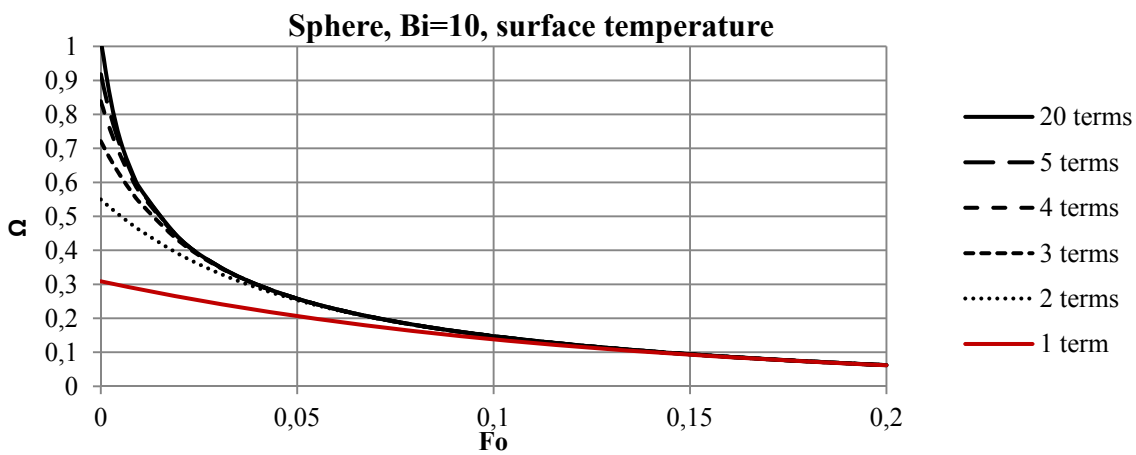
Figure 7.18 Convergence of the series expansion using an increasing number of terms for the surface temperature of a sphere with a Biot number of 10

From the graphs in figure 7.17 and 7.18 it can be seen that for a series expansion solution for the surface temperature many terms are needed to describe the very initial phase, where a dramatic change in the temperature is occurring very early in the process.

7.4.2 Sensitivity for the parameters in the series expansion.

In this section the sensitivity of the parameters included in the series expansion solution is discussed. The focus in this investigation is the Biot number and Biot number related sensitivity. In the investigation the temperature dependence of the thermophysical properties are not considered. In generalized form, the series expansion describes the correlation between a time input and a temperature output based on the physical phenomenon of heat transfer. The series expansion solution is recapitulated below. For this investigation the 1st term approximation for the centre temperature is used to exemplify the sensitivity of parameters.

$$\Omega = \left(\frac{T_s - T}{T_s - T_0}\right) = a_1 e^{-b_1 \cdot Fo}$$

The equation is expanded below to highlight the parameters:

$$\Omega = \left(\frac{T_s - T}{T_s - T_0}\right) = f(Bi)e^{-f(Bi)\cdot\frac{k}{\rho\cdot c_p\cdot R^2}t}$$

Expanding the Biot number:

$$\Omega = \left(\frac{T_s - T}{T_s - T_0}\right) = f\left(\frac{h\cdot R}{k}\right) \cdot e^{-f\left(\frac{h\cdot R}{k}\right)\cdot\frac{k}{\rho\cdot c_p\cdot R^2}t} \qquad\qquad [7.5]$$

From this expanded version of the Fourier expansion the sensitivity can be studied more directly.

The sensitivity of the density (ρ), and the specific heat capacity (c_p), is directly coupled with the exponent, and has thus a high sensitivity to the output of the equation. The density and the heat capacity can often be determined with adequate precision based on the composition of the food. The characteristic dimension (R) has a high impact on the calculation as it is influencing the exponent squared. The characteristic dimension is often not a big challenge to measure for elemental and general geometries. If the geometry is complex, the dimensions are difficult to determine, however the series expansion is less suited for very complex geometries where a numerical solution is more suited.

The sensitivity of the thermal conductivity is important because it is a part of both the Fourier number and the Biot number, and also the sensitivity of the thermal conductivity is dependent on the value of the Biot number. This is best described through the lumped capacitance equation in extended form (equation 7.3) valid for (Bi<0.1) where the sensitivity of the conductivity is 0. If Bi is approaching infinity, the influence of the thermal conductivity for the calculation is directly proportional to the exponent. The thermal conductivity is more difficult to measure than the density and the heat capacity, and also the temperature dependency of the thermal conductivity is larger.

Sensitivity of the Biot number

The sensitivity of the Biot number as most directly explained through the sensitivity of the lag factor and the Fourier exponent which are both a function of the Biot number. This is presented above in equation 7.5. The sensitivity of these two parameters is evaluated by utilizing the normalized Biot number presented in chapter 3.

$$Bi_{norm} = \frac{Bi}{1 + Bi}$$

The relation between the normalised Biot number and the lag factor a_c and the Fourier exponent λ^2 can be seen in figure 7.19 and 7.20.
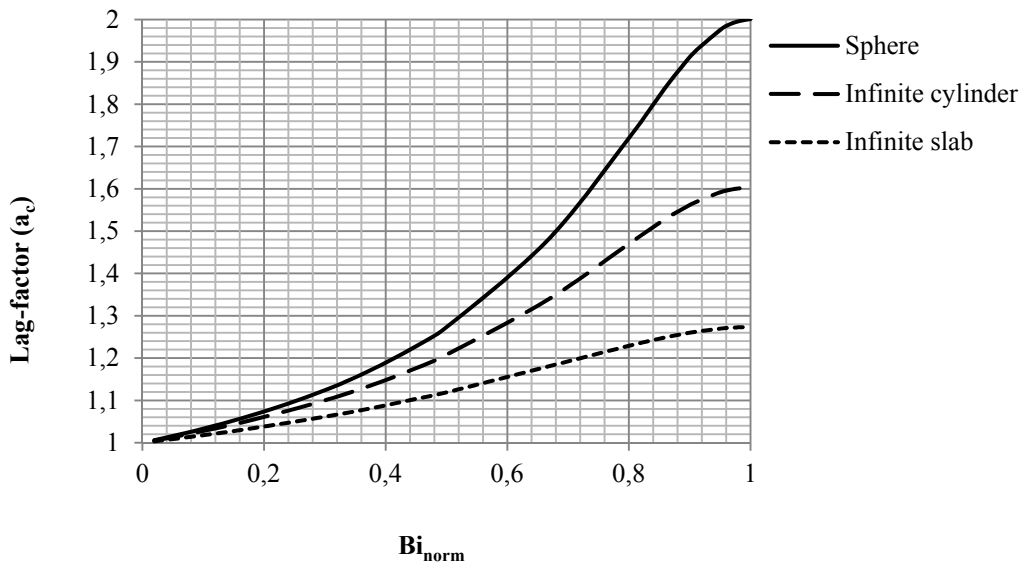
Figure 7.19 Relation between the normalised Biot number and the lag factor for infinite slabs
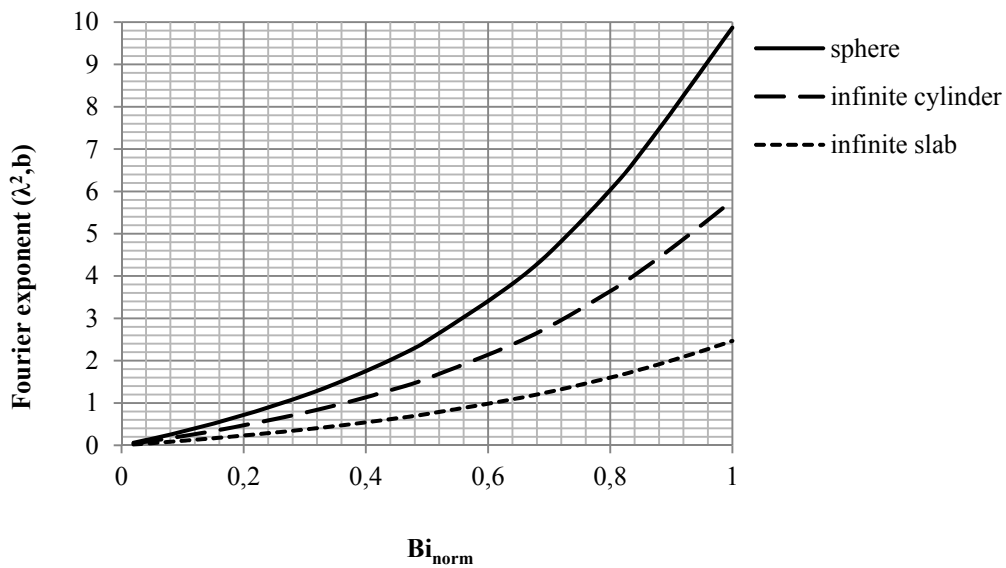
Figure 7.20 Relation between the normalised Biot number and the first Fourier exponent

The close relation between the sensitivity of the normalised Biot number to both the lag factor and the Fourier exponent makes the normalised Biot number an easy way to investigate the sensitivity in the calculations with the Fourier series expansion. This is exemplified by 4 examples:

A Biot number in a process has been determined with an accuracy of +/-20% (due to uncertainties in the determination of the dimension R, the thermal conductivity k and the heat transfer coefficient h) the four determined Biot numbers are in this case 0.2, 1, 5 and 20. Calculation of the normalised Biot number:

3. $Bi_{norm} = \frac{0.2}{0.2+1} = 0.166$

4. $Bi_{norm} = \frac{1}{1+1} = 0.5$

5. $Bi_{norm} = \frac{5}{5+1} = 0.833$

6. $Bi_{norm} = \frac{20}{20+1} = 0.952$

The implications of an uncertainty of 20 % is calculated and the variety in the normalized is presented as:

1. $Bi_{norm} = \frac{0.16}{0.16+1} \rightarrow \frac{0.24}{0.24+1} = 0.14 - 0.19$

2. $Bi_{norm} = \frac{0.8}{0.8+1} \rightarrow \frac{1.2}{1.2+1} = 0.44 - 0.55$

3. $Bi_{norm} = \frac{4}{4+1} \rightarrow \frac{6}{6+1} = 0.8 - 0.86$

4. $Bi_{norm} = \frac{16}{16+1} \rightarrow \frac{24}{24+1} = 0.94 - 0.96$

From this small investigation it can be seen that the determination of the Biot number is most sensitive at Biot numbers close to 1 as a function of the Fourier number. If the Biot number is very high or very small it is less sensitive to its determination. However, it should be noticed that the propagation of the error is dependent on the process time as well, and that processes at very low Biot numbers are finalized at much higher Fourier numbers. This can be seen in figure 7.21 where a 1st term approximation of the 4 presented Biot numbers are presented with indication of the 20% error line.
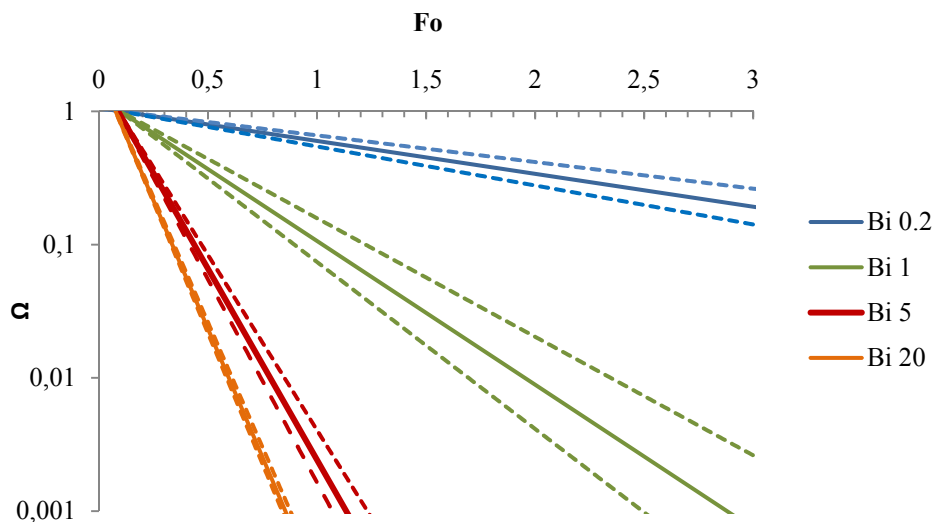
Figure 7.21 Propagation of the prediction of the centre temperature of a sphere at selected Biot numbers. The y axis is logarithmic to compare the error related to the Fourier number. The dashed lines indicates the consequence of a 20% error in the estimation of the Biot number

If the error propagation is investigated in form of the prediction error of Ω as a function of the target point e.g. 0.1 the result is somewhat different. This can be viewed in figure 7.22.
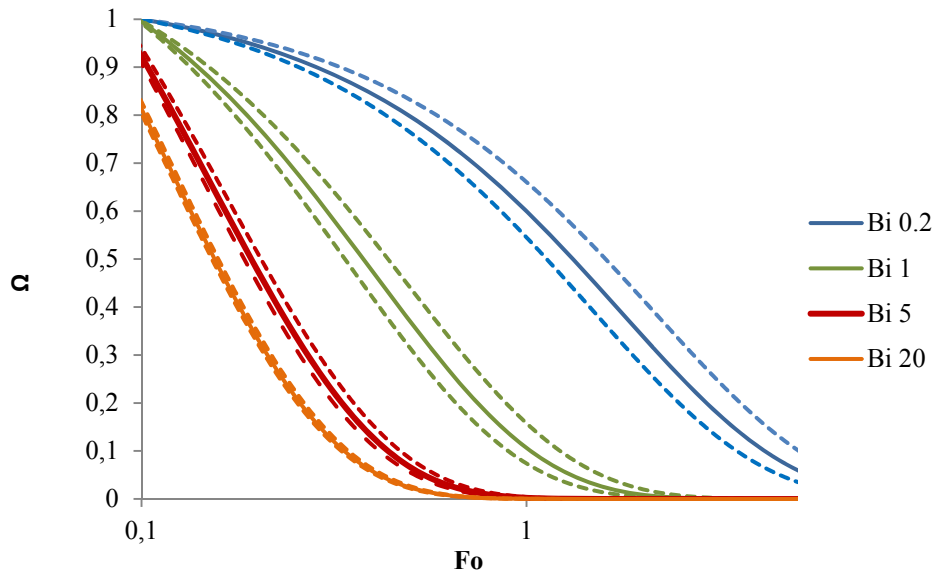
Figure 7.22 Propagation of the prediction of the centre temperature of a sphere at selected Biot numbers. The x axis is logarithmic to compare the implication related to Ω. The dashed lines indicates the consequence of a 20% error in the estimation of the Biot number

From figure 7.21 and 7.22 the propagation of the prediction error is presented. In figure 7.21 it is seen that the error as a function of the Fourier number is largest at Bi 1, which is expected through the normalised Biot number. However the propagated error when the target temperature is in focus the error is large at the low Biot numbers, and negligible at very high Biot numbers. This can also be seen in the asymptotes of the 1st term approximation to the series expansion, presented below for a sphere.

$$\Omega = e^{-3 \cdot Bi \cdot Fo} \text{ (For Bi < 0.1)} \hspace{3cm} [7.6]$$

$$\Omega = 2 \cdot e^{-\pi^2 \cdot Fo} \text{(for Bi} \rightarrow \text{infinity)} \hspace{3cm} [7.7]$$

From equation 7.6 (generalised lumped capacitance) it is seen that the sensitivity of the Biot number is high at very low Biot numbers. For very large Biot numbers only the parameters in the Fourier number are important, the thermal diffusivity α and the characteristic dimension (equation 7.7). For the majority of food processing the Biot number is intermediate (0.1-20), ranging from ambient air-cooling of small products to steaming of large products.

To assess the real implications of the sensitivity of the parameters it needs to be coupled with uncertainty, as a very sensitive parameter is more crucial of the determination if it also has a high uncertainty. How uncertainty and sensitivity is coupled needs a thorough investigation such as exemplified by the study of contact baking by Feyissa et al. (2012) and will not be treated further in this study. For the investigation of the coupled uncertainties and sensitivities a numerical model is more suitable because many calculations can be conducted fast after the model is build.

It is important to emphasize that the parameters will not necessarily vary independently. The thermo physical properties are all related to the composition of the product and the heat transfer coefficients sensitivity is dependent on the magnitude of the Biot number, which is also influenced by the thermo-physical properties and the characteristic dimension. If uncertainties are coupled in the sensitivity analysis it is important to know both the uncertainty due to measurements/assumptions and the variation of the parameters.

7.4 Summarised conclusions

The presented analysis of the induced uncertainties emphasise some concerns with regards to the generally assumed criteria in the choice of solution method to the Fourier equation.

For the use of the lumped capacitance model at Bi<0.1, the recommended solution should be guided with a description of the induced error ($\Delta\Omega$) which as in worst case (sphere at Bi=0.1) 3%. It is found that the error in the lumped capacitance criterion is largest at low Fourier numbers and do not increase with time. The criterion should be changed to 0.02 where the static error ($\Delta\Omega$) is below 1% for all elemental geometries.

For the case of the high process times (Fo>0.2) the uncertainties induced are too large to recommend the use of the 1st term approximation in this area, especially because the largest error is observed at very common Bi numbers (0.5-10). The problem is even more evident in the construction of general geometries (cans and boxes) where the dimensions are multiplied, and the worst case (a box where all three dimensions have a Biot number around 2) gives prediction errors of up to 6%.

As a result the criteria for using the 1st term approximation should be changed to Fo>0.3. This is problematic as the Heissler charts originally produced to cover the low process times is only covering 0<Fo<0.2, and do not include the volume average temperatures. Thus new charts are needed if the graphical solution should provide sufficient accuracy.

The analysis also shows that the convergence between the 1st term approximation and the complete solution is faster in positions in between the centre and the surface. This information is useful in the determination of heat transfer coefficients as presented in chapter 6.

It is shown that the number of terms needed in a series expansion solution in many cases is rather few. For the centre temperature only 3 terms can predict the full temperature history as long as the criterion ($\Omega \leq 1$) is acknowledged. For the volume average temperature and the surface temperature more terms are needed.

The use of the developed equations (4.9 and 4.10) has no restriction criteria and they can be readily applied without any graphs for all Biot numbers above 0.02 and for all Fourier numbers without the use of any graphs.

8 Discussion

The formulation of engineering equations is an academic tradition at technical universities. It is important to continuously develop and validate engineering equations that can be used in the industry and assist the transfer of knowledge. It is important to continuously develop and validate engineering equations in order to exploit the qualitative and quantitative understanding of physical phenomena.

This study has presented and validated engineering equations suited for the calculations of heating and cooling of solids. This with an improved window of operation compared to classical 1st term approximations without making the solution more complex.

Results of the individual contributions in this study have been discussed in the previous chapters. Because the results are connected they are summarised briefly to get an overview of the results. Following is the discussion of the combined work and the application of the contributions.

The formulation and validation of predictive calculations is an academic task to ensure a broad application and to promote equations governed by understanding of prevailing physical phenomena. The use of predictive calculations is however seldom an academic task, which emphasise the importance of simplicity in the formulation.

8.1 Individual contributions

Determination of Fourier exponents
In chapter 3 the proposed normalised Biot number (Bi_{norm}) and its use in determination of the first Fourier exponent is presented. This method eliminates the need for charts and tables to acquire the exponents. The prediction of Fourier exponents was compared to three related studies. All the studies were providing adequate accuracy, but the solution based on Bi_{norm} is more transparent and simple.
In addition Bi_{norm} can be used as sensitivity measure of Bi and the derived Fourier exponents and lag factors, and could be a useful tool invalidation of predictive calculations.

Simplified predictions for low Fourier numbers
In chapter 4 the modelling of the residual between a 1st term approximation and a complete solution to the Fourier heat equation is presented and validated. The proposed solution provides a tool where the initial heating/cooling phase can be evaluated by a modified 1st term approximation for the centre temperature and for the volume average temperature. The formulated equation is expanding the workspace of the 1st term approximation in a simplified manner.

Numerical validation of industrial examples
The combined methods from chapter 3 and 4 were validated in chapter 5 through two industrial examples, showing good compliance with a numerical simulation. To ensure wide industrial application the formulated equation should be validated in industrial setups for a variety of processes involving heating/cooling of solids.

Handling of irregular geometries

From investigation of previous publications it seems that no simple solutions provide accuracy and wide application for irregular geometries. But a promising procedure of calculating irregular geometries as a corresponding general geometry with a respective A/V ratio could be considered. Following the analogy that sphere like objects can be calculated as a sphere (Uyar and Erdogdu 2012), most objects has a geometry that can be related to a general geometry and thus be calculated as the corresponding (e.g. can, box or prism) with an equal A/V ratio. Because the formulated equations have a large operational window (Fo>0, Bi>0.02 for all elementary and general geometries) they are suited for such investigations. The scope of this study has not been to investigate irregular geometries; however the formulated equations set a framework where it could be possible to make further adaptions.

Determination of heat transfer coefficients

In calculation of heating and cooling of solids it is important that correct inputs are used in the equations. Often the thermo-physical properties can be determined with adequate precision from product composition, whereas the heat transfer coefficient is often determined or assumed with less accuracy. In chapter 6 two methods for determining heat transfer coefficients are presented. It is shown that the heat transfer coefficients can be determined by matching a temperature curve with a simple expression; the lumped capacitance model for aluminium replica, and a 1st term approximation for position temperatures inside real food objects. The possibility of using simple expressions in the determination is important for industrial application of these methods.

Continuity and sensitivity of the series expansion

Utilization of the Fourier series expansion solution has been thoroughly analysed in terms of the work frame for simplified solutions in form of the lumped capacitance method and the 1st term approximation. It is found that the errors induced by generally acknowledged assumptions are not acceptable. It is also found that convergence of the 1st term approximation to the complete series expansion depends on position inside the solid.

I propose that the limit for the 1st term approximation is changed to Fo>0.3 to avoid prediction errors for general geometries and that the criterion for the use of the lumped capacitance method is revised to Bi<0.02 to avoid a static prediction error.

The simplified equation given in chapter 4 and the non-iterative determination of the Fourier exponent through the normalised Biot number in chapter 3 expands the work-frame for the 1st term approximation to cover all Fourier numbers and all relevant Biot numbers (0.02>Bi). When the developed method is used only the criteria for the lumped capacitance model (proposed Bi<0.02) is needed.

It has been shown in chapter 7 that convergence of the 1st term approximation towards the complete series expansion is highly position dependent. This should be stated along with the criteria for a deeper insight into the dynamics of the series expansion solution. Especially because this information can be used actively as shown in the calculation of fluid-to-particle heat transfer coefficients. The faster convergence of a relative

position between the centre and the surface of a particle enabled determination of the heat transfer coefficient through calculation of a 1st term approximation at Fourier numbers below 0.2 with good accuracy.

The adequate number of terms needed for an accurate temperature prediction was investigated. Results pointed out that for the centre temperature very few terms are needed for accurate prediction. This is important because there is no need for using excessive calculations. In the area of process control it is an advantage to have as simple calculations as possible, especially when using more information than the temperature history.

Simplification
In order to formulate a simple model that provides adequate precision two general procedures can be followed. Either a complex model can be formulated and subsequently simplified to fulfil a precision criterion, or a simplicity criterion can be formulated and the model optimised to achieve the best precision in fulfilment with the simplicity criteria. The two approaches differ substantially in scope and procedure but also in the solution provided. As discussed in Chwif and Baretto (2000) it is important to incorporate simplicity in the initial phase and to only include parameters needed in the intended use in the formulation of the scope of the calculations.

Because the provided contribution in the simplification of the series expansion in this study has the same scope as Ramaswamy et al. (1982) it is of interest to compare the procedures and resulting solutions. In both of the related studies an accuracy criteria was formulated and used for simplification in a multiple regression approach. Their solution meets the accuracy criteria but is complex with many parameters making the application difficult. In the procedure presented in this study (chapter 3 and 4) a simplicity criteria was formulated with the 1st term approximation as the reference, subsequently the 1st term approximation was expanded to cover the wanted operation window. The solution is very simple with no new parameters and only one constant for each of the elementary geometries. The two proposed solution procedures actually provide equal accuracy.

8.2 Application of combined contributions
In some cases it is necessary to evaluate the thermal history and predicted process time along with calculations of several unit operations in order to investigate a process line. In process scheduling and de-bottlenecking operations this is often the case. In these cases it is convenient to have the calculations in the same program frame e.g. a spreadsheet solution. A specific programmed solver for each of the unit operations could hamper the interfaces in the calculations.

The presented equations are less precise than a numerical solution, but the precision more than meets the needs of practice. The formulated equations are very versatile under the given assumptions that only heat transfer is dominating and it can be used directly without programming.

The target group for the utilization of the developed methods is employees and students in food process engineering. This group has extensive qualitative knowledge of product quality, biological materials and food processing. But has traditionally less focus on quantitative process knowledge as they have not necessarily had a full engineering training. The formulated equations improve the accessibility of predictive calculations on heating and cooling of solids. This is an advantage for food process engineers with tight

schedules, and for food science students pursuing a career in food engineering. The accessibility is facilitated by expanding the operation window for simple calculations with adequate precision and eliminating the need for graphs and tables.

It should be noted that for all calculations of heating and cooling of solids it is a prerequisite that the thermo physical properties are known, that the geometry is well defined and that the heat transfer coefficients can be measured or assumed with reasonable precision. In addition the reliability of the solution implies that both mass transport and phase change should be negligible.

The contribution of this study is equations for simple calculations of the temperature history for all general geometries where transient conduction is the only dominating phenomena. The equations should be used as a foundation where more phenomena can be adapted. It could possibly be used as a reference frame for calculations of irregular geometries, and it is assumed that small contributions of phase change and internal heat generation can be incorporated as proposed for the complete series expansion by e.g. Dincer (1993).

Food manufacture

In general food manufacture it would be beneficial to have more simple tools for crude calculations in order to conduct rational production planning and ease the introduction of new products to existing process lines. The developed equations could serve as an important tool to minimize the time used in trials for implementation of new procedures. The equations proposed in the submitted papers would be applicable to many unit operations where mass transfer and phase changes are negligible, where the obvious example is cooling operations of finished products, ingredients or meal elements.

Food process design

In the design of process equipment numerical solutions are often most suited for design optimization. The optimal design of process equipment might be different depending on the product characteristics in the process line where it is used. In the design of process equipment it is thus valuable to know the implications the designed equipment has on food processing. Because process equipment manufacturers are producing equipment for a massive variety of product characteristics it is valuable to have a set of simple equations for crude evaluation of process impact on products.

Automation

In automation and process control the primary goal is to ensure that a process is producing products within acceptable specifications. By feedback control the process settings are adjusted to ensure that specifications are met. An incorporation of a predicted temperature history into the control system is believed to improve the process control.

Education

It is also worthy to elaborate on the education of new food engineering graduates. For this is important to establish a description of the food industry, as it is the education of their future employees that sets a part of the frame for their process calculation capabilities.

In food science and food technology educations we refer to the series expansion in order to enable students to be able to carry out crude calculations and physical based decision making in food manufacture to evaluate kinetic reactions of either food safety or food quality issues. Often the crude calculation of process time and temperature history is used for evaluation of process lines and conduction of process scheduling. The presented extension to the 1st term approximation enables that these crude calculations are conducted more easily without the use of charts and tables and that solutions are adequately accurate for a larger part of the process.

Authorities

For authorities assuring food safety it would be beneficial to have a simple tool to fast evaluate whether e.g. the cooling guidelines could be met by a specific procedure described in a company's own control documents, and also enable an evaluation whether a deviation from the procedure is problematic or not. For these purposes the presented solution could be beneficial as it can be implemented in simple software and the solution is very versatile for crude calculations, especially for cooling operations.

9 Conclusion and perspectives

The overall research question for this dissertation was whether it was possible to formulate and validate engineering equations for heat transfer that are user friendly and provide adequate precision. The challenge was divided into four objectives: a non-iterative determination of Fourier exponents, a simple equation also valid for low Fourier numbers, determination of heat transfer coefficients and an analysis of the series expansion to understand the work frame for the developed equations.

With the contributions provided with this thesis, it is shown that it is possible to formulate new engineering equations for heat transfer in food processing. The formulation of the normalised Biot number and the developed method for determination of the first Fourier exponent, eigenvalue and lag factor has made the use of the calculations more user-friendly by eliminating the necessity of charts and tables.

It has been shown that the application frame for a traditional 1st term expansion can be increased to also cover the initial phase (Fo<0.2) for all Biot numbers, for all elementary and general geometries with a good accuracy (prediction error <1%). This precision is within acceptance and will serve adequate in most situations. The provided solution is validated for the calculation of the centre temperature and the volume average temperature. Furthermore the developed equations have been validated against numerical simulations of real processing situations with promising results. It was possible to achieve an accurate prediction of the cooling profile for the cooling of a packaged product with an apparent headspace using the new equation. The developed equation was also validated against a numerical solution to a 3 step process where a change in the boundary condition occurred. The new equation matched the prediction from the numerical solution.

The study provides methods for determining heat transfer coefficients in food manufacture. It was shown that a 1st term approximation can be used for inverse calculation of the temperature curve with good accuracy for the determination of fluid-to-particle heat transfer coefficients by using an observed gelatinisation front in potatoes.

Based on the investigation of the sensitivity of the Fourier series-expansion and the continuity of the simplified solutions, two new discoveries are presented: The error induced by using a 1st term approximation is not adequate at Fo=0.2 (errors of up to 6%) and the criteria should be revised. The prediction error when using the lumped capacitance model for Bi=0.1 (up to 3%) is primarily static, and caused primarily by the lag factor. In determination of heat transfer coefficients where an aluminium replica product is used, a static error is less problematic than a dynamic error. However the criterion could easily be changed to 0.02 where the error is less than 1% for all elementary geometries. The proposed equation in this study is validated from Bi>0.02 ensuring convergence between the solutions.

It has been shown that the series expansion converges more rapidly for positions in between the surface and the centre (more than twice as fast for the half radius point) which is an advantage in inverse calculations used for the determination of heat transfer coefficients.

The proposed normalised Biot number can be used as a fast and crude evaluation of the sensitivity of the Biot number to assess heat transfer calculations. This can be used to assess the needed accuracy in the determination of heat transfer coefficients.

Overall, the accessibility of heat transfer calculations in the food industry has been enhanced by expanding the work space for the simplified calculations, and by eliminating the necessity of charts and tables in the calculations.

The format of the supplied equations allow for implementation into various software applications, which favours that the calculations are performed as a general activity as a part of process-planning, -scheduling, and –optimisation.

9.1 Perspectives and future work

The presented equations have been formulated for the centre temperature and volume average temperature evolution. It is a goal to also formulate analogue relations to cover temperatures for relative positions inside solids to enable a prediction of the temperature distribution.

The presented equations have been validated for the elementary and general geometries and for two industrial examples. It is a big motivation to expand this validation to cover more products and processes together with the industry. By using an analogy to the procedure presented for sphere like objects (Uyar and Erdogdu 2012) it could be investigated whether irregular geometries in general can be represented by a general geometry with a close relation to the irregular geometry by using the respective V/A ratio.

In the future it is also a clear goal to expand the applications of the developed equations to also cover areas where other phenomena are present. The formulated equations can probably be used as a foundation for the incorporation of additional physical phenomena (e.g. phase-change and mass transfer), provided their contribution to the overall energy balance is relatively small compared to contribution of conduction through the solid. For the complete series expansion it has already been suggested that small contributions can be incorporated by adaptations to the expansion by correcting the heat transfer coefficient (Dincer 1993) or the Foruier exponent (Cuesta and Lamua 2009). A future focus is to investigate whether small adaptations to the presented simplified equations can be used for predictions where other phenomena play a role.

Because the same mathematical expressions are used in mass transfer and heat transfer, it is a possibility that an analogy to the developed equations could be formulated to cover mass transfer processes, such as salting and brining operations. In salting and brining operations the volume average concentration is often more critical than local concentrations and often the Fourier number in such processes are very low. A future focus is to formulate equations with an increased precision for the volume average concentration in the very initial phase.

References

Amezquita, A., Wang, L., Weller, C. L. (2005). Finite element modelling and experimental validation of cooling rates of large ready-to-eat meat products in small meat-processing facilities. *ASAE American Society of Agricultural Engineers ISSN 0001-2352*

Augusto, P. E. D., Pinheiro, T. F., Cristianini, M. (2012). Determining convective heat transfer coefficient for heating and cooling of bottles in water immersion. *Journal of Food Process Engineering 35 pp. 54-75*

Awuah, G. B., Ramaswamy, H. S., Simpson, B. K. (1992). Surface heat transfer coefficients associated with heating of food particles in cmc solutions. *Journal of Food Process Engineering 16 pp. 39-57*

Baïri, A., Laraqi, N (2003). Diagrams for fast transient conduction in sphere and long cylinder subject to sudden and violent thermal effects on its surface. *Applied Thermal Engineering 23 pp.1373-1390*

Balasubramaniam, V. M., Sastry, S. K. (1994). Liquid to particle convective heat transfer in non-Newtonian carrier medium during continuous tube flow. *Journal of Food Engineering 23 pp. 169-187*

Ball, C. O. (1923). Determining, by methods of calculation, the time necessary to process canned foods. *Bulletin of the National Research Council 7 (37) pp. 9-76.*

Baptista, P. N., Oliviera, F. A. R., Oliviera, J. C., Sastry, S. K. (1997). Dimensionless analysis of fluid-to-particle heat transfer coefficients. *Journal of Food Engineering 31 pp. 199-218*

Barigou, M., Mankad S., Fryer P. (1998). Heat transfer in two-phase solid-liquid food flows: A review. *Food and Bio products Processing, 76,* 3-29.

Bird R. B., Stewart W. E., Lightfoot E. N. (Eds.) (2001). Transport phenomena. (2nd ed.). *John Wiley and Sons Inc., New York.*

Bhutta, M. M. A., Hayat, N., Basir, M. H., Khan, A. R., Ahmad, K. N., Khan, S. (2012). CFD approach in various heat exchanger design: A review. *Journal of Applied Thermal Engineering 32 pp. 1-12*

Bouvier, L., Moreau A., Line A., Fatah N., Delaplace G. (2011). Damage in Agitated Vessels of Large Visco-Elastic Particles Dispersed in a Highly Viscous Fluid. *Journal of Food Science, 76(5),* 384-391.

Cacace, D., Palmieri, L., Pirone, G., Dipollina, G. (1994). Biological validation of mathematical modelling of the thermal processing of particulate foods: the influence of heat transfer coefficient determination. *Journal of Food Engineering 23 pp. 51-68*

Carslaw, H. S., Jaeger, J. C. (1959). Conduction of heat in solids 2nd ed. *Oxford University Press 1959.*

Çengel, Y. A., Ghajar, A. J. (2011). Heat and Mass Transfer 4th ed. *McGraw Hill*

Choi, Y. Okos, M., R. (1986). Effects of temperature and composition on thermal properties of foods. *Food Engineering and Process Applications 1 pp. 93-101*

[3]Christensen, M. G., Feyissa, A. H., Adler-Nissen, J. (2011). Computer aided simulation for developing a simple model to predict cooling time of packaged foods. *In proceedings of ICEF11 Athens, Greece, MCF378 http://www.icef11.org/main.php?fullpaper&categ=MCF*

Chwif, L., Baretto, M. R. P. (2000). On simulation model complexity. *Proceedings of the 2000 Winter Simulation Conference pp.449-455*

Cleland, D. J., Cleland, R. L., Earle, R. L., Byrne, S. J. (1987). Prediction of freezing and thawing times for multi-dimensional shapes by numerical methods. *International Journal of refrigeration 10 pp.32-39*

Cleland, A. C., Earle, R., L. (1982). A simple method for prediction of heating and cooling rates of solids of various shapes. *Revue Internationale du Froid 5(2) pp.98-105*

Cuesta, F. J., Lamúa, M. (1995). Asymptotic modelling of the transient regime in heat conduction in solids with general shapes. *Journal of Food Engineering 24 pp.295-320*

Cuesta, F. J., Lamúa, M. (2009). Fourier series solution to the heat conduction equation with an internal heat source linearly dependent on temperature: application to chilling of fruit and vegetables. *Journal of Food Engineering 90 pp. 291-299*

Datta, A. K. (2008). Status of physics-based models in the design of food products, processes and equipment. *Comprehensive Reviews in Food Science and Food Safety 28 (3) pp. 121-129*

Dehghannya, J., Ngadi, M., Vigneault, C. (2010). Mathematical model procedures for airflow, heat and mass transfer during forced convection cooling of produce: a review. *Food Engineering Reviews 2010 (2) pp. 227-243*

Denys, S., Pieters, J. G., Dewettinck, K. (2003). Combined CFD and Experimental Approach for Determination of the Surface Heat Transfer Coefficient During Thermal Processing of Eggs. *Journal of Food Science 68 (3) pp. 943-951*

Dincer, I. (1993). Transient temperature distributions within spherical products with internal heat generation and transpiration: experimental and analytical results. *International Journal of Heat and Mass Transfer 36 (7) pp. 1998-2003*

Feyissa, A. H., Gernaey, K. V., Adler-Nissen, J. (2012).Uncertainty and sensitivity analysis: Mathematical model of coupled heat and mass transfer for a contact baking process. *Journal of Food Engineering 109 pp.281-290*

Fourier, J. (1822). Théorie analytiqu de la chaleur. *Chez Firmin Didot, Pére Et Fils.*

Freeman, A. (1872). Analytical theory of heat. Translated with notes from: Fourier, J. (1822)"Théorie analytique de la chaleur". *Cambridge University press.*

Gurnay, H. P., Lourie, J. (1923). Charts for estimating temperature distributions in heating or cooling solid shapes. *Industrial and Engineering Chemistry Vol 15 (11) pp. 1170-1172.*

---

[3] The paper is not published in a scientific journal, but is found through the presented link, the paper is also attached in appendix 3.

Hayakawa, K-I. (1969). Estimating the central temperatures of canned food during the initial heating or cooling period of heat process. *Food Technology 23 pp. 1473-1477*

Hayakawa, K-I., Ball, C. O. (1971). Theoretical Formulas for temperatures in cans of solid food and for evaluating various heat processes. *Journal of Food Science 36 pp. 306-310*

Heissler, M. P. (1947). Temperature charts for induction and constant-temperature heating. *American Society of Mechanical Engineers ASME Semi-annual meeting, Detroit Michigan, June 17-20, 1946* .

Incropera, F. P., DeWitt, D. P. (1996). Introduction to Heat Transfer 3rd ed. *Wiley*

Kantt C., Schmidt S., Sizer C., Palaniappan S., Litchfield J. (1998). Temperature mapping of particles during aseptic processing with Magnetic Resonance Imaging. *Journal of Food Science, 63(2),* 305-311.

Lacroix, C., Castaigne, F. (1987). Simple method for freezing time calculations for infinite slabs, infinite cylinders and spheres. *Canadian Institute of Food Science and Technology vol 20 (4) pp. 251-259.*

Lemus-Mondaca, R. A., Vega-Gálvez, A., Moraga, N. O. (2011). Computational simulation and developments applied to food thermal processing. *Food Engineering Reviews 2011 (3) pp. 121-135*

Lü, X., Lu, T., Viljanen, M. (2006). A new analytical method to simulate heat transfer in buildings. *Applied Thermal Engineering 26 pp.1901-1909*

Maesmans, G., Hendrickx, M., DeCordt, S., Fransis, A., Tobback, P. (1992). Fluid to particle heat transfer coefficient determination of heterogeneous foods: a review. *Journal of Food Processing and Preservation 16 pp. 29-69*

Maesmans, G., Hendrickx, M., Decordt, S., & Tobback, P. (1994). Feasibility of the use of a Time-Temperature Integrator and a Mathematical-Model to Determine Fluid-To-Particle Heat-Transfer Coefficients. *Food Research International, 27(1),* 39-51.

Merts, I., Bickers, E. D., Chadderton, T. (2007). Application and testing of a simple method to predicting chilling times for hoki (*Macruronus novaezlandiae). Journal of Food Engineering 78 pp. 162-173*

Mills, A. F. (1995). Heat And Mass Transfer. *Richard D. Irwin, Inc.*

Myhrvold, N., Young, C. and Bilet, M. (2011). *Modernist Cuisine: The art and science of cooking. The cooking lab*; Spi Har/Pa edition, Bellevue, WA 98005, USA

National Food Institute DTU www.foodcomp.dk

Narasimhan, T. N. (1999). Fourier´s heat conduction equation: history, influence and connections. *Review of Geophysics 37 (1) pp. 151-172*

Nesvadba, P. (2014). Thermal properties of unfrozen foods. In M. A. Rao, S. H. Rizvi, A. K. Datta et al. (Eds.), *Engineering Properties of Foods. (4th ed., pp. 223-245). CRC Press, Broken Sound Parkway NW.*

Newman, A. B. (1936). Heating and cooling rectangular and cylindrical solids. *Industrial and Engineering Chemistry* 28 pp. 545-548.

Norton, T., Sun, Da-Wen. (2006) Computational Fluid Dynamics – an effective and efficient design and analysis tool for the food industry: A review. *Trends in Food Science and Technology 17 pp. 600-620*

Ostrogorsky, A. G. (2009). Simple explicit equations for transient heat conduction in finite solids. *Journal of Heat Transfer 131 pp. 011303-1 – 011303-11.*

Ostrogorsky, A. G., Mikic, B. B. (2008). Explicit solutions for boundary problems in diffusion of heat and mass. *Journal of Crystal Growth 310 pp. 2691-2696.*

Ostrogorsky, A. G., Mikic, B. B. (2009). Explicit equations for transient heat conduction in finite solids for Bi>2. *Heat Mass Transfer 45 pp. 375-380.*

Pflug, I. J., Bleidsdell, J. L., Kopelman, J. (1965). Developing temperature-time curves for objects that can be approximated by a sphere, infinite plate, or Infinite cylinder. *ASHRAE semi-annual meeting January 25th - 28th 1965 Chicago, Michigan.*

R Development Core Team (2008). R: A language and environment for statistical computing. *R Foundation for Statistical Computing, Vienna, Austria. ISBN 3-900051-07-0, URL* http://www.R-project.org.

Ramaswamy H., Awuah G., Simpson B. (1997). Heat transfer and lethality considerations in aseptic processing of liquid/particle mixtures: A review. *Critical reviews in food science and nutrition, 37(3),* 253-286.

Ramaswamy, H. S., Lo, K. V., Tung, M. A. (1982). Simplified equations for transient temperatures in conductive foods with convective heat transfer at the surface. *Journal of Food Science 47 pp. 2042-2047.*

Ramaswamy, H. S., Shreekanth, S. (1999). Simplified equations for transient temperature prediction in solids during short time heating or cooling. *Canadian Agricultural Engineering 41(1) pp. 59-64*

Saguy, I. S., Singh, R. P., Johnson, T., Fryer, P. J., Sastry, S. K. (2013). Challenges facing food engineering. *Journal of food engineering 119 pp. 332-342*

[4]Singh, R. P., Heldman, D. R. (2013). *Introduction to Food Engineering* 5th ed. Elsevier.

Stoforos, N. G., Merson, R. L. (1990). Estimating Heat Transfer Coefficients in Liquid/Particulate Canned Foods using Only Liquid Temperature Data. *Journal of Food Science 55 (2) pp. 478-483*

Taylor, F. W. (1919) The principles of scientific management. Monograph. *Harpers and brothers publishers*

Teixeira, A. A., Dixon, J. R., Zahradnik, J. W., Zinsmeister, G. E. (1969). Computer optimization of nutrient retention in the thermal processing of conduction-heated foods. *Food Technology 23 pp. 845–850*

Tijskens, L., Hertog, L., Nicolaï, B. (2001). *Food Process Modelling.* Woodhead Publishing Series in Food Science and Technology. Woodhead

Trystram, G. (2012). Modelling of food and food processes. *Journal of food Engineering 110 (2) pp. 269-277*

---

[4] The publication year is 2014 according to the publication information in the book, according to Wiley it is published August 2013

Uyar, R., Erdogdu, F. (2012). Numerical validation of spherical geometry approximation for heating and cooling of irregular shaped food products. *Journal of food science 77 (7) pp. E166-E175*

van der Sman, R. G. M. (2003). Simple model for estimating heat and mass transfer in regular-shaped foods. *Journal of Food Engineering 60 pp. 383-390*

Verboven, P., Nicolaï, B. M., Svheerlinck, N., De Baerdemaeker, J. (1997). The local surface heat transfer coefficient in thermal food process calculations: A CFD approach. *Journal of Food Engineering 33 pp.15-35*

Weng, Z., Hendrickx, M., Maesmans, G., Tobback, P (1992). The use of a time-temperature-integrator in conjunction with mathematical modelling for determining liquid/particle heat transfer coefficients. *Journal of Food Engineering 16 pp. 197-214*

Zuritz A. Carlos, McCoy C. Steven & Sastry K. Sudhir (1990). Convective heat transfer coefficients for irregular particles in non-Newtonian fluid during tube flow. *Journal of Food Engineering 11 pp. 159-174*

Åström, A., Bark, G. (1994). Heat transfer between fluid and particles in aseptic processing. *Journal of Food Engineering 21 pp. 97-125*

Appendices

Appendix 1: Submitted paper: Proposing a normalised Biot number: For simpler determination of Fourier exponents and for sensitivity analysis of heating and cooling of solids

Appendix 2: Submitted paper: Simplified equations for transient heat transfer problems at low Fourier numbers

Appendix 3: Conference paper: Computer aided simulation for developing a simple model to predict cooling of packaged foods

Appendix 4: Submitted paper: Potatoes as potential devices for studying fluid to particle heat transfer in vessel cooking processes

Appendix 5: Regression polynomials for modelling low Fourier numbers

Appendix 6: Convergence of between the lumped capacitance model and the series expansion at low Fourier numbers

Appendix 7: HEATMAN Manual

Appendix 8: Boling induced heat transfer in vessel cooking

Joint author statement

If a thesis contains articles (i.e. published journal and conference articles, unpublished manuscripts, chapters etc.) made in collaboration with other researchers, a joint-author statement verifying the PhD student's contribution to each article should be made by all authors. However, if an article has more than three authors the statement may be signed by a representative sample, cf. article 12, section 4 and 5 of the Ministerial Order No. 1039 27 August 2013 about the PhD degree. We refer to the Vancouver protocol's definition of authorship.

A representative sample of authors is comprised of
- Corresponding author and/or principal/first author (defined by the PhD student)
- 1-2 authors (preferably international/non-supervisor authors)

Titel of the article	Proposing a normalized Biot number: For simpler determination of Fourier exponents and for sensitivity analysis of heating and cooling of solids
Author(s)	Martin Gram Christensen, Jens Adler-Nissen
Journal/conference * if applicable	Applied Thermal Engineering (Submitted)
Name of PhD student	Martin Gram Christensen
Date of Birth	19th of September 1981

Description of the PhD student's contribution to the abovementioned article

Martin Gram Christensen as the first author proposed the idea of the normalized Biot number, carried out calculations and validations and have written the full manuscript. Jens Adler-Nissen as co-author reviewed the full manuscript and came with corrections and advices through the writing process.

Signature
of the PhD student _(signature)_ Date 25-9-2014

Signatures of co-authors

As a co-author I state that the description given above to the best of my knowledge corresponds to the process and I have no further comments.

Date (DD/MM/YY)	Name	Signature
25/09/2014	Jens Adler-Nissen	_(signature)_

Joint author statements shall be delivered to the *PhD administration* along with the PhD thesis

Appendix 1

Corresponding Author: Mr. Martin Gram Christensen, m.sc

Corresponding Author's Institution: Technical University of Denamrk

First Author: Martin Gram Christensen, m.sc

Order of Authors: Martin Gram Christensen, m.sc; Jens Adler-Nissen, dr.techn. Professor

Abstract: This paper presents a normalization of the Biot number, which enables the Fourier exponents to be fitted with a simple 3rd order polynomial (R2>0.9999). The method is validated for Biot numbers ranging from 0.02 to ∞, and presented graphically for both the Fourier exponents and the lag factors needed in the series expansion. The lag factors and Fourier exponents are validated with an average variation coefficient (CVRMSD) less than 0.006. The resulting prediction error of the thermal response is <0.6°C for spheres and <0.3°C for slabs and cylinders. The normalized Biot number also facilitates an easy investigation of the sensitivity in heat transfer calculations. The simplicity of the solution facilitates its implementation in the industry and curricula for engineers that needs crude calculation methods for thermal calculations, e.g. food science and food technology educations.

Proposing a normalized Biot number: For simpler determination of Fourier exponents and for sensitivity analysis of heating and cooling of solids

Christensen, M. G.[*] & Adler-Nissen, J.[*]

Department of Industrial Food Research, The National Food Institute, Technical University of Denmark

Corresponding author: Martin Gram Christensen, email: mgch@food.dtu.dk, phone: +45 27138244

Abstract

This paper presents a normalization of the Biot number, which enables the Fourier exponents to be fitted with a simple 3rd order polynomial ($R^2 > 0.9999$). The method is validated for Biot numbers ranging from 0.02 to ∞, and presented graphically for both the Fourier exponents and the lag factors needed in the series expansion. The lag factors and Fourier exponents are validated with an average variation coefficient (CVRMSD) less than 0.006. The resulting prediction error of the thermal response is <0.6°C for spheres and <0.3°C for slabs and cylinders. The normalized Biot number also facilitates an easy investigation of the sensitivity in heat transfer calculations. The simplicity of the solution facilitates its implementation in the industry and curricula for engineers that needs crude calculation methods for thermal calculations, e.g. food science and food technology educations.

Keyword: Normalization; Biot number; Transient heat transfer; Series expansion; Eigenvalues; Fourier exponent; Lag factor

1. Introduction

The calculation of heating and cooling of solids is a traditional engineering task in several industries, also in food manufacture. The production of food is conducted in large scale factories often expanded from smaller productions, based on a history of trial and error. To ensure safe products and to evaluate the quality of manufactured food, it is crucial to know the thermal history that the products undergo during processing, cooling, storage and distribution. The staff at most current food production sites often do not have an advanced engineering training, and they must rely on simple, robust calculations in their daily process evaluation and performing scheduling activities. This paper is proposing an easy way to evaluate thermal response based on a normalized Biot number, suited for such calculations.

For evaluation of the thermal response in solid foods the series expansion to the Fourier equation for non-stationary conductive heat transfer is the standard procedure for food products which approximately can be described by ideal geometries (infinite slab, infinite cylinder and sphere) and cross-sections of the first two.

Nomenclature			
Bi	Biot number $Bi = \frac{h}{k} \cdot L$ [-]	J_0	0th order of the Bessel function of the first kind
Bi_norm	Normalized Biot number $Bi = \frac{Bi}{Bi+1}$ [-]	J_1	1st order of the Bessel function of the first kind
$a_{c,1}$	Lag factor (center temperatures) in the series expansion [-]	k	Thermal conductivity [W/m²]
$a_{m,1}$	Lag factor (average temperatures) in the series expansion [-]	Ω	Dimensionless temperature difference $\Omega = \frac{(T_s - T)}{(T_s - T_0)}$ [-], subscripts *s* is the surrounding temperature, *0* is the initial temperature

b_i	Fourier exponent $b_i = \lambda_i^2$ [-]	ρ	Density [kg/m³]
c_p	Specific heat capacity [J/kg·K]	λ_1	The first eigenvalue to respective root functions [-]
α	Thermal diffusivity $\alpha = \frac{k}{\rho \cdot c_p}$ [m²/s]	R	Determining dimension (1/2 height for slabs, radius for cylinders and spheres) [m]
h	Heat transfer coefficient [W/m²K]	Fo	Fourier number, dimensionless process time $Fo = \frac{\alpha}{R^2} \cdot t$ [-]
t	Time [s]		

The mathematical apparatus for calculating non-stationary heat transfer using the series expansion is thoroughly described by Carslaw and Jaeger [1]. It is the standard for predictive heat transfer calculations, and it is presented in most textbooks on the subject [2, 3]. The series expansion is presented below in condensed form for ideal geometries (infinite slabs, infinite cylinders and spheres).

The series expansion for heat transfer:

$$\Omega = \left(\frac{T_s - T}{T_s - T_0}\right) = \sum_i^\infty a_i e^{-b_i \cdot Fo} \tag{1}$$

Where the Fourier number (Fo):

$$Fo = \frac{\alpha}{R^2} \cdot t \tag{2}$$

The Fourier exponent b_i in eq.1 is calculated from the eigenvalue (λ_i) to the respective root functions:

$$b_i = \lambda_i^2 \tag{3}$$

The eigenvalues are calculated by iteration from the root functions in Table 1 based on the Biot number. The equations for the derived Fourier exponents (b_i) and lag factors (a_i) are presented along in Table 1.

Table 1 Mathematical presentation of the respective root function for the ideal geometries, lag factors for center temperatures (a_c), the positional lag factors ($a_{x/R}$) and the lag factors for mean temperatures (a_m),

Geometry	Root function λ_i	a_c	$a_{x/R}$	a_m
Inf. Plate	$Bi = \lambda_i tan\lambda_i$	$\dfrac{2sin\lambda_i}{\lambda_i + sin\lambda_i cos\lambda_i}$	$a_c \cdot cos\left(\lambda_i \dfrac{x}{L}\right)$	$a_c \cdot \dfrac{sin(\lambda_i)}{\lambda_i}$
Inf. cylinder	$Bi = \dfrac{\lambda_i J_1(\lambda_i)}{J_0(\lambda_i)}$	$\dfrac{2J_1(\lambda_1)}{\lambda_i(J_0^2(\lambda_i) + J_1^2(\lambda_i))}$	$a_c \cdot J_0\left(\lambda_i \dfrac{r}{R}\right)$	$a_c \cdot 2\dfrac{J_1 \lambda_i}{\lambda_i}$
Sphere	$Bi = 1 - \lambda_i cot\lambda_i$	$\dfrac{2(sin\lambda_i - \lambda_i cos\lambda_i)}{\lambda_i - sin\lambda_i cos\lambda_i}$	$a_c \cdot \dfrac{sin\left[\lambda_i\left(\frac{r}{R}\right)\right]}{\lambda_i\left(\frac{r}{R}\right)}$	$a_c \cdot 3 \cdot \dfrac{sin(\lambda_i) - \lambda_i cos(\lambda_i)}{\lambda_i^3}$

J_0 and J_1 is the Bessel function of the 1st kind with 0th and 1st order respectively.

The Biot number (Bi) is the ratio between the external and internal resistance to heat transfer and is calculated using eq. 4:

$$Bi = \frac{h}{k}R \tag{4}$$

Where h is the heat transfer coefficient, k is the thermal conductivity and R is the characteristic dimension.

The lag factor *a* can be calculated from the equations in Table 1, where index c denotes the center temperature, index *x/r* denotes a position relative to the center and *m* denotes the volume average temperature .

The developed series applies for ideal geometries that can be described in simple coordinate systems (the infinite slab in Cartesian coordinates, the infinite cylinder in cylindrical coordinates and spheres in a spherical coordinate system). For calculating geometries that can be expressed as the cross section of ideal geometries [4] the thermal response can be calculated from eq. 5, here exemplified by the calculation of a can-shaped geometry.

$$\frac{(T_s-T)}{(T_s-T_0)} = \Omega_{can} = \Omega_{\frac{1}{2}height} \times \Omega_{radius} \qquad [5]$$

In the early-mid 20th century heat transfer calculations were time-consuming to conduct without the availability of computers; thus several graphical methods and tabulated values for determining the Fourier exponents and lag factors have been constructed. They are presented also in recent standard textbooks on the subject [2, 3]. For a fast evaluation of thermal response as a function of Bi and Fo several graphical methods have also been reported such as the Guernay-Lourie plots and the Heissler charts [5, 6]. The series expansion solutions to non-stationary heat transfer have been thoroughly mathematically described [1], and they are presented in a more condensed format applied to food processing [7]. The solutions from [7] are still rendered in textbooks today [2, 3]. Even though several more advanced tools and techniques (simulation software, and finite element calculations) are widely applied in research, they are rarely used in the food manufacturing industry or in teaching for several reasons: the software is expensive and the training needed for the employees or students in order to conduct and utilize the obtained information from these calculations is intensive.

In many processing situations it is often adequate to acquire information on the thermal response in the last part of the process. In these situations the dimensionless temperature difference will be low and the Fourier number will be fairly large (Fo>0.2). For calculations where the Fourier number is above 0.2 the 1st term in the series expansion is assumed adequate for evaluating the thermal response [2]. Christensen and Adler-Nissen [8] showed that also the initial phase in heating and cooling of solids can be modelled by an extended 1st term approximation where the first eigenvalue is the only needed input parameter to cover 0<Fo→∞.

One of the big challenges using the solutions devised by [7] is the determination of the Fourier exponents given by the eigenvalues to the respective root functions (Table 1). As mentioned, the root functions are of iterative character and are thus cumbersome to solve. Alternatively, the exponents can be found tabulated in textbooks or papers on the subject [3, 7], where it is often needed to interpolate between tabulated values, or they can be found in charts [2] where there is a risk of misreads. Neither the tabulated values nor the graphical representation are suited for implementation in simple programs or spreadsheets. Thus, it would be a great advantage to develop non-iterative equations for calculating the Fourier exponents, and a few authors have presented such equations, as discussed in the following.

Ramaswamy, Lo and Tung [9] fitted the Fourier exponents to ideal geometries using trigonometric regressions of the Biot number with good precision. Lacroix and Castaigne [10] used a logarithmic polynomial fit to determine the Fourier exponents. Ostrogorsky and Mikic [11], developed explicit equations for the determination of Fourier exponents with a good precision at Bi<2. Ostrogorsky and Mikic [12] also determined explicit equations for the Fourier exponents for Bi>2 with a good prediction. All four studies provide non-iterative solutions that could be incorporated into spreadsheets. However the suggested solutions

by [9, 10] are rather complex for easy interpretation and are thus difficult to teach students and the industry, hence the application of these fits has not spread outside academia or made its presence in textbooks on the subject. The solutions from Ostrogorsky and Mikic [11, 12] are split into two sets of equations one for Bi<2 and another set for Bi>2, which is less practical. Additionally Ostrogorsky [13] published other simple explicit equations for the whole Biot range with a good overall precision. The methodology and robustness of [13] is, however, less transparent.

This paper focuses on the series expansion solution to non-stationary heat transfer. We propose a new way of calculating the first Fourier exponent ($b_1=\lambda_1^2$) which is more transparent and intuitive. The calculation is based on a normalization of the Biot number which results in smooth, monotonically increasing and simple regression functions.

The series expansion only including the 1st term is presented in equation 6.

$$\Omega = a \cdot e^{-b \cdot Fo}$$ [6]

Where $a=a_c$ is the lag factor for the center, $a=a_m$ is the lag factor for the volume average temperature, $a=a_{x/R}$ is the lag factor for positions within the geometry. b is the first Fourier exponent and Fo is the Fourier number.

Historically, the nomenclature has not been concise throughout the development of the field; hence a summation of the nomenclature is presented in table 2 for easier interpretation of the present work.

Table 2 Nomenclature of present study and the standard references

	Definition	This study	Singh and Heldman (2013)	Mills (1995)	Ramaswamy, Lo and Tung (1982)	Pflug, Bleidsdell and Kopelman (1965)
Biot number		Bi	N_{Bi}	Bi	Bi	N_{Bi}
Fourier number	$(\alpha/R^2)t$ [-]	Fo	N_{Fo}	Fo	Fo	-
Lag factor	table 1 [-]	a	A	A	R	j
Fourier exponent	table 1 [-]	b, λ^2	b, λ^2	λ^2	S	β^2
Dimensionless temperature difference	$(T_a-T)/(T_a-T_0)$ [-]	Ω	-	Θ	U	-

- *Means that no particular symbol is used*

2. Materials and methods

The Biot number, describing the ratio between the internal and external resistance to heat transfer, is recapitulated below for better interpretation of the procedure in formulating a normalized Biot number.

$$Bi = \frac{h}{k} \cdot R$$ [4]

For easier calculation of the Fourier exponents, we introduce the normalized Biot number [Bi_{norm}] in equation 7. [Bi_{norm}] is basically the fraction of internal resistance to overall heat transfer resistance. The internal resistance to heat transfer (R/k) is described as the characteristic dimension (R) divided by the thermal

conductivity (k).The external resistance to heat transfer is the reciprocal heat transfer coefficient (1/h). The total resistance to heat transfer can be defined as:

$$total\ recistance = \frac{1}{h} + \frac{R}{k}$$

And the ratio of the internal resistance to the total resistance will be defined as:

$$ratio\ of\ internal\ resistance = \frac{\frac{R}{k}}{\frac{1}{h} + \frac{R}{k}}$$

Multiplying with the heat transfer coefficient [h] gives a rational description of [Bi$_{norm}$]:

$$Bi_{norm} = \frac{\frac{h}{k} \cdot R}{\frac{h}{h} + \frac{h}{k} \cdot R} = \frac{Bi}{Bi+1} \qquad [7]$$

The constructed normalized Biot number has some advantages: it has an s-shaped curvature as a function of [Bi] enabling a more simple expression to determine Fourier exponents without iteration, because the Fourier exponents and the lag factor also have an s-shaped curvature as a function of the Biot number. Furthermore the normalized Biot number has a finite scale [0→1] which enables the Fourier exponent to be expressed in a linear scale in a graphical presentation instead of a logarithmic scale for [Bi], which notoriously has been a road to misreads. The basic procedure is exemplified graphically in figure 1.
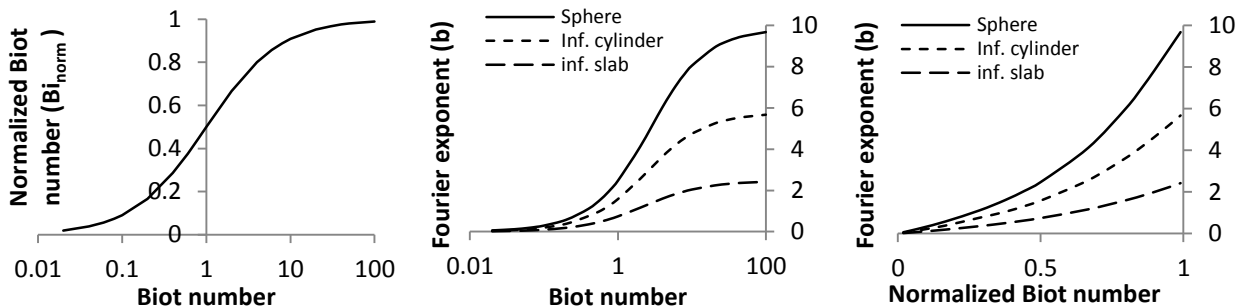
Figure 1 Normalization of the Biot number to the left, Fourier exponents as a function of the Biot number in the middle and the Fourier exponents as a function of the normalized Biot number to the right. Fourier exponents are from [2] p. 173.

The normalized presentation of the Biot number has the advantage of having the same s-shaped curvature as the Fourier exponents, making Bi$_{norm}$ easier to utilize as a base for regression determination of Fourier exponents (b, λ^2) as can be seen from figure 1. In figure 2, 3 and 4 it is shown that the behavior of the Fourier exponent is monotonically increasing as a function of Bi$_{norm}$, where both the 1st and the 2nd derivative are positive, making polynomial fitting suitable with very small residuals.

In this study 21 Biot numbers (Bi) have been chosen to illustrate the procedure (0.02; 0.04; 0.06; 0.08; 0.1; 0.2; 0.4; 0.6; 0.8; 1; 2; 4; 6; 8; 10; 20; 30; 40; 50; 100; ∞) (data from [2]). The Fourier exponents are plotted as a function of the normalized Biot number, and they are fitted by a polynomial regression of the third order to gain a reasonable fit. The plots are shown in figure 2-4, and the regression equations are summarized in Table 3.

Appendix 1
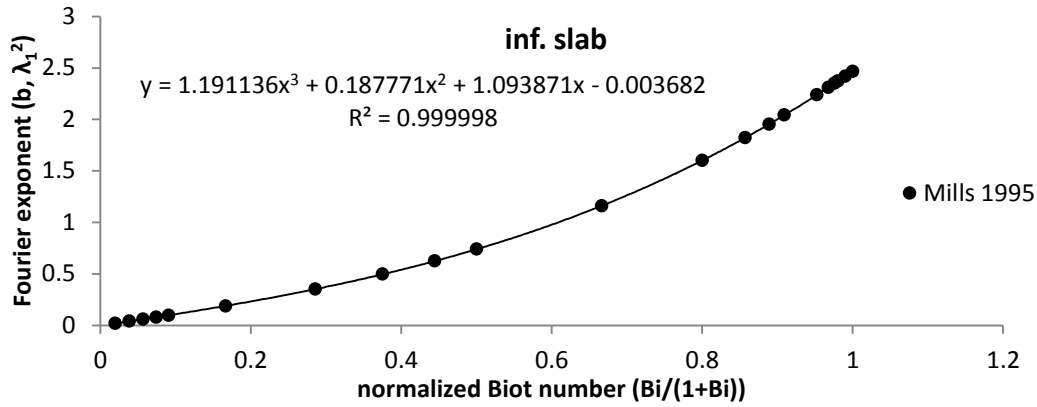
Figure 2 The Fourier exponents (b, λ_1^2) as a function of the normalized Biot number, the dots represents the Fourier exponents from [2], the line represents the polynomial fit.
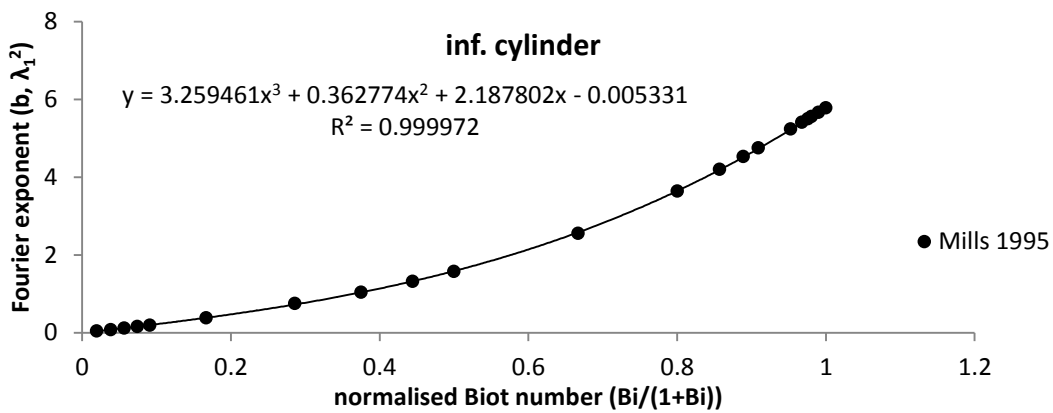
Figure 3 The Fourier exponents (b, λ_1^2) as a function of the normalized Biot number, the dots represents the Fourier exponents from [2], the line represents the polynomial fit.
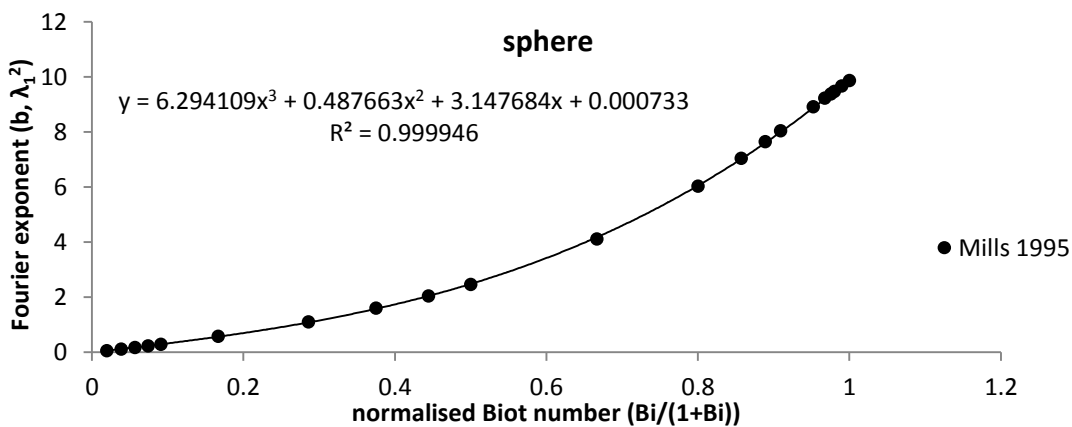
Figure 4 The Fourier exponents (b, λ_1^2) as a function of the normalized Biot number, the dots represents the Fourier exponents from [2], the line represents the polynomial fit.

Figure 2, 3 and 4 demonstrate that, the Fourier exponents can be predicted fairly precise by the 3rd order polynomial regressions (R^2>0.9999). By this procedure the calculation of the Fourier exponents, eigenvalues and lag factors associated with the series expansion can be determined using considerably more simple equations than in [9], [10] and [13].

Table 3 Summation of the regression polynomia to determine the Fourier exponents for the series expansion

Geometry	Regression polynomia
Inf. slab	$b = \lambda_1^2 = 1.1911 \cdot (Bi_{norm})^3 + 0.1878 \cdot (Bi_{norm})^2 + 1.0939 \cdot (Bi_{norm}) - 0.0037$
Inf. cylinder	$b = \lambda_1^2 = 3.2595 \cdot (Bi_{norm})^3 + 0.3628 \cdot (Bi_{norm})^2 + 2.1878 \cdot (Bi_{norm}) - 0.0053$
Sphere	$b = \lambda_1^2 = 6.2941 \cdot (Bi_{norm})^3 + 0.4877 \cdot (Bi_{norm})^2 + 3.1477 \cdot (Bi_{norm}) + 0.00073$

As seen from the equations in table 3, all the polynomial regressions have positive coefficients and they are monotonically increasing. The residual in the regressions should optimally be 0 for Biot numbers approaching 0. The residuals are indeed very small, but it is not recommended to force the regression through (0,0). However when the Biot number is approaching 0, then the Fourier number is approaching infinity for all t > 0; thus the series expansion is not valid for Bi → 0. Instead, the lumped capacitance assuming no internal resistance to heat transfer model should be used. In practice, when the Biot number is below 0.1 the lumped capacitance model (eq. 8) is adequate [2, 3].

$$\Omega = e^{-\frac{h \cdot A}{m \cdot c_p} \cdot t} \tag{8}$$

Where h is the heat transfer coefficient, A is the surface area where the heat is transferred, m is the mass of the product and c_p is the specific heat capacity.

The regression polynomial can be used for Biot numbers as low as 0.02 and still gives accurate values of the Fourier exponent, ensuring adequate overlap with the region where the lumped capacitance model can be used.

3. Results and validation

The polynomial regression fit is used to determine Fourier exponents and the eigenvalues for the series expansion based on the equations from Table 3. The results are validated by comparison with tabulated values from [2]. The results are presented in figure 5 for the Fourier exponent (b_1).
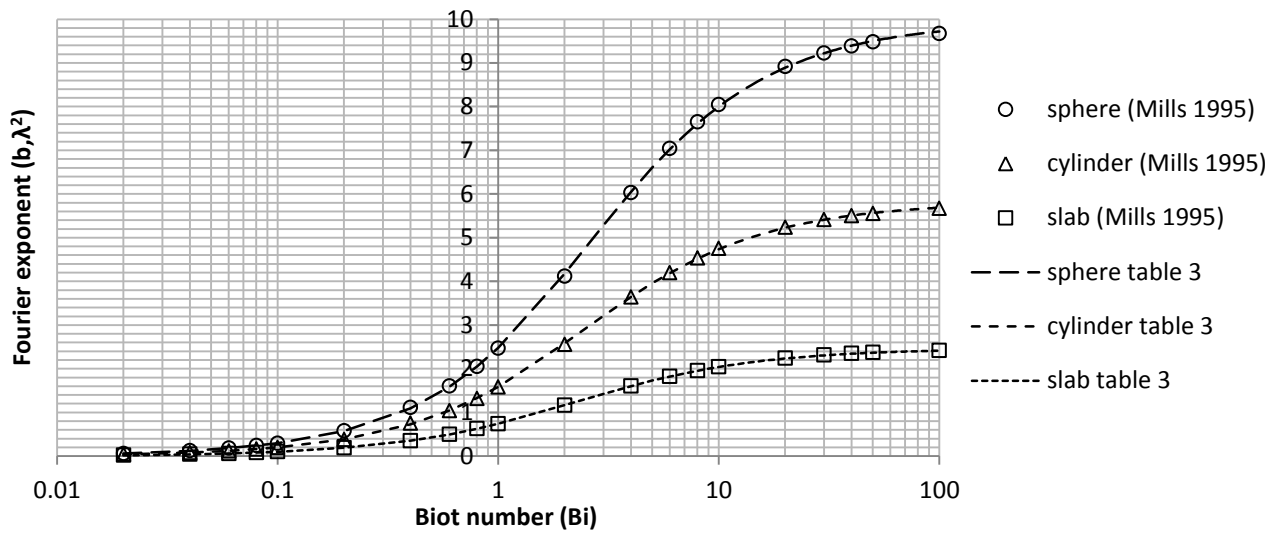
Figure 5 Validation of the calculated Fourier exponents (b_1, λ_1^2) on the polynomial fits. The dashed lines are calculated values, the open dots represents data from [2].

From figure 5 it is clear that the calculated Fourier exponents match the actual values rather precisely. It is thus reasonable to believe that the regressions will also predict the exponents in between the tabulated values and hence interpolation is not necessary using this new approach.

To validate that the approach could also be used for calculating the lag factors used in the series expansion, the eigenvalues from the regressions are used to calculate the lag factors from the equations in table 2. These are presented in figure 6 for the lag factor (a_c) used when considering center temperatures, and figure 7 for lag factors (a_m) considering the volume averaged temperatures. The calculated values are compared with tabulated values from [2].
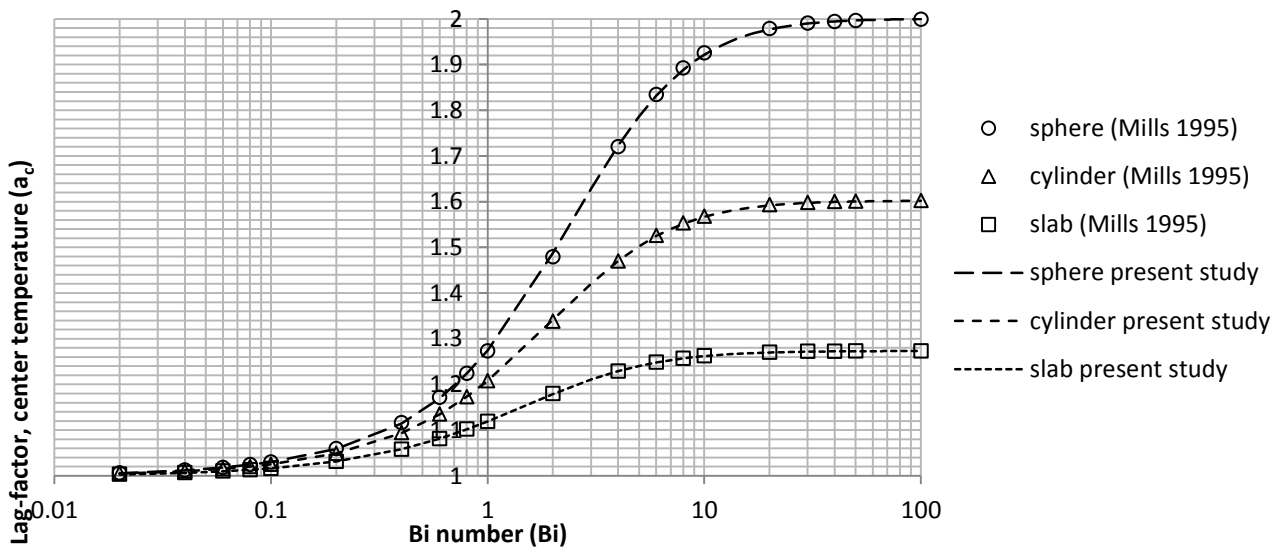
Figure 6 Validation of the calculated lag factors for center temperatures (a_c) in the Fourier expansion compared to tabulated values from [2]
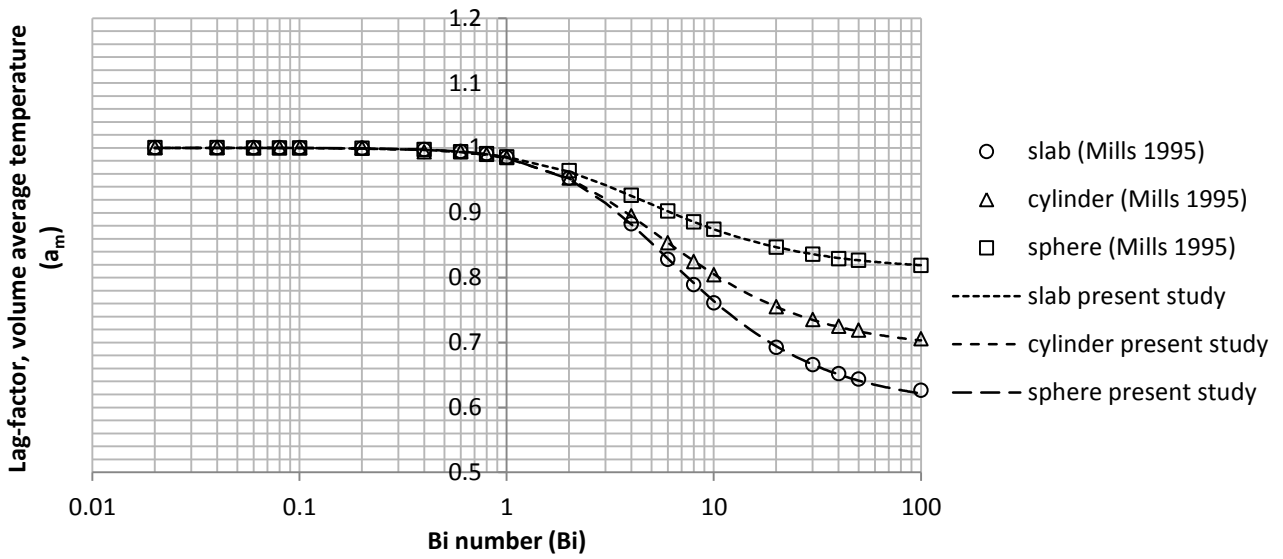
Figure 7 Validation of the calculated lag factors for volume averaged temperatures (a_m) in the Fourier expansion compared to tabulated values from [2]

From the validation of the lag factors in figure 6 and figure 7 it is seen that the derived lag factors based on the eigenvalues calculated from the equations in table 3 have a good fit with the actual lag factors presented in [2]. The average variation coefficients, CVRMSD (Coefficient of Variation of the Root Mean Squared Deviance) (eq. 9) for the fit are presented in table 4.

$$CVRMSD = \frac{1}{\bar{x}_2} \sqrt{\sum_{t=1}^{n} \left(\frac{(x_{1,t} - x_{2,t})^2}{n} \right)}$$ [9]

Table 4 CVRMSD values for the fit of the Fourier exponents and the lag factors needed in the series expansion calculation for non-stationary heat transfer for center and volume average temperatures

	Fourier exponent (b, λ_1^2)	Lag factor center (a_c)	Lag factor mean (a_m)
Inf. Slab	0.0011	0.00033	0.00034
Inf. Cylinder	0.0043	0.00076	0.00082
Sphere	0.0059	0.0018	0.0017

Because the positional lag factors ($a_{x/R}$) are also derived from the same eigenvalues as the center lag factor (a_c) they can also be precisely calculated from this approach.

The precision of the present approach is comparable to the precision of related studies [9, 10 and 13]. The error of prediction (eq.10) from the three studies are compared to the present study in figure 8, 9 and 10

$$error = \frac{\lambda_{1,calculated}^2 - \lambda_{1,actual}^2}{\lambda_{1,actual}^2}$$ [10]
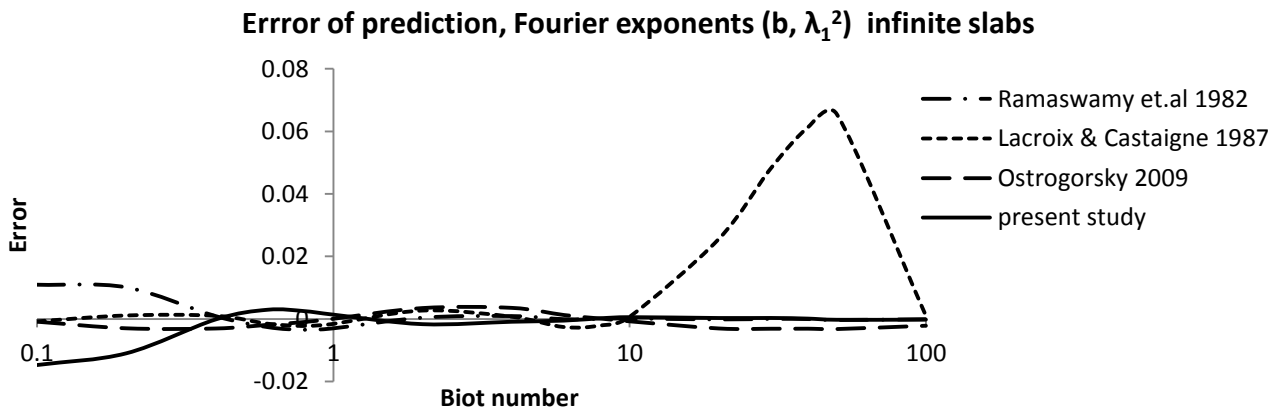
Figure 8 Comparison of prediction errors for related studies for infinite slabs
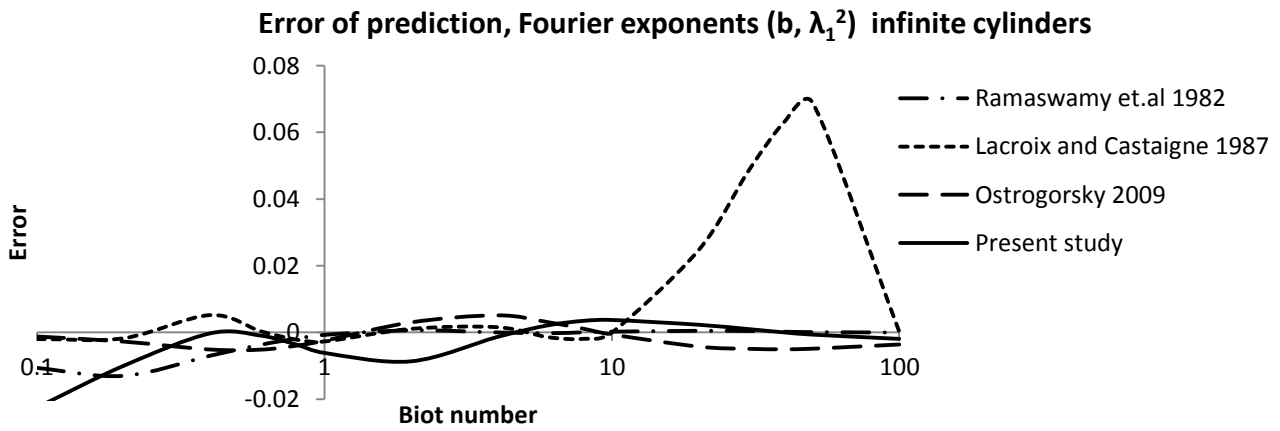
Figure 9 Comparison of prediction errors for related studies for infinite cylinders

Error of Fourier exponents (b, λ_1^2) prediction spheres
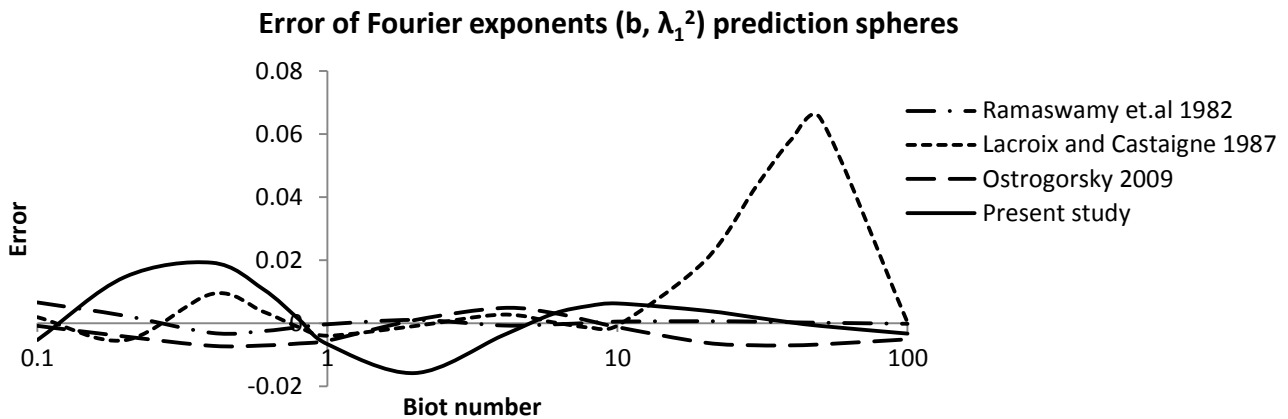
Figure 10 Comparison of prediction errors for related studies for spheres

From the comparison between the related studies in figure 8, 9 and 10 it can be extracted that all the studies are promoting a good fit for Bi<10 with an overall prediction error <0.02 for all the studies. The study by Lacroix and Castaigne [10] is not suited for high Biot numbers (10-100) because of the high error. The best overall fit is performed by Ramaswamy et.al [9] with an overall maximum error<0.01. The present study has the same overall maximum error of 0.01 for the slab at all Biot numbers and for the cylinder at all Bi > 0.2. These the two geometries are by the far the most relevant in sterilization processes, and situations where Bi < 1 rarely occur for such processes. Because the infinite cylinder and the infinite slab is used for the calculation of general geometries (box, prism and can) the accuracy of these two elementary geometries is most critical.

The simplicity of the present study and the transparency of the methodology is an advantage in many situations involving teaching and knowledge transfer to the food producing industry. The consequences of the error in the prediction of the Fourier exponents are evaluated in the worst case scenarios for the three dimensions which are at Biot 2 and 10 following the error graphs in figure 8, 9 and 10. The consequences are presented as the residual ($\Omega_{actual}-\Omega_{predicted}$) the propagation of the error is presented in figure 11.
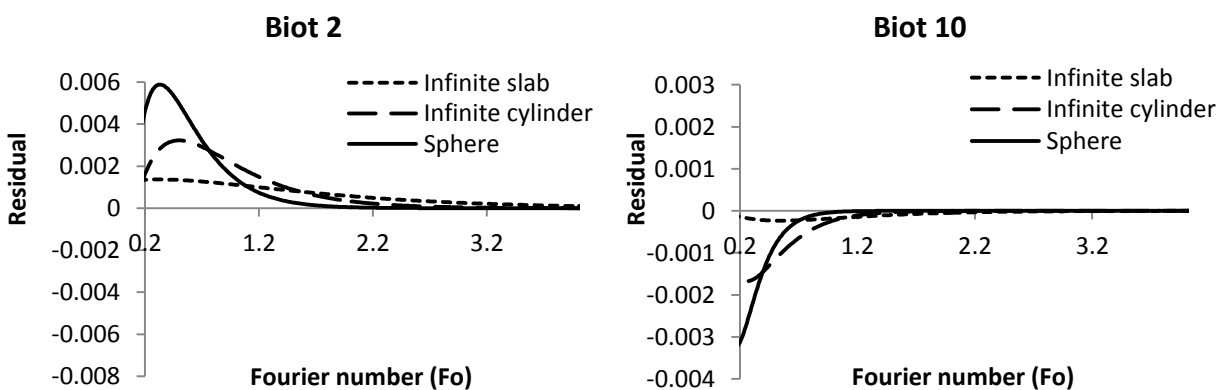
Figure 11 Residual logarithmic temperature difference ($\Delta\Omega$) for the worst case predictions of the center temperatures of infinite slabs, infinite cylinders and spheres for Fo>0.2

From figure 11 the residual can be extracted to a maximum of $\Delta\Omega$=0.006 for spheres at Bi=2. In food processing the driving temperature difference will seldom be above 100°C in situations where mass transfer and phase changes can be neglected. Thus the maximum residual will induce an error in the predicted temperature of maximum 0.6°C for spheres. For the infinite slabs and infinite cylinders the residuals are

considerably lower (<0.3°C); therefore the construction of finite bodies by cross products of these will not induce any appreciable error.

4. Sensitivity of the series expansion

In generalized form, the series expansion describes the correlation between a time input to a temperature output based on the physical phenomenon of heat transfer. To investigate the consequences of a variability is the input to the variability of the output an analysis of the sensitivity of the parameters is used. The series expansion solution is recapitulated below. For this investigation the 1st term approximation for the center temperature is used to exemplify the sensitivity of parameters. The series expansion is expanded below to highlight the parameters where the lag factor is a function f(Bi_{norm}) and the Fourier exponent is a function g(Bi_{norm}):

$$\Omega = \left(\frac{T_S - T}{T_S - T_0}\right) = f(Bi_{norm})e^{-g(Bi_{norm}) \cdot \frac{k}{\rho \cdot c_p \cdot R^2} t} \qquad [11]$$

The sensitivity of the density ρ, and the heat capacity c_p, is directly coupled with the exponent, and has thus a high sensitivity to the output of the equation. The density and the heat capacity can often be determined with adequate precision based on the composition of the food. The characteristic dimension R is very sensitive for the calculation as it is influencing the exponent squared. The characteristic dimension is often not a big challenge to measure for elemental and general geometries. If the geometry is complex, the dimensions are difficult to determine; however, the series expansion is less suited for very complex geometries where a numerical solution is more suited.

The sensitivity of the thermal conductivity is important because it is a part of both the Fourier number and the Biot number. The sensitivity of the thermal conductivity is dependent on the value of the Biot number. This is best described through the lumped capacitance equation where the sensitivity of the conductivity is 0. For Bi→∞, the sensitivity of the thermal conductivity to the output is directly proportional to the exponent.

The uncertainty in the Biot number is often most influenced by the uncertainty in the heat transfer coefficient determination. The consequence of an uncertainty of the determined heat transfer coefficient is evaluated through the sensitivity of the Biot number.

4.1 Sensitivity of the Biot number

The sensitivity of the Biot number is most directly explained through the sensitivity of the lag factor and the Fourier exponent which are both a function of the normalized Biot number. This is presented above in equation 11. The sensitivity of these two parameters is evaluated by utilizing the normalized Biot number:

$$Bi_{norm} = \frac{Bi}{1 + Bi}$$

The relation between the normalized Biot number and the lag factor and the Fourier exponent can be seen in figure 12 and 13.
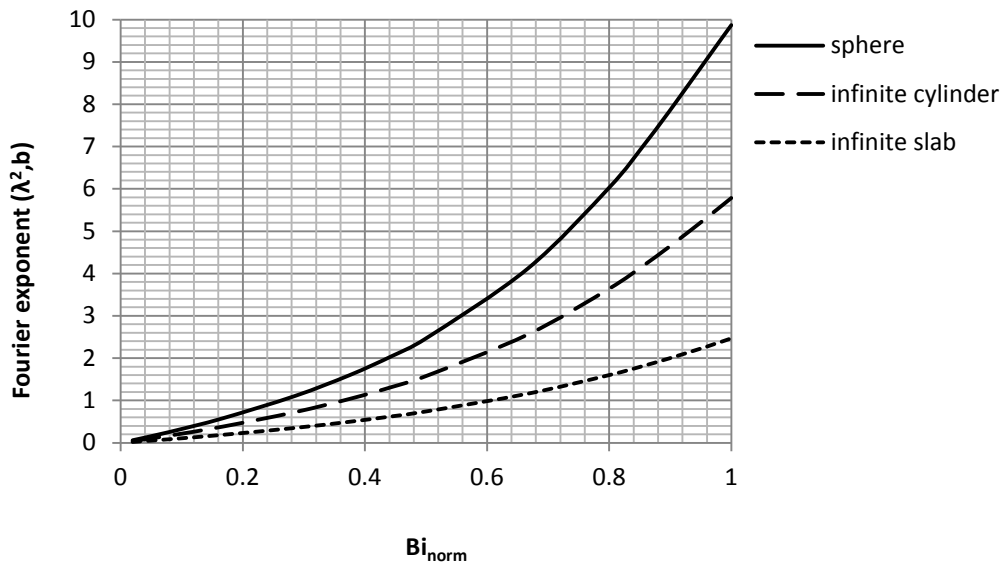
Figure 12 Relation between the normalized Biot number and the 1st Fourier exponent
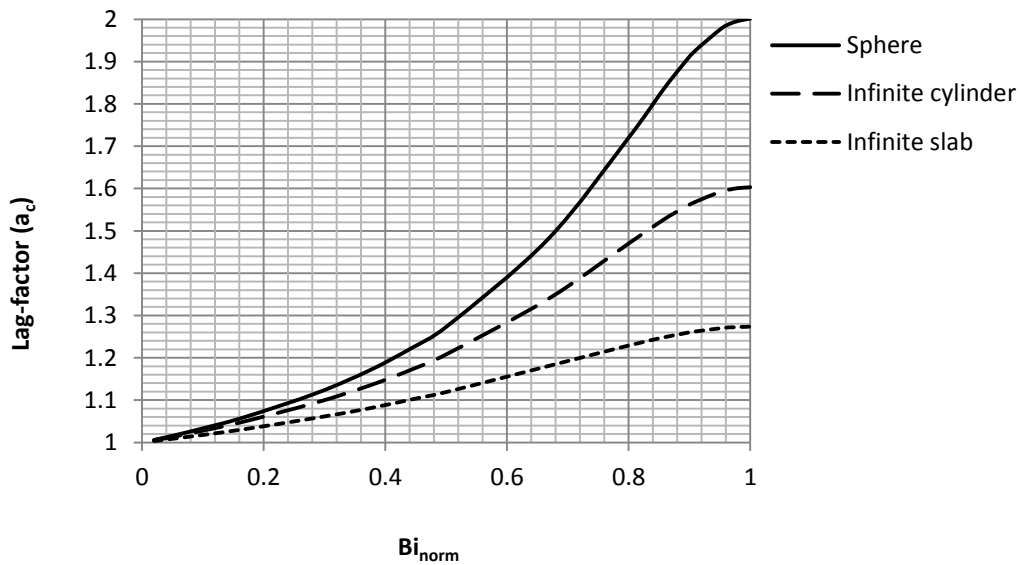
Figure 13 Relation between the normalized Biot number and lag factor for the center temperature

The simple relation between the normalized Biot number to both the lag factor and the Fourier exponent makes the normalized Biot number an easy way to investigate the sensitivity of the Biot number in the calculations with the Fourier series expansion.

5. Discussion

The determination of the eigenvalues and hence Fourier exponents to the series expansion without the need for iterations and interpolation is a clear advantage if simple programs for evaluating thermal history are to be constructed. Especially, the possibility of incorporating the equations into simple spreadsheet programs

will serve as an advantage for food manufacturers lacking more advanced dedicated software, and for the teaching of students in food technology. The presented approach is validated at Biot numbers above 0.02. In situations with Biot numbers below 0.1 it will in most cases be sufficient to use the lumped capacitance model assuming no internal resistance to heat transfer, thus for Biot numbers below 0.02 it will be meaningless to use the series expansion in most cases. Because the presented solution in this study is based on a normalized Biot number, there is no upper limit for the value of the Biot number.

In addition [Bi_{norm}] is a more direct description of the influence of internal and external resistance to heat transfer. This is valuable in assessing the sensibility in heat transfer calculations, especially the determination of heat transfer coefficients and thermal conductivity. For example if [Bi] is calculated to be 10 based on an average heat transfer coefficient of $100 +/-20$ [W/m^{2}K], the implications can be seen directly. By means of the resulting [Bi] (8, 10 and 12) the sensibility in the estimation of [h] is difficult to assess. By using [Bi_{norm}], however the internal fraction of the resistance is calculated in the 3 possible situations to be: 0.89, 0.91 and 0.923. The presentation of the sensibility in terms of internal resistance is more direct because the Fourier equation is a calculation of internal conduction, based on an external impact.

If a Biot number is calculated to be 2 average heat transfer coefficient of $100 +/-20$ [W/m^{2}K] the uncertainty in the Biot number is (1.6, 2, 2.4). The resulting Bi_{norm} is 0.615, 0.667 and 0.706 respectively. From the normalized Biot numbers it can be concluded that the determination of low Fourier numbers are more sensitive than the determination of high Biot numbers. This is important in heat transfer coefficient determination.

This study presents a solution for calculating Fourier exponents that has similar precision as reported in earlier studies [9, 10, 11, 12 and 13], but provides a more intuitive and transparent solution based on a normalized Biot number. This enables a more intuitive understanding of the parametric variability and transparency in the procedure. In addition the provided solution improves the simplicity in the calculation of the whole Fo regime presented by [9]

6. Conclusion

A new method to determine the Fourier exponents needed to calculate the series expansion for non-stationary heat transfer has been developed. The developed method utilizes our finding that a normalization of the Biot number enables a simple polynomial fit of the first Fourier exponents. The polynomial is monotonically increasing yielding a high robustness in the parametric variability. The polynomial regression is validated with a low error for the range of Biot numbers (0.02<Bi<∞)**.** The study will facilitate the generation of more general and simple programming in spreadsheets to handle non-stationary heat transfer problems.

Aknowledgements

References

[1] Carslaw, H. S., Jaeger, J. C. Conduction of heat in solids 2nd ed. *Oxford University Press 1959.*

[2] Mills, A. F. Heat And Mass Transfer. Richard D. Irwin, Inc. 1995

[3] Singh, R. P. and Heldman, D., R. *Introduction to Food Engineering* 5th ed. Elsevier. 2013.

[4] Newman, A.B. Heating and cooling rectangular and cylindrical solids. Industrial and Engineering Chemistry, 28, pp. 545-548. 1936

[5] Gurnay, H. P. and Lourie, J. Charts for estimating temperature distributions in heating or cooling solid shapes. Industrial and Engineering Chemistry Vol 15 (11) pp. 1170-1172. (1923)

[6] Heissler, M. P. Temperature charts for induction and constant-temperature heating. American Society of Mechanical Engineers ASME Semi-annual meeting, Detroit Michigan, June 17-20, 1946.

[7] Pflug, I. J., Bleidsdell, J. L., and Kopelman, J. Developing Temperature-Time Curves for Objects That Can Be Approximated By a Sphere, Infinite Plate, or Infinite Cylinder. ASHRAE semi-annual meeting January 25-28 1965 Chicago, Michigan. 1965

[8] Christensen, M. G., Adler-Nissen, J. Simplified equtions for transient heat transfer problems at low Fourier numbers. Applied Thermal Engineering, Submitted July 2014

[9] Ramaswamy, H. S., Lo, K. V., Tung, M. A. Simplified equations for transient temperatures in conductive foods with convective heat transfer at the surface. Journal of Food Science (47) pp. 2042-2047. 1982

[10] Lacroix, C., Castaigne, F. Simple method for freezing time calculations for infinite slabs, infinite cylinders and spheres. Canadian Institute of Food Science and Technology vol 20 (4) pp. 251-259. 1987

[11] Ostrogorsky, A. G., Mikic, B. B. Explicit solutions for boundary problems in diffusion of heat and mass. Journal of Crystal Growth (310) pp. 2691-2696. 2008

[12] Ostrogorsky, A. G., Mikic, B. B. Explicit equations for transient heat conduction in finite solids for Bi>2. Heat Mass Transfer (45) pp. 375-380. 2009

[13] Ostrogorsky, A. G. Simple explicit equations for transient heat conduction in finite solids. Journal of Heat Transfer (131) 011303-1 – 011303-11. 2009

Joint author statement

If a thesis contains articles (i.e. published journal and conference articles, unpublished manuscripts, chapters etc.) made in collaboration with other researchers, a joint-author statement verifying the PhD student's contribution to each article should be made by all authors. However, if an article has more than three authors the statement may be signed by a representative sample, cf. article 12, section 4 and 5 of the Ministerial Order No. 1039 27 August 2013 about the PhD degree. We refer to the Vancouver protocol's definition of authorship.

A representative sample of authors is comprised of
- Corresponding author and/or principal/first author (defined by the PhD student)
- 1-2 authors (preferably international/non-supervisor authors)

Titel of the article	Simplified equations for transient heat transfer problems at low Fourier numbers
Author(s)	Martin Gram Christensen, Jens Adler-Nissen
Journal/conference * if applicable	Applied Thermal Engineering (Submitted)
Name of PhD student	Martin Gram Christensen
Date of Birth	19th of September 1981

Description of the PhD student's contribution to the abovementioned article

Martin Gram Christensen as first author formulated the idea and approach, carried out the deduction of new equations, numerical modelling and validation, and have written the full manuscript. Jens Adler-Nissen as co-author reviewed the full manuscript and came with corrections, comments and advices to the manuscript and approach.

Signature
of the PhD student _____ Date 25 - 9 - 2014

Signatures of co-authors

As a co-author I state that the description given above to the best of my knowledge corresponds to the process and I have no further comments.

Date (DD/MM/YY)   Name   Signature

25/09/2014   Jens Adler-Nissen   _____

Joint author statements shall be delivered to the *PhD administration* along with the PhD thesis

Appendix 2

Corresponding Author: Mr. Martin Gram Christensen, m.sc

Corresponding Author's Institution: Technical University of Denamrk

First Author: Martin Gram Christensen, m.sc

Order of Authors: Martin Gram Christensen, m.sc; Jens Adler-Nissen, professor

Abstract: This paper proposes an analytical solution to transient heat transfer, which also applies for the initial heating/cooling period (Fo<0.2) of solids with simple geometries subjected to convective boundary conditions, with negligible mass transfer and phase-change. The new equation is presented and validated for infinite slabs, infinite cylinders, spheres and by an industrial application example, covering the center temperature and the volume average temperature. The approach takes ground in the residual difference between the 1 term series solution and a 100 term solution to the Fourier equation of the thermal response for solids subjected to convective heat transfer. By representing the residual thermal response as a function of the Biot number and the first eigenvalue, the new approach enables the description of the thermal response in the whole Fourier regime. The presented equation is simple and analytical in form, which allows an easy implementation into spreadsheets and thus serves as a transparent and fast tool for crude process calculations in e.g. process planning or introduction of new products to existing lines. The prediction error of the new equation is low (RMSD<0.015) for 0<Fo<0.2 and 0.1<Bi<100 for infinite slabs, infinite cylinders, spheres and typical examples of finite bodies.

Simplified equations for transient heat transfer problems at low Fourier numbers

Martin Gram Christensen, Jens Adler-Nissen

Department of Industrial Food Research, National Food Institute, Technical University of Denmark

Email: mgch@food.dtu.dk Phone number: +45 27138244

Abstract

This paper proposes an analytical solution to transient heat transfer, which also applies for the initial heating/cooling period (Fo<0.2) of solids with simple geometries subjected to convective boundary conditions, with negligible mass transfer and phase-change. The new equation is presented and validated for infinite slabs, infinite cylinders, spheres and by an industrial application example, covering the center temperature and the volume average temperature. The approach takes ground in the residual difference between the 1 term series solution and a 100 term solution to the Fourier equation of the thermal response for solids subjected to convective heat transfer. By representing the residual thermal response as a function of the Biot number and the first eigenvalue, the new approach enables the description of the thermal response in the whole Fourier regime. The presented equation is simple and analytical in form, which allows an easy implementation into spreadsheets and thus serves as a transparent and fast tool for crude process calculations in e.g. process planning or introduction of new products to existing lines. The prediction error of the new equation is low (RMSD<0.015) for 0<Fo<0.2 and 0.1<Bi<100 for infinite slabs, infinite cylinders, spheres and typical examples of finite bodies.

Keywords: Modeling; heat-transfer; analytical solutions; low Fourier-numbers

1. Introduction

The calculation of non-stationary convective heat transfer into solids is important in several engineering fields, such as aeronautics, metallurgy, building construction and food technology [1,2,3]. For elementary geometries (infinite slab, infinite cylinder, sphere), the standard approach is to solve the Fourier differential equation through a series expansion [4,5]. The solution assumes convective uniform boundary conditions with no or insignificant mass transfer, no internal heat generation and negligible changes in geometry. Despite these restrictions, many practical engineering problems of convective heating or cooling of solids can be approximated by the situation with ideal geometries or cross-sections of them. In food engineering, calculation of the sterilization process in the canning industry is the classical example [6,7]. Also calculation of cooling processes is an often encountered issue in the food industry where it is important for the safety and quality of the food to ensure that a target temperature of a solid food product is reached before it enters a chilled storage.

In recent decades research in heat transfer, also within food engineering, has focused on modeling and simulations in often advanced software such as the MATLAB based COMSOL Multiphysics® [8,9]. The simulations have the advantage that more complex physics can be included into the models accounting for mass transfer, geometry changes, chemical reactions and structure

changes within the products [10]. An example of this modeling approach is a study of the convective roasting of meat [11], where heat and mass transfer is coupled with a geometrical change (shrinkage) during processing. Such simulations are precise and can handle real processing situations; however, they are often targeted at specific products in specific processes making them less versatile for general engineering calculations. In addition, many engineers in the food producing industry do not have access to suitable software nor the time needed to conduct simulations in their daily work. This means that there is still a need for classical engineering equations to handle the calculation of the thermal history of solid foods, preferably by using simple, commonly used software such as spreadsheets.

2. Theory

For the infinite slab, the infinite cylinder, and the sphere the temperature history can be calculated using eq. 1-7 below [5], assuming convective boundary conditions with no or insignificant mass transfer and disregarding the influence of chemical reactions and possible changes in geometry.

Nomenclature			
α	Slope of regression curves	J_0	0th order of the Bessel function of the first kind [-]
a_i	Lag factor in the series expansion to the heat transfer equation [-]	J_1	1st order of the Bessel function of the first kind [-]
Bi	Biot number $Bi = \frac{h}{k} \cdot L$ [-]	k	Thermal conductivity [W/m^2]
c_p	Specific heat capacity [J/kg·K]	λ_i	The eigenvalue to respective root functions [-]
C	Intercept of regression curves	L	Determining dimension [m]
ε	Residual dimensionless temperature difference [-]	Ω	Dimensionless temperature difference $\Omega = \frac{(T_s - T)}{(T_s - T_0)}$ [-], subscripts s is surrounding temperature, 0 is initial temperature
Fo	Fourier number (dimensionless process time) $Fo = \frac{k}{L^2 \cdot \rho \cdot c_p} \cdot t$ [-]	ρ	Density [kg/m^3]
h	Heat transfer coefficient [W/m^{2}K]	x	Relative position in geometry, x=0 for center, 1 for surface
T	Temperature [°C]	t	Time [s]

$$\Omega = \sum_{i=1}^{\infty} a_i \cdot e^{-\lambda_i^2 \cdot Fo} \tag{1}$$

λ_i is the eigenvalue to the representative root functions eq. 2, 3 and 4, for the 3 elementary geometries.

$$\text{inf. slab: } Bi = \lambda_i tan\lambda_i \tag{2}$$

$$\text{inf. cylinder: } Bi = \frac{\lambda_i J_1(\lambda_i)}{J_0(\lambda_i)} \tag{3}$$

$$\text{sphere: } Bi = 1 - \lambda_i cot\lambda_i \tag{4}$$

The lag factor (a_i) is calculated for the three geometries as a function of the respective eigenvalue to the root functions in equation 5, 6 and 7. *L* is the characteristic dimension, which is half thickness for slabs, and the radius for cylinders and spheres.

$$\text{inf. slab (point): } a_i = \frac{2sin\lambda_i}{\lambda_i + sin\lambda_i cos\lambda_i} \cdot cos\left(\lambda_i \frac{x}{L}\right) \tag{5}$$

$$\text{inf. cylinder (point): } a_i = \frac{2J_1(\lambda_i)}{\lambda_i[J_0^2(\lambda_i) + J_1^2(\lambda_i)]} \cdot J_0\left(\lambda_i \frac{x}{L}\right) \tag{6}$$

$$\text{sphere (point): } a_i = \frac{2(sin\lambda_i - \lambda_i cos\lambda_i)}{\lambda_i - sin\lambda_i cos\lambda_i} \cdot \frac{sin\left(\lambda_i \frac{x}{L}\right)}{\lambda_i \frac{x}{L}} \tag{7}$$

For estimating the center temperature in finite bodies such as cans, boxes and prisms the cross-products of the elementary geometries is the standard solution [12]. The resulting dimensionless temperature difference (Ω) is the product of the individual contributions, here exemplified by the calculations of a finite box:

$$\Omega_{box} = \Omega_{length} \cdot \Omega_{width} \cdot \Omega_{height} \tag{8}$$

$$\Omega_{box} = \left[\sum_{i=1}^{\infty} a_i \cdot e^{(-\lambda_i^2 \cdot Fo)}\right]_{length} \cdot \left[\sum_{i=1}^{\infty} a_i \cdot e^{(-\lambda_i^2 \cdot Fo)}\right]_{width} \cdot \left[\sum_{i=1}^{\infty} a_i \cdot e^{(-\lambda_i^2 \cdot Fo)}\right]_{height} \tag{9}$$

Applying only the first term of the expansion is considered adequate if the Fourier number exceeds 0.2 [5]. However, for finite bodies each dimension is usually different, and the corresponding Fourier number will be different for the same process time. For example, for a finite box where one of the dimensions is two times larger than the smallest dimension, the Fourier number will be four times lower. This means that at e.g. Fo = 0.3 for the smallest dimension, the largest dimension will have Fo = 0.075 which introduces a significant error in the calculation, if only 1 term is applied. For calculations involving finite bodies more terms in the expansion are therefore often needed even if the smallest dimension has a Fo-number that exceeds 0.2. Alternatively, charts can be used to evaluate the thermal response at Fo < 0.2 [1,13,14,15,16]. Both the approach of using more terms in the series expansion and the use of charts is feasible. However, using more terms in the expansion requires dedicated software or programming (in Matlab, R, etc.), whilst the graphical method is less precise, time consuming and not readily incorporated into spreadsheet solutions.

The aim of this study is to derive more simple equations which are valid for all Fourier numbers, also for Fo < 0.2, where the standard solutions require the use of graphs. Studies directed towards more simple engineering equations to handle low Fourier numbers are scarce, and they are neither widely implemented in the industry nor presented in textbooks. Hayakawa [15] reported charts and tables to estimate the initial center temperature response for canned foods, but the solutions are limited to the geometry of a finite cylinder. Ramaswamy and Shreekanth [17] used a stepwise multiple regression approach to approximate the summarized series solution at Fo<0.2 for infinite geometries. Their general idea was to model the residual between the summarized series and the 1 term approximation, as is also done in the present study. Their solution included 13 new parameters for each of the three infinite geometries in a set of three equations [17]. As it will be shown, we propose a simpler solution of sufficient precision with only 1 new parameter included in a single equation for handling the prediction of the center temperature and the volume average

temperature. The solution covers a wide application area (0<Fo, 0.1<Bi<100) for the elementary geometries and their cross-sections, cans, prisms, and boxes.

3. Materials and methods

The solution to the series expansion (eq. 1) is obtained using the freeware program R [18], where 100 terms represent the virtually exact solution to the entire expansion based on the equations 1-7. The difference between the 100 term solution and the 1 term solution (residual) is then evaluated for 16 Biot numbers (0.1; 0.2; 0.4; 0.6; 0.8; 1; 2; 4; 6; 8; 10; 20; 30; 40; 50; 100) for the three elementary geometries. Because the residual between the 1 term solution and the 100 term solution to the thermal history is only of practical significance at Fo<0.2 the analysis of the residual is conducted for the range 0<Fo<0.2.

Following Ramaswamy and Shrekanth [17] we handle the approximate solution to eq. 1 by splitting the series expansion into the 1st term minus a residual, where the residual will be the difference between the infinite series and the 1st term:

$$\Omega = a_1 \cdot e^{-\lambda_1^2 \cdot Fo} - \epsilon \tag{10}$$

where:

$$\epsilon = \Delta\Omega = \left(a_1 \cdot e^{-\lambda_1^2 \cdot Fo} - \sum_{i=1}^{\infty} a_i \cdot e^{-\lambda_i^2 \cdot Fo} \right) \tag{11}$$

The method represented by eq. 10 is illustrated in figure 1, where Ω for a sphere of Bi=4 is plotted against the Fourier number [0:0.2] for the 1st term solution, the 100 term solution and the residual (eq. 11).
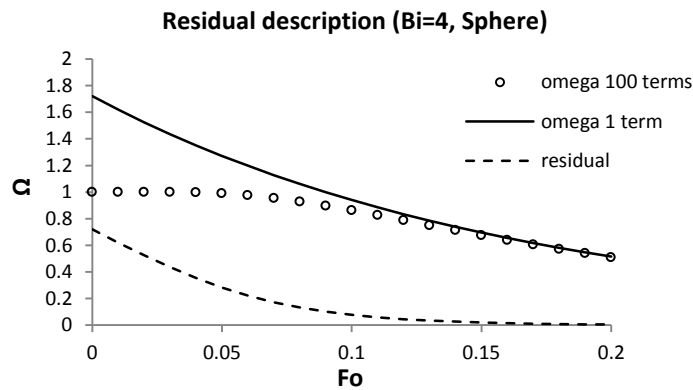
Figure 1 Graphical method description of equation 11

3.1 Center temperatures – derivation of equations

The natural logarithm to the residual ($\epsilon = \Omega_{1\ term} - \Omega_{100\ terms}$) is investigated as a function of the Fo-number [0; 0.2; 0.01] in order to express the residual in the same format as the first term expansion. In figure 2 it is exemplified for a sphere with a Biot number of 4. Because we want the residual at Fo=0 to be equal to the difference between the 1 term solution and the exact solution to the heat equation, the intercept in the regression is forced at $\ln(a_{c,1}-1)$. $a_{c,1}$ is calculated from equation 5, 6 and 7.

Appendix 2
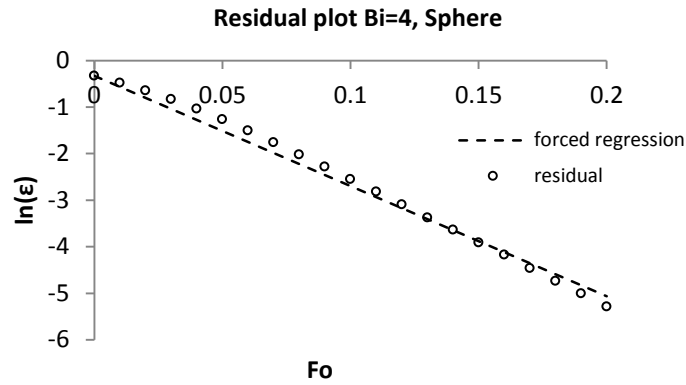
Figure 2. Regression plot of the residual (eq. 11) as a function of the Fourier number, for a sphere with a Biot number of 4, fitted by a minimal squared error regression with a forced intercept

The regression equation 12 crudely represents the development in the residual over process time (Fo):

$$\ln \epsilon = \alpha \cdot Fo + \ln(a_{c,1} - 1) \tag{12}$$

All the regression lines are presented in appendix A1 for infinite slabs, A2 for infinite cylinders and A3 for spheres. The regression coefficients from appendix (A1, A2, A3) for the 16 tested Biot numbers are plotted (open circles) against ln(Bi) for infinite slabs (figure 3), for infinite cylinders (figure 4) and for spheres (figure 5).

Because it is desirable to introduce as few new variables as possible in the calculation of the residual we have chosen to express the regression coefficients as a function of the Biot number and the first eigenvalue (λ_1) to the respective root function. Testing a number of simple combinations we found that the regression coefficients (α) follow rather closely equation 13:

$$\alpha = -(\lambda_1 \cdot \ln(Bi) + C) \tag{13}$$

Where C is a constant which depends on the geometry and equals the coefficient at Bi=1. The predicted regression coefficients from equation 13 are presented in figure 3, 4 and 5 as dotted curves.

Appendix 2
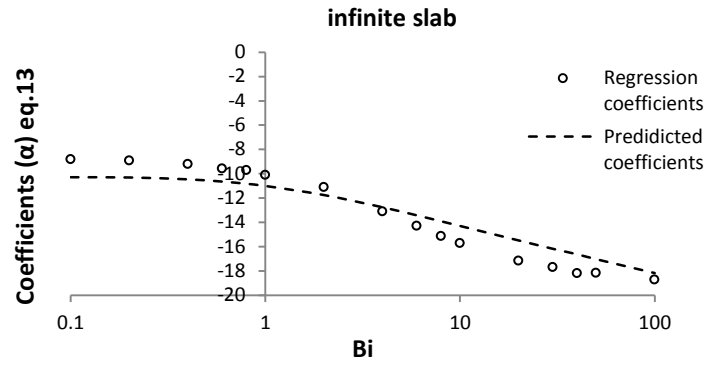
Figure 3. Plot of the slopes of the residual plots as a function of ln(Bi) for infinite slabs, the line represents the predicted coefficients from equation 13.
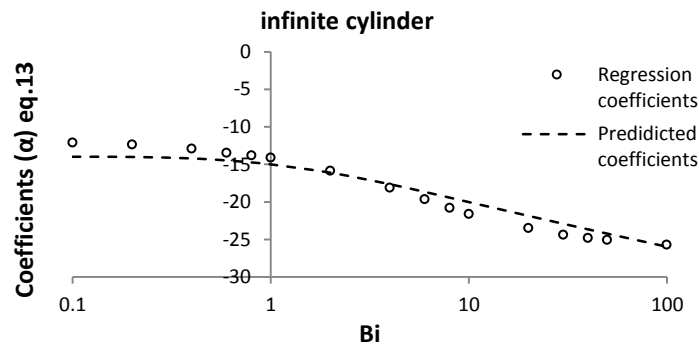
Figure 4. Plot of the slopes of the residual plots as a function of ln(Bi) for infinite cylinders, the line represents the predicted coefficients from equation 13.
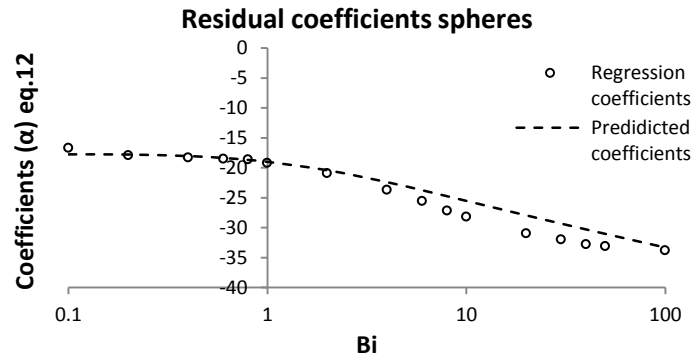
Figure 5. Plot of the slopes of the residual plots as a function of ln(Bi) for spheres, the line represents the predicted coefficients from equation 13.

Inserting eq.13 in eq.12 gives:

$$\ln(\epsilon) = -(\lambda_1 \cdot \ln(Bi) + C) \cdot Fo + (a_{c,1} - 1) \tag{14}$$

Taking the antilogarithm to eq. 14 and rearranging gives:

$$\epsilon = (a_{c,1} - 1) \cdot e^{-\lambda_1 \cdot \ln(Bi) \cdot Fo} \cdot e^{-C \cdot Fo} \tag{15}$$

Equation 15 may be simplified to:

$$\epsilon = (a_{c,1} - 1) \cdot Bi^{-\lambda_1 \cdot Fo} \cdot e^{-C \cdot Fo} \tag{16}$$

For the infinite slab, the infinite cylinder and the sphere, the rounded values of *C* equals: 11, 15, 19, respectively.

Equation 15 predicts that the residual, ε approaches 0 when the Fourier number becomes large and approaches $a_{c,1}$ when the Fourier number approaches 0, in full accordance with the exact solution of the series expansion (eq. 1). For Bi<0.1 $a_{c,1}$ approaches 1 and the residual is negligible, and in these cases the lumped capacitance method can be used [21]. For Bi>100 the surface resistance is negligible and these situations can be calculated as if Bi=100. The parameter C is not sensitive to small variations; however, the global fit of the model is best at the suggested values of C. The inputs needed are summarized in table 1.

Table 1 Formulae input to calculate the thermal history based with the suggested equation

Geometry	λ_1	a_c	a_m	C
Inf. plate	$Bi = \lambda_1 tan\lambda_1$	$\dfrac{2sin\lambda_1}{\lambda_i + sin\lambda_1 cos\lambda_1}$	$a_c \cdot \dfrac{sin(\lambda_i)}{\lambda_i}$	11
Inf. cylinder	$Bi = \dfrac{\lambda_1 J_1(\lambda_1)}{J_0(\lambda_1)}$	$\dfrac{2J_1(\lambda_1)}{\lambda_1(J_0^2(\lambda_1) + J_1^2(\lambda_1))}$	$a_c \cdot 2\dfrac{J_1\lambda_i}{\lambda_i}$	15
sphere	$Bi = 1 - \lambda_1 cot\lambda_1$	$\dfrac{2(sin\lambda_1 - \lambda_1 cos\lambda_1)}{\lambda_1 - sin\lambda_1 cos\lambda_1}$	$a_c . 3 \cdot \dfrac{sin(\lambda_i) - \lambda_i cos(\lambda_i)}{\lambda_i^3}$	19

The values of λ_1, $a_{c,1}$ and $a_{m,1}$ for different Biot numbers are presented in most textbooks on the subject based on the equations in table 1, alternatively, non-iterative solutions [19,20] can applied with small errors.

Inserting eq. 16 into eq. 10 gives:

$$\Omega = a_{c,1} \cdot e^{-\lambda_1^2 \cdot Fo} - (a_{c,1} - 1) \cdot Bi^{-\lambda_1 \cdot Fo} \cdot e^{-C \cdot Fo} \tag{17}$$

For an improved precision at Fo<≈0.05-0.08, where eq. 17 tends to overshoot the predicted value of Ω (see figure 6 later), the rational restriction Ω≤1 should be applied, since a value of Ω>1 is unphysical because no internal heat generation is considered.

$$\Omega = a_{c,1} \cdot e^{-\lambda_1^2 \cdot Fo} - (a_{c,1} - 1) \cdot Bi^{-\lambda_1 \cdot Fo} \cdot e^{-C \cdot Fo} \qquad [\text{ where } \Omega \leq 1]$$
$$\tag{18}$$

3.2 Volume average temperatures

The same procedure as in section 2.1 is used for constructing a similar equation for the volume average temperature:

$$\Omega = a_{m,1} \cdot e^{-\lambda_1^2 \cdot Fo} - (a_{m,1} - 1) \cdot Bi^{-3 \cdot \lambda_1 \cdot Fo} \cdot e^{-C \cdot Fo} \tag{19}$$

The exponential term (3·λ·Fo) is larger than in eq. 17 because the 1-term approximation is converging more rapidly for the volume average temperature than for the center temperature. The restriction Ω≤1 needs not to be applied in this case.

3.3 Finite bodies

For the calculation of finite bodies that can be represented as cross sections of infinite bodies (cans, boxes and infinite prisms) the method suggested by Newman [12] can be adopted with the new approach in the same manner as presented in equation 8, keeping in mind that the restriction (eq.18) should be applied for all individual dimensions. This is exemplified in section 4.1 by a case from industry.

4. Results and Discussion

To test the validity of the new equation (eq.18) it is compared with the solution to eq. 1 at representative Biot numbers (1 and 10 for the center, 4 and 20 for the volume average). The validation is presented in the figures 6.a-f for the center temperature and 7.a-f for the volume average temperature. The validation is presented for $0<Fo<0.2$. At higher Fourier numbers the solutions of both the 1-term solution and the new equation converge with the 100 term solution. The rational restriction $\Omega \leq 1$ is included in the figures.
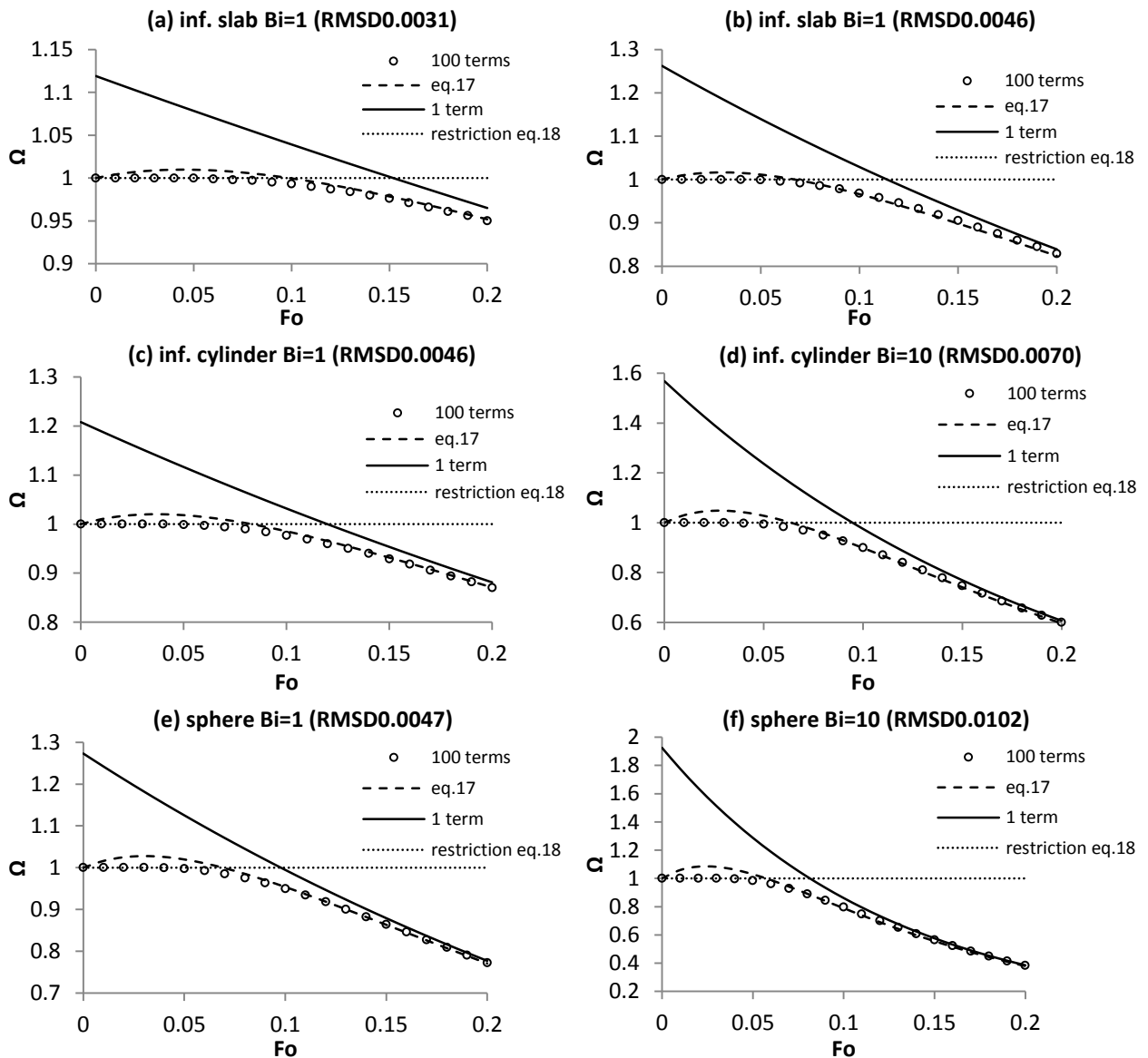
Figure 6. a-f. Center temperature validation by comparing the 1- term solution (eq. 1), the exact solution with 100 terms (eq. 1), and the new equation (eq. 18).

Figure 6 shows that eq. 17) generally overshoots slightly at low Fo; by including the restriction ($\Omega \leq 1$) in eq. 18 predicts the temperature response in the center with good precision at all Fo numbers.

The results from the validation of the volume average temperature calculation (eq.19) are presented in figure 7. a-f.
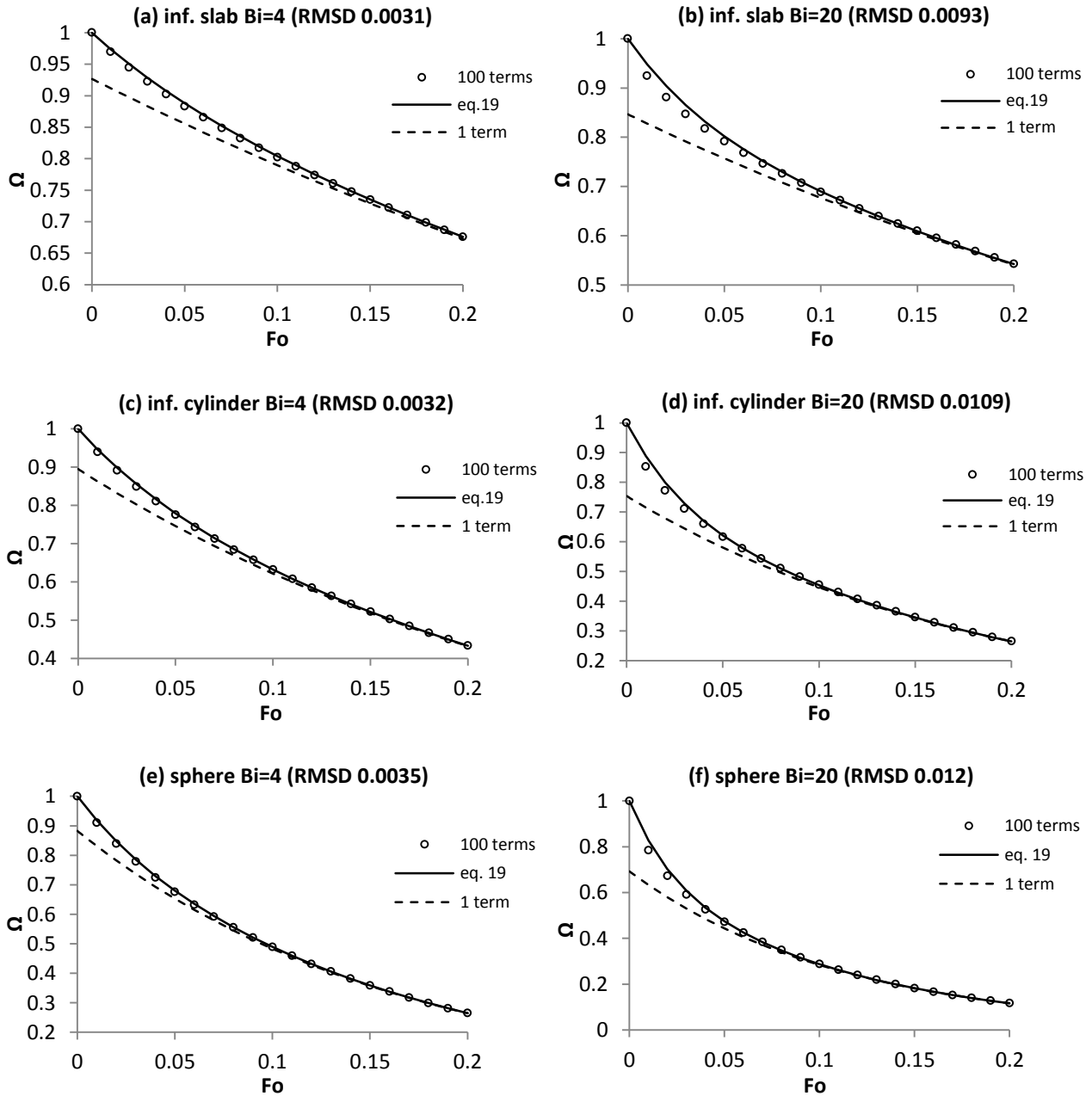
Figure 7. a-f. Volume average temperature validation by comparing by comparing the 1- term solution (eq. 1), the exact solution with 100 terms (eq. 1), and the new equation (eq. 19)**.**

As for the center temperature, the precision of the prediction is good also at low Fo numbers as can be observed in the graphs in figure 7.a-f.

The validation of the new equation is supported by the calculation of the error of prediction in terms of Root Mean Squared Difference (RMSD) (eq.20) for comparison between the 100 term solution and equations 18 and 19, respectively. The RMSD values of all the tested geometries are presented in table 2.

$$RMSD = \sqrt{\sum_{t=1}^{n}\left(\frac{(x_{1,t}-x_{2,t})^2}{n}\right)} \tag{20}$$

Table 2 The calculated RMSD values for the comparison between the new equation and the 100 term solution at 0<Fo<0.2 for the center temperature and volume average temperature.

	Center temperature (eq. 18) (Restriction: $\Omega \leq 1$)			Volume average temperature (eq. 19)		
Bi	Inf. slab RMSD	Inf. cyl RMSD	sphere RMSD	Inf. slab RMSD	Inf. cyl RMSD	sphere RMSD
0.1	0.0008	0.0010	0.0005	-	-	-
0.2	0.0013	0.0017	0.0012	-	-	-
0.4	0.0019	0.0026	0.0021	-	-	-
0.6	0.0024	0.0034	0.0030	-	-	-
0.8	0.0030	0.0041	0.0039	-	-	-
1	0.0031	0.0046	0.0047	0.0007	0.0006	0.0011
2	0.0035	0.0060	0.0072	0.0020	0.0018	0.0022
4	0.0031	0.0066	0.0089	0.0031	0.0032	0.0035
6	0.0035	0.0067	0.0101	0.0046	0.0047	0.0045
8	0.0041	0.0066	0.0102	0.0058	0.0062	0.0067
10	0.0046	0.0070	0.0102	0.0068	0.0074	0.0080
20	0.0046	0.0074	0.0103	0.0093	0.0109	0.0121
30	0.0041	0.0077	0.0107	0.0085	0.0123	0.0135
40	0.0042	0.0080	0.0115	0.0108	0.0126	0.0140
50	0.0037	0.0086	0.0124	0.0105	0.0128	0.0141
100	0.0041	0.0111	0.0161	0.0101	0.0123	0.0140

- At Bi<1, the error (RMSD) is insignificant for the volume average temperature because $a_{m,1} \approx 1$

As seen from the RMSD values in table 2, it is obvious that the error of the new equation is increasing at higher Biot numbers. The maximum error is for spheres (Bi=100) with a maximum RMSD of 0.016. In general RMSD is about 0.01 or lower, and this precision is adequate in most practical situations.

4.1 Validation of finite geometries – Cream cheese case study

To validate the developed equations in an industrial setup, the cooling of a packaged cream cheese is chosen, where the developed equations (18 and 19) are compared to a numerical simulation of the Fourier equation (eq. 21) conducted in COMSOL Multiphysics®.

$$\rho c_p \frac{\partial T}{\partial t} = \nabla \cdot (k\nabla T) = k\left[\frac{\partial^2 T}{\partial x^2} + \frac{\partial^2 T}{\partial y^2} + \frac{\partial^2 T}{\partial z^2}\right] \tag{21}$$

The simulation describes the temperature as a function of time and position using the following boundary conditions:

$$-k\frac{\partial T}{\partial x} = h_x(T - T_{air})$$

$$-k\frac{\partial T}{\partial y} = h_y(T - T_{air})$$

$$-k\frac{\partial T}{\partial z} = h_z(T - T_{air})$$

The packaged cream cheese is considered as a box with the dimensions (20×80×120 [mm]) and an apparent headspace of 2 [mm] on the top boundary caused by an attached lid, see figure 8.
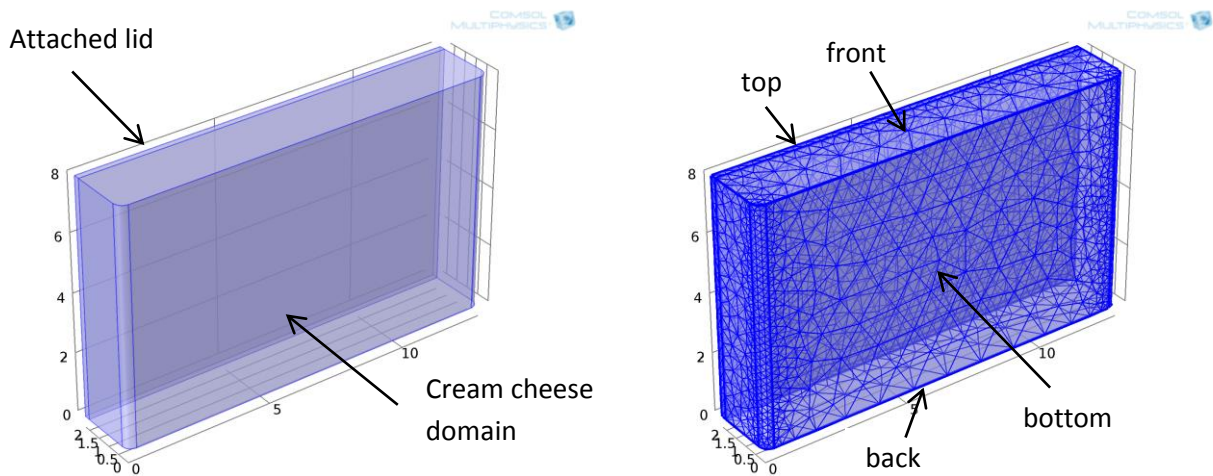
Figure 8. The constructed geometry for the modeling of cream cheese to the left and the applied mesh to the right. The dimension unit is [cm]. The attached lid is positioned at the top, the cream cheese domain is in the bottom.

The cream cheese is cooled in a conventional cooling tower by circulating air in a perpendicular airstream inducing a non-uniform heat transfer around the package. In a separate project we had measured the following heat transfer coefficients for the individual surfaces:

Dimension	Heat transfer coefficient
Top	30 [W/m^{2}K]
Bottom	10 [W/m^{2}K]
Sides	22 [W/m^{2}K]
Back	18 [W/m^{2}K]
Front	35 [W/m^{2}K]

The headspace below the lid acts as an insulating layer, and the heat transfer coefficient to the top of the cream cheese is therefore equal to the total heat transfer coefficient U:

$$\frac{1}{U} = \frac{1}{h} + \frac{k_{air}}{L_{headspace}} = \frac{1}{\left(\frac{1}{30} + \frac{0.0237}{0.002}\right)} = 7.5 \; [\text{w}/m^2\text{K}]$$

For the simplified calculation in the present work, the average values of h in each dimension are used, cf. the boundary conditions above:

- Top/bottom: 8.75 [w/m^{2}K] $\left(\frac{7.5+10}{2}\right)$
- Sides: 22 [w/m^{2}K] $\left(\frac{22+22}{2}\right)$
- Front/back: 26.5 [w/m^{2}K] $\left(\frac{18+35}{2}\right)$

The thermo physical properties of the cream cheese are (T, 50°C) : ρ_{cheese}=998 [kg/m^3], k_{cheese}=0.45[w/m·K], $c_{p,cheese}$=3261[J/kgK], $k_{headspace}$=0.0237[w/m·K].

Process description: The cream cheese is to be pre cooled before storage to allow the gel to set at a volume average temperature of 30°C, the initial temperature is 70°C and the surrounding temperature is 0°C. The volume average temperature is important as a set point for the cooling process, but also the center temperature (more precisely the global maximum temperature) is important in order to conduct process evaluation at the production site, as this can be directly measured.

The results from the simulation are the temperature history of the volume average temperature and the global maximum. Figure 9 shows the simulation results compared with the calculations using eq. 19 and eq. 18. The figure demonstrates also in this case a good agreement between the numerical simulations and the calculations according to the new equations developed in the present work.
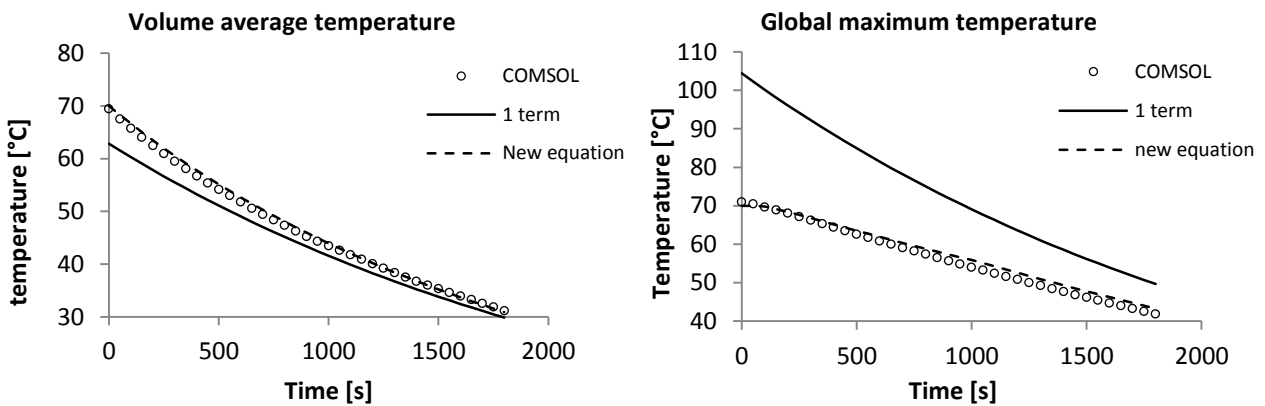
Figure 9 Comparison between the 1 term series expansion solution and the present work with the model result from COMSOL for the thermal history of the average temperature (left) and the global maximum temperature (right) for the original simulation setup described in the case

4.2 Implementation and parameter variability of the model

The developed equation (eq.18 for center temperature and eq.19 for volume average temperature) is immediately applicable in spreadsheets where the equation can be directly solved for any timescale. The input parameters needed in the calculations are the thermo-physical data calculated from the content of macro-nutrients, the product geometry, the heat transfer coefficient and the Fourier exponents (λ_1^2), thus the same inputs as if only the 1 term solution is applied, but with an additional constant C for each of the 3 ideal bodies. The needed eigenvalues (λ_1) and

Fourier exponents (λ_1^2) can be found in charts or tables in textbooks [3,5]. Alternatively they can be calculated by utilizing a non-iterative approximation procedure [19,20]. For finite bodies that can be presented as cross products of infinite elements, the solution by Newman [12] can be adopted as presented in the industrial case.

The only input parameter to the new equation that can vary independently is the constant C. The suggested values of C, (11 for infinite slabs, 15 for infinite cylinders and 19 for spheres) represent the best global fit for the tested Biot numbers. The other input parameters (Bi, λ_1, $a_{c,1}$, $a_{m,1}$) are given by the boundary conditions and the geometry of the body.

5. Conclusion and perspectives

The proposed equation gives good precision for the thermal response in the center and for the volume average temperature of simple geometries (slabs, cylinders, spheres, cans, boxes and prisms), covering the whole process time (Fo>0) and all Biot numbers in the range 0.1<Bi<100. In general, RMSD is about 0.01 or lower; for the sphere at high Bi the prediction error (RMSD) increases up to 0.016. This precision is adequate in most practical situations, considering that the driving temperature difference in most cases in the food industry is below 100°C. The variable input to the new equation is identical to the information needed in a 1-term solution to non-stationary heat transfer problems and an additional constant depending on the geometry. The equation can be applied by engineers for process evaluation, and it is directly implementable in spreadsheet solutions.

Acknowledgements

Appendix A

Table A1 Regression line coefficients and intercepts for the tested Biot numbers for infinite plates. The lag-factors $a_{c,1}$ and the eigenvalues (λ_1) are extracted from Mills [5]

Bi	$a_{c,1}$	λ_1	intercept ln $(a_{c,1}-1)$	Coefficient (α)	Bi	$a_{c,1}$	λ_1	Intercept ln $(a_{c,1}-1)$	Coefficient (α)
0.1	1.016	0.133	-4.135	-8.813	6	1.248	1.349	-1.394	-14.305
0.2	1.031	0.433	-3.474	-8.920	8	1.257	1.398	-1.359	-15.133
0.4	1.058	0.593	-2.847	-9.201	10	1.262	1.429	-1.339	-15.714
0.6	1.081	0.705	-2.513	-9.594	20	1.270	1.496	-1.309	-17.158
0.8	1.102	0.791	-2.283	-9.712	30	1.272	1.520	-1.302	-17.678
1	1.119	0.860	-2.129	-10.107	40	1.272	1.533[*]	-1.302	-18.179
2	1.180	1.077	-1.715	-11.119	50	1.273	1.539	-1.298	-18.174
4	1.229	1.265	-1.474	-13.101	100	1.273	1.555	-1.298	-18.712

Corrected value due to typing error in Mills 1995

A2

Table A2 Regression line coefficients and intercepts for the tested Biot numbers for infinite cylinders. The lag-factors $a_{c,1}$ and the eigenvalues (λ_1) are extracted from Mills [5]

Bi	$a_{c,1}$	λ_1	intercept ln $(a_{c,1}-1)$	Coefficient (α)	Bi	$a_{c,1}$	λ_1	Intercept ln $(a_{c,1}-1)$	Coefficient (α)
0.1	1.025	0.442	-3.689	-12.09	6	1.526	2.049	-0.642	-19.63
0.2	1.049	0.617	-3.016	-12.36	8	1.553	2.128	-0.592	-20.78
0.4	1.094	0.869	-2.364	-12.91	10	1.568	2.179	-0.566	-21.62
0.6	1.135	1.018	-2.002	-13.47	20	1.593	2.288	-0.523	-23.49
0.8	1.173	1.149	-1.754	-13.82	30	1.598	2.326	-0.514	-24.38
1	1.208	1.256	-1.570	-14.11	40	1.600	2.345	-0.511	-24.81
2	1.338	1.599	-1.085	-15.86	50	1.601	2.357	-0.509	-25.06
4	1.470	1.908	-0.755	-18.10	100	1.602	2.381	-0.507	-25.69

A3

Table A3 Regression line coefficients and intercepts for the tested Biot numbers for spheres. The lag-factors $a_{c,1}$ and the eigenvalues (λ_1) are extracted from Mills [5]

Bi	$a_{c,1}$	λ_1	intercept ln $(a_{c,1}-1)$	Coefficient (α)	Bi	$a_{c,1}$	λ_1	Intercept ln $(a_{c,1}-1)$	Coefficient (α)
0.1	1.030	0.542	-3.507	-16.79	6	1.834	2.654	-0.182	-25.64
0.2	1.059	0.759	-2.830	-17.89	8	1.892	2.765	-0.114	-27.16
0.4	1.116	1.052	-2.154	-18.31	10	1.925	2.836	-0.078	-28.21
0.6	1.171	1.264	-1.766	-18.52	20	1.978	2.986	-0.022	-31.01
0.8	1.224	1.432	-1.496	-18.58	30	1.990	3.037	-0.010	-32.03
1	1.273	1.570	-1.298	-19.19	40	1.994	3.063	-0.006	-32.71
2	1.479	2.029	-0.736	-20.89	50	1.996	3.079	-0.004	-33.10
4	1.720	2.456	-0.329	-23.67	100	1.999	3.110	-0.001	-33.78

References

[1] Baïri, A., Laraqi, N. Diagrams for fast transient conduction in sphere and long cylinder subject to sudden and violent thermal effects on its surface, Applied Thermal Engineering (2003) 23 1373-1390

[2] Lü, X., Lu, T., Viljanen, M., A new analytical method to simulate heat transfer in buildings, Applied Thermal Engineering 26 (2006) 1901-1909

[3] R.P. Singh, D.R. Heldman, Introduction to Food Engineering, 5th ed. Cpt. 4 pp. 339-366 Elsevier (2013)

[4] H.S. Carslaw, J.C. Jaeger, Conduction of Heat in Solids, second ed., Oxford University Press, Oxford, UK, 1959

[5] A.F. Mills, Heat And Mass Transfer *Cpt. 3* pp. 123-173. Richard D. Irwin, Inc. (1995)

[6] C.O. Ball, Determining By Methods of Calculation The Time Necessary To Process Canned Foods, Bulletin of the National Research Council, Volume 7 (37): pp. 9-76 (1923-1924)

[7] I.J. Pflug, J.L. Bleidsdell, J. Kopelman, Developing Temperature-Time Curves for Objects That Can Be Approximated By a Sphere, Infinite Plate, or Infinite Cylinder, Transaction of ASHRAE 71: pp. 230-239 (1965)

[8] G. Trystram, Modeling of food and food processes, Journal of food Engineering 110: pp. 269-277 (2012)

[9] J. Dehghannya, M. Ngadi, C. Vigneault, Mathematical model procedures for airflow, heat and mass transfer during forced convection cooling of produce: a review, Food Eng. Rev 2010 (2)(2010) : pp. 227-243

[10] R.A. Lemus-Mondaca, A. Vega-Gálvez, N.O. Moraga, Computational simulation and developments applied to food thermal processing, Food Eng. Rev 2011 (3) (2011): pp. 121-135

[11] A.H. Feyissa, K.V. Gernaey, J. Adler-Nissen,3D Modeling of coupled heat and mass transfer for a convective oven roasting process. Meat Science, volume 93 (4) (2013): pp. 810-820

[12] A.B. Newman, Heating and cooling rectangular and cylindrical solids, Industrial and Engineering Chemistry, 28 (1936): pp. 545-548

[13] H.P. Gurnay, J. Lurie, Charts for estimating temperature distributions in heating or cooling solid shapes. Industrial and Engineering Chemistry Vol 15 (11) (1923): pp. 1170-1172.

[14] M.P. Heissler, Temperature charts for induction and constant-temperature heating, Transaction of ASME 69 (1947): pp. 227-236

[15] K-I. Hayakawa, Estimating the central temperatures of canned food during the initial heating or cooling period of heat process, Food Technology 23: (1969) :pp. 1473-1477

[16] A. Baïri, N. Laraqi, N. Alilat, Z. Zouaoui, Fast transient conduction in infinite plate subject to violent thermal effects, Applied Thermal Engineering 24 (2004) pp. 1-15.

[17] H.S. Ramaswamy, S. Shreekanth,(1999). Simplified equations for transient temperature prediction in solids during short time heating or cooling, Canadian Agricultural Engineering 41(1) (1999): pp. 59-64

[18] R Development Core Team (2008). R: A language and environment for statistical computing. R Foundation for Statistical Computing, Vienna, Austria. ISBN 3-900051-07-0, URL http://www.R-project.org.

[19] H.S. Ramaswamy, K.L. LO, M.A. Tung, Simplified equations for transient temperatures in conductive foods with convective heat transfer at the surface, Journal of Food Science (47) (1982): pp. 2042-2047

[20] A.G. Ostrogorsky, Simple explicit equations for transient heat conduction in solids, Journal of Heat Transfer 131 (2009) pp. 011303.1-011303.11

[21] A. F. Mills, Heat And Mass Transfer *Cpt. 3* pp. 32. Richard D. Irwin, Inc. (1995)

Joint author statement

If a thesis contains articles (i.e. published journal and conference articles, unpublished manuscripts, chapters etc.) made in collaboration with other researchers, a joint-author statement verifying the PhD student's contribution to each article should be made by all authors. However, if an article has more than three authors the statement may be signed by a representative sample, cf. article 12, section 4 and 5 of the Ministerial Order No. 1039 27 August 2013 about the PhD degree. We refer to the Vancouver protocol's definition of authorship.

A representative sample of authors is comprised of
- Corresponding author and/or principal/first author (defined by the PhD student)
- 1-2 authors (preferably international/non-supervisor authors)

Titel of the article	Computer aided simulation for developing a simple model to predict cooling of packaged foods
Author(s)	Martin Gram Christensen, Aberham Hailu Feyissa, Jens Adler-Nissen
Journal/conference * if applicable	Internation Conference of Engineering and Food (ICEF11)
Name of PhD student	Martin Gram Christensen
Date of Birth	19th of September 1981

Description of the PhD student's contribution to the abovementioned article

Martin Gram Christensen as the first author formulated the idea, carried out the experimentals, deduced the equations and was main writer of the manuscript. Aberham Hailu Feyissa as co-author carried out the numerical simulations and contributed in the writing of the manuscript and the experimental setup. Jens Adler-Nissen as co-author reviewed the full manuscript and gave comments and suggestions to the manuscript and approach.

Signature
of the PhD student _____ Date 25-9-2014

Signatures of co-authors

As a co-author I state that the description given above to the best of my knowledge corresponds to the process and I have no further comments.

Date (DD/MM/YY)	Name	Signature
25/09/2014	Jens Adler-Nissen	
25/09/2014	Aberham Hailu Feyissa	

Joint author statements shall be delivered to the *PhD administration* along with the PhD thesis

Computer aided simulation for developing a simple model to predict cooling of packaged foods

Martin Gram Christensen[a], Aberham Heilu Fayissa[a], Jens Adler-Nissen[a]

[a] National Food Institute, DTU, Lyngby, Denmark (mgch@food.dtu.dk)

ABSTRACT

A new equation to predict equilibrium temperatures for cooling operations of packaged foods has been deducted from the traditional 1st order solution to Fourier's heat transfer equations. The equation is analytical in form and only requires measurable parameters, in form of area vs. volume ratio (A/V), thermo-physical properties calculated from the recipe, and the heat transfer coefficients measured in the equipment. The equation is based on an overall Biot number. The simple deducted model was tested and validated with experimental and simulated setups. Simulations have been performed using COMSOL Multiphysics, commercially available software, to test the new equation. Additionally, an experiment with all boundary conditions known, and the three dimensional coordinates of the position of six thermocouples were conducted. The COMSOL simulation showed very good conformity with experimental results matching all individual thermocouples. Simulations are used as a validation tool for cooling predictions. This was done by comparing the simulated equilibrium temperature with the calculated using the new equation. The simulations are able to evaluate cooling situations in the industry where experiments are too laborious or impossible to conduct. The deducted equation was tested for irregular geometries, unequal heat transfer and headspace restrictions. The new equation predicted equilibrium temperature curves of the simulated cooling with a low error (1.5°C for Fourier numbers below 0.3) and good precision at the target temperature (error below 0.5°C for Fourier numbers above 0.3).

Keywords: Cooling; Finite Element Method; Irregular geometry; Heat Transfer; Modelling

INTRODUCTION

Cooling operations are important unit operations in the food industry. Often, it is a big challenge to find the appropriate cooling time because the optimal set-point is to achieve the correct equilibrium temperature in the product before it is conveyed to the cold storage. As the product eventually will obtain the same temperature in the cold storage it is economically advantageous only to cool until the cold storage equilibrium temperature is met. However, it is difficult to conduct experiments for measuring the equilibrium temperature over time, especially in industrial setups. This necessitates fast calculations to manage prediction of the equilibrium temperature during daily operation management. So far, simple equations have only been developed to handle calculations of the equilibrium temperature of simple geometries for cooling processes where the solutions suggested by Pflug *et.al* [1] can be used. The scope of this project is to derive such models by using finite element modelling (FEM) in COMSOL Multiphysics to conduct *in silico* experiments for the validation of the models. In this paper the first developed model based on A/V (area to volume) ratio and an overall Biot-number is validated. The models must be analytical for implementation in commercial software, easy to use, and still provide more precision than the traditional 1st order approximations of Fourier's equations for Fo> 0.3 and simple geometries.

Traditionally, the equations used for calculation of cooling operation times in the food industry have been based on a 1st order approximation of Fourier's heat transfer equations (1). This is done by utilising a-values (a_m for the equilibrium temperature) as described by Pflug and Kopelman as a j-factor [1], and b values as described by Ball [2] as an f-factor.

$$\Omega = \sum_{i}^{\infty} a_i e^{-b_i \cdot Fo} \quad (1)$$

For non-ideal geometries the approach suggested by Newman [3] has been utilised. However, due to unequal boundary conditions and lack of symmetry these methods are not very precise under real life conditions. Simple model solutions have been suggested by Cleland and Earle [4] and Merts, Bickers and Chadderton [5]

for centre temperature prediction during cooling and these simple solutions requires thorough geometrical calculations.

Alternatively, and pushed by the technological advance in IT, calculations of cooling times have been performed using finite element modelling by Wang and Sun [6] and Amézquita, Wang and Weller [7]. These studies have also been focussing on point temperatures, and are conducted with assumed equal boundary condition, or calculated based on air velocity, which can be very difficult to measure in industrial setups.

FEM methods are precise but unfortunately time consuming and demand trained personnel. Further it necessitates that the boundary conditions are well described. When utilised properly FEM modelling can handle the unequal boundaries and asymmetrical geometries present in industrial cooling operations, and can serve as a powerful tool in validating and testing simple, deduced analytical models, when experiments are too laborious or impossible to conduct.

Many food products are cooled in the package, which often can be described as a semi-filled un-symmetrical plastic package with an air filled headspace. The products are typically cooled with a perpendicular airflow across the packages. This highlights the two major challenges when a simple equation should be developed for cooling processes: the boundary conditions are not equal and must be determined individually, and the geometry is asymmetrical. Thus the widely used method described by Newman [3] is not applicable in many situations, according to his own conclusions. However, by utilising the A/V ratio as the determining dimension, a different view on the geometry is achieved which is not dependent on the geometrical shape.

The Biot number in blast cooling is usually fairly low (below 5). In blast cooling operations the equilibrium temperature is often the target and the dimensionless temperature Ω will be low ($\Omega<0.5$), therefore the Fourier number will be fairly high (above 0.2). This favours a simplification by utilising a 1st order approximation. In earlier studies [8] the Biot numbers of known geometries (infinite slab, infinite cylinders, spheres and cubes) have been investigated for Biot numbers below 5. An overall Biot number ($Biot_d$) of a specimen have been suggested to give similar results in cooling process evaluations compared to single dimension Biot numbers. The geometry´s overall Biot number is suggested to be calculated based on A/V ratio, for the three finite specimens in the x,y,z domain as presented in eq. 2 and 3:

$$\frac{1}{Biot_d} = \frac{1}{Biot_x} + \frac{1}{Biot_y} + \frac{1}{Biot_z} \ (2)$$
$$Biot_d = \frac{h}{k} \cdot \frac{V}{A} \ (3)$$

Where V [m³] is the volume of the geometry, A [m²] is the surface area of the geometry, h [W/m²K] is the heat transfer coefficient, and k is the thermal conductivity of the food. Eq. 2 is suggested to apply for all irregular, asymmetric geometries [8].
The overall Biot number enables a single equation description of the heat transfer in 3-dimensional geometries. This requires that the "a"- and "b"- values can be expressed as single values for the specimen. To achieve this, the b values are plotted as b/Biot (4) as a function of $Biot_d$ (3).

$$y = \frac{b}{Biot} \ (4)$$

For the known infinite geometries (inf. slab, inf. cylinder and sphere) the b values can be expressed by eq. 5 by utilising a geometry factor, n [7] (slab=1, cyl=2, sphere=3) by curve fitting of b-values.

$$y = 0.0325 \cdot n^{1.35} \cdot Biot_d - 0,279 \cdot n^{0.65} \cdot Biot_d + 1 \ (5)$$

Where n is the dimensionality, and $Biot_d$ is the overall Biot number. The same relationship is utilised when handling irregular geometries.

As the a_m values for the first order approximation are determined based on point measurements [1], the solution suggested by [3] does not apply for modelling equilibrium temperatures. Thus no overall

determination of the a_m-value for finite elements exists. In this study the a_m values are proposed to follow eq. (6) based on the assumption that a_m values for finite elements can be calculated by a plot fit of the a_m for single dimensions as a function of the overall Biot number ($Biot_d$) and a dimensional factor (n), and the overall Biot number [8].

$$a_m = \left(\frac{4 \cdot n - 2}{100}\right) \cdot Biot_d + 1,01 \ (6)$$

The expression of the b-values in eq. 4 gains continuity between the 1st order approximation of Fourier's equations and the lumped form used when no heat gradient is considered (for Biot→ 0, y→ 1). In the approach the y factor is denoted as b/Biot fulfilling the assumption of obtaining continuity. When the three known geometries are expressed by an overall Biot number, the "a" and "b" values can be calculated using eq. 5 and 6. The relationship between Ω and time (t) is then deduced to the following:

$$\Omega = a_m \cdot e^{-y \cdot \frac{A \cdot h}{V \cdot \rho \cdot C_p} \cdot t} \ (7)$$

In eq. 7 the 1st order solution for Fourier's equations presented in eq. 1 is reduced from three equations down to one explaining all three dimensions for equilibrium temperatures, where ρ [kg/m^3] is the density of the food and c_p [J/(kgK)] the specific heat capacity. The equation has been tested against a 6th order solution to Fourier's equation for cylinders, cubes and spheres with comparable results for Biot numbers below 5 [8] with good agreement, and with an advantage of handling irregular geometries, where three single Biot numbers are not determinable.

In this study the governing equations of Fourier in eq. 8 have been solved for the experimental geometry using COMSOL Multiphysics to simulate the conducted wet experiments.

$$\rho c_p \left(\frac{\partial T}{\partial t}\right) = k \left[\frac{\partial^2 T}{\partial x^2} + \frac{\partial^2 T}{\partial y^2} + \frac{\partial^2 T}{\partial z^2}\right] \ (8)$$

MATERIALS & METHODS

For the experimental validation of the new developed equation a puree was made of soaked, boiled and blended chickpeas as a model system. The dry matter content of the puree was 25 % [w/w], and the thermo-physical properties calculated to; thermal conductivity 0.538 [W/(mK)], density 1072 [kg/m^3], heat capacity 3591 [J/(kgK)]. The chickpea puree was cooled in a blast freezer and the temperature measured by T-type thermo couples in seven measuring points through a custom made geometry (100x100x300mm aluminium with a thickness of 2 mm), as presented in figure 1.

Figure 1 Geometrical setup of the experiments in the blast cooler

To determine the local heat transfer in the blast cooler, a solid aluminium block was used. The aluminium block was isolated from all sides except one using polystyrene, and placed in the cooler to determine the temperature history of all six sides of the block singularly, using T-type thermo couples. The local heat transfer was calculated based on the lumped equation for transient heat transfer, assuming a very low Biot number for the aluminium block (<0.01).

The experiments were simulated using COMSOL Multiphysics, with the measured local heat transfer coefficients as boundary conditions. The x,y,z-coordinates of the T-couples in the simulation was compared with the experimental results based on six point temperature curves to validate the conformity between the simulations and experiments. The calculated equilibrium temperatures from the simulations have been used

for validation of the simple model. Further validation of the new equation (7) is conducted by comparison with a 6th order solution to Fouriers series (in eq. 1) in an excel-based program, BIC-Simula, developed at the institute by associate professor Jørgen Risum. Calculations based on the programme is in this article noted BIC-Simula.

RESULTS & DISCUSSION

The local heat transfer coefficients were measured in a blast cooler to determine the boundary conditions for the simulations of cooling processes in the equipment. Based on the heat flux across a solid aluminium block, the heat transfer coefficient was calculated based on the lumped equation for transient heat transfer. It is clear that the local heat transfer coefficients are different on the six boundaries in table 1. Thus the COMSOL simulations should preferably be computed using the local heat transfer coefficients. The results also indicate that in case of headspace in the packaging material the local heat transfer is reduced significant, (from 30 to 10 [W/(m²K)]), but is still too high to neglect and use the approach suggested by [3].

Table 1. Local heat transfer coefficients

Geometry position	Local heat transfer coefficient [W/m²K]
back	24,5
sides	27
front	33
bottom	35
isolated bottom	0
top	
-direct flow	32
-headspace 28 mm	7
headspace 10 mm	9
headspace 5 mm	10
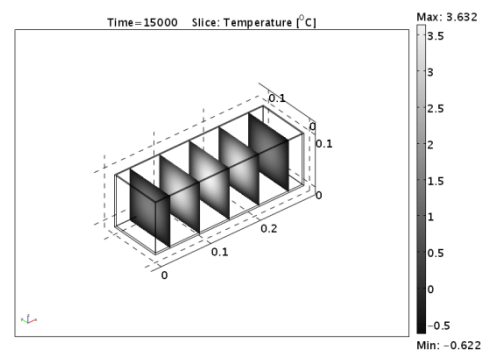
Figure 2 Temperature distribution at t=15000s for the COMSOL simulation

The COMSOL simulation is compared with the experiments in figure 3 for six measurements during blast cooling of chickpea puree.
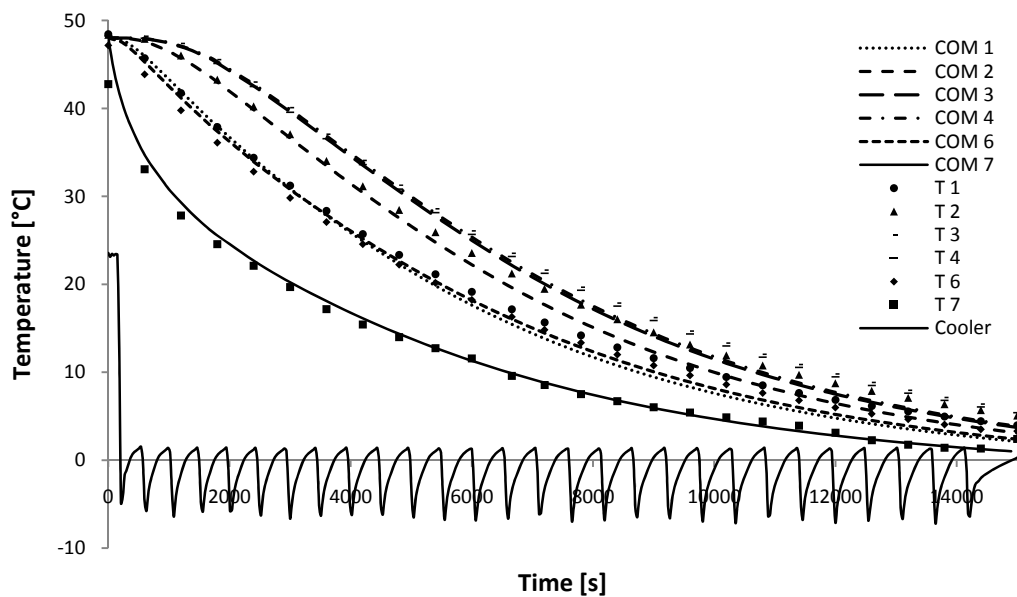
Figure 3 Comparison of the measured Temperature points during cooling of chickpea puree in a blast cooler (T1, T2, T3, T4, T6, T7), with the corresponding simulated temperature curves (COM1, COM2, COM3, COM4, COM6, COM7) at the x,y,z points in COMSOL.

The simulated and experimental results show good agreement with only minor deviations at the positions close to the centre (-2°C). The simulations are thus used as *in silico* experiments for the validation of the new model for equilibrium temperature. The equilibrium temperature are calculated from the simulation and used for comparison with the developed eq. 7. This approach will make it possible to test irregular geometries with unequal boundary conditions and headspace in simulations to further validate the new eq. 7. The simulation and the developed model are compared in figure 4, 5, 6 and 7 for different geometries. In Table 2, the maximum error between the simulation and the simple model are listed. The simulated cooling curve for equilibrium temperature is compared to the calculated cooling curve from eq. 7, and a 6th order approximation for finite elements.
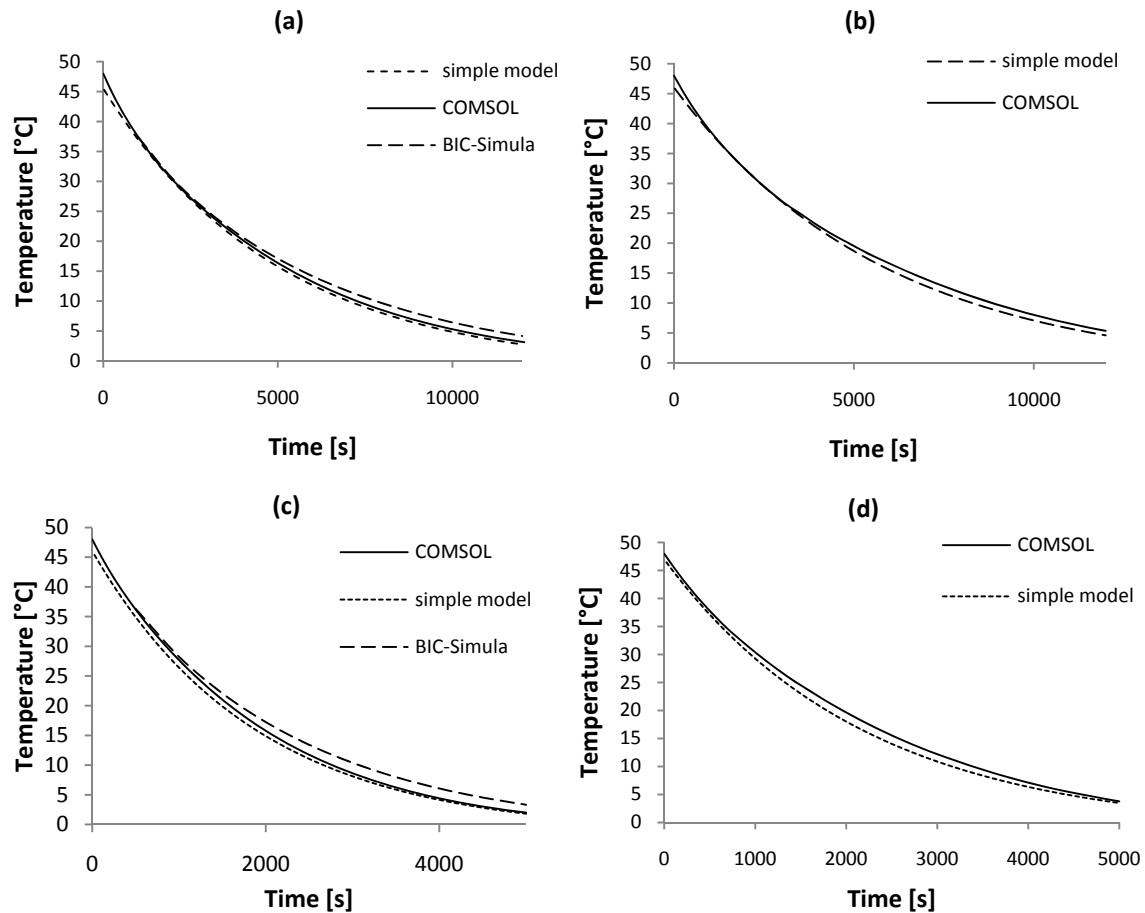
Figure 4 Comparison of the simulated temperature curves by COMSOL and the calculated equilibrium temperature using the new model (7), the four graphs presented are free standing geometry (a)(100x100x300mm), free standing geometry with headspace (b)(100x100x300mm), free standing geometry (c)(50x50x150mm) and a free standing geometry with headspace (d)(50x50x150mm).

From the results in Figure 4, the new model is able to describe the evolution of the equilibrium temperature with good precision. At high Fourier numbers, the simple model predicts the same equilibrium temperatures as found in the COMSOL simulations.

Table 2. Maximal error in degrees centigrade between simulated equilibrium temperatures and prediction of the temperatures using the new model.

Geometry	Centigrade error maximum	Error at target (5°C)
Geometry (a)	+1,5 [°C]	<0.5[°C]
Geometry (b)	+2 [°C]	<1 [°C]
Geometry (c)	+1.5 [°C]	<0.5 [°C]
Geometry (d)	+2 [°C]	<0.5 [°C]

The results presented in Figure 4 and the errors summed in Table 2 indicate good precision in predicting equilibrium temperatures using the new equation. An important notice is that the error in the latter part of the prediction curve is very small (large Fo-numbers). Thus in the final equilibrium temperature prediction the error is insignificant compared to experimental error, because the target of importance during cooling is the final equilibrium temperature. The simplification has not harmed the prediction of equilibrium temperatures when compared to the BIC-SIMULA calculations.

It should be noted that the suggested solution to handle cooling and equilibrium temperatures are only validated for specimens with a Biot number below 5. The future scope is to further develop the simple model, with respect to the equation description of the "a" and "b" values, to enable handling products with larger Biot numbers, and to investigate the possibility of incorporating mass transfer into a single equation.

CONCLUSION

An experimental setup has been used to enable simulations for the prediction of equilibrium temperature during cooling of foods in packaging materials. The simulation has proved a powerful tool for the validation of simple prediction models.

It is possible to conduct easy calculation of cooling times for foods in packaging materials in industrial applications, where the boundary conditions are unequal, and the package is asymmetrical, by utilising the simple model presented in eq. 7.

The newly developed model has proven quite precise in equilibrium temperature prediction in the performed simulations based on a few industrial measurable variables (A/V ratio, thermo physical data and heat-flux). The temperature error was low (<0.5°C) in the final equilibrium temperature prediction. Due to the analytical form of the model it is implementable in excel spreadsheets and could serve as a powerful tool for fast and easy cooling time prediction in daily operations in the food industry.

REFERENCES

[1] Pflug, I. J., Bleidsdell, J. L., Kopelman, J. (1965) Developing Temperature-Time Curves for Objects That Can Be Approximated By a Sphere, Infinite Plate, or Infinite Cylinder *ASHRAE semiannual meeting January 25-28 1965 in Chicago, Michigan*

[2] Ball, C., O. (1923-1924) Determining, By Methods of Calculation, The Time Necessary To Process Canned Foods. *Bulletin of the National Research Council, Volume 7 (37):9-76*

[3] Newman, A.B. (1936) Heating and cooling rectangular and cylindrical solids. *Industrial and Engineering Chemistry*, 28, 545-548

[4] Cleland, A.C. and Earle, R.L. (1982) A simple method for prediction of heating and cooling rates in solids of various shapes. *International Journal of Refrigeration*, 5 , 2, 98–106

[5] Merts, I. Bickers, E.D. and Chadderton, T. (2007) Application and testing of a simple method for predicting chilling times for hoki (*Macruronus novaezelandiae*). *Journal of Food Engineering*, 78, 162-173

[6] Wang, L. and Sun, D. W. (2002) Modelling three conventional cooling processes of cooked meat by finite element method. *International Journal of Refrigeration*, 25, 100-110

[7] Amézquita, A., Wang, L., Weller, C. L. (2005) Finite Element Modeling and Experimental Validation of Cooling Rates of Large Ready-To-Eat Meat Products in Small Meat-Processing Facilities. *ASAE American Society of Agricultural Engineers ISSN 0001-2352*

[8] Christensen, M. G., Adler-Nissen, J (2010). Robust Modeling for Processing of Ready-Made Meals. *Conference paper: Food Factory of the Future.* Gothenburg 1. July 2010

Joint author statement

If a thesis contains articles (i.e. published journal and conference articles, unpublished manuscripts, chapters etc.) made in collaboration with other researchers, a joint-author statement verifying the PhD student's contribution to each article should be made by all authors. However, if an article has more than three authors the statement may be signed by a representative sample, cf. article 12, section 4 and 5 of the Ministerial Order No. 1039 27 August 2013 about the PhD degree. We refer to the Vancouver protocol's definition of authorship.

A representative sample of authors is comprised of
- Corresponding author and/or principal/first author (defined by the PhD student)
- 1-2 authors (preferably international/non-supervisor authors)

Titel of the article	Potatoes as potential devices for studying fluid to particle heat transfer in vessel cooking processes
Author(s)	Aberham Hailu Feyissa, Martin Gram Christensen, Søren Juhl Pedersen, Minka Hickman, and Jens Adler-Nissen
Journal/conference * if applicable	
Name of PhD student	Martin Gram Christensen
Date of Birth	19th of September 1981

Description of the PhD student's contribution to the abovementioned article

Feyissa as first author has made the numerical simulations and data treatment, contributed with ideas to the experimental design and has been heavily involved in writing the full manuscript. Christensen has as co-author conducted the literature review in the introduction, contributed to the writing process of the full manuscript, conducted the sensitivity analysis of the analytical calculations, and together with co-author Pedersen designed, constructed and tested the experimental setup with the half-vessel. Pedersen has, in addition to development of the experimental setup, contributed in the review of the full manuscript. Hickman as co-author carried out the experimental work as part of her Master thesis work (supervised by Adler-Nissen and Feyissa), and established the imaging technique for measuring the progression of the gelatinisation front. Adler-Nissen as co-author has coordinated the full manuscript, contributed to the idea development and reviewed/edited the full manuscript. All authors have contributed in discussions, writing and reviewing of the manuscript.

Signature of the PhD student _(signature)_ Date 25-9-2014

Signatures of co-authors

As a co-author I state that the description given above to the best of my knowledge corresponds to the process and I have no further comments.

Date (DD/MM/YY)	Name	Signature
23/09/14	MINKA HICKMAN	
25/07/14	Søren Juhl Pedersen	
25/09/14	Aberham Hailu Feyissa	
25/09/14	Jens Adler-Nissen	

Joint author statements shall be delivered to the *PhD administration* along with the PhD thesis

Appendix 4

Manuscript Number:

Title: Potatoes as potential devices for studying fluid-to-particle heat transfer in vessel cooking processes

Article Type: Research Article

Corresponding Author: Dr. Aberham Hailu Feyissa, Ph.D

Corresponding Author's Institution: Technical University of Denmark, DTU

First Author: Aberham Hailu Feyissa, Ph.D

Order of Authors: Aberham Hailu Feyissa, Ph.D; Martin Gram Christensen, MSc; Søren Juhl Pedersen, MSc; Minka Hickman, MSc; Jens Adler-Nissen, Professor, dr.techn.

Abstract: This paper presents and demonstrates a novel idea of using spherical potatoes as a dispensable, cheap device for studying fluid-to-particle heat transfer in vessel cooking processes. The transmission of heat through the potato can be traced by measuring the distance from the surface to the gelatinization front, which is easy to identify visually. Knowing this distance, the gelatinization temperature, the period of immersion, and the average radius of the potato allow for the assessment of the heat transfer coefficient by fitting a simple numerical model (FEM) of non-stationary heat transfer into a sphere with the thermo-physical properties of potatoes. Alternatively, an analytical one-term solution of the Fourier equation can be applied. The gelatinization temperature of the potatoes used was assessed to be 67oC by a direct temperature measurement while visually following the progression of the gelatinization front in a half potato attached to a window in the cooking vessel.

Potatoes as potential devices for studying fluid-to-particle heat transfer in vessel cooking processes

Aberham Hailu Feyissa, Martin Gram Christensen, Søren Juhl Pedersen, Minka Hickman, and Jens Adler-Nissen

Food Production Engineering, DTU Food, Technical University of Denmark, Søltofts Plads 227, DK-2800 Lyngby, Denmark

Abstract

This paper presents and demonstrates a novel idea of using spherical potatoes as a dispensable, cheap device for studying fluid-to-particle heat transfer in vessel cooking processes. The transmission of heat through the potato can be traced by measuring the distance from the surface to the gelatinization front, which is easy to identify visually. Knowing this distance, the gelatinization temperature, the period of immersion, and the average radius of the potato allow for the assessment of the heat transfer coefficient by fitting a simple numerical model (FEM) of non-stationary heat transfer into a sphere with the thermo-physical properties of potatoes. Alternatively, an analytical one-term solution of the Fourier equation can be applied. The gelatinization temperature of the potatoes used was assessed to be 67°C by a direct temperature measurement while visually following the progression of the gelatinization front in a half potato attached to a window in the cooking vessel.

Keywords:

Heat transfer coefficient – potato – fluid-to-particle heat transfer – gelatinization – FEM

Highlights:

- Determination of fluid-to-particle heat transfer coefficient for food particles in vessel cooking processes by using spherical potatoes as model particles.
- The progression of the gelatinization front during heating is easy to identify visually and gives the moving position of the 67°C isotherm.

2

- Solving the Fourier equation numerically or analytically gives a model which can predict the relation between the heat transfer coefficient and the position of the 67$^{\text{o}}$C isotherm with time.

1. Introduction

Heating of suspended particles in a liquid is a very common operation in the food industry, for example in many canning processes (Meng & Ramaswamy 2005), in continuous aseptic processing (Ramaswamy et al. 1997), or in vessel cooking of soups and sauces with suspended pieces of meat and/or vegetables (Bouvier et al. 2011). It is the vessel cooking process that is the focus of this paper. The common practice in industry is first to make the base soup or sauce and then add the solid food pieces at prescribed intervals. At the time of addition, the solid food pieces are colder than the fluid, or even frozen; this can cause a significant drop in the temperature of the fluid. After processing the product needs to be cooled, and this also induces considerable temperature gradients between the fluid and the particles.

To evaluate if the suspended food particles have received an adequate heat treatment in the course of the process it is necessary to know the geometry and thermo-physical properties of the food particles and also to have a rough assessment of the fluid-to-particle heat transfer (h_{fp}) under the prevailing process conditions. Determination of the thermo-physical properties from knowledge of the composition of the food can be done with reasonable accuracy (Nesvadba 2014; Singh and Heldman 2014: 275-282), while determination of the fluid-to-particle heat transfer is not a trivial task.

In the literature several different techniques have been reported for estimating fluid-to-particle heat transfer coefficients in food processes, primarily in continuous heat treatment processes or in canned foods processed in rotating autoclaves. A complete listing of references is out of scope here, as the literature (the majority of references are from the 1980s and 1990s) is well covered by three extensive reviews (Maesmans et al. 1992; Ramaswamy et al. 1997; Barigou et al. 1998). The most common approach is to measure the temperature-time profile inside a real food particle or replicas of either materials having thermal properties close to food products or of a highly conductive material, usually aluminium. By fitting the temperature-time curve to a mathematical solution of the Fourier equation for non-stationary convective heat transfer into a body of the relevant geometry,

usually a sphere, it is possible to estimate the particle-to-fluid heat transfer coefficient (Maesmans et al 1992; Barigou et al. 1998). Three examples of studies using this approach are: one represents particles in tube flow (Ramaswamy & Zareifard 2000, another is dealing with the determination of h_{fp} for surface pasteurisation of eggs (Denys et al. 2003), the third is a study of the autoclaving of a canned, viscous model food with particles (Meng & Ramaswamy 2005).

The advantage of using particle replicas of metal, for which the Biot number is very low (Bi < 0.1), is that the solution to the heat transfer equation is simple and allows a high precision in the determination of h_{fp} (Barigou et al. 1998), and that the position of the temperature sensor inside the body is not critical (Ramaswamy et al. 1997). The use of particles with food-like thermo-physical properties (Bi > 0.1) generally results in a less precise determination of h_{fp}, and the heat transfer equation must be solved by a more complicated series expansion of the Fourier equation (Maesmans et al 1992; Barigou et al. 1998). However, an advantage of using model particles with food-like thermo-physical properties is that the heat transfer conditions are more realistic than for metal replicas ; this holds in particular for cases in which were natural convection is a significant (Åström & Bark 1994). The different solutions to the heat transfer equation at Bi>0.1 are presented in standard textbooks (Mills 1995: 167-176; Singh & Heldman 2014: 355-383), and need not be expounded here.

The recording of the temperature inside the particle represents a major experimental obstacle in nearly all processes since the food pieces are normally free flowing in the liquid, and a connecting wire will restrict the particle flow. Alternative, wireless methods are therefore much sought for (Maesmans et al. 1992). Time-temperature-integrators based on the kinetics of microbial inactivation have been proposed and tested, but the method requires calibration and does not seem to be precise for determination of h_{fp} (Maesmans et al. 1994). The method is, however, useful for studying the temperature distribution in agitated vessels (Mehauden 2008). Particles with embedded liquid crystals, which are heat sensitive and change colour with temperature have been tested (Balasubarminan & Sastry 1994). Calibration is difficult and the use of the technique is restricted to transparent liquids in transparent equipment (Ramaswamy et al. 1997; Barigou et al. 1998). A promising technique is magnetic resonance imaging (MRI) which has been tested in continuous aseptic processing of potato cubes (Kantt et al. 1998). The method relies on the temperature dependence of the proton resonance frequency, and it does seem to produce a reliable image of the

temperature distribution inside the potato cubes, from which h_{fp} may be calculated by numerical modelling and fitting. The method requires a metal-free imaging region (Kantt et al. 1998) which may be difficult to achieve experimentally in vessel cooking. Tessneer and co-workers (2001) have demonstrated that the mechanism of ablation heat transfer could be used for determining h_{fp} in tube flow. Spheres of ice were introduced into the tube flow and recovered after leaving the tube. From the weight difference an energy balance can be set up, allowing the calculation of h_{fp}. The method could be applied in the fluid temperature range of 3°C to 10°C; this speaks against the feasibility of this method because the viscosity and hence h_{fp} at those temperatures would be much different from the viscosity in vessel cooking in the typical temperature range of 75°C to 100°C.

As appears from the above discussion of the literature, there are only few studies concerned directly with the study of fluid-to-particle heat transfer in vessel cooking. In this paper we propose to use spherical potatoes as a dispensable, cheap device for studying fluid-to-particle heat transfer in such processes. The idea is based on the fact that the gelatinization of potato starch occurs in a narrow temperature interval around 67.5^{o}C (Pravisani et al. 1985; Verlinden et al. 1995). Above this temperature, the activation energy for the gelatinization reaction is very high, meaning that reaction will be completed rapidly, while it is rather slow at lower temperatures (Verlinden et al. 1995). This explains why the gelatinization front is easily identified visually and is rather sharp (Derbyshire & Owen 1988; Lamberg & Olsson 1989).

Assuming that mass transfer during the initial cooking period is negligible, Derbyshire and Owen (1988) found in a small experiment that the center temperature of a potato plunged into boiling water can be described by the standard Fourier equation for non-stationary conductive heat transfer into a sphere. In their modelling they assumed that the resistance to convective heat transfer was negligible, which is sensible because the heat transfer coefficient is high in boiling water due to the rapid movement and low viscosity of the fluid.

However, the fluid-to-particle heat transfer coefficient in cooking processes is rarely as high as it is when using boiling water as the medium of heat transfer. In industrial recipes for soups and gravies containing pieces of vegetables, meat, or fish, vigorous boiling is avoided to reduce evaporation and minimize over-cooking of the particles. In addition, soups and gravies have higher viscosity than water, which also reduces the fluid-to-particle heat transfer coefficient. This means that the thermal

history of a food particle will be determined by non-stationary heat transfer into the particle at middle-range Biot numbers (typically Bi = 1 to 20). A theoretical calculation of h_{fp} under these conditions is very difficult, if not close to the impossible, because of the complicated movement of the particles. In agitated vessels the mode of heat transfer cannot be expected to be fully forced convection, because suspended particles generally follow the movement of the liquid, the slip velocities are low, and natural convection must contribute to the heat transfer as well. Natural convection will evidently dominate if stirring is not applied or only used intermittingly to minimize mechanical damage (Bouvier et al. 2011).

From these considerations we came across the idea of experimentally determine the progression of the gelatinization front during cooking of potatoes and use this information to obtain information about the fluid-to-particle heat transfer coefficient. The purpose of the present work is to investigate the feasibility of this idea.

The first step in this work is to develop a simple procedure for determining the progression of the gelatinization front in potatoes immersed for a given time in a medium. The second step is to study more closely the progression of the gelatinization front and the temperature profile in real time. In this experiment we could validate the expected gelatinization temperature of about 67°C. The third step is to establish a Finite Element Model (FEM) of this experiment to validate that the temperature profile could be described by non-stationary conductive heat transfer and that the model correctly described the temperature profile using a realistic, average value of the fluid-to-particle heat transfer coefficient. The fourth step is to establish a physical-mathematical model for predicting the progression of the gelatinization front and determining its sensitivity with respect to the heat transfer coefficient, the diameter of the potato and the gelatinization temperature. This predictive model can then be used to assess the fluid-to particle heat transfer coefficient by fitting the predicted and experimental distances of the gelatinization front.

2. Materials and Methods

Potatoes of the Danish varieties *Marbelle* and *Folva* were bought in a local supermarket, and the most spherical potatoes were selected for the experiments. The smaller *Marbelle* variety (diameter around 36-38 mm) was used in 2.1 (imaging of gelatinization front), and the larger *Folva* variety (diameter around 41- 49 mm) in 2.2 and 2.3 (the internal temperature measurements).

2.1 Interval heating of potatoes and identification of gelatinization front

The potato samples (*Marbelle*) were heated in hot water at 90°C in a cooking vessel for 1 min, 2 min, 3 min, 5 min and 6 min. At the indicated times a potato was taken out, cut in half and immediately cooled in ice water bath containing 4% citric acid. After cooling, the potato samples were dried for half an hour at room temperature. The two halves of each potato sample were sliced (in approximately 2 mm thickness) parallel to the cut surface. One of the slices was stained by placing it in Lugol's iodine solution for one minute and then rinsed in distilled water for one minute. The composition of the Lugol's iodine solution was 2 g KI in 50 ml distilled water and adding 0.2 ml iodine stock solution (Lamberg and Olsson 1989).

All the samples, both the unstained and the stained samples, were photographed using a Canon 500D camera with Macro lens EF-S 60 mm 1:2.8 USM. For all the samples, the distance from the surface to the gelatinization front (which was clearly visible, see Figure 4 later) was determined from the images using Adobe Photoshop CS4. The distance was measured at 30° intervals around the periphery of the potato, and the distance was reported as the average of these 12 measurements.

2.2 Real-time study of the gelatinization front

A cast iron pot was cut in half along the vertical symmetry plane, and a glass plate was glued onto the open half with a temperature-tolerant adhesive. This formed a window that allowed visual inspection of the cooking processes. The idea is inspired by Myhrwold et al. (2011). The vessel was heated by placing it on a contact frying rig where the contact temperature can be controlled and the temperature of the fluid and evaporative mass loss can be measured continuously (Ashokkumar & Adler-Nissen, 2011). A spherical potato (*Folva*) was cut in half and attached to the window using a conventional laboratory clamp. In order to measure the actual gelatinization temperature, in one of the experiments a T-type thermocouple was placed between the glass wall and the potato surface about one-third of the distance from the periphery to the center of the potato (see Fig. 6 later). Hot water at 80°C was poured into the half vessel, and the water temperature was maintained at around 77.5^{o}C by manually adjusting the contact temperature of the frying rig to compensate for the heat loss from the vessel. The camera was mounted on a tripod and placed in horizontal alignment with the sample in the pot (Fig. 1). Ambient light illumination was used and the distance from the sample

was 0.3-0.4 m. The setup allowed continuous imaging by video of the submerged potato through the glass plate (Fig. 1).
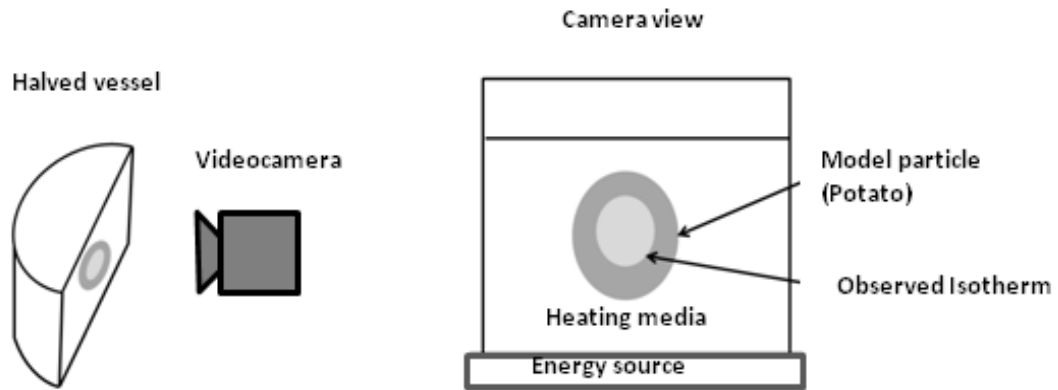
Figure 1   Experimental setup for video inspection of particle heating in a liquid media

2.3 Measuring temperature profiles and the gelatinization front

Similarly to the set-up in 2.2, three T-type thermocouples were attached and placed at different positions (A, B, and C, Fig. 2) between the half potato and the glass window of the half-vessel. This potato was particularly selected for its spherical shape; its diameter of 48.7mm was calculated as the average of the minimum (48.4 mm) and maximum (48.9) diameter of the potato. The exact positions of the data loggers were determined from the images that were taken from the video setup: the positions of the thermocouples were 0 mm, 9.8 mm and 20.5 mm from the center for the position A, B, and C, respectively. All the temperature sensors (T-type thermocouples) were connected to the computer with a data logger (Tc-08 Pico Technology, Cambridgeshire, UK) where the temperatures were recorded every second.

Appendix 4
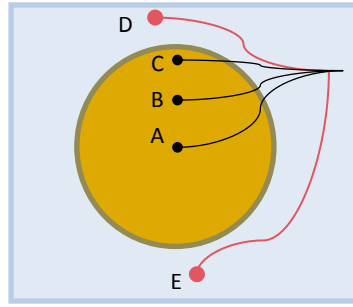
Figure 2: Temperature sensor position within half potato (A = center, B = 9.8 mm from the center,, C = 20.5 mm from the center . D and E are temperature sensor position within the fluid in the top and bottom sides, respectively. Diameter of the potato is 48.7 mm.

2.4 Modelling of heat transfer

Model formulation: The governing heat transfer inside the model food (potato) and through the glass is described by Eq. (1) and Eq. (2), respectively (Bird et al., 2001).

Heat transfer within the potato, (Fig. 2 domain 1):

$$\rho_p c_{p,\text{p}} \left(\frac{\partial T}{\partial t} \right) = k_p \nabla^2 T \tag{1}$$

Heat transfer within glass (Pyrex glass) (Fig. 2 domain 2):

$$\rho_g c_{p,\text{g}} \left(\frac{\partial T}{\partial t} \right) = k_g \nabla^2 T) \tag{2}$$

where T is the temperature [K], t is time [s], k_p and k_g is the thermal conductivity of the product and the glass, respectively [W/(m·K)], and $c_{p,\text{p}}$ and $c_{p,\text{g}}$ is the specific heat capacity of the product and the glass, respectively [J/(kg·K)], and ρ_p *and* ρ_g is the density of the product and the glass, respectively [kg/m^3].

Boundary conditions:

The boundary of potato surfaces that is exposed to fluid (*n* is the normal vector):

$$-n \cdot \left(k_p \nabla T \right) = h_{fp} \left(T_{fluid} - T_s \right) \tag{3}$$

Interior boundary, interface between the glass and the potato:

9

$$-n \cdot \left(k_p \nabla T\right) = -n \cdot \left(k_g \nabla T\right) \tag{4}$$

The glass-air interface (the boundary exposed surrounding air):

$$-n \cdot \left(k_g \nabla T\right) = h_{air}\left(T_{air} - T_s\right) \tag{5}$$

The glass-fluid interface (the boundary of glass wall that exposed to fluid):

$$-n \cdot \left(k_g \nabla T\right) = h_{fg}\left(T_{fluid} - T_s\right) \tag{6}$$

Where h_{fp} is the heat transfer coefficient between the fluid (heating medium) and the particle (in the case potato), [W/(m^2·K], h_{air} is the heat transfer coefficient between the glass and the surrounding air, [W/(m^2·K)], h_{fg} is the heat transfer coefficient between the glass and fluid, [W/(m^2·K)], T_{air} and T_{fluid} are the temperature of the surrounding air and the heating medium (fluid), respectively. The values of these input parameters are given in Table 1.
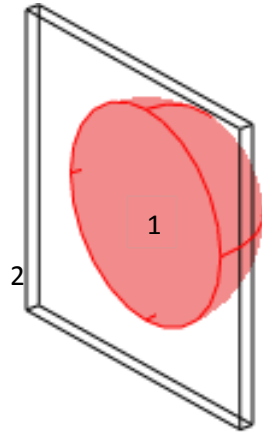
Figure 3. The geometry: domain 1(product) and domain 2 (the glass) modeled in COMSOL

Solution: The mathematical model (the partial differential equations, equation 1 and 2) that describes heat transfer together with boundary condition (Eq. 3-5) was solved using the *Finite Element Method* in COMSOL Multiphysics®3.5. The set up in COMSOL consists of two domains: the product (domain 1, in Fig. 3) and the glass (domain 2, in Fig. 3). The governing equations of heat transfer were set for each domain. The initial value was obtained from the measurements; the

values of the input parameters used in the model are given in the Table 1. The model prediction was compared with the obtained experimental temperature profile. The unknown parameter (heat transfer coefficient) in the model was estimated by manual tuning its value until it matched the measured temperature profile at the center of the product.

Appendix 4

Table 1 Thermophyical properties of the potato and the glass and other input parameters

Parameter	Value	Reference	parameter	Value	Reference
k_p	0.54 W/(m·K)	estimated	k_g	1.3 W/(m·K)	Bejan (1993)
$C_{p,p}$	3671.6 J/(kg·K)	estimated	$c_{p,g}$	750 J/(kg·K)	Bejan (1993)
ρ_p	1076 kg/m^3	estimated	ρ_g	2210 kg/m^3	Bejan (1993)
T_{air}	25 °C	measured	T_{fluid}	77.5 °C	measured
T_o	20 °C	measured	h_{air}	10 W/(m^2·K)	estimated

2.5 Progression front and sensitivity analysis

The progression of the gelatinization front was determined using a mathematical model of heat transfer solved in COMSOL, but in a simplified form: a whole spherical potato was immersed in the fluid instead of modelling a hemispherical potato attached to a glass wall (section 2.4). Using this model the moving isotherm at the gelatinization temperature of 67 °C was tracked, and the **distance** of the **front** from the **surface** (*dfs*) was predicted as function of time.

The sensitivity of the position of the gelatinization front was investigated with respect : 1) the heat transfer coefficient – higher values ($h = 240$ W/m^2·K, $h = 300$ W/m^2·K and $h = 360$ W/m^2·K) and lower values ($h = 80$ W/m^2·K, $h = 100$ W/m^2·K and $h = 120$ W/m^2·K); 2) the gelatinization temperature of potato starch – in this case gelatinization temperatures of 66.5 °C, 67 °C and 67.5 °C were considered; and 3) the size of the potato – the diameter of the potato were varied as follows: 0.032 m, 0.036 m, 0.04 m, 0.044m, 0.048 m and 0.056 m. The two ranges of *h* were chosen as they represent typical upper and lower values of experimentally determined fluid-to-particle heat transfer coefficients (h_{fp}) reported for conditions prevailing in vessel cooking, namely natural convection and for viscous liquids also forced convection (Maesmans et al. 1992).

3. Results and discussion

3.1. Validation of gelatinization front by imaging

The first step (section 2.1) was to check if it is possible to observe the gelatinization front from the photos. Fig. 4 shows the images obtained: a) without iodine and b) with iodine. The front observed in the two images agrees well, which indicates that the moving front is due to the gelatinization, see Fig. 5. In the unstained samples the gelatinization front is visible as a sharp change in translucency – the inner, un-gelatinized part of the potato being more opaque than the outer part of the potato. The iodine staining confirms that the outer part is gelatinized.

a)   b)

Figure 4 a) image of sliced sample without iodine treatment b) image of sliced sample stained with iodine (average diameter = 38 mm)
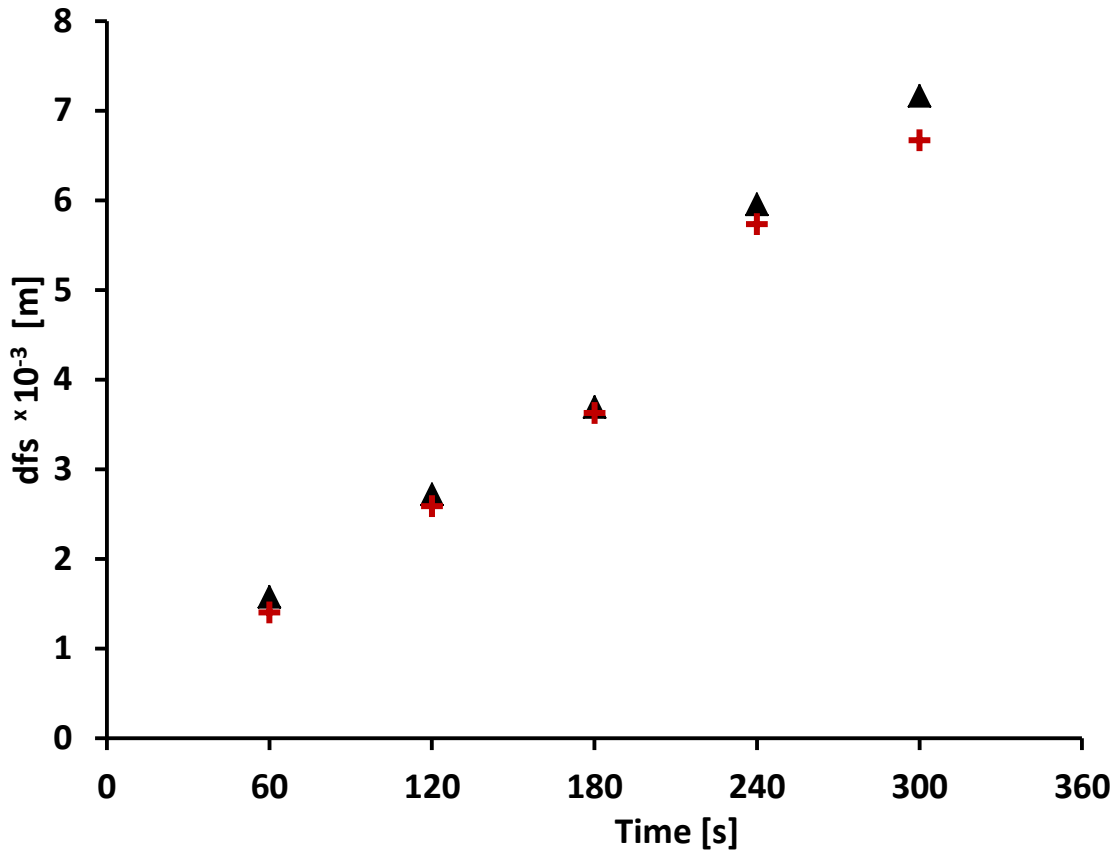
Figure 5 the position of front from surface vs the time: where the distance obtained from a) the image of sliced sample (black triangle) and b) image of the sample stained with iodine (red +)

3.2 Validation of the gelatinization front using the measured temperature

The next step was to validate the gelatinization temperature using the data from the real-time study (section 2.2) .Figure 6a, 6b and 6c show that the images of the potato at 300 s, 360 s and 420 s, respectively. The position of the thermocouple is shown by the red circle, and the images show that the moving front had passed this position at a time between 360 s and 420 s. The temperature measured at that position is shown in Fig. 7.

The distance from the surface, dfs, was measured on the images as described in 2.1. At 360 s (Fig. 6b), *dfs* = 6.40 mm and at 420 s (Fig 6c), *dfs* = 7.23 mm from the surface. The time at which the

moving front reached the position of the temperature sensor (6.68 mm from the surface) was determined by linear interpolation to be 380 s (6.3 min). This distance corresponds to a temperature of around 67°C, as shown in Figure 7. This is in agreement with what could be expected from the kinetic studies discussed in the introduction (Verlinden et al. 1995; Pravisani et al. 1985).

a)   300 s   b) 360 s   c) 420 s
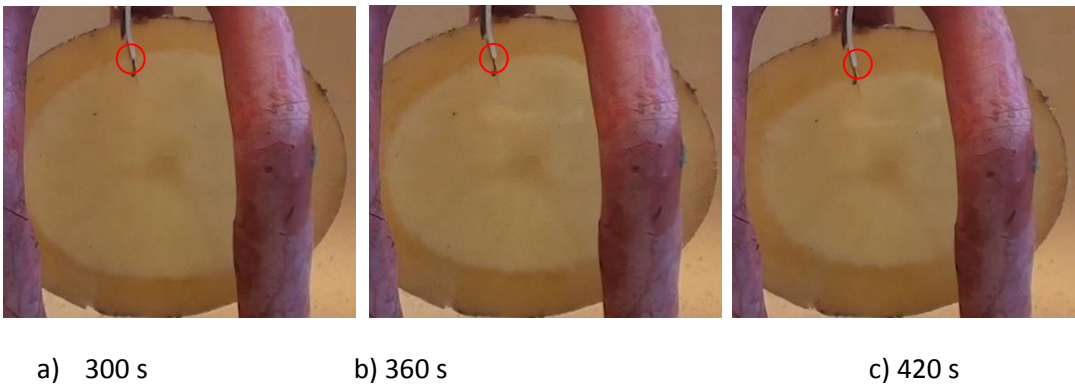
Figure 6: images of the front and the measured temperature: a) image at 300 s (5min), b) image at 360 s (6 min), c) image at 420 s (7 min) and at the sensor position (red circle) for the temperature measurement
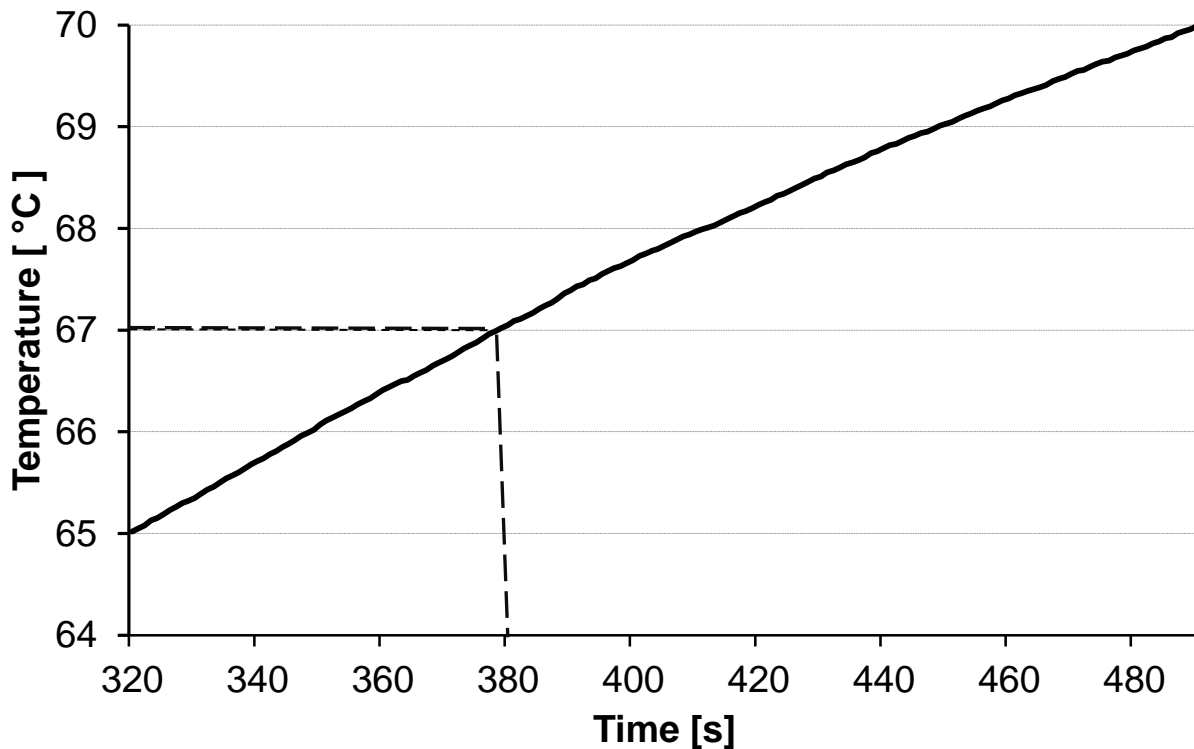
Figure 7 the measured temperature at the position indicated with red circle in Fig. 6, the dashed line indicates the 67 °C (gelatinization temperature of the potato) at 380 s

3.3. Comparison of simulated and measured temperature profile

The simulation was performed in *COMSOL-MATLAB®3.5* (as described in Section 2.4) and the obtained temperature profiles at position A, B and D (Fig. 2) are presented in Fig. 8 with blue, black and red lines, respectively. The simulated and the measured temperatures were compared, and the fluid-to-particle heat transfer coefficient was estimated (Fig. 8). The temperature profile was simulated at different values of the heat transfer coefficient (varied from 200 to 700 W/(m^2·K), first in large steps and later steps with smaller and smaller steps. For each step the calculated temperature profiles were compared with the measured temperature profiles. The best fit was obtained with the heat transfer coefficient value (rounded) of 300 W/(m^2·K) under the current experimental set up.
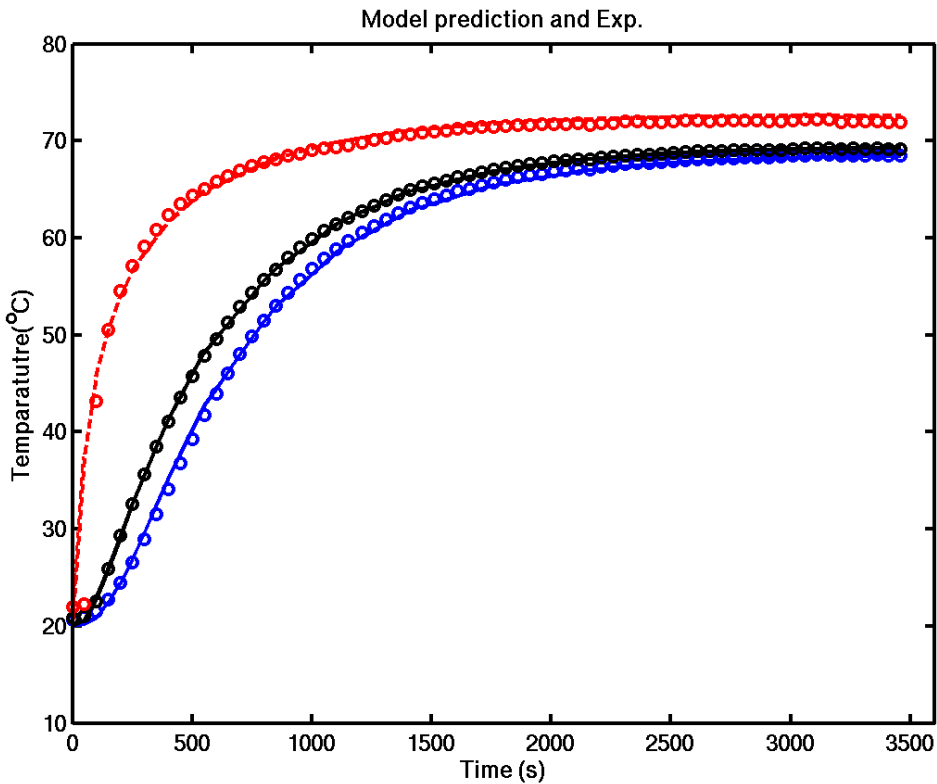
Figure 8 comparison the measured temperature and the simulated temperature (o measured and the line is simulation, red is the close to surface (at the position C, Fig. 2), black is the middle (at the position B, Fig. 2) and blue is the center (at the position A), (h$_{fp}$ = 300 W/m^2·K) and the diameter of potato is 48.7 mm.

3.4. Effect of heat transfer coefficient, gelatinization temperature and the size of potato

The **distance** of the **front** from the **surface (***dfs***)** was calculated as function of time at different values of the heat transfer coefficient as described in the section 2.5. Fig. 9 shows the effect of the heat transfer coefficient on the *dfs* profile for a sphere of the same size (diameter 48.7 mm) and thermo-physical properties as the potato in 3.3 and with the same fluid temperature (77.5°C. The obtained *dfs profiles* exhibit more sensitivity – understood as how large the relative horizontal distance is between the curves for a variation in h of ±20% – at the lower heat transfer coefficient (*h* =100 W/m^2·K) than at higher heat transfer coefficient (300W/m^2·K). The calculated difference in sensitivity is in accordance with what could be expected from the calculated values of the Biot numbers of 4.5 and 13.5, respectively. The greater sensitivity at *h* =100 W/m^2·K is promising with regard to the practical use of the suggested method for measuring fluid-to-particle heat transfer coefficients in soups and sauces, since values of h_{fp} of this magnitude or lower are frequently reported for viscous fluids (Chandarana & Gavin 1990; Awuah et al. 1992; Maesmans et al. 1992). Fig. 10 shows the effect of the gelatinization temperature of (66.5 °C, 67 °C and 67.5 °C) on the *dfs* profiles. The curves lie close to each other, showing that the exact determination of the gelatinization temperature is not critical. This issue will be briefly discussed in section 4.

Appendix 4
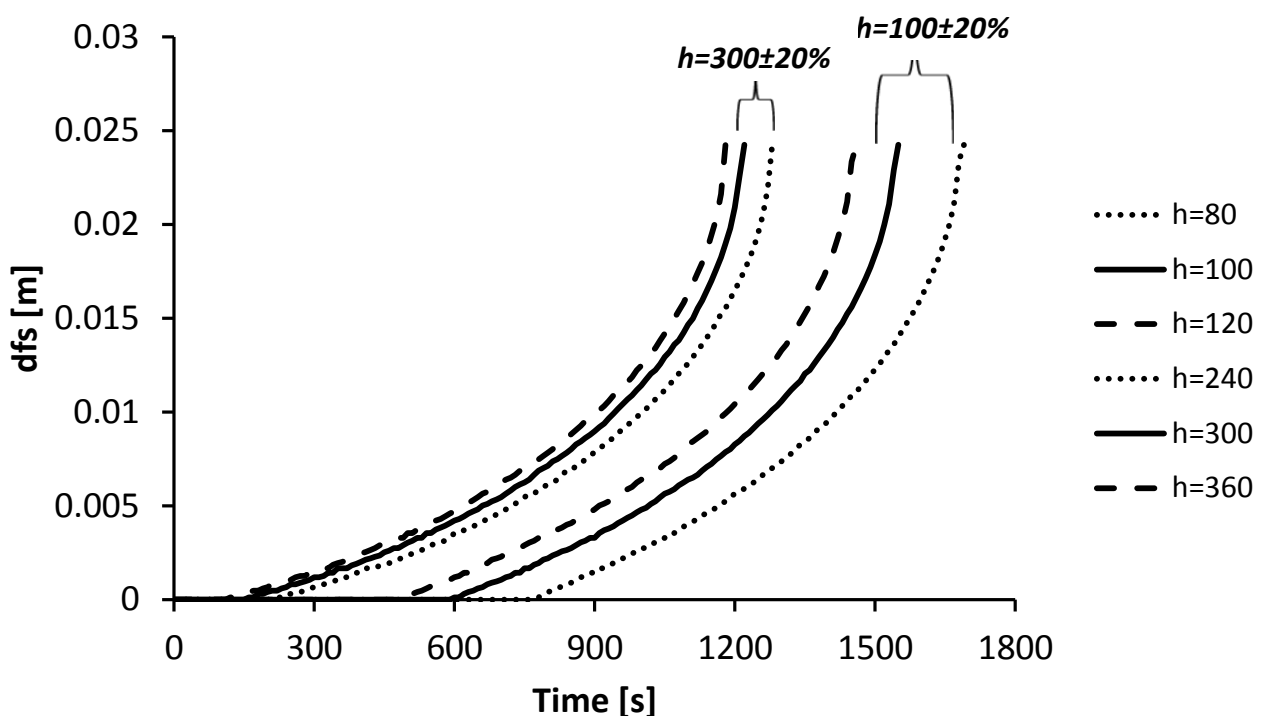
Figure 9 Effect of heat transfer coefficient (100±20 W/m2.K and 300 ±60 W/m².K). The diameter is 48.7 mm.
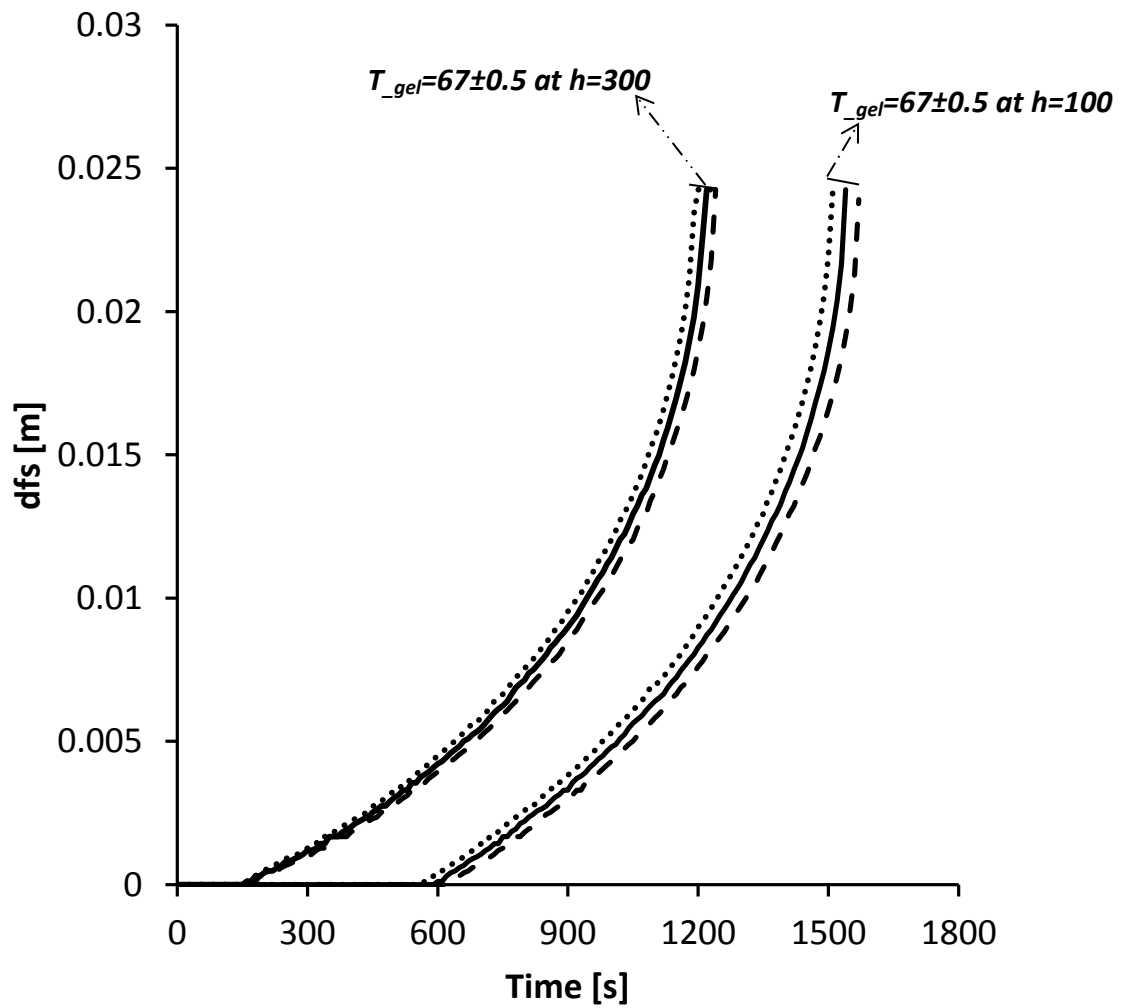
Figure 10 Effect of gelatinization temperature (67 ±0.5 ᵒC): $T_{\_gel}$=66.5 ᵒC (dashed line), $T_{\_gel}$=67 ᵒC (dotted line) and $T_{\_gel}$= 67.5 ᵒC (solid line). h=100 W/(m². K) and h =300 W/(m²·K) and diameter is 48.7 m.
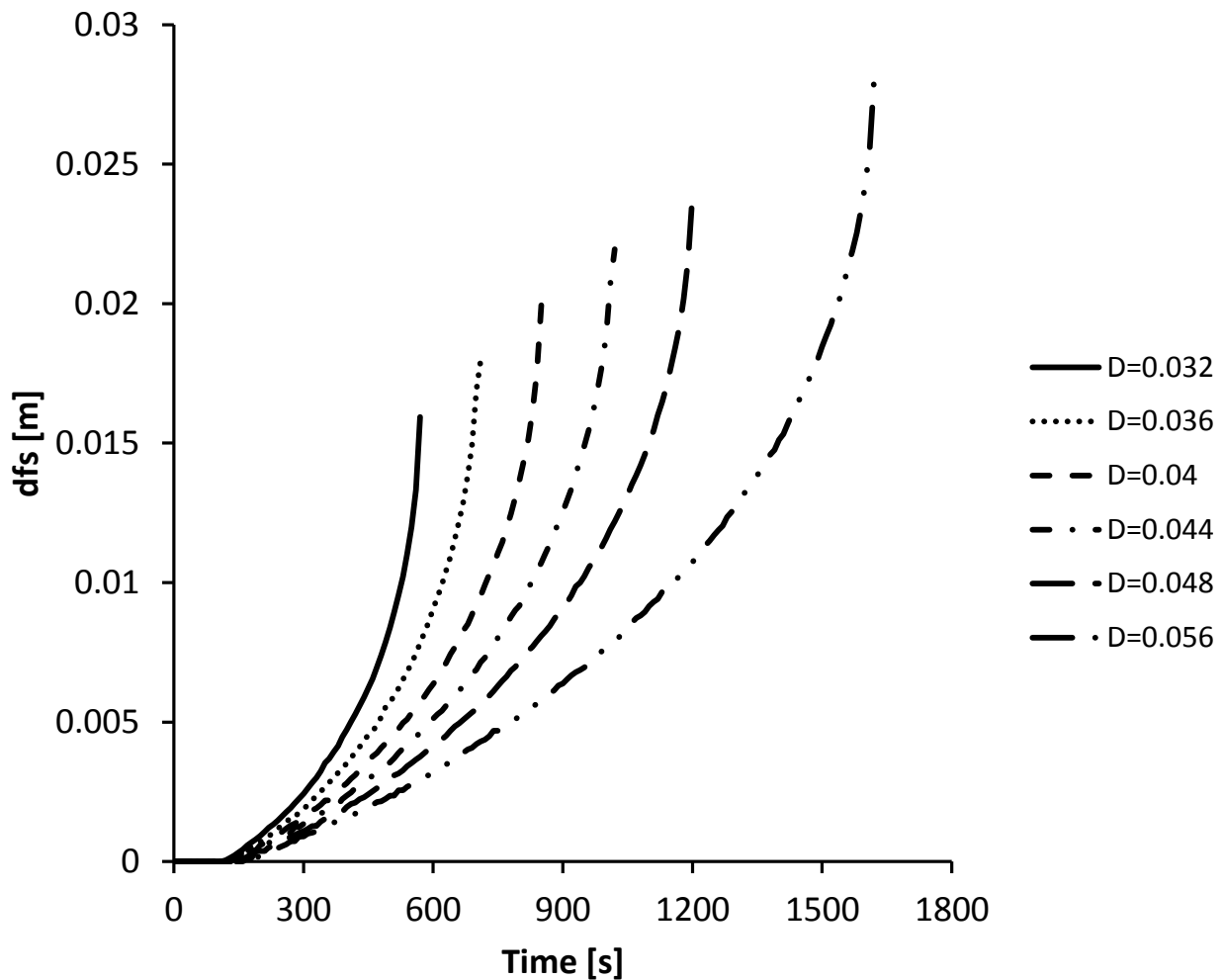
Figure 11 Effect of the size of the potato (diameter = 0.032, 0.036, 0.04, 0.044, 0.048 and 0.056 m). h=300 W/m²·K)

Fig 11 shows the effect of different sizes of potato on *dfs* as a function of time. The sensitivity with respect to size is large; however, this is hardly problematic since the average diameter of an approximately spherical potato can be measured with high precision using a Vernier caliper.

3.5. General discussion – application of the method and its limition

From the experimental results reported in section 3.1 and 3.2, it can be concluded that the gelatinisation front is easily observed, also without the use of iodine staining, and that its distance from the surface (*dfs*) can be measured with high precision from photos of the potato cut in half, as described. The gelatinization temperature can be determined experimentally using the set-up with the half-vessel. Since the modelling in section 3.3 shows that the exact gelatinization temperature is not very critical, it is reasonably safe to use either the measured temperature of 67°C or the value of 67.5°C reported in the literature. It would

however, be advantageous to develop a more simple method for measuring the gelatinization temperature on the same batch of potatoes as is used for experimentally determining fluid-to-particle heat transfer coefficients. This is addressed in the conclusion in section 4.

As described, the postion of the gelatinization front as a function of time can be calculated using the developed model (FEM). When the model is first established, it is easy to vary the radius of the potato or the heat transfer coefficient in the model. It is also possible to rely on classical analytical procedures for modelling the progression of the gelatinization front by solving the Fourier equation using the series expansion. From the data in Fig. 9 we calculated the Fourier number (Fo) at the time, when dfs was half the radius of the potato and found that Fo increased from Fo = 0.23 at h =360 W/m^2·K to Fo = 0.34 at h =80 W/m^2·K. It was also interesting to note that a similar calculation using the data in Fig. 11 showed that Fo only varied slightly with the diameter of the potato, from Fo = 0.23 at D = 0.056 m to 0.27 at D = 0.032 m. Since Fo>0.2 in all cases this means that a rather precise analytical solution can be obtained using only the first term of the series expansion of the Fourier equation (Mills 1995, 167-176). Calculations also show that if the fluid temperature is higher, Fo will be lower when dfs reaches half the radius of the potato, and for potatoes in boiling water Fo will be around 0.12. One of us (Christensen 2014) has, however, shown that the expansion series solution to the Fourier equation converges particularly rapidly for the sphere at positions about half-way between center and surface, and Christensen's study indicates that the one-term solution is applicable down to Fo around 0.12. Taken together, these calculations demonstrate that a simple analytical one-term solution can be applied for a relevant range of fluid-to-particle heat transfer coefficients as well as particle sizes.

In general, we found that a value of dfs > about 0.6×radius is less applicable because the gelatinisation front tends to become blurred when the temperature gradient becomes less steep later in the cooking process.

Measurements of the fluid-to-particle heat transfer coefficients in different set-ups is carried out by plunging a potato in the liquid for a given time and removing it, cutting it in half and measure the dfs of the gelatinization front, as described in 2.1. From the image, the average radius of the potato can also be measured with high precision. These two measured distances plus the time are input to the model, be it numerical or analytical, and h is then varied until the predicted dfs fits with the measured value.

4. Conclusion and perspective

In the present paper we have demonstrated the feasibility of using spherical potatoes as a dispensable, cheap device for studying fluid-to-particle heat transfer in vessel cooking processes. The method is based on the observation that the transmission of heat through the potato can be traced by measuring the distance from the surface to the gelatinization front. Knowing this distance, the period of immersion and the average radius of the potato allows for the assessment of the heat transfer coefficient by fitting a simple numerical model (FEM) of a sphere with the thermo-physical

properties of potatoes. Alternatively, an analytical one-term solution of the Fourier equation can be applied.

The gelatinization temperature of the potatoes used was assessed to be $67^{\circ}C$ by a direct temperature measurement while visually following the progression of the gelatinization front in the vessel-with-window setup. This setup also allows for studying other physical phenomena such as uneven transfer of heat under natural convection and for visualising particle and liquid movements.

As an alternative way to measure gelatinization temperature of a particular batch of potatoes we suggest to immerse some of the potatoes in vigorously boiling water. This ensures that the Biot number is so high that the progression of the gelatinization front will be independent of the actual value of the fluid-to-particle heat transfer coefficient. As before, *dfs* is measured after a given time. The only unknown variable in the model is now the temperature of the gelatinization isotherm.

Future studies of the proposed method should concentrate on further validation and of adapting the method to industrial practice.

References

Ashokkumar, S. & Adler-Nissen, J. (2011). Evaluating the Non-Stick Properties of Different Surface Materials for Contact Frying. *Journal of Food Engineering, 105 (3),* 537-544.

Åström, A., & Bark, G. (1994). Heat transfer between fluid and particles in aseptic processing. *Journal of Food Engineering, 21,* 97-125.

Awuah, G. B., Ramaswamy, H. S., & Simpson, B. K. (1992). Surface heat transfer coefficients associated with heating of food particles in cmc solutions. *Journal of Food Process Engineering, 16,* 39-57.

Balasubramaniam, V. M., & Sastry, S. K. (1994). Liquid to particle convective heat transfer in non-newtonian carrier medium during continuous tube flow. *Journal of Food Engineering, 23,* 169-187.

Barigou, M., Mankad S., & Fryer P. (1998). Heat transfer in two-phase solid-liquid food flows: A review. *Food and Bioproducts Processing, 76,* 3-29.

Bejan, A. (1993). Heat transfer. *John Wiley and Sons, Inc*. New York.

Bird, R.B., Stewart W.E., & Lightfoot E.N. (2001). *Transport Phenomena.* (2nd edn.). John Wiley and Sons, Inc, New York.

Appendix 4

Bouvier, L., Moreau A., Line A., Fatah N., & Delaplace G. (2011). Damage in Agitated Vessels of Large Visco-Elastic Particles Dispersed in a Highly Viscous Fluid. *Journal of Food Science, 76(5)*, 384-391.

Chandarna, D. I., & Gavin, A. (1990). Particle/fluid interface heat transfer under UHT conditions at low particle/fluid relative velocities. *Journal of Food Process Engineering, 13,* 191-206.

Christensen, M. G. (2014). *Formulation and validation of applied engineering equations for the calculation of heat transfer processes in the food industry*. Ph.D.-thesis (to be submitted 30 September), Technical University of Denmark.

Denys, S., Pieters, J.G. & Dewettinck, K. (2003). Combined CFD and experimental approach for determination of surface heat transfer coefficient during thermal processing of eggs. *Journal of Food Science 68(3),* 943-951.

Derbyshire, P.M., & Owen, I. (1986). Transient heat transfer in boiled potato: a study related to food process engineering. *International Journal of heat and fluid flow, 9,* 254-256*.

Kantt C., Schmidt S., Sizer C., Palaniappan S., & Litchfield J. (1998). Temperature mapping of particles during aseptic processing with Magnetic Resonance Imaging. *Journal of Food Science, 63(2),* 305-311.

Lamberg, I., & Olsson, H. (1989). Starch gelatinization temperatures within potato during blanching. *International Journal of food science and technology, 2,* 487-494.

Maesmans, G., Hendrickx, M., DeCordt, S., Fransis, A., & Tobback, P. (1992). Fluid to particle heat transfer coefficient determination of heterogeneous foods: a review. *Journal of Food Processing and Preservation, 16,* 29-69.

Maesmans, G., Hendrickx, M., Decordt, S., & Tobback, P. (1994). Feasibility of the use of a Time-Temperature Integrator and a Mathematical-Model to Determine Fluid-To-Particle Heat-Transfer Coefficients. *Food Research International, 27(1),* 39-51*.

Mehauden, K., Bakalis, S., Cox, P. W., Fryer, P. J., & Simmons, M. J. H. (2008). Use of time temperature integrators for determining process uniformity in agitated vessels. *Innovative Food Science and Emerging Technologies, 9,* 385-395.

Meng, Y., & Ramaswamy, H. (2005). Heat transfer coefficients associated with canned particulate/non-Newtonian fluid (CMC) system during end-over-end rotation. *Food and Bioproducts Processing, 83(3),* 229-237*.

Mills, A. F. (1995). *Heat and Mass Transfer*. Chicago: Irwin*.

Myhrvold, N., Young, C., & Bilet, M. (2011). *Modernist Cuisine: The art and science of cooking*. The cooking lab; Spi Har/Pa edition, Bellevue, WA 98005, USA.

Nesvadba, P. (2014). Thermal properties of unfrozen foods. *In M. A. Rao, S. H. Rizvi, A. K. Datta et al. (Eds.), Engineering Properties of Foods.* (4th edn., pp. 223-245). *CRC Press, Broken Sound Parkway NW.*

22

Appendix 4

Pravisani, C.I., Califano, A.N., & Calvelo, A. (1985). Kinetics of starch gelatinization in potato. Journal *of Food Science, 50 (3)*, 657-660.

Ramaswamy H., Awuah G., & Simpson B. (1997). Heat transfer and lethality considerations in aseptic processing of liquid/particle mixtures: A review. *Critical reviews in food science and nutrition, 37(3),* 253-286.

Ramaswamy H., & Zareifard M. (2000). Evaluation of factors influencing tube-flow fluid-to-particle heat transfer coefficient using a calorimetric technique*. Journal of Food Engineering, 45(3),* 127-138*.*

Singh, R. P., & Heldman, D. R. (2014). *Introduction to Food Engineering* 5th ed. London: Academic Press.

Tessneer W., Farkas B., & Sandeep K. (2001). Use of ablation to determine the convective heat transfer coefficient in two-phase flow. *Journal of Food Process Engineering, 24(5),* 315-330.

Verlinden, B.E., Nicola, B. M., De Baerdemaeker, J. (1995). The starch gelatinization in potatoes during cooking in relation to the modelling of texture kinetics. *Journal of Food Engineering, 24 (2),*165-179.

Appendix 5

Appendix 5A Center temperature

Table A1 Regression line coefficients and intercepts for the tested Biot numbers for infinite plates. The lag-factors $a_{c,1}$ and the eigenvalues (λ_1) are extracted from Mills [5]

Bi	$a_{c,1}$	λ_1	intercept ln $(a_{c,1}-1)$	Coefficient (α)	Bi	$a_{c,1}$	λ_1	Intercept ln $(a_{c,1}-1)$	Coefficient (α)
0.1	1.016	0.133	-4.135	-8.813	6	1.248	1.349	-1.394	-14.305
0.2	1.031	0.433	-3.474	-8.920	8	1.257	1.398	-1.359	-15.133
0.4	1.058	0.593	-2.847	-9.201	10	1.262	1.429	-1.339	-15.714
0.6	1.081	0.705	-2.513	-9.594	20	1.270	1.496	-1.309	-17.158
0.8	1.102	0.791	-2.283	-9.712	30	1.272	1.520	-1.302	-17.678
1	1.119	0.860	-2.129	-10.107	40	1.272	1.533 *	-1.302	-18.179
2	1.180	1.077	-1.715	-11.119	50	1.273	1.539	-1.298	-18.174
4	1.229	1.265	-1.474	-13.101	100	1.273	1.555	-1.298	-18.712

Corrected value due to typing error in Mills 1995

Table A2 Regression line coefficients and intercepts for the tested Biot numbers for infinite cylinders. The lag-factors $a_{c,1}$ and the eigenvalues (λ_1) are extracted from Mills [5]

Bi	$a_{c,1}$	λ_1	intercept ln $(a_{c,1}-1)$	Coefficient (α)	Bi	$a_{c,1}$	λ_1	Intercept ln $(a_{c,1}-1)$	Coefficient (α)
0.1	1.025	0.442	-3.689	-12.09	6	1.526	2.049	-0.642	-19.63
0.2	1.049	0.617	-3.016	-12.36	8	1.553	2.128	-0.592	-20.78
0.4	1.094	0.869	-2.364	-12.91	10	1.568	2.179	-0.566	-21.62
0.6	1.135	1.018	-2.002	-13.47	20	1.593	2.288	-0.523	-23.49
0.8	1.173	1.149	-1.754	-13.82	30	1.598	2.326	-0.514	-24.38
1	1.208	1.256	-1.570	-14.11	40	1.600	2.345	-0.511	-24.81
2	1.338	1.599	-1.085	-15.86	50	1.601	2.357	-0.509	-25.06
4	1.470	1.908	-0.755	-18.10	100	1.602	2.381	-0.507	-25.69

Table A3 Regression line coefficients and intercepts for the tested Biot numbers for spheres. The lag-factors $a_{c,1}$ and the eigenvalues (λ_1) are extracted from Mills [5]

Bi	$a_{c,1}$	λ_1	intercept ln $(a_{c,1}-1)$	Coefficient (α)	Bi	$a_{c,1}$	λ_1	Intercept ln $(a_{c,1}-1)$	Coefficient (α)
0.1	1.030	0.542	-3.507	-16.79	6	1.834	2.654	-0.182	-25.64
0.2	1.059	0.759	-2.830	-17.89	8	1.892	2.765	-0.114	-27.16
0.4	1.116	1.052	-2.154	-18.31	10	1.925	2.836	-0.078	-28.21
0.6	1.171	1.264	-1.766	-18.52	20	1.978	2.986	-0.022	-31.01
0.8	1.224	1.432	-1.496	-18.58	30	1.990	3.037	-0.010	-32.03
1	1.273	1.570	-1.298	-19.19	40	1.994	3.063	-0.006	-32.71
2	1.479	2.029	-0.736	-20.89	50	1.996	3.079	-0.004	-33.10
4	1.720	2.456	-0.329	-23.67	100	1.999	3.110	-0.001	-33.78

Appendix 5B Volume average temperature

Table B1 Regression line coefficients and intercepts for the tested Biot numbers for infinite plates. The lag-factors $a_{m,1}$ and the eigenvalues (λ_1) are extracted from Mills [5]

Bi	$a_{m,1}$	λ_1	intercept ln $(1-a_{m,1})$	Coefficient (α)	Bi	$a_{m,1}$	λ_1	Intercept ln $(1-a_{m,1})$	Coefficient (α)
1	0.986	0.860	-4.265	-13.3	20	0.846	1.496	-1.874	-29
2	0.965	1.077	-3.346	-16.5	30	0.836	1.520	-1.806	-30
4	0.927	1.265	-2.613	-20	40	0.829	1.523	-1.769	-31
6	0.902	1.349	-2.325	-22	50	0.826	1.540	-1.750	-32
8	0.886	1.398	-2.170	-24	100	0.818	1.555	-1.706	-30
10	0.874	1.429	-2.074	-25					

Table B2 Regression line coefficients and intercepts for the tested Biot numbers for infinite cylinders. The lag-factors $a_{m,1}$ and the eigenvalues (λ_1) are extracted from Mills [5]

Bi	$a_{m,1}$	λ_1	intercept ln $(1-a_{m,1})$	Coefficient (α)	Bi	$a_{m,1}$	λ_1	Intercept ln $(1-a_{m,1})$	Coefficient (α)
1	0.983	1.256	-4.099	-17.6	20	0.754	2.288	-1.402	-37.3
2	0.954	1.599	-3.070	-20.5	30	0.735	2.326	-1.329	-38.8
4	0.895	1.908	-2.252	-25.2	40	0.724	2.345	-1.287	-40.3
6	0.852	2.049	-1.914	-28	50	0.718	2.357	-1.265	-41.7
8	0.824	2.129	-1.736	-30	100	0.705	2.381	-1.220	-42.4
10	0.803	2.179	-1.627	-32.5					

Table B3 Regression line coefficients and intercepts for the tested Biot numbers for spheres. The lag-factors $a_{m,1}$ and the eigenvalues (λ_1) are extracted from Mills [5]

Bi	$a_{m,1}$	λ_1	intercept ln $(1-a_{m,1})$	Coefficient (α)	Bi	$a_{m,1}$	λ_1	Intercept ln $(1-a_{m,1})$	Coefficient (α)
1	0.985	1.570	-4.220	-21.3	20	0.692	2.986	-1.179	-46
2	0.953	2.029	-3.062	-27	30	0.666	3.037	-1.096	-49
4	0.883	2.456	-2.145	-33	40	0.652	3.063	-1.055	-50
6	0.828	2.654	-1.760	-35	50	0.643	3.079	-1.031	-53
8	0.789	2.765	-1.556	-38	100	0.626	3.110	-0.983	-54
10	0.761	2.836	-1.430	-40					

Appendix 6 The convergence between the series expansion and the lumped capacitance model.

6A, For infinite slabs:

From the definition of the Fourier exponents:

$$b_1 = \lambda_1^2$$

With the root function

$$Bi = \lambda_1 \cdot \tan \lambda_1 \qquad \text{[A1]}$$

Which is an iterative root function to be solved, an explicit form of the equation [A1] can be obtained by expanding the tangent:

$$\tan \lambda_1 = \lambda_1 + \frac{\lambda_1^3}{3} + \frac{2\lambda_1^5}{15} + \cdots$$

For small values of λ_1:

$$\tan \lambda_1 = \lambda_1 \qquad \text{[A2]}$$

Thus for small values of λ_1 inserting A2 into A1:

$$Bi = \lambda_1^2 = b$$

6B, For infinite cylinders:

From the definition of the Fourier exponents:

$$b_1 = \lambda_1^2$$

With the root function

$$Bi = \frac{\lambda_1 J_1(\lambda_1)}{J_0(\lambda_1)} \qquad \text{[B1]}$$

Where J_1 and J_0 is Bessel functions of the First kind with 1st and 0th order. The Besselfunctions can be expanded following for small values of λ_1 and Bi:

$$J_0(\lambda_1) = 1 - \frac{\left(\frac{\lambda_1}{2}\right)^2}{(1!)^2} + \frac{\left(\frac{\lambda_1}{2}\right)^4}{(2!)^2} - \cdots = 1 - \frac{\lambda_1^2}{4} + \frac{\lambda_1^4}{64} - \cdots \qquad \text{[B2]}$$

$$J_1(\lambda_1) = \frac{\lambda_1}{2} - \left(\frac{\frac{\lambda_1}{2}}{1!2!}\right)^3 + \left(\frac{\frac{\lambda_1}{2}}{2!3!}\right)^5 - \cdots = \frac{\lambda_1}{2} - \frac{\lambda_1^3}{16} + \frac{\lambda_1^5}{386} - \cdots \qquad \text{[B3]}$$

For very small values of λ_1 only the first terms in equation [B2] and [B3] becomes determining. Inserted into [B1]

$$Bi = \frac{\lambda_1 \cdot \frac{\lambda_1}{2}}{1} = \frac{\lambda_1^2}{2} \leftrightarrow b = \lambda_1^2 = 2 \cdot Bi \qquad\qquad [B4]$$

6C, for spheres:

From the definition of the Fourier exponents:

$$b_1 = \lambda_1^2$$

With the root function

$$Bi = 1 - \lambda_1 \cdot \cot \lambda_1 \qquad\qquad [C1]$$

Expanding Cotangent yields:

$$\cot \lambda_1 = \frac{1}{\lambda_1} - \frac{\lambda_1}{3} - \frac{\lambda_1^3}{45} - \cdots$$

For very small values of λ_1:

$$\cot \lambda_1 = \frac{1}{\lambda_1} - \frac{\lambda_1}{3}$$

Inserting into [C1]

$$Bi = 1 - \lambda_1 \cdot \left(\frac{1}{\lambda_1} - \frac{\lambda_1}{3} \right)$$

$$Bi = 1 - \left(\frac{\lambda_1}{\lambda_1} \right) + \frac{\lambda_1^2}{3} \leftrightarrow b = \lambda_1^2 = 3 \cdot Bi \qquad\qquad [C2]$$

heatman man

Peter Stubbe
Fødevareinstituttet DTU

14. september 2012

`heatman` is a library for R, that implements solutions for transient heat conduction problems.

Geometries

The four simple shapes, infinite plate, infinite cylinder, sphere, and halfspace are implemented aswell as combinations totalling thirteen different geometries.

Compound geometry	Elements
plate	plate
cylinder	cylinder
sphere	sphere
halfspace	halfspace
prism	plate and plate
box	plate and plate and plate
platecorner	plate and halfspace and halfspace
finite cylinder	cylinder and plate
plate edge	plate and halfspace
prismend	plate and plate and halfspace
cylinderend	cylinder and halfspace
edge	halfspace and halfspace
corner	halfspace and halfspace and halfspace

Boundary Conditions

`heatman` solves for three boundary conditions. Type 1, or Dirichlet states that the surface has a fixed temperature, type 2, or von Neumann states that there is a fixed heatflux at the surface, and type 3, or Robin states that there is convection at the surface.

Functions starting with "`conv`" solves for a Robin boundary condition, or a Dirichlet if the Biot number is very high. Functions starting with "`q`" solves for a von Neuman boundary condition.

Sequences

The simple solutions to instationary heat conduction problems will only solve for one step change in temperature or flux. However using Duhamel integration it is possible to calculate more complicated problems involving several steps. All functions ending in `seq` will solve for a sequence of changing temperatures, where the parameter `T0` is the starting temperature and the parameter `seq` is a vector with alternating times in seconds and temperatures (or fluxes). E.g. `c(0,100,2000,20)`, will give a step from T0 to 100 ^oC at the time 0, and a step from 100 ^oC to 20 ^oC at the time 2000 seconds.

Arguments and Results

Arguments

n	number of terms in solution
T	temperature $[^oC]$
Bi	Biot number $\frac{hL}{k}$
time	time $[s]$
alpha	thermal diffusivity $\frac{k}{\rho c_p}$
L	half thickness of plate $[m]$
R	radius of cylinder og sphere $[m]$
root	roots as calculated by `convplateroot()`, `convcylroot()`, or `convsphereroot()`
x	dimensionless position
y	dimensionless position
z	dimensionless position
r	dimensionless position
h	heat transfer coefficient $[\frac{W}{m^2K}]$
k	thermal conductivity $[\frac{W}{mK}]$
X	position $[m]$
Y	position $[m]$
Z	position $[m]$
T0	initial temperature $[^oC]$
seq	sequence temperatures
w	angular velocity $[rad/s]$

Results

n	number of terms in solution
cp	labeled table of heat capacities
k	labeled table of thermal conductivities $[\frac{W}{mK}]$
rho	labeled table of densities
alpha	labeled table of thermal diffusivities $\frac{k}{\rho c_p}$
root	vector of roots
t	dimensionless temperature $t = \frac{T_\infty - T}{T_\infty - T_0}$
T	temperature $[^oC]$
X	position $[m]$
time	time $[s]$
a	dimensionless temperature amplitude $a = \frac{T_\infty - T}{T_\infty - T_0}$

Time and position arguments can be scalars or vectors. Vector arguments will result in a vector or at most a two dimensional table. If more than two arguments are vectors, only the first element will be used from the time, and maybe the z dimension.

t	res
t[ ]	res[t]
t,x	res
t,x[ ]	res[x]
t[ ],x	res[t]
t[ ],x[ ]	res[t,x]
t,x,y	res
t,x,y[ ]	res[y]
t,x[ ],y	res[x]
t[ ],x,y	res[t]
t,x[ ],y[ ]	res[x,y]
t[ ],x,y[ ]	res[t,y]
t[ ],x[ ],y	res[t,x]
t[ ],x[ ],y[ ]	res[x,y] only calculated for t[1]
t,x,y,z	res
t,x,y,z[ ]	res[z]
t,x,y[ ],z	res[y]
t,x[ ],y,z	res[x]
t[ ],x,y,z	res[t]
t,x,y[ ],z[ ]	res[y,z]
t,x[ ],y,z[ ]	res[x,z]
t,x[ ],y[ ],z	res[x,y]
t[ ],x,y,z[ ]	res[t,z]
t[ ],x,y[ ],z	res[t,y]
t[ ],x[ ],y,z	res[t,x]
t,x[ ],y[ ],z[ ]	res[x,y] only calculated for z[1]
t[ ],x[ ],y[ ],z	res[x,y] only calculated for t[1]
t[ ],x[ ],y,z[ ]	res[x,z] only calculated for t[1]
t[ ],x,y[ ],z[ ]	res[y,z] only calculated for t[1]
t[ ],x[ ],y[ ],z[ ]	res[x,y] only calculated for t[1] and z[1]

Functions

n<-heatinit(n)

Sets the number of terms to use in the solution, and calculates some roots. The function is called when the library is loaded, and is only needed if more or fewer than the standard number of 100 are needed.

Example:
```
> heatinit(100)
[1] 100
```

cp<-foodspecheat(T)

Calculates the heat capacity for food constituents.

Example:
```
> foodspecheat(25)
  protein       fat     carbo     fibre       ash     water       ice
 2037.602  2018.032  1594.150  1888.758  1137.539  4177.349  2214.223
```

k<-foodconduct(T)

Calculates the heat conductivity for food constituents.

Example:
```
> foodconduct(25)
    protein        fat      carbo      fibre        ash      water        ice
  0.2070064  0.1115891  0.2333880  0.2125723  0.3628307  0.6109627  2.1268400
```

rho<-fooddensity(T)

Calculates the density of food constituents.

Example:
```
> fooddensity(25)
    protein        fat      carbo      fibre        ash      water        ice
  1316.9400  915.1508  1591.3385  1302.3528  2416.7843  994.9102  913.6223
```

alpha<-fooddiffusivity(T)

Calculates the thermal diffusivity of food constituents.

Example:
```
> fooddiffusivity(25)
       protein           fat         carbo         fibre           ash
  7.969313e-08  9.561082e-08  9.265388e-08  8.556387e-08  2.102600e-08
         water           ice
  1.457979e-07  1.082916e-06
```

```
root<-convplateroot(Bi)
```

Calculates roots for use by `convplate` functions.

Example:
```
> convplateroot(5)
  [1]    1.313838    4.033568    6.909596    9.892753   12.935221   16.010659
  [7]   19.105520   22.212556   25.327648   28.448314   31.572985   34.700624
 [13]   37.830519   40.962167   44.095206   47.229363   50.364435   53.500262
 [19]   56.636721   59.773715   62.911164   66.049003   69.187181   72.325653
 [25]   75.464383   78.603341   81.742501   84.881839   88.021338   91.160980
```

```
root<-convcylroot(Bi)
```

Calculates roots for use by `convcyl` functions.

Example:
```
> convcylroot(5)
  [1]    1.989815    4.713142    7.617708   10.622300   13.678558   16.762984
  [7]   19.863966   22.975361   26.093678   29.216811   32.343419   35.472615
 [13]   38.603785   41.736495   44.870430   48.005354   51.141087   54.277491
 [19]   57.414458   60.551901   63.689750   66.827948   69.966450   73.105215
 [25]   76.244213   79.383414   82.522797   85.662342   88.802031   91.941849
```

```
root<-convsphereroot(Bi)
```

Calculates roots for use by `convsphere` functions.

Example:
```
> convsphereroot(5)
  [1]    2.570432    5.354032    8.302929   11.334826   14.407971   17.503428
  [7]   20.612031   23.728945   26.851418   29.977779   33.106961   36.238251
 [13]   39.371158   42.505330   45.640512   48.776510   51.913179   55.050405
 [19]   58.188099   61.326189   64.464619   67.603342   70.742318   73.881515
 [25]   77.020907   80.160471   83.300188   86.440040   89.580014   92.720097
```

```
t<-convplate(time,alpha,L,root,x)
```

Infinite plate.

Example:
```
> r<-convplateroot(4)
> convplate(10000,1.5e-7,0.04,r,0)
[1] 0.2743694
```

```
t<-convplatemean(time,alpha,L,root)
```

Calculates mean dimensionless temperature of an infinite plate.

Example:
```
> r<-convplateroot(4)
```

```
> convplatemean(10000,1.5e-7,0.04,r)
[1] 0.2068708
```

T<-convplateseq(time,alpha,L,root,T0,seq,x)

Example:
```
> r<-convplateroot(4)
> convplateseq(1:10*1000,1.5e-7,0.04,r,10,c(0,100,2000,20),0.2)
 [1]   12.58958   21.75389   29.67680   30.80363   29.88442   28.64529
 [7]   27.47372   26.44070   25.54574   24.77403
```

t<-convcyl(time,alpha,R,root,r)

Infinite cylinder.

Example:
```
> r<-convcylroot(4)
> convcyl(10000,1.5e-7,0.04,r,0)
[1] 0.04840784
```

T<-convcylseq(time,alpha,R,root,T0,seq,r)

Example:
```
> r<-convcylroot(4)
> convcylseq(1:10*1000,1.5e-7,0.04,r,10,c(0,100,2000,20),0.2)
 [1]   16.45635   36.50776   48.59939   43.85653   37.45027   32.47183
 [7]   28.87465   26.30964   24.48526   23.18828
```

t<-convcylmean(time,alpha,R,root)

Calculates mean dimensionless temperature for an infinite cylinder.

Example:
```
> r<-convcylroot(4)
> convcylmean(10000,1.5e-7,0.04,r)
[1] 0.0294773
```

t<-convsphere(time,alpha,R,root,r)

Sphere.

Example:
```
> r<-convsphereroot(4)
> convsphere(10000,1.5e-7,0.04,r,0)
[1] 0.0060308
```

```
T<-convsphereseq(time,alpha,R,root,T0,seq,r)
```

Example:
```
> r<-convsphereroot(4)
> convsphereseq(1:10*1000,1.5e-7,0.04,r,10,c(0,100,2000,20),0.2)
 [1]  22.44514  52.54141  61.71087  46.69276  35.39916  28.76728
 [7]  24.98270  22.83114  21.60858  20.91395
```

```
t<-convspheremean(time,alpha,R,root)
```

Calculates mean dimensionless temperature for a sphere.

Example:
```
> r<-convsphereroot(4)
> convspheremean(10000,1.5e-7,0.04,r)
[1] 0.003095588
```

```
t<-convhalfspace(time,alpha,h,k,X)
```

Halfspace. X is from the surface in.

Example:
```
> convhalfspace(10000,1.5e-7,100,1,0.05)
[1] 0.7191208
```

```
T<-convhalfspaceseq(time,alpha,h,k,T0,seq,X)
```

X is from the surface in.

Example:
```
> convhalfspaceseq(1:10*1000,1.5e-7,100,1,20,c(0,100,1000,20),0.05)
 [1]  20.10602  21.49944  22.76919  23.11955  23.05246  22.84367
 [7]  22.60162  22.36645  22.15165  21.96029
```

```
time<-convhalfspacetcrit(alpha,h,k,L)
```

Calculates the critical time when a finite body with characteristic length L, is no longer considered a halfspace.

Example:
```
> convhalfspacetcrit(1.5e-7,100,1,0.04)
[1] 53.22256
```

```
X<-convhalfspacedepth(time,alpha)
```

Calculates the position where the change is 1% of the change at the surface. This function requires a Dirichlet type boundary.

Example:
```
> convhalfspacedepth(3600,1.5e-7)
[1] 0.08458596
```

```
t<-convhalfspacecycl(time,alpha,w,X)
```

Calculates the dimensionless temperature for a periodic changing surface temperature. This function requires a Dirichlet type boundary.

Example:
```
> convhalfspacecycl(1:10*1000,1.5e-7,0.1,0.01)
 [1]    0.0031081451    0.0026467118    0.0014564740   -0.0001348218   -0.0016889927
 [6]   -0.0027780788   -0.0031021868   -0.0025720697   -0.0013337017    0.0002719175
```

```
a<-convhalfspacecyclamp(alpha,w,X)
```

Calculates the dimensionless amplitude at depth X for a periodic changing surface temperature. This function requires a Dirichlet type boundary.

Example:
```
> convhalfspacecyclamp(1.5e-7,0.1,0.01)
[1] 0.003108849
```

```
X<-convhalfspacecycldepth(alpha,w)
```

Calculates the position where the amplitude is 1% of the amplitude at the surface. This function requires a Dirichlet type boundary.

Example:
```
> convhalfspacecycldepth(1.5e-7,0.1)
[1] 0.007976094
```

```
T<-convedge(time,alpha,h,k,X,Y)
```

Edge made by combining two halfspaced in a quaterspace.

Example:
```
> 100-90*convedge(1000,1.5e-7,100,1,0:4*0.01,0:4*0.001)
          [,1]      [,2]      [,3]      [,4]      [,5]      [,6]
 [1,]  87.46730  86.22918  85.02327  83.85213  82.71808  81.62316
 [2,]  76.78711  74.49389  72.26032  70.09114  67.99067  65.96268
 [3,]  70.42228  67.50027  64.65426  61.89032  59.21390  56.62985
 [4,]  67.60319  64.40268  61.28543  58.25804  55.32653  52.49619
 [5,]  66.68123  63.38964  60.18367  57.07013  54.05519  51.14431
```

```
T<-convedgeseq(time,alpha,h,k,T0,seq,X,Y)
```

Example:
```
> convedgeseq(1:10*1000,1.5e-7,100,1,20,c(0,100,2000,20),0.01,0.001)
 [1]   77.32790   86.10485   32.60156   25.98499   23.55295   22.36627
 [7]   21.69332   21.27339   20.99320   20.79669
```

```
T<-convplateedge(time,alpha,h,k,L,rootp,X,y)
```

The edge of a plate made by combining a plate and a halfspace. X is from the edge in, y is perpendicular to the plate.

Example:
```
> r<-convplateroot(4)
> convplateedge(2000,1.5e-7,100,1,0.04,r,0:4*0.01,0:5/5)
            [,1]      [,2]      [,3]      [,4]      [,5]      [,6]
  [1,]  0.2565338  0.2496956  0.2288429  0.1934302  0.1438284  0.0824123
  [2,]  0.4909100  0.4778241  0.4379199  0.3701531  0.2752340  0.1577064
  [3,]  0.6675154  0.6497219  0.5954622  0.5033162  0.3742497  0.2144415
  [4,]  0.7816971  0.7608599  0.6973188  0.5894108  0.4382669  0.2511227
  [5,]  0.8449244  0.8224018  0.7537212  0.6370851  0.4737160  0.2714347
```

```
T<-convplateedgeseq(time,alpha,h,k,L,rootp,T0,seq,X,y)
```

Example:
```
> r<-convplateroot(4)
> convplateedgeseq(1:5*1000,1.5e-7,100,1,0.04,r,20,c(0,100,2000,20),0.01,0)
[1] 45.58249 60.69006 45.03981 36.69718 31.68164
```

```
T<-convprism(time,alpha,Lx,Ly,rootx,rooty,x,y)
```

Infinite prism made by combining two plates.

Example:
```
> rx<-convplateroot(4)
> ry<-convplateroot(8)
> convprism(2000,1.5e-7,0.04,0.08,rx,ry,0:4/4,0:5/5)
            [,1]      [,2]      [,3]      [,4]      [,5]      [,6]
  [1,]  0.8920063  0.8892088  0.8707244  0.7978764  0.6045528  0.2565338
  [2,]  0.8547572  0.8520766  0.8343641  0.7645581  0.5793075  0.2458213
  [3,]  0.7405276  0.7382052  0.7228598  0.6623826  0.5018889  0.2129698
  [4,]  0.5475475  0.5458303  0.5344839  0.4897670  0.3710976  0.1574702
  [5,]  0.2865599  0.2856612  0.2797230  0.2563203  0.1942145  0.0824123
```

```
T<-convprismseq(time,alpha,Lx,Ly,rootx,rooty,T0,seq,x,y)
```

Example:
```
> convprismseq(1:5*1000,1.5e-7,0.04,0.08,rx,ry,20,c(0,100,2000,20),0,0)
[1] 21.26784 28.52842 36.83955 38.72358 37.63141
```

```
T<-convfincyl(time,alpha,L,R,rootp,rootc,x,r)
```

Finite cylinder made by combining a cylinder and a plate.

Example:
```
> rp=convplateroot(4)
> rc=convplateroot(4)
```

```
> convfincyl(1000,1.5e-7,0.04,0.04,rp,rc,0,0)
[1] 0.9929876
```

T<-confincylseq(time,alpha,L,R,rootp,rootc,T0,seq,x,r)

Example:
```
> convfincylseq(1:5*2000,1.5e-7,0.04,0.04,rp,rc,20,c(0,100,2000,20),0,0)
[1] 45.00618 47.75520 36.09905 28.87323 24.87264
```

T<-convcylend(time,alpha,h,k,R,rootc,X,r)

Cylinder end made by combining a cylinder and a halfspace. X is from the end in.

Example:
```
> convcylend(3600,1.5e-7,100,1,0.04,rc,0.04,0)
[1] 0.6040951
```

T<-convcylendseq(time,alpha,h,k,R,rootc,T0,seq,X,r)

Example:
```
> convcylroot(4)
> convcylendseq(1:5*2000,1.5e-7,100,1,0.04,r,20,c(0,100,2000,20),0.04,0)
[1] 41.23253 42.89996 34.93199 29.58732 26.28932
```

T<-convbox(time,alpha,Lx,Ly,Lz,rootx,rooty,rootz,x,y,z)

Box made from three plates.

Example:
```
> rx=convplateroot(4)
> ry=convplateroot(8)
> rz=convplateroot(12)
> convbox(2000,1.5e-7,0.04,0.08,0.12,rx,ry,rz,0:4/4,0:5/5,0)
           [,1]       [,2]       [,3]       [,4]       [,5]        [,6]
 [1,]   0.8920057  0.8892083  0.8707239  0.7978759  0.6045525  0.25653365
 [2,]   0.8547567  0.8520760  0.8343636  0.7645576  0.5793071  0.24582113
 [3,]   0.7405271  0.7382047  0.7228593  0.6623822  0.5018886  0.21296962
 [4,]   0.5475472  0.5458300  0.5344836  0.4897667  0.3710974  0.15747015
 [5,]   0.2865597  0.2856610  0.2797228  0.2563202  0.1942144  0.08241225
```

T<-convboxseq(time,alpha,Lx,Ly,Lz,rootx,rooty,rootz,T0,seq,x,y,z)

Example:
```
> convboxseq(1:5*2000,1.5e-7,0.04,0.08,0.12,rx,ry,rz,20,c(0,100,2000,20),0:5/5,0,0)
```

```
           [,1]      [,2]      [,3]      [,4]      [,5]      [,6]
  [1,]  28.41832  30.32031  36.12009  45.96851  59.75526  74.70055
  [2,]  38.75008  38.50181  37.56941  35.51940  31.98668  26.99010
  [3,]  35.85708  35.37138  33.93414  31.61019  28.52083  24.85177
  [4,]  31.79186  31.41769  30.31841  28.56259  26.26058  23.55828
  [5,]  28.29985  28.03585  27.26062  26.02342  24.40288  22.50211
```

T<-convprismend(time,alpha,h,k,Ly,Lz,rooty,rootz,X,y,z)

Prism end made by combining two plates and a halfspace. X is from the end in.

Example:
```
> convprismend(2000,1.5e-7,100,1,0.08,0.12,ry,rz,1:5*0.02,0,0)
[1] 0.7470260 0.9455668 0.9926337 0.9986923 0.9991119
```

T<-convprismendseq(time,alpha,h,k,Ly,Lz,rooty,rootz,T0,seq,X,y,z)

Example:
```
> convprismendseq(2000,1.5e-7,100,1,0.08,0.12,ry,rz,20,c(0,100,2000,20),1:5*0.02,0,0)
[1] 40.22157 24.33829 20.57295 20.08826 20.05469
```

T<-convplatecorner(time,alpha,h,k,Lp,rootp,x,Y,Z)

Corner of a plate made by combining two halfspaces and a plate. x is theough the plate.

Example:
```
> convplatecorner(1:4*2000,1.5e-7,100,1,0.08,ry,0,0:5/5,0)
              [,1]        [,2]        [,3]        [,4]        [,5]        [,6]
  [1,]  0.08249303  0.2870908  0.2870908  0.2870908  0.2870908  0.2870908
  [2,]  0.04499723  0.2096538  0.2096538  0.2096538  0.2096538  0.2096538
  [3,]  0.02961359  0.1654376  0.1654380  0.1654380  0.1654380  0.1654380
  [4,]  0.02109360  0.1345273  0.1345333  0.1345333  0.1345333  0.1345333
```

T<-convplatecornerseq(time,alpha,h,k,Lp,rootp,T0,seq,x,Y,Z)

Example:
```
> convplatecornerseq(1:4*2000,1.5e-7,100,1,0.08,ry,20,c(0,100,2000,20),0:4/4,0,0)
            [,1]      [,2]      [,3]      [,4]      [,5]
  [1,]  93.39401  93.44441  93.74220  95.06866  96.79903
  [2,]  22.99966  23.06915  23.16829  22.74727  21.10702
  [3,]  21.23069  21.23208  21.16825  20.89033  20.33230
  [4,]  20.68160  20.66368  20.58902  20.41947  20.15134
```

T<-convcorner(time,alpha,h,k,X,Y,Z)

Corner made from three halfspaces yielding an eigthsspace.

Example:
```
> convcorner(1:4*2000,1.5e-7,100,1,0,0:5/5,0)
```

```
           [,1]        [,2]        [,3]        [,4]        [,5]        [,6]
[1,]  0.023724328  0.08256499  0.08256499  0.08256499  0.08256499  0.08256499
[2,]  0.009886650  0.04606447  0.04606447  0.04606447  0.04606447  0.04606447
[3,]  0.005735449  0.03204133  0.03204141  0.03204141  0.03204141  0.03204141
[4,]  0.003854456  0.02458231  0.02458341  0.02458341  0.02458341  0.02458341
```

T<-convcornerseq(time,alpha,h,k,T0,seq,X,Y,Z)

Example:
```
> convcornerseq(1:4*2000,1.5e-7,100,1,20,c(0,100,2000,20),0,0:5/5,0)
          [,1]       [,2]       [,3]       [,4]       [,5]       [,6]
[1,]  98.10205   93.39480   93.39480   93.39480   93.39480   93.39480
[2,]  21.10701   22.92004   22.92004   22.92004   22.92004   22.92004
[3,]  20.33210   21.12185   21.12185   21.12185   21.12185   21.12185
[4,]  20.15048   20.59672   20.59664   20.59664   20.59664   20.59664
```

T<-qplate(time,Q,alpha,k,L,x)

Infinite plate.

Example:
```
> qplate(2000,100,1.5e-7,1,0.05,0:4/4)
[1] 0.07443634 0.14210821 0.39388593 0.95372513 1.95445847
```

T<-qplateseq(time,alpha,k,L,T0,seq,x)

Example:
```
> qplateseq(1:4*2000,1.5e-7,1,0.05,20,c(0,100,2000,0),0)
[1] 20.07449 20.38705 20.53420 20.57986
```

T<-qcyl(time,Q,alpha,k,R,r)

Infinite cylinder.
Example:
```
> qcyl(2000,100,1.5e-7,1,0.05,0:4/4)
[1] 0.2385702 0.3330883 0.6548711 1.2941657 2.3324804
```

T<-qcylseq(time,alpha,k,R,T0,seq,r)

Example:
```
> qcylseq(1:4*2000,1.5e-7,1,0.05,20,c(0,100,2000,0),0)
[1] 20.23744 20.96130 21.15870 21.19291
```

T<-qsphere(time,Q,alpha,k,R,r)

Sphere.

Example:
```
> qsphere(2000,100,1.5e-7,1,0.04,0:4/4)
[1] 1.091374 1.208209 1.564374 2.172220 3.041007
```

```
T<-qsphereseq(time,alpha,k,R,T0,seq,r)
```

Example:
```
> qsphereseq(1:4*1000,1.5e-7,1,0.04,20,c(0,100,2000,0),0:4/4)
          [,1]      [,2]      [,3]      [,4]      [,5]
 [1,]   20.19588  20.26863  20.52107  21.03185  21.86482
 [2,]   21.10398  21.20809  21.56449  22.17212  23.03298
 [3,]   21.98535  22.03638  22.15610  22.26773  22.30883
 [4,]   22.20957  22.21754  22.23595  22.25272  22.25879
```

```
T<-qhalfspace(time,Q,alpha,k,X)
```

Halfspace. X is from the surface in.

Example:
```
> qhalfspace(2000,100,1.5e-7,1,0:4/100)
[1] 1.9544100 1.1150526 0.5719636 0.2611839 0.1052952
```

```
T<-qhalfspaceseq(time,alpha,k,T0,seq,X)
```

Example:
```
> qhalfspaceseq(1:4*2000,1.5e-7,1,20,c(0,100,2000,0),0:4/100)
          [,1]      [,2]      [,3]      [,4]      [,5]
 [1,]   21.95441  21.11505  20.57196  20.26118  20.10530
 [2,]   20.80954  20.76327  20.64027  20.47902  20.32091
 [3,]   20.62118  20.60041  20.54222  20.45764  20.36116
 [4,]   20.52368  20.51124  20.47565  20.42180  20.35656
```

```
T<-qedge(time,Q,alpha,k,X,Y)
```

Edge made from two halfspaces giving a quarterspace.

Example:
```
> qedge(2000,100,1.5e-7,1,0:4/100,0.01)
[1] 3.069463 2.230105 1.687016 1.376237 1.220348
```

```
T<-qedgeseq(time,alpha,k,T0,seq,X,Y)
```

Example:
```
> qedgeseq(2000,1.5e-7,1,20,c(0,100,500,0),0:4/100,0.01)
[1] 20.49967 20.47565 20.41611 20.34825 20.29444
```

```
T<-qplateedge(time,Q,alpha,k,Lp,X,y)
```

Edge of a plate made by combining a plate and a halfspace. X is from the edge in, y is through the plate.

Example:
```
> qplateedge(2000,100,1.5e-7,1,0.04,0:4/100,0)
[1] 2.1650013 1.3256439 0.7825548 0.4717751 0.3158864
```


```
T<-qplateedgeseq(time,alpha,k,Lp,T0,seq,X,y)
```

Example:
```
> qplateedgeseq(1:4*1000,1.5e-7,1,0.04,20,c(0,100,2000,0),0:4/100,0)
          [,1]      [,2]      [,3]      [,4]      [,5]
 [1,]   21.40665  20.63079  20.23778  20.08325  20.03702
 [2,]   22.16504  21.32568  20.78259  20.47182  20.31593
 [3,]   21.49583  21.40345  21.17776  20.92547  20.72618
 [4,]   21.45230  21.40603  21.28303  21.12178  20.96367
```


```
T<-qprism(time,Q,alpha,k,Lx,Ly,x,y)
```

Infinite prism made by combining two plates.

Example:
```
> qprism(2000,100,1.5e-7,1,0.04,0.08,0:4/100,0)
[1] 0.2120094 0.2121468 0.2125590 0.2132463 0.2142089
```


```
T<-qprismseq(time,alpha,k,Lx,Ly,T0,seq,x,y)
```

Example:
```
> qprismseq(2000,1.5e-7,1,0.04,0.08,20,c(0,100,1500,0),0:4/4,0)
[1] 20.21130 20.29408 20.53223 20.83370 20.98004
```


```
T<-qprismend(time,Q,alpha,k,Ly,Lz,X,y,z)
```

Prism end made by combining two plates and a halfspace. X is from the end in.

Example:
```
> qprismend(2000,100,1.5e-7,1,0.04,0.08,0:4/100,0,0)
[1] 2.1664195 1.3270621 0.7839731 0.4731933 0.3173046
```


```
T<-qprismendseq(time,alpha,k,Ly,Lz,T0,seq,X,y,z)
```

Example:
```
> qprismendseq(2000,1.5e-7,1,0.04,0.08,20,c(0,100,1500,0),0:4/100,0,0)
[1] 21.18851 21.04037 20.73062 20.46675 20.31624
```


```
T<-qbox(time,Q,alpha,k,Lx,Ly,Lz,x,y,z)
```

Box made by combining three plates.

Example:
```
> qbox(2000,100,1.5e-7,1,0.04,0.08,0.012,0:4/4,0:5/5,0)
```

```
            [,1]      [,2]      [,3]      [,4]      [,5]      [,6]
 [1,]   2.512009  2.517526  2.556915  2.730617  3.267727  4.465001
 [2,]   2.599824  2.605340  2.644729  2.818431  3.355541  4.552816
 [3,]   2.884875  2.890392  2.929781  3.103482  3.640592  4.837867
 [4,]   3.419679  3.425196  3.464585  3.638286  4.175397  5.372671
 [5,]   4.257246  4.262763  4.302152  4.475854  5.012964  6.210238
```

T<-qboxseq(time,alpha,k,Lx,Ly,Lz,T0,seq,x,y,z)

Example:
```
> qboxseq(2000,1.5e-7,1,0.04,0.08,0.012,20,c(0,100,1500,0),0:4/4,0:5/5,0)
           [,1]      [,2]      [,3]      [,4]      [,5]      [,6]
 [1,]   22.08488  22.09039  22.12976  22.30004  22.73058  23.06066
 [2,]   22.16765  22.17317  22.21253  22.38282  22.81336  23.14344
 [3,]   22.40580  22.41132  22.45068  22.62097  23.05151  23.38159
 [4,]   22.70727  22.71279  22.75215  22.92244  23.35298  23.68306
 [5,]   22.85362  22.85913  22.89850  23.06878  23.49932  23.82940
```

T<-qfincyl(time,Q,alpha,k,L,R,x,r)

Finite cylinder made by combining a cylinder and a plate.

Example:
```
> qfincyl(2000,100,1.5e-7,1,0.04,0.04,0:4/4,0:5/5)
            [,1]       [,2]      [,3]      [,4]      [,5]      [,6]
 [1,]   0.7967771  0.8645958  1.073162  1.435446  1.966321  2.675842
 [2,]   0.8845915  0.9524102  1.160976  1.523261  2.054135  2.763656
 [3,]   1.1696428  1.2374615  1.446028  1.808312  2.339187  3.048707
 [4,]   1.7044469  1.7722657  1.980832  2.343116  2.873991  3.583511
 [5,]   2.5420141  2.6098329  2.818399  3.180683  3.711558  4.421079
```

T<-qfincylseq(time,alpha,k,L,R,T0,seq,x,r)

Example:
```
> qfincylseq(1:4*2000,1.5e-7,1,0.04,0.04,20,c(0,100,2000,0),0,0)
[1] 20.79591 22.06207 22.22798 22.24702
```

T<-qcylend(time,Q,alpha,k,R,X,r)

Cylinder end made by combining a cylinder and a halfspace. X is from the end
in.

Example:
```
> qcylend(2000,100,1.5e-7,1,0.04,0:4/100,0:5/5)
```

```
             [,1]      [,2]      [,3]     [,4]     [,5]     [,6]
  [1,]  2.5405959  2.6084147  2.8169808  3.179265  3.710140  4.419661
  [2,]  1.7012385  1.7690573  1.9776234  2.339908  2.870783  3.580303
  [3,]  1.1581495  1.2259683  1.4345344  1.796819  2.327693  3.037214
  [4,]  0.8473697  0.9151885  1.1237546  1.486039  2.016914  2.726434
  [5,]  0.6914810  0.7592998  0.9678659  1.330150  1.861025  2.570546
```

`T<-qcylendseq(time,alpha,k,R,T0,seq,X,r)`

Example:
```
> qcylendseq(2000,1.5e-7,1,0.04,20,c(0,100,1500,0),0:4/100,0)
[1] 21.56015 21.41202 21.10226 20.83840 20.68789
```

`T<-qcorner(time,Q,alpha,k,X,Y,Z)`

Corner made by combining three halfspaces.

Example:
```
> qcorner(2000,100,1.5e-7,1,0:4/100,0.01,0.01)
[1] 4.184515 3.345158 2.802069 2.491289 2.335400
```

`T<-qcornerseq(time,alpha,k,T0,seq,X,Y,Z)`

Example:
```
> qcornerseq(2000,1.5e-7,1,20,c(0,100,1500,0),0:4/100,0.01,0.01)
[1] 22.63535 22.48721 22.17746 21.91359 21.76308
```

`T<-qplatecorner(time,Q,alpha,k,Lp,x,Y,Z)`

Corner of a plate made by combining a plate and two halfspaces. x is through the plate.

Example:
```
> qplatecorner(2000,100,1.5e-7,1,0.04,0:4/4,0.01,0.01)
[1] 2.440697 2.528511 2.813562 3.348366 4.185934
```

`T<-qplatecornerseq(time,alpha,k,Lp,T0,seq,x,Y,Z)`

x is through the plate.

Example:
```
> qplatecornerseq(2000,1.5e-7,1,0.04,20,c(0,100,1500,0),0:4/4,0.01,0.01)
[1] 21.86802 21.95080 22.18895 22.49042 22.63676
```

16

Appendix 8

A8.1 Boiling induced heat transfer coefficients

In this section the influence of induced boiling in a non-Newtonian liquid is studied in order to investigate the resulting fluid to particle heat transfer coefficient. The setup and model food dimension is not representative for suspended particles and the investigation is only comparative.

A8.1.1 Experimental setup

To investigate the heat transfer coefficients from fluid to particles during vessel-boiling, an experimental setup has been created based on the lumped capacitance determination with an aluminium block, presented in figure 6.4.
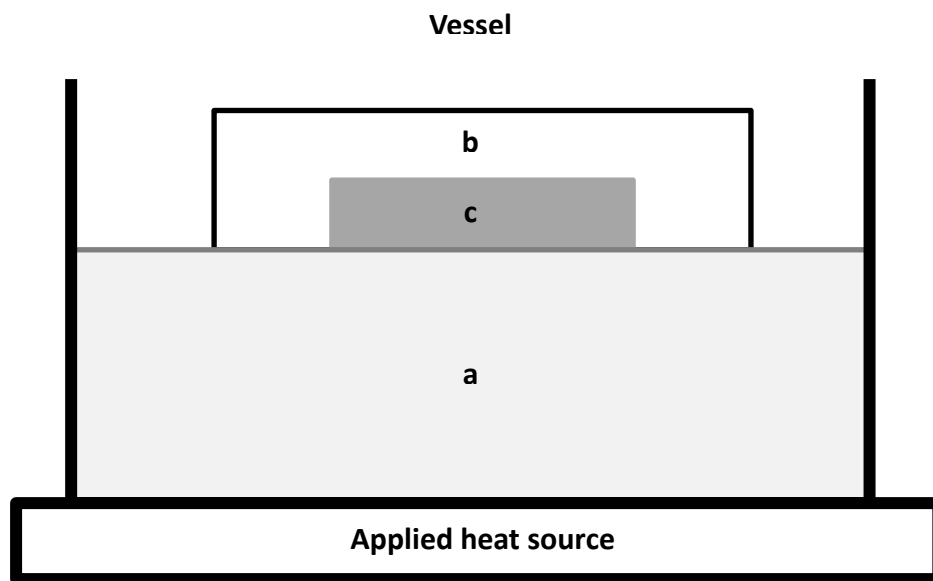

Vessel

Figure 1 Schematic experimental setup for determination of heat transfer coefficients. Domain a is the heating media, for this experiment three different types of soups, and water was used. Domain b is a polystyrene mold used to insulate the aluminum block. Domain c is the aluminum block.

The experimental setup presented in figure 1 is measuring the energy transferred from the liquid (a) to an aluminium block (c). The aluminium block is insulated with polystyrene (b) only exposing the surface contacting the liquid below it.

Polystyrene is used in the experimental setup for two specific reasons; to enable the aluminium block to float and to insulate the other boundaries of the aluminium block.

It is well acknowledged that the experimental setup will not determine the actual heat transfer coefficients for a suspended particle, as the flow pattern across a horizontal surface at the top of the liquid is different from a submerged particle. The goal of this experiment is to investigate at a comparative level the influence of boiling in media of different rheological characterization.

Four different medias was investigated, water and three commercial soups; tomato soup, curry soup and a Tuscany soup (basically a tomato soup with a high concentration of small pieces of vegetables). The setup

from figure 1 is placed on a temperature controlled frying rig, where the surface temperature of the heating source is controlled and the mass loss can be recorded (Ashokkumar and Adler-Nissen 2011). The temperature settings of the frying-rig resulted in a measured steady state temperature inside the vessel as reported in table 6.3. The temperatures chosen for the media was different because high temperatures of the frying rig created residues at the vessel bottom, due to the lack of agitation for especially the curry soup.

Table 1 Experimental settings and resulting steady state temperatures in the liquid media below the aluminium block in the conducted experiments

	Temperature setting of the frying rig, and resulting averaged temperature in the liquid media [°C]		
Frying rig settings	120	140	160
Water temperature	86	97	100
Frying rig settings	100	120	140
Tomato soup temperature	63	85	100
Frying rig settings	100	120	140
Tuscany soup temperature	*60*	*90*	*100*
Frying rig settings	80	100	120
Curry soup temperature	37	55	100

A8.1.2 Rheological characterization

The rheological characterization of the soups was carried out on a Stresstech high resolution rheometer (ATS RheoSystems) in a bop-cup setup, where the rheolgical characterization was performed under assumption that a power law model could crudely describe the behaviour (equation 1). The rheometer was set to apply an increasing stress stepwise (0.01 – 273 [Pa] in 10 steps). The characterization was carried out at 25-95 [°C], with an increment of 5[°C].

$$\tau = K \cdot \gamma^N \hspace{4cm} [1]$$

Where τ is the shear stress [Pa], γ is the shear rate [s^{-1}], k is the consistency index [Pa·s^n] and N is the power-law exponent [-]. More elaborations on rheological characterization will not be expounded here as it is not the scope to make a deterministic model based on rheology, but to serve as a characterisation measure.

The characterization of the water and the soups are carried out in the temperature range that was also investigated in the vessel. The characterization of the Tuscany soup cannot be conducted in a traditional rheometer due to the high concentration of particles and it was strained before the characterization. The viscous behaviour for water as a function of temperature is known, and since it is Newtonian it is presented as a viscosity. The rheological behaviour is presented in figure 2 for the consistency index K. The power-law exponent N was not significantly inflicted by the temperature increase. Because the experiments are conducted without agitation, the flow behaviour index is less important.
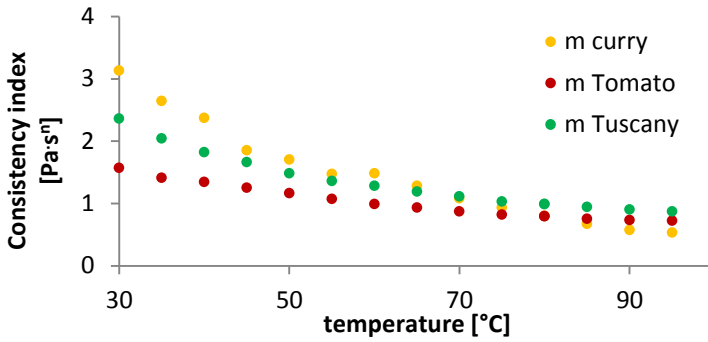
Figure 2 Consistency index for the characterization of the investigated soups

From figure 2 it is seen that the consistency index is higher for the curry Tuscany soup and the curry soup. When the soup temperature approaches the boiling point, the difference in rheological behaviour is less significant.

A8.1.3 Results from the determination of heat transfer coefficients

The determination of the heat transfer coefficients is carried out using equation 6.1. The heat transfer coefficients are presented in figure 3-5(a, b) as a function of temperature and as a function of the rate of boiling. The rate of boiling is calculated is the effect [W] used for water evaporation based on measured mass loss from the liquid media, through equation 2.

$$rate\ of\ boiling = \frac{\Delta m_{evap} \cdot \Delta H_{evap}}{t}\ [\text{J/s}] \quad\quad\quad [2]$$

Where m_{evap} [kg] is the mass-loss due to evaporation, ΔH_{evap} [J/kg] is the specific energy needed for evaporation of water (2290 [KJ/kg]) and t is the time. The measured heat transfer coefficients are presented as a function of temperature and as a function of the rate of boiling in figure 3 for water, in figure 4 for tomato soup, and in figure 5 for Tuscany soup and curry soup (as they showed similar heat transfer).
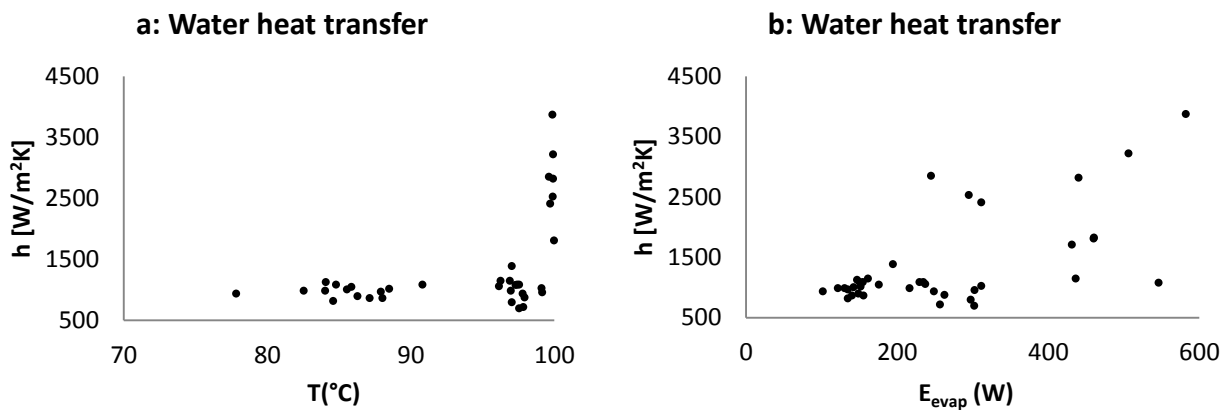

Figure 3 The heat transfer coefficient, h, from water to the aluminium block measured at the surface as a function of the temperature (left) and the rate of boiling (right)

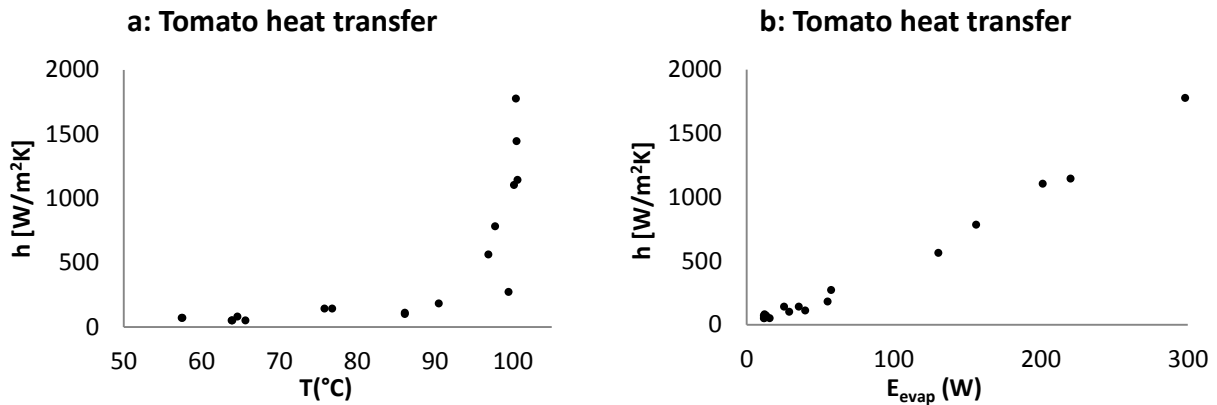## a: Tomato heat transfer

b: Tomato heat transfer

Figure 4 The heat transfer coefficient, *h*, from tomato soup to the aluminium block measured at the surface as a function of the temperature (left) and the rate of boiling (right)

a: Toscany/curry heat transfer

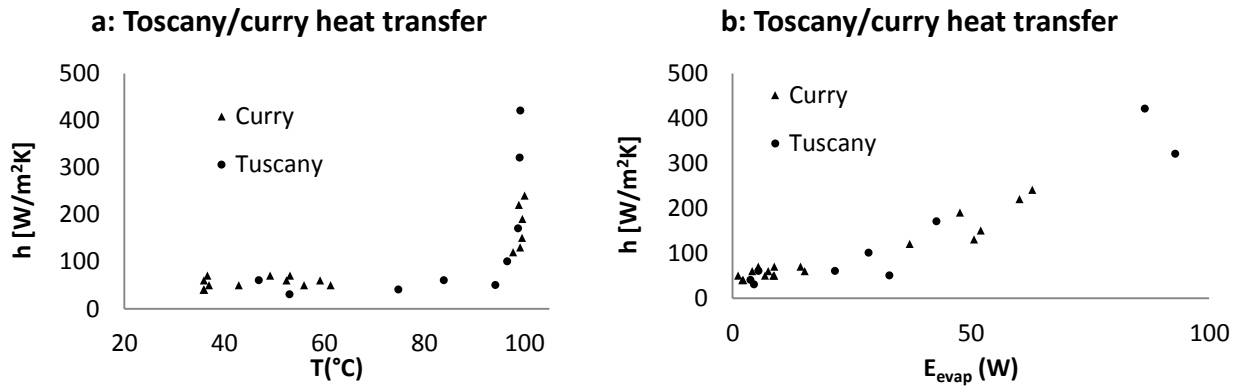## b: Toscany/curry heat transfer

Figure 5 The heat transfer coefficient, *h*, from curry soup and Tuscany soup to the aluminium block measured at the surface as a function of the temperature (left) and the rate of boiling (right)

The results presented in figure 3-5 show a huge difference in the heat transfer coefficient for different liquid media. At sub boiling temperature the heat transfer coefficient is primarily dominated by convection, thus a fluid with a higher viscosity (consistency index for non-Newtonian fluids) is promoting smaller heat transfer coefficients. For water the sub-boiling heat transfer coefficient is observed at a range of 700-1400 [W/m^{2}K], 60-100 [W/m^{2}K] for tomato soup and 40-70 [W/m^{2}K] for curry and Tuscany soup. The results also indicate a big increase in the heat transfer coefficient above the boiling point of the media. The increase in heat transfer coefficients induced by boiling is explained by two phenomena: condensation of vapour bubbles from the liquid to the solid and enhanced convection, (Incropera and DeWitt 1996).

A8.1.4 Influence of the heat transfer coefficient on the resulting heating time of suspended particles

The sensitivity of the uncertainty in h_{fp} is investigated through a small theoretical study where four different food particles (green peas, frankfurter sausages, carrot cubes and potatoes) are heated with varying heat transfer coefficients. In the study only heat transfer is included as a phenomenon. The heating time for the particles is defined as: the time to reach 78°C in the centre. Heating time for the four particles is presented in figure 6. The calculations are performed by solving the series expansion recapitulated below.

$$\Omega = \left(\frac{T_s - T}{T_s - T_0} \right) = \sum_i^\infty a_i e^{-b_i \cdot Fo}$$

Figure 6 represents the heating time to reach 78°C from an initial temperature of 20°C as a function of the heat transfer coefficient. The thermal properties of the particles are calculated from the composition. The characteristic dimensions of the investigated particles are: Peas (r=0.003 [m], sphere), frankfurters (r=0.095 [m], infinite cylinder), carrot cubes (L=0.005 [m], cubic) and potatoes (r=0.02 [m], sphere).
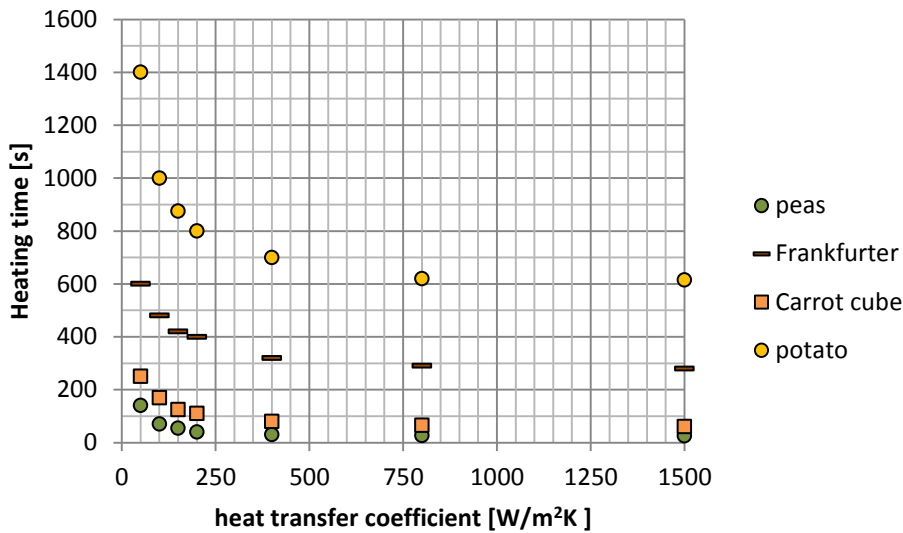

Figure 6 Heating time for selected food particles as a function of the fluid to particle heat transfer coefficient

From figure 6 it can be observed that the heating time for investigated particles does not decrease substantially with an increase in the heat transfer coefficient above app. 500 [w/m^{2}K]. This is an interesting result because the convective heat transfer coefficient in water at sub boiling temperatures can be above this value. In addition, it is observed that there is an increase in the heating time for heat transfer coefficients varying from 50-250 [W/m^{2}K]. This is also an important observation because the fluid to particle heat transfer coefficients for commercial soups (the three tested) can be as low as 50 [W/m^{2}K] at sub boiling temperatures. If a heat transfer coefficient higher than 50 [W/m^{2}K] is wanted it could be necessary to either increase the convection through agitation or by inducing boiling.

An important notice is that the conducted experiments can only be used for comparison because the geometry and position of the aluminium block is very different from a suspended food particle.

National Food Institute
Technical University of Denmark
Mørkhøj Bygade 19
DK - 2860 Søborg

Tel.   35 88 70 00
Fax   35 88 70 01

www.food.dtu.dk

ISBN: 87-93109-51-2